

POLARSTERN ARKTIS XVII/2
Cruise Report: AMORE 2001
(Arctic Mid-Ocean Ridge Expedition)

by J. Thiede
and the Shipboard Scientific Party

Ber. Polarforsch. Meeresforsch. 421 (2002)
ISSN 1618 - 3193

POLARSTERN ARK XVII/2
CRUISE REPORT / FAHRTBERICHT: AMORE 2001
by J.Thiede and the Shipboard Scientific Party

Contents	Page
AMORE 2001: Executive Summary	4-6
AMORE 2001: Zusammenfassung	7-9
1 Introduction	10
1.1 Structure and Composition of the Crust in the Eastern Arctic Ocean.....	10-13
1.2 The Partner Ship USCGC HEALY.....	13-17
1.3 Joint Operations of HEALY and POLARSTERN.....	18-20
1.4 Short Biography of Yakov Gakkel.....	21-22
2. Expedition Narrative.....	23-40
3. Meteorological Conditions	41-49
4. Sea Ice Measurements and Sampling	50
4.1 Ice Conditions along the Cruise Track.....	51-53
4.2 NOAA-AVHRR Imagery.....	53-56
4.3 Ice Thickness Measurements.....	56-67
4.4 Laser Profiling of Pressure Ridges.....	67-69
4.5 Spectral Albedo and Areal Coverage of Various Surface Types.....	70-75
4.6 Salinity, Density and Texture of Ice Cores.....	76-77
4.7 The Role of Sea Ice on the Transport of Radionuclides.....	77-79
4.8 Biological Studies.....	79-81
4.9 Particulate Matter in Snow and Ice.....	82-84
4.10 Icebergs: Types and Sediment Content.....	84-85
4.11 Deployment of Drifting Meteorological Buoys.....	85-86
4.12 A "Fishermans Camp".....	86-88
5. Hydrography	89
5.1 Secchi Depth Measurements.....	89-90
5.2 Evidence for Hydrothermal Activity, Gakkel Ridge.....	90-93
6. Bathymetry	94-99

7.	Sediment Distributions	100
7.1	Parasound-Data.....	100-110
7.2	Sediment Cores.....	111-115
7.3	Sediment Geochemistry.....	116-117
8.	Petrogenesis of Crustal Rocks	118
8.1	Introduction.....	118-120
8.2	Planning and Operations.....	120-128
8.3	Samples.....	129-132
8.4	Observations.....	132-141
8.5	Discussion.....	142-162
8.6	Conclusions.....	162-164
9.	Geophysical Investigations	165
9.1	Introduction.....	165-169
9.2	Seismic Reflection Experiments.....	169-173
9.3	Refraction Experiments along Seismic Reflection Transects.....	174-177
9.4	Seismic Refraction Experiment along the Gakkel Ridge.....	178-180
9.5	Gravimetric Measurements.....	181
9.6	Helicopter Based Magnetic.....	181-185
9.7	Heat Flow Measurements.....	186-190
9.8	Seismological Studies.....	191-201
9.9	Magnetotellurics on Drifting Ice Floes.....	201-206
10.	Plans for Future Work	207-210
11.	Public Relations	211-213
12.	Acknowledgements	214-216
13.	References	217-222
Appendices		
	Contents Appendices.....	223
1.	Scientific Party ARK XVII/2.....	224-225
2.	Participating Institutions ARK XVII/2.....	226-227
3.	Ship's Crew ARK XVII/2.....	228-229
4.*	Scientific Party on HEALY.....	230
5.	Station Log POLARSTERN.....	231-234

6.*	Station Log HEALY.....	235-240
7.*	Petrology: Sampling Technologies.....	241-245
8.*	Petrology: Sample Descriptions.....	246-281
9.*	Thin Sections Overview.....	282-288
10.*	Thin Section Descriptions.....	289-335
11.*	MAPR.....	336-341
12.*	TV-Grab Video.....	342
13.*	OFOS Observations.....	343
14.*	Sediment Core Descriptions.....	344-350
15.*	Geophysical Investigations: Experience Report.....	351-387
16.*	Polar University.....	388
17.	List of Abbreviations and Acronyms.....	389-390
18.*	Karasik Seamount.....	391-397

*** - only on CD**

AMORE 2001: Executive Summary

The AMORE 2001 (Arctic Mid-Ocean Ridge) expedition to the central Eastern Arctic Ocean combined the operations of 2 research ice-breakers to make certain investigations possible at all, to improve progress, efficiency and safety in the ice. The main target area was the ridge crest of the western Gakkel Ridge. Traverses from the north-eastern Barents Sea shelf to the Gakkel Ridge and from to the Lomonosov Ridge were used for continuous seismic reflection profiles across the Nansen and Amundsen basins.

The two ships operated in tandem for geophysics operations, and were able to either work together or to separate for sampling operations. Sampling was to be conducted via dredge, TV-grab, gravity and rock cores from both ships. At sea observations include hand sample descriptions of all rock types encountered, preliminary geochemistry (carried out on HEALY) and thin section analyses (carried out on POLARSTERN).

HEALY and POLARSTERN reached the North Pole on September 6, 2001. On August 23 a historic meeting of 3 research ice-breakers occurred on top of the Gakkel Ridge. More than 250 crew and scientists from 17 nations on HEALY, the Swedish ODEN and POLARSTERN exchanged data and samples; the gathering on the ice comprised more scientists than ever had met at the same time and place in the central Arctic Ocean.

Both ships succeeded in charting by multibeam sounding systems (SEABEAM on HEALY, HYDROSWEEP on POLARSTERN) 33 000 square kilometres of the Arctic Ocean floor, mostly of the Gakkel Ridge, including its shallowest (566 m) and deepest (5670 m) points, with unprecedented precision and detail.

Multichannel seismic reflection profiles have been shot continuously along the transit trips across the Nansen and Amundsen basins, as well as up to 30 NM long segments along the Gakkel Ridge, interspersed with rock sampling operations. A substantial number of heat flow measurements has been conducted along the return trip from Lomonosov to Gakkel Ridge and along its ridge crest / rift valley. The values increase towards the active Gakkel Ridge in general, but the stations from the rift valley are highly variable.

Both ships carried 2 helicopters each, for logistic and scientific purposes. POLARSTERN succeeded to deploy routinely helicopters for airborne investiga-

tions: HELI-MAG-surveys of the magnetic anomalies of various ridge segments, deployment of long-term geophysical stations on the ice, beside cargo and personnel transport between the two ships and ice reconnaissance.

Systematic sampling of crustal rocks from the Gakkel Ridge has been carried out for petrological studies, at more than 200 stations between the 2 ships, with the recovery of various types of basalts, peridotites, gabbros, breccias and hydrothermal deposits, in total weighing almost 20 t between the 2 ships. The dominant lithology consisted of various types of basalt, but one ridge segment produced a substantial number of peridotite and gabbro samples. The rock types sampled on Gakkel Ridge record the magmatic, hydrothermal and tectonic evolution of the world's most slowly spreading mid-ocean ridge. During 40 days of sampling, 96 total basement sampling stations were carried out on POLARSTERN. The lithologies recovered confirm the position of Gakkel Ridge as one of the geologically most unusual and interesting mid-ocean ridges. Peridotites sampled along the magmatically starved segments show indications for generally low degrees of partial melting, as do the basalts. Basalts are also generally quite primitive, suggesting the absence of a thick crust required for significant processing. Weighing against these observations are the increasing abundances of basalt to the east of the magmatically starved section. This runs contrary to all theory concerning mid-ocean ridges. Mantle temperature is probably a stronger input into the overall degree of melting than was previously thought to be the case.

Sediment cores have been recovered at the heat flow stations in the central Eastern Arctic ocean containing records of the history of the Arctic sea ice cover and of several Eurasian continental glaciations. Two provinces of somewhat different depositional environments were sampled along the Gakkel Ridge during the expedition. In general, all sediments consist of hemipelagic silty to sandy muds with little to no microfossil content. In the western province (around 0° latitude), the brownish to olive sediments show evidence for variable current sorting effects on deposition, which may relate to a variable inflow of Atlantic waters. In the eastern province (around 75°E), the sediments display a cyclic deposition of dark grey, olive and brownish sediments. Variations in bioturbation and the content of ice-rafted debris suggest that these cycles reflect climatic variations from warmer to colder phases (and vice versa), some of which had glaciations of continental areas in northern Eurasia.

Ice-thickness and other glaciological measurements over long distances have been collected by means of a HEM-bird, of a SEM-probe deployed from a crane in front of POLARSTERN's bow and during visits in a substantial number of ice floes. The average ice thickness of the floes in the investigated area was 1,95 m, approximately 20 % less than 10 years ago. Ice-cores at numerous locations permitted independent checks to verify ice-thicknesses as well as to collect fauna (various small invertebrates) living in the ice. Their species composition was determined and they were cultivated for nutrition experiments.

AMORE 2001: Zusammenfassung

Die AMORE 2001 (Arctic Mid-Ocean Ridge) Expedition (31.07. Tromsø bis 07.10. Bremerhaven für POLARSTERN, 31.07. Tromsø bis 03.10. Tromsø für HEALY) in den zentralen östlichen Arktischen Ozean wurde durch die beiden Forschungseisbrecher POLARSTERN und HEALY durchgeführt. Die HEALY ist ein neuer Eisbrecher der US Küstenwache, die in diesem Sommer ihre wissenschaftliche Jungfernfahrt durchgeführt hat. Die gemeinsamen Operationen der zwei Eisbrecher ermöglichten eine Reihe von sonst nicht möglichen Untersuchungen, weil einer der beiden Eisbrecher als führendes Schiff den laufenden Fortschritt garantieren konnte. Die beiden Eisbrecher ergänzten sich auch in ihrer wissenschaftlichen Effizienz und ihrer Sicherheit. Das wichtigste Zielgebiet war der westliche Gakkel-Rücken (beide Rückenschultern und das Rift-Tal), aber Traversen von der nordöstlichen Barentssee zum Gakkel-Rücken und vom Gakkel-Rücken zum Lomonosov-Rücken wurden für kontinuierliche reflektionsseismische Arbeiten durch das Nansen- und das Amundsen-Becken genutzt.

USCGC HEALY und POLARSTERN erreichten den Nordpol am 06.09.2001. Unterwegs (am 23.08.) trafen sich den schwedischen Eisbrecher ODEN und ein historisches Treffen von drei Forschungseisbrechern wurde in der Gegend des Gakkel-Rückens abgehalten. Die ODEN hatte gemeinsam mit der POLARSTERN bereits am 07.09.1991 den Nordpol erreicht und damit erstmals bewiesen, dass konventionell angetriebene Forschungsschiffe im zentralen Arktischen Ozean erfolgreich operieren können. Durch das gemeinsame Treffen von HEALY, ODEN und POLARSTERN versammelten sich mehr als 250 Besatzungsmitglieder und WissenschaftlerInnen zu einem gemeinsamen Treffen auf dem Eis; gleichzeitig wurden wissenschaftliche Daten und Proben ausgetauscht. Dieses Treffen der drei Forschungseisbrecher bedeutet einen historischen Höhepunkt der Erforschung des zentralen Arktischen Ozeans.

HEALY und POLARSTERN waren beide mit kompatiblen Fächerecholoten ausgerüstet (auf der HEALY ein SEABEAM-System, auf der POLARSTERN ein HYDROSWEEP-System) und es gelang, insgesamt 33.000 km² des Arktischen Meeresbodens in bisher unerreichtem Detail zu kartieren. Der größte Teil der Kartierarbeiten konzentrierte sich auf die Gipfel-Flur des Gakkel-Rückens und umfaßte den flachsten (566 m) sowie tiefsten Punkt (5.670 m) im östlichen Arktischen Ozean. Das Segment des Gakkel-Rückens war bisher völlig unbekannt und zählt nun zu den best untersuchtesten Gebieten auf der ganzen Erde.

Die geophysikalischen Untersuchungen umfaßten Multikanals-Reflektions-Profile, die entlang der gesamten Transitstrecke über das Nansen- und das Amundsen-Becken vermessen wurden. Zusätzlich wurden bis zu 30 nm lange Segmente entlang der Rückenachse des Gakkel-Rückens vermessen, um die Krustendicke zu bestimmen. Auch wurden an einer beträchtlichen Anzahl von Stationen Wärmestrommessungen vorgenommen, einmal entlang des Profils vom Lomonosov-Rückens zum Gakkel-Rücken und entlang der Rückenachse des Gakkel-Rückens, dabei vor allem im Rift-Tal. Generell steigen die Wärmestromwerte in Richtung auf den aktiven Gakkel-Rücken, aber erstaunlicherweise sind die Stationen im eigentlichen Rift-Tal höchst variabel.

Beide Schiffe transportierten jeweils zwei Helikopter, die für logistische und wissenschaftliche Ziele eingesetzt werden konnten. Die POLARSTERN hat ihre beiden Helikopter systematisch für wissenschaftliche Untersuchungen eingesetzt, wobei die HELI-MAG-Untersuchungen der magnetischen Anomalien von verschiedenen sehr detailliert aufgenommenen Rücken-Segmenten hervorzuheben sind und wobei auch geophysikalische Stationen (REFTEK u. a.) auf dem Eis ausgebracht werden konnten. Neben den geophysikalischen Arbeitsgruppen konnten auch glaziologische Arbeitsgruppen auf das Eis ausgefliegen werden und es konnte erstmals eine elektromagnetische Sonde zur Eisdickenbestimmung unter dem Helikopter eingesetzt werden, um weiträumig Eisdickenuntersuchungen vorzunehmen.

Beide Schiffe haben mit Hilfe ihrer Windensysteme eine systematische Beprobung der Krustengesteine des Gakkel-Rückens durchgeführt. Insgesamt konnten mehr als 200 Stationen von beiden Schiffen beprobt werden, wobei es gelang, eine breite Suite von verschiedenen Typen von Tiefsee-Basalten und Peridotiten, Gabbros und Brekzien zu gewinnen. An einer Station konnten hydrothermale Ablagerungen (Eisensulfid-Vererzung) gewonnen werden. Insgesamt sind mehr als 20 t Gestein von beiden Schiffen geborgen wurden, wobei die dominierende Lithologie aus verschiedenen Basalt-Typen besteht, die Peridotit- und Gabbro-Proben sich aber auf ein spezielles Rückensegment konzentrieren. An zahlreichen Positionen konnten hydrothermale Quellen nachgewiesen werden.

An den Wärmestromstationen konnten in der Regel auch relativ lange Sedimentkerne gewonnen werden, die es erlauben, die Ablagerungsgeschichte des quartären Arktischen Ozeans im Detail zu beschreiben. Sie dokumentieren, dass der Arktische Ozean schon seit vielen Hunderttausend Jahren durch Mee-

reis bedeckt ist und dass das eistransportierte Material den Einfluss von Eisschilden von benachbarten Kontinenten belegt (dieses war besonders interessant, weil wir uns entlang der östlichen Grenze des Arktischen Eurasischen Eisschildes während der letzten Vereisung bewegten). Die glaziologische Arbeitsgruppe konnte die Eismächtigkeit und eine Suite von ergänzenden glaziologischen Messungen durchführen. Neu war der erstmalige technische Routineinsatz einer elektromagnetischen Sonde vom Helikopter (HEM-Bird), während gleichzeitig vom Bug der POLARSTERN eine elektromagnetische Sonde zur routinemäßigen Vermessung der Eismächtigkeit vor dem Bug der POLARSTERN vorgenommen wurde. Eine Zusammenschau der Messergebnisse ermöglicht die Aussage, dass sich in diesem Gebiet die Eismächtigkeit von etwa 2,5 m im Jahre 1991 auf 1,95 m im Jahre 2001 reduziert hat. Die Eiskerne enthielten an zahlreichen Lokalitäten Fauna (verschiedene kleine Invertebraten), die sich an den extremen Lebensraum in den Solekanälen des Eises angepasst haben. Die Artenzusammensetzung dieser Organismen wurde bestimmt und sie wurden für Ernährungsexperimente in den Aquarien der POLARSTERN gehalten.

1. Introduction

1.1 Structure and Composition of the Crust in the Eastern Arctic Ocean

(J.Thiede)

The Arctic Ocean (Fig. 1) is divided in deep sea basins, which have been formed through seafloor spreading since the middle Mesozoic and structural highs that can consist of volcanic structures or of continental crust with a relatively thin younger pelagic sediment cover. The AMORE 2001 (= ARK XVII/2) expedition of the research icebreaker POLARSTERN, which has been carried out in the late summer of the year 2001 together with new US-American research icebreaker USCGC HEALY, has tried to collect extensive knowledge on structure and composition of the oceanic crust in the eastern Arctic Ocean deep sea basin between Spitzbergen and Gakkel Ridge (= Nansen Basin incl. Barents Abyssal Plain), Gakkel Ridge and Lomonosov Ridge (= Amundsen Basin incl. Pole Deep Abyssal Plain). Both scientific parties had extensively planned their joint operations; a special Memorandum of Understanding (MOU) was developed and signed during the cruise to define the division of responsibilities between the scientific parties on the 2 ships.

The Eastern Arctic deep basin has developed since the late Paleocene through the detachment of a narrow strip of continental crust, which today builds the foundation of the Lomonosov Ridge from the Eurasian continental margin. The area was visited by POLARSTERN in 1987 (Thiede et al., 1988) and 1991 (Fütterer et al., 1992). Today the Gakkel Ridge is the most prominent structural feature of the Eastern Arctic Ocean. Based on the pattern and age of seafloor-spreading type linear magnetic anomalies it has developed over the past 55 Mio. years after the margins of Lomonosov Ridge began to separate from the Eurasian continental margin. It is an outstanding and clearly defined feature of this deep-sea basin, but because of the exploration history of the Arctic Ocean its existence has only been known for less than 50 years. The naming of the Gakkel Ridge has gone through several decades and it took a substantial time until the scientific community had settled the question of the name of this ridge. It is only lately that the term Gakkel Ridge has been generally accepted. It is equivalent to the following names, which have been used in previous publications: Arctic Mid-Ocean Ridge, Arctic Mid-Oceanic Cordillera, Nansen Ridge and Nansen-Gakkel Ridge.

While marine-geophysical and seismological investigations during former expeditions have already revealed a framework of the tectonic structure of this deep sea-basin, the petrology of the volcanic rocks along Gakkel Ridge (active mid-ocean ridge with the slowest spreading rate in comparison to all other mid-ocean ridge systems) was largely unknown prior to AMORE 2001. Volcanic rocks were found rather accidentally during a former POLARSTERN expedition (1987) at one station, which – however - could hardly give information on the variety of rocks in their unique quality and distinction of this ridge system. Jointly POLARSTERN and HEALY have executed a systematic dredging program, in order to grasp the different lithologies of volcanic rocks in this area and to point to the history of origin of the attributes of the Gakkel Ridge. The joint operation of POLARSTERN and HEALY posed a special challenge on the nautical proficiency of the crews of both research icebreakers.

The examination of the composition of the oceanic crust was supplemented by marine-geophysical and seismological experiments, in order to collect further data to the tectonic structure of the area of investigation. Surveys of the detailed bathymetry must be considered as an integrated component of this program. Also the suspected formation of hydrothermal mineral accumulations, which are indicators for the appearance of hydrothermal systems, stood in close connection to the volcanic processes at Gakkel Ridge.

While the main focus of the scientific programs during this expedition was based on the geological and geophysical properties of the oceanic crust, additional programs for physical sea-ice qualities, for bacterial communities, biological studies as well as sediment probes for paleo-environmental examinations have played only a relatively subordinate role. However, they could be executed because both research icebreakers performed a long and carefully planned advance into the central eastern Arctic Ocean in the summer of 2001 and each of these efforts provided unique possibilities for sample material for the described problems.

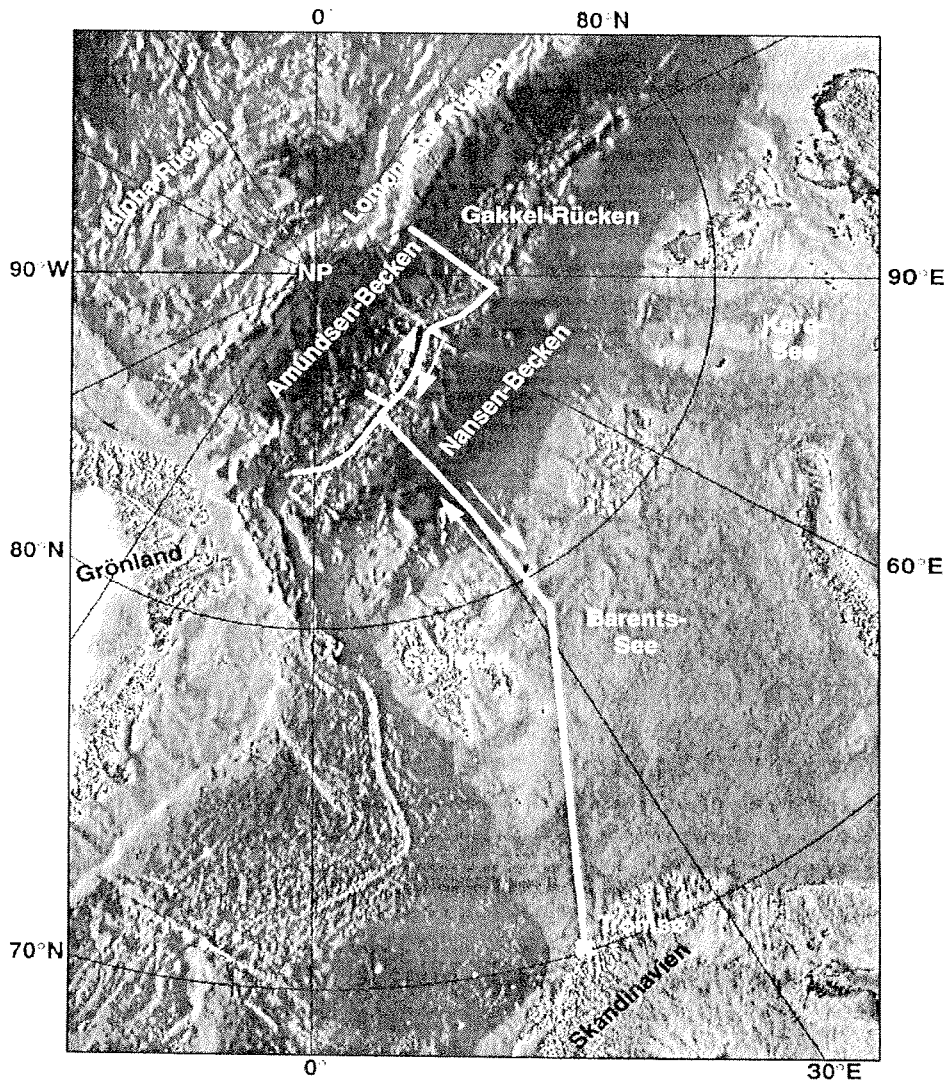


Fig. 1: Planned region of main operations of AMORE 2001.

In Figure 1, the bathymetry of the Arctic Ocean is illustrated and clearly shows its structure of deep-sea basins and ridge systems together with the planned region of operations of AMORE 2001. Figure 2 shows the expedition route, which took the vessels from Tromsø eastwards of Spitzbergen into the central part of the eastern Arctic basin with a main focus of investigations along Gakkel Ridge. Individual excursions have addressed the border structure of the deep-sea basins to the continental-edge in front of Barents Sea and Lomonosov Ridge. The expedition began on July 31. in Tromsø and it has been completed at the beginning of October, after POLARSTERN returned back to Bremerhaven and HEALY exchanged her scientific party in Tromsø for another venue in the Arctic later.

The AMORE 2001 expedition to the Gakkel-Ridge has been a two-ship-operation with USCGC HEALY (WABG-20) of the US Coast Guard and PFVS POLARSTERN of the AWI joining forces (Fig. 2). The HEALY was on her scientific maiden voyage and beautifully performed as a research icebreaker. Both ships met and jointly left Tromsø, but they had to part on September 26 after leaving the Gakkel Ridge, because POLARSTERN was unexpectedly assigned acoustic testing close to Bergen/Stavanger-Norway as part of her return trip to Bremerhaven. During sampling operations both ships operated separately but during transit either of them could take the lead. During geophysical profiling they sailed in convoy, HEALY (Fig. 3a) as the more capable icebreaker clearing a lead, POLARSTERN (Fig. 3b) following at a close distance with her geophysical gear (airgun array, streamer) deployed (Table 1).

1.2 The Partner Ship USCGC HEALY

(mainly based on information on USCGC HEALY copied from a brochure provided by the Public Affairs Officer: FPO AP 9667-3918)

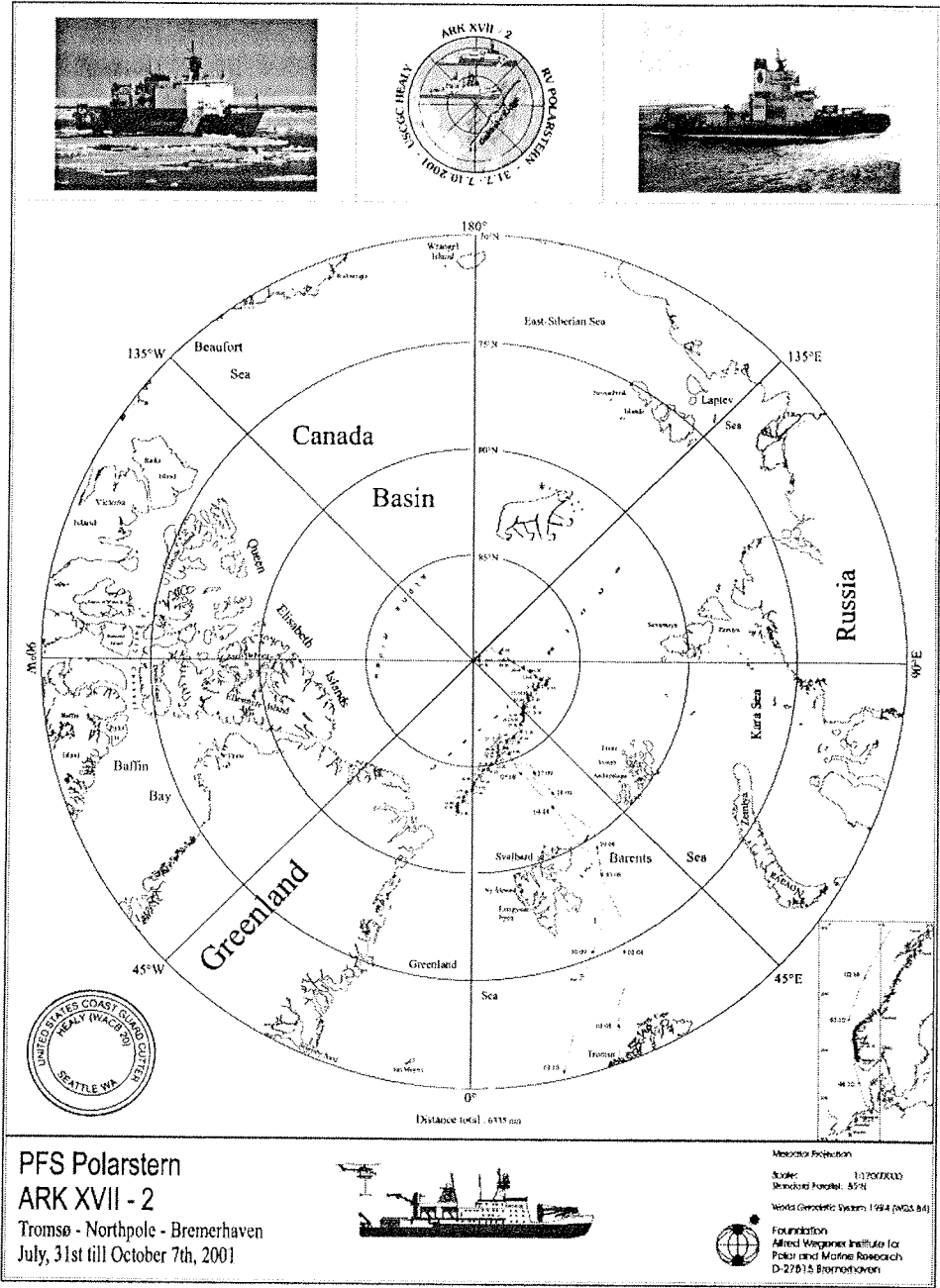


Fig. 2: POLARSTERN-Route during AMORE 2001.

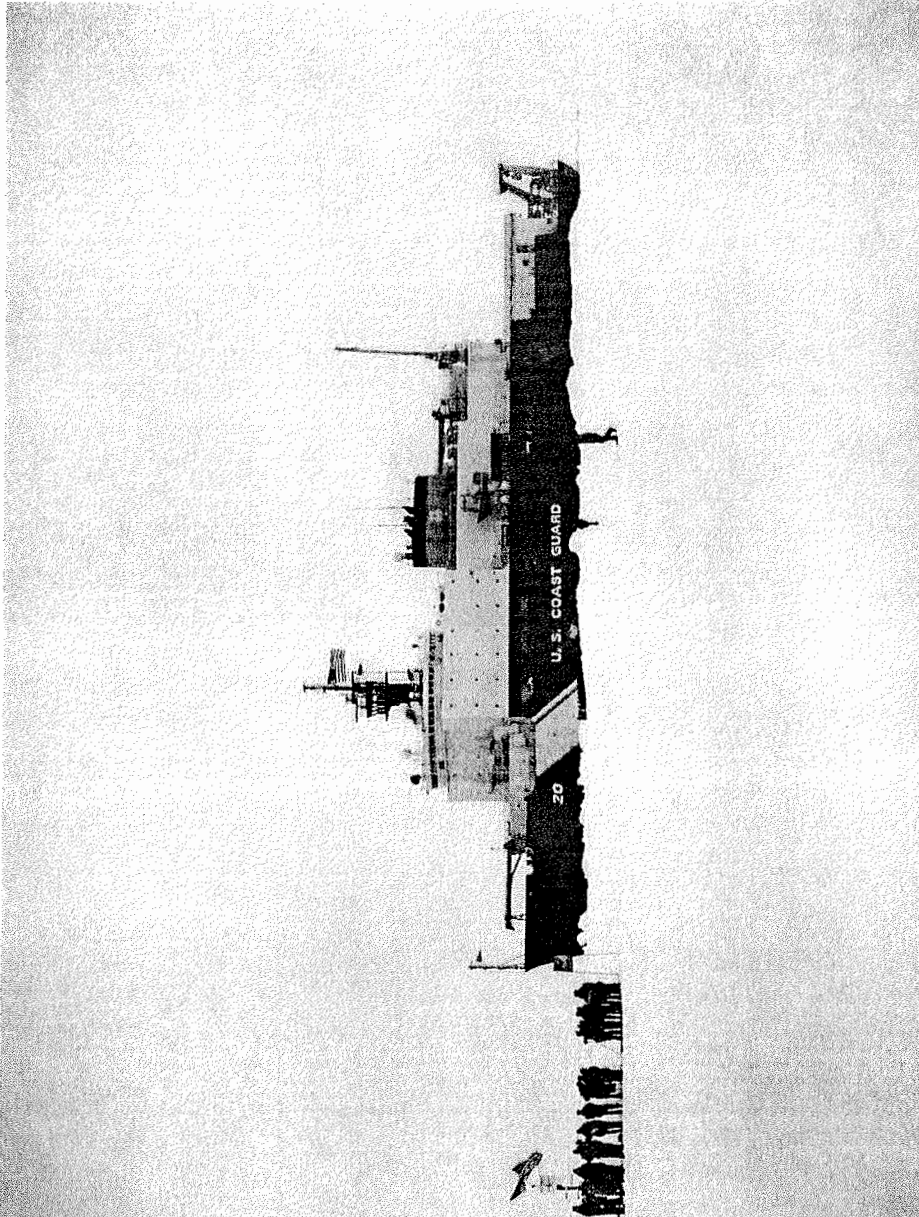


Figure 3a: USCGC HEALY during AMORE 2001.

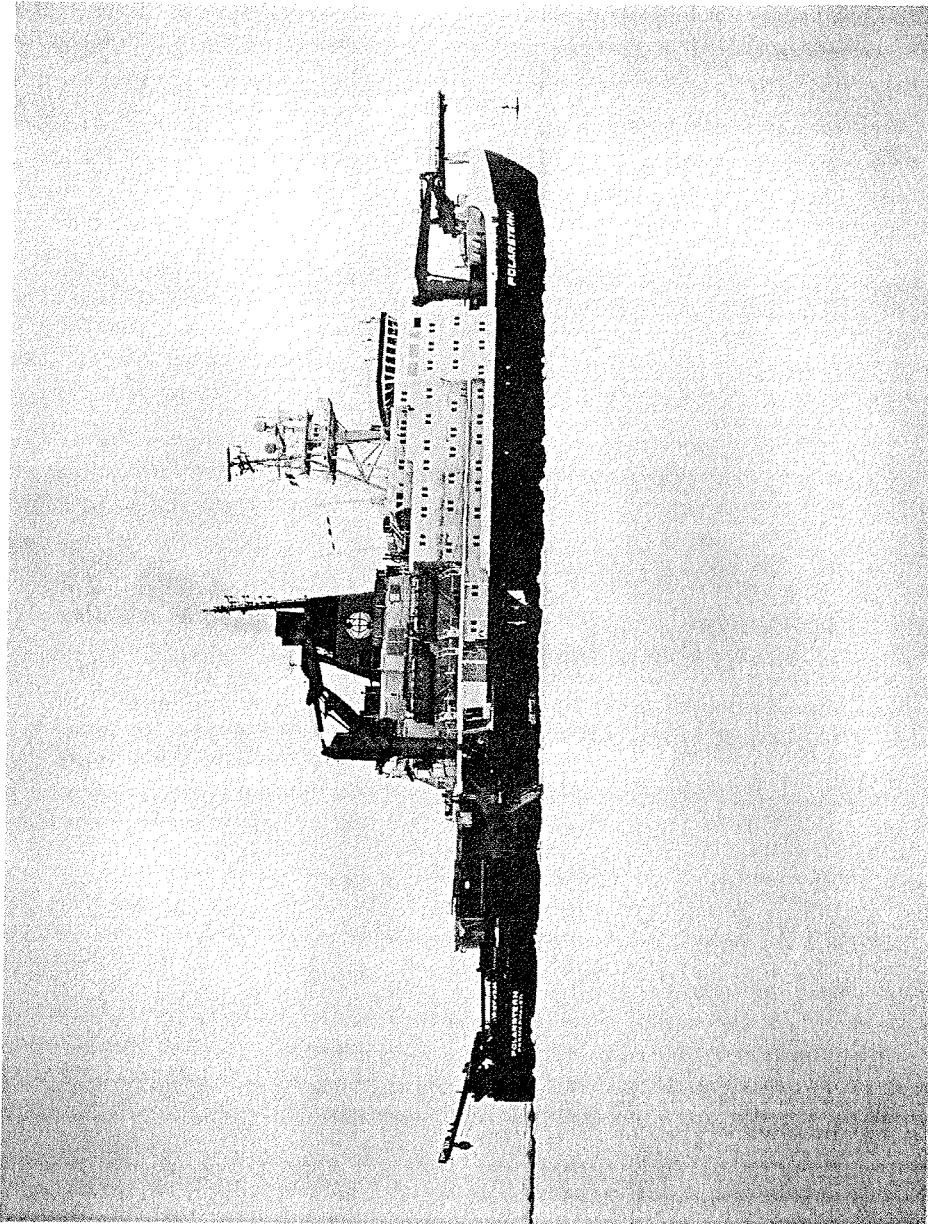


Figure 3b: PVFS POLARSTERN during AMORE 2001.

In 2001 USCGC HEALY was a brand new ship on her scientific maiden voyage. The acquisition of the HEALY was a joint effort between the US Coast Guard and the US Navy. The contract to design and construct the ship was awarded to Avondale Industries in 1993; the contract was for building a multimission ice-breaking research vessel capable of effectively performing operations satisfying a broad spectrum of scientific and icebreaking requirements in all polar regions. It was designed to commercial, military and international standards. The HEALY is named in commemoration of Captain Michael A. Healy, U. S. Revenue Marine. Captain Healy was most notable as a foremost seaman and navigator of his time in the Bering Sea and Alaskan Arctic regions while commanding Officer of the U. S. Revenue Cutter BEAR 1886-1895.

The modern HEALY is a very capable icebreaker, which performed excellently during AMORE 2001. She is 128 m long, with a displacement of 16 000 LT. Her diesel electric propulsion system provides 30 000 horsepower's on 2 fixed pitch propellers. She can break ice of 1,37 m at 3 knots continuously, 2,44 m by backing and ramming. Accommodations are provided for a total of 92 persons with 35 additional berths reserved for scientists. She can also carry 2 helicopters.

1.3 Joint Operations of HEALY and POLARSTERN: Assessment of Watch Going Officer of POLARSTERN

(J. Keil)

The icebreaking in convoy was a new experience for both sides and therefore created new demands on both bridge watches. The exchange of information about ice conditions and visibility was successful depending upon the actual conditions. The communication between two ships did not cause any problems. All in all, the co-operation between the both ships was positive and an advantage for each other.

The following problems needed special attention.

- The co-operation between both ships while travelling in convoy was excellent. For example, the HEALY bridge watch was careful to announce in time the reduction of speed while travelling through thick ice or backing and ramming. This was very important because the POLARSTERN could not set the propeller pitch astern to stop the ship while the geophysics array or even the streamer were outside of the ship.
- During the travel through the wake behind HEALY, a minimum distance of 3 cables should not be exceeded or undergone. Because of frequent fog with visibility below 200 m, the ship ahead disappeared and the wake was barely visible.
- As requested by the POLARSTERN, the HEALY tried to keep the distance close between the ships, so that the gully between the two ships could not close. But it seemed that this information was not transmitted during the handing over of the watches, because this request had to be repeated on many occasions. Frequent appeals of the bridge watch to the HEALY, to not make sharp route corners (over 90 degrees or too great changes of the course) only showed an effect after some time.
- Due to the better manoeuvring capabilities of the HEALY (very small turning circle, quick acceleration), the distance between the ships often increased rapidly and the POLARSTERN could not follow, especially when the air-gun and / or the streamer stuck in the fast closing ice, which necessitated the pulling in of the array.
- As a result of the better capabilities of steering of the HEALY in comparison to the POLARSTERN, it was sometimes difficult to follow the open wake after great changes of the course by the HEALY. Because of the extreme rudder position while attempting to cut off the corner in a tight turn, ice often

was washed in between the airgun array and the ship, and this led to the array being lifted out of the water and dragged across the ice.

- The performance of helicopter flights during convoy travel of the part of HEALY was very disruptive, causing the leading ship to stop and heave to.
- It is important to highlight the immediate readiness of the HEALY to offer ice breaking without request, in cases where the POLARSTERN, could not free itself, which was practised successfully.
- To improve possible co-operation in the future, the nautical officers of both ships should consider a meeting for the preparation of the expedition, to solve these kinds of problems and to sharpen the appreciation for them in advance.

Table 1. Times of convoy operations of HEALY and POLARSTERN.

Date	Time (UTC)	–	–	Miles	Convoy Time [h]	Remarks
04.08.01	08.30	81°50,1'N	029°13,2'E	310	53,8	BZ = UTC
06.08.01	14.16	85°44,9'N	015°07,1'E			
07.08.01	09.15	85°30,1'N	015°25,9'E	39	7,5	BZ = UTC +1h
07.08.01	16.45	85°06,7'N	010°47,7'E			
08.08.01	09.59	84°58,9'N	009°03,1'E	24	4,8	BZ = UTC +1h
08.08.01	14.45	84°47,2'N	005°02,5'E			
09.08.01	13.51	84°25,6'N	002°25,1'E	25	7,1	BZ = UTC +1h
09.08.01	20.55	84°04,9'N	000°01,6'E			
10.08.01	12.28	84°09,1'N	000°25,8'E	40	15,2	BZ = UTC +1h
11.08.01	03.40	83°35,6'N	003°20,2'W			
11.08.01	10.45	83°33,9'N	003°32,4'W	24	5,3	BZ = UTC +1h
11.08.01	16.05	83°15,0'N	005°36,8'W			
27.08.01	09.11	85°56,5'N	023°25,1'E	28	10,4	BZ = UTC + 2h
27.08.01	19.36	86°00,7'N	029°57,8'E			
28.08.01	21.58	86°04,1'N	032°11,6'E	22	9,3	BZ = UTC + 3h
29.08.01	07.15	86°20,2'N	038°21,1'E			
29.08.01	22.26	86°22,5'N	038°00,3'E	18	6,6	BZ = UTC + 3h
29.08.01	05.00	86°30,6'N	042°11,9'E			
30.08.01	19.14	86°31,2'N	042°06,9'E	26	10,9	BZ = UTC + 3h
31.08.01	06.09	86°42,7'N	048°49,6'E			
02.09.01	01.37	86°53,6'N	063°22,0'E	19	5,8	BZ = UTC + 4h
02.09.01	07.27	86°42,5'N	068°07,2'E			
03.09.01	15.02	86°15,0'N	072°36,0'E	200	49,8	BZ = UTC + 5h
05.09.01	16.52	89°00,7'N	130°03,3'E			
26.09.01	02.05	85°40,5'N	020°38,1'E	27	6,4	BZ = UTC + 3h
26.09.01	08.31	85°13,1'N	020°45,9'E			
26.09.01	13.35	85°04,9'N	020°40,0'E	10	1,9	BZ = UTC + 3h
26.09.01	15.30	84°55,4'N	020°06,7'E			
28.09.01	03.10	84°25,1'N	028°01,2'E	32	6,9	BZ = UTC + 3h
28.09.01	10.06	83°53,1'N	028°06,8'E			
28.09.01	18.25	83°52,3'N	027°36,6'E	19	4,5	BZ = UTC + 3h
28.09.01	23.00	83°33,2'N	027°20,7'E			
Gesamt:				863	205,9 = 8 d 14 h	

* direct distances between the starting and end coordinates.

1.4 Short Biography of Yakov Gakkel

(According to documentation obtained from the archives of the AARI, St. Petersburg)

Yakov Gakkel (1901-1965) was a prominent Russian polar researcher and a well-known professor in geography. One of his major fields of study was polar geography and he was involved in developing the Russian Arctic and the Northern Sea Route. After he graduated from the Department of Geography of Leningrad University (now St. Petersburg State University) he worked at the State Arctic and Antarctic Research Institute (AARI) for 40 years. He published more than 140 scientific papers, which are noteworthy for general geographic topics and for their thorough analyses. The results presented in these publications were based on his own observations collected during 21 expeditions, incl. 16 to high-latitude Arctic regions. These included his participation in expeditions on the icebreakers SIBIRYAKOV and CHELYUSKIN. The most prominent publications are monographs on "Continental Slope of the Arctic Ocean" and "Science in Developing the Arctic" where he distinguished a circum-polar (Arctic) geographic zonation of the coastal landscapes with respect to meteorology, hydrology, glaciology, zoogeography, etc. 1960 the Geographic Society awarded him the S. Dezhnev Prize for one of his monographs.

Having processed and generalized numerous bathymetric soundings obtained during expeditions to high northern latitudes and from the NORTH POLE drift stations, Yakov Gakkel compiled bathymetric and morphologic maps of the Arctic Ocean distinguished for their well defined geomorphology and interpretation of origin as well as age relationships of the seafloor physiography. He recognized a substantial number of large morphostructures consisting of ridges and isometric rises. Certain structures which were predicted by him on theoretic assumptions, such as Mendeleev Ridge and "Arctic Mid-Ocean Ridge" (now the Gakkel Ridge), were later confirmed and introduced into the maps. Another outstanding geographic event, the discovery of the Lomonosov Ridge, is also related to Yakov Gakkel's name.

Yakov Gakkel is well known for his wide-ranging scientific interests and substantial contributions to a number of science fields: cartography, oceanology, glaciology, Earth's magnetism, astronomy, paleogeography, tectonics, geology, and astronomic geology. As oceanographer, he studied the circulation of the currents over the Chuckchi Plateau and peculiarities of the Arctic Ocean hydrography over the continental slope. He discovered and studied the rotation of the

earlier unknown drift of the ice fields. As geologist and astronomic geologist he developed the tectonic concept of "wave formation" of folds and rupture dislocation, and he studied formation, migration and inversion of geosynclines and deep structures of the Arctic Basin lithosphere.

His wide-ranging and deep insight into nearly all disciplines of the Earth sciences were brilliantly presented in this book "Science in Developing the Arctic", where he considered Arctic energy issues, Arctic paleogeography, deformation processes in the ice cover, the Earth's crust and other media in terms of physical geography and planetology. This book also initiated new developments in cryotectonics, a new branch of glaciology. He published papers related to Antarctica, over themes such as "Lomonosov and Antarctic" or "On Possible Influence of the Earth's Rotation Forces on Arctic and Antarctic Morphostructures", which are widely known as well.

2. Expedition Narrative AMORE-2001

(J. Thiede)

Week 31 (July 31- August 5, 2001)

POLARSTERN completed her expedition ARK XVII/1 on July 29 in Tromsø/ Norway after completing a substantial program of multidisciplinary oceanographic investigations in the Fram Strait and in the western Greenland Sea. She changed crew and scientific participants on July 30 and 31 and was ready to leave the same day in the evening after a press conference and a reception for dignitaries from various institutions and authorities in Tromsø as well as from the 2 ships (PFVS POLARSTERN and USCGC HEALY) which were to conduct the coming AMORE-2001 expedition jointly.

The weather in Tromsø had been rainy and miserable, as it was when POLARSTERN at 20.00 hrs. started to proceed through the wide fjord on its way to the open ocean. USCGC HEALY was berthed at a Norwegian navy base a few kilometres South of Tromsø; she was to cast off lines the same day close to midnight, leaving the fjord through the western approaches directly to the open sea. The two ships therefore navigated separately until they met close to Bear Island from where they travelled jointly up the edge of the Arctic ice pack. Crew and scientists on POLARSTERN woke up the next morning feeling the effects of a storm (with a strength of up to 8-9 Bft. and waves of up to 5 m high) which developed under the influence of a meteorological low just outside the fjord mouth (close to Fugløya). However, that bad weather abated rapidly and we were then able to proceed under rather favourable conditions towards the North. Weather and ice conditions were indeed favourable that we could reach a high latitude (84°33'N) in the ice during this first week of the expedition.

Most of the first days of the expedition were spent in transit to the ice-covered region of the Arctic Ocean to the Northeast of Svalbård. POLARSTERN passed Kvitøya in the west, while HEALY took a short cut around its eastern shores, and we all remembered that on this forbidden island the remains of André and his men had been found after their fateful attempt to use a balloon for polar research in the Arctic. The ice edge was reached on Saturday, August 4 and we were able to start a program of seismic reflection measurements after having conducted the first bathymetric survey already in the eastern Barents Sea. HEALY took the lead and POLARSTERN followed having its seismic gear (seismic array with airguns and 300 m long streamer) launched and trying to

use the channel cut by HEALY through the ice. Coordination of the scientific program between the ships was achieved through frequent radio calls and occasional visits by helicopter. Each of the ships carried two helicopters and flying time was readily available as long as we had suitable weather conditions. In the meantime we also succeeded in establishing radio contact with the Swedish icebreaker ODEN, which conducted oceanographic and meteorological research close to the Northpole, and which, together with POLARSTERN, had reached this magic point on September 7, 1991. This was the first time ever that conventionally powered research vessels had reached the Northpole.

The seismic data of the first week resulted in the resolution of a faintly recognisable basement under a thick and poorly stratified sediment cover in the Nansen Basin. The internal structures of the sediment cover suggest a discontinuous history of deposition, which was obviously very different in the Nansen Basin from that of the Amundsen Basin North of Gakkel Ridge. Beside seismic reflection we collected refraction data while PARASOUND and HYDROSWEEP were run continuously en-route. They will help us to establish a precise correlation to the bathymetry of the Gakkel Ridge established by the US-American SCICEX program. Even though the ice was fragile during these early days of the expedition, when our sea ice group conducted the first thickness measurements from ice flows. The other scientific working groups used these early days to install their lab equipment. Petrologic sampling of crustal rocks of the Gakkel Ridge will receive heavy emphasis during this expedition but can only start when we have reached the Gakkel Ridge itself.

Week 32 (August 5-12, 2001)

Sunday, August 12, HEALY and POLARSTERN had reached the western end of the Gakkel Ridge, located to the North of Lena Trough and Fram Strait. This was the first real working week of the expedition, bringing much success to both ships. The weather was excellent and we enjoyed several days of clear sky with sunshine. A relatively warm air mass covered the bottom near layer of polar cold air, with the consequence that the bottom near inversion produced a high potential for the unpredictable occurrence of local fog patches; on the other hand relatively high temperatures made it easy to work on deck. Ice conditions were highly variable; for long distances the sea ice was loose and easy to transit. We had several exchanges by helicopter with our colleagues (mostly petrologists) from HEALY; the scientific participants of POLARSTERN com-

prised an international group of geophysicists, glaciologists, biologists, petrologists, geodetics, sedimentologists and paleoceanologists with members from Germany, Russia, China, Italy and USA.

The seismic profiles of the geophysics groups required that both ships travel in tandem close behind each other, with HEALY ahead. The acquired data were of extraordinary quality, resolving the structure and morphology of the Gakkel Ridge, its rift valley and flanks. Early during this week we completed a seismic transect through the entire Nansen Basin; while its present seafloor is flat like in an abyssal plain, the seismic data revealed that the sediments have covered basement elevations up to 2000 m high during the past 50 mill. years. Since reaching the Gakkel Ridge we have conducted deep seismic experiments to determine crustal thicknesses. The two helicopters of POLARSTERN permitted to establish REFTEK-stations on the ice at various locations to conduct seismic refraction experiments for many hours. In addition seismic stations were placed on a big ice flow to collect data on seismicity and a magnetic station was placed on the ice. The heat flow of the rift valley inner regions was determined by means of a gravity corer or a metal spear outfitted with several thermistors at various depths below the sea floor.

Sea ice investigations concentrated on the question: Does the ice around the Northpole decrease (instigated by the year 2000 news that there was a hole in the ice at the Northpole)? For the AWI, however, such studies are by no means new, but our sea ice group has acquired a long time series, gaining new data for an additional year. The most important parameter to be measured was sea ice thickness. Two biologists investigated at the same time occurrences of fauna and flora within the sea ice; they measured temperature, salinity and chlorophyll concentrations along profiles through the sea ice, and they collected the sympagic meiofauna in the ice. Typical elements of these faunas were copepods and several worm-like taxa. Sea ice sampling is particularly cumbersome during the summer because of the special environmental conditions. The most difficult task was the crossing of small (melt-) lakes, which covered 20-30 % of the ice surface. The EM-probe was therefore stowed into a kayak, which was then pulled for kilometres over the ice. Melt water lakes had to be crossed under the constant danger of breaking through the fragile lake bottom, into the sea below. Fog sometimes impeded the trips to the ice flows as well as the polar bear watches.

Sampling and petrologic characterisation of the rocks of the oceanic crust of the Gakkel Ridge received particular attention during this expedition. The Gakkel Ridge is an active mid-ocean ridge, but it spreads slower than any other segment of the circumglobal mid-ocean system. The sampling program of this week was extremely successful, because we collected more than 800 kg rock from 6 TV-grabs and 5 dredges. They comprised various basalts, peridotites, gabbros and breccias. In addition it was possible to use the NOAA MAPR's to determine the hydrographic properties of the water column for locating escape regions of hydrothermal fluids in the rift valley. Hundreds of rock samples were cleaned, numbered, photographed, cut and curated; several thin sections provided excellent material for petrographic descriptions. They will reveal the secrets of the Gakkel Ridge origin.

The times when the Arctic Ocean represented the loneliest sea of the world are long gone by now. A Russian nuclear icebreaker carrying tourists from the Northpole to Svalbard passed us behind the horizon and we had daily radio contacts to the ODEN on station for oceanographic and meteorological measurements very close to the Northpole.

Week 33 (August 12-19, 2001)

Early during this week HEALY and POLARSTERN investigated the complicated western end of the Gakkel Ridge and its transition into the Lena Trough, where plate tectonics have not yet been resolved convincingly. Since then both ships returned to easterly courses to investigate the rift valley, HEALY emphasizing the northern, POLARSTERN the southern shoulder of the valley. Sunday, August 19, both ships had reached 84°40'N 4°25'E, after a week of almost continuously poor weather. Frequent snowfall, fog, the danger of icing and sometimes icy rain limited possibilities of using the helicopters. This weather mode was caused by the repeated formation of meteorological lows over the Barents Sea which resulted in the influx of humid and relatively warm air masses from northern Russia in the lower troposphere.

Because of the bad weather conditions the sea ice group could not be transferred to the ice by helicopter, but in most instances it had to climb into the "mummy"-chair using the crane on the bow of the ship for transfer to the ice. At the westernmost point of this expedition close to Greenland we encountered highly variable ice consisting of a mixture of old and young floes. Many floes

carried high-pressure ridges and in many instances also large amounts of sediments whose composition will allow pinpointing the source area of the ice. Large sediment accumulations on sea ice are an indication of old ice floes. In the mean time all melt water ponds had been covered by recent snowfalls and the snow cover was stable enough to carry a person. The SIMS (Sea Ice Monitoring System) installed in front of the ship's bow had been taken into use. It was to continuously measure ice thicknesses along the ship's track.

The petrologists deployed the TV grab at 7 dredges at 9 locations. From 15 stations they acquired valuable rock samples in sufficient quantity. In addition 2 sediment cores also contained volcanic glass and the MAPR-systems had been deployed at several stations so that we then had hydrographic sections from a total of 6 positions. In total during this week we have collected more than 2 t of rock which had to be cleaned, numbered, described and stored. 20 out of 75 thin sections have also been described. The western segment of Gakkel Ridge produced mainly basalt samples and virtually no peridotite, in stark contrast to the segment following in the East. Proof of hydrothermal activity was found in the fragments of iron sulphide "smokers" dredged by our colleagues on HEALY. The hydrographic profiles had already suggested areas of hydrothermal activity, but it remained impossible to locate them precisely. The success rate of the petrologic sampling activities was far beyond expectations.

Heat flow measurements at 3 locations resulted in relatively high values, as expected from an active volcanic ridge. At the same time we collected sediment cores of up to 660 cm in length. The deposits comprised fine-grained clayey-silty muds, which accumulated under the influence of deep-sea currents. The relatively thick interglacial intervals will later allow detailed investigations of the water mass exchange between the deep Arctic Ocean with other basins of the World Ocean. The scarcity of coarse terrigenous ice-rafted debris in these cores was particularly noteworthy.

The marine geophysics groups deployed seismometers at 4 stations on the ice. They have been able to discern large earthquakes under the Japanese islands (Hokkaido, magn. 6,3) from numerous small "ice quakes" generated by ice flow collisions. Attempts to deploy magnetotelluric probes on the ice were promising; they were aimed at measuring the conductivity of rocks from crust and mantle. The continuation of the HELI-MAG-flying program was hindered by bad weather. Towards the end of the week the intensive studies of structure and petrology of the Gakkel Ridge were continued in an easterly direction, where a

principally different morphology already suggested a different tectonic style of the ridge.

Week 34 (August 19-26, 2001)

On Sunday, August 26 POLARSTERN's position was at 85°47'N 20°15'E. The course of both ships followed in general easterly directions after they had reached the south-western end (in approx. 250 km distance from Greenland) of Gakkel Ridge last week. The weather of this week was under the influence of a meteorological high between Svalbard and the Kara Sea which led to an influx of relatively warm air into the area of the expedition where it cooled over the ice, producing freezing fog of various intensities. Therefore the HELI-MAG-program was curtailed, but it was still possible to deploy a magnetotelluric station and a seismic array on the ice for 4 days.

The polar ecology working group drilled several ice cores from the sea ice. On-board POLARSTERN these samples were allowed to melt in the dark at 4°C. The chlorophyll contents allowed conclusions about the amount of algae in the ice, which showed maximum occurrences in the lowermost part of the ice cores. The sea ice (physicists) group was still trying to determine sea ice thickness along profiles over distances of 1-2 km every day. Several true icebergs were sighted; they came in all probability from the shores of the Laptev Sea and could harbour also important information about the source region of the surrounding sea ice. One of these icebergs was broken into 2 pieces, each of them approx. 100 m in length, which were tipped on the side revealing an internal stratification. It carried sediments and rocks consisting of greywackes and slates, typical for northern Siberia. Similar lithologies have also been found in a deep-water dredge nearby.

The detailed bathymetry of the Gakkel Ridge provided the basic data for planning sampling sites. The topography of the seafloor was determined continuously by means of the multibeam HYDROSWEET System on POLARSTERN while a SEASBEAM-System has been installed on HEALY. The combined data sets from both ships cover the entire crestal area of the Gakkel Ridge and we expected to be able to present a complete and detailed map of the entire segment of the Gakkel Ridge, which has been visited during the AMORE 2001 expedition. A sediment core has been collected from 5330 m water depth, at the same time a heat flow measurement has been performed, both at greater depth

than ever before anywhere in the Arctic Ocean. The sediments are very fine-grained and the heat flow was established at 500 mW/m².

The petrologists continued their successful efforts sampling for basement rocks at an additional 19 locations, collecting > 1 t materials. Onboard thin section microscopy demonstrated that the frequency of diopsid in the peridotites of the Gakkel Ridge was higher than in similar samples from other active spreading ridges because of reduced melting rates of mantle materials. This result offers an answer to the most important petrologic question of the AMORE 2001 expedition and provides a substantial base for planning future geochemical investigations (for example Osmium isotopy).

One of the highlights of this week was encountering the Swedish icebreaker ODEN that was on her return trip from an expedition to the Northpole (Fig. 4). ODEN and POLARSTERN had visited the Northpole already on September 7, 1991 as the first conventionally driven ships to reach this location. The meeting of the 3 research icebreakers HEALY, ODEN and POLARSTERN marked a new era of peaceful, systematic research in the Arctic. Our sea ice group selected a suitable ice flow to dock the 3 ships simultaneously. Beside the scientific exchange (and the transfer of a limited amount of fuel from ODEN to POLARSTERN and samples between HEALY and POLARSTERN) we used the occasion to celebrate, by offering games on the ice, several hours "open ship" on all three vessels, with the possibility of buying stamps and souvenirs, and a grand barbecue in the hangar of HEALY. The certified DFB-referee (Mr. H. Erdmann) declared 1,4 m ice thickness sufficient for a set of formal football games (every ship against every other) which the POLARSTERN team succeeded in winning (price 1 bottle of "Rotkäppchen"-Sekt). Fate was just and we lost rope towing against the ODEN. The international atmosphere with citizens of 17 nations present bore a promise for the continuation of this type of peaceful polar research in the future.



Fig. 4: ODEN in the foreground, POLARSTERN behind and HEALY at a distance in the mist, on August 23, 2001.

Week 35 (August 26- September 2, 2001)

Sunday, September 2 POLARSTERN had reached 86°40'N 68° 40'E, after continuing its scientific program together with HEALY along easterly courses. Fog and weak winds dominated the weather; henceforth visibility was bad and we saw the sun only Tuesday morning for a few hours.

The scientific program of this week comprised a transit with geophysics; this and the deteriorating ice conditions resulted also in fewer samples for the petrologists. Despite these obstacles they have been able to conduct 12 successful sampling stations (7 TV grabs and 5 dredges). The peculiar lithologies of the rocks from the Gakkel Ridge contributed to the motivation of our petrology groups. The research area of the AMORE expedition comprised the segment of the global mid-ocean ridge system with the lowest spreading rates as compared to all other regions world-wide (approx. 5-13 mm/a). The degree of melting of peridotites from where basaltic magmas are produced, is therefore very low. Such low-grade partial melts are a product of the melting process under each volcano, but their chemical signatures, like on Hawaii or the Aetna, are later blurred by additional melting. The peridotites collected from the Gakkel Ridge were of exceptional quality. They will allow analyses, which have never been applied to this type of rock because seafloor peridotites are usually heavily weathered. In the AMORE area the peridotites and the resulting basalts have been sampled in large quantities; thus this expedition has been an astounding success for the petrologic working groups.

PARASOUND-measurements to decipher the high-resolution stratigraphy of the upper sediment layers have been carried out along the entire cruise track around the clock. Sediment rich localities have been detected in the axial valley, despite its irregular topography, which degrades the data quality. Such localities are of particular interest for the selection of sampling points for gravity cores (=heat flow measurements) and box cores.

Early during this week we carried out seismic refraction work between dredge stations, which provided sufficient distance. Decreasing fog frequencies also allowed for the deployment and recovery of seismic stations from the ice. The quality of the recovered data was adequate for solving the geophysical questions to be addressed by these stations. Deplorably the weather had not improved sufficiently to allow for enough HELI-MAG-flights, whose number is far behind expectations. We did not deploy long-term seismologic and magnetotel-

luric stations because of the relatively fast easterly progress of both ships along Gakkel Ridge.

The sea ice group continued its work with daily stations on large ice flows. After an interruption of 3 weeks it measured height and frequencies of ice pressure ridges by means of a laser altimeter from the helicopter. After some technical problems it was also possible to conduct the first flight for the electromagnetic ice thickness probe (HEM-Bird). This probe is towed on a 20 m long cable under the helicopter approx. 10-20 m above the ice; this manoeuvre is a particular challenge for the helicopter pilots. The first data promised to be able to replace the time-consuming ice thickness measurements of a ground party by deploying the bird more frequently.

All working groups looked toward the future when we hoped to reach a zone of active volcanism in the rift valley of Gakkel Ridge.

Week 36 (September 2-9, 2001)

The program of this week did not develop according to our expectations at the end of the preceding week. A geophysical transect from Gakkel to Lomonosov Ridge which had been planned for much later during the expedition was executed due to the favourable ice conditions along its route, as predicted from satellite pictures made available on HEALY. We therefore crossed the Amundsen Basin following HEALY and towing a streamer/ airgun array to the foot of the Lomonosov Ridge. From there we proceeded to the North and together with our partner reached the North Pole on Thursday, September 6. Late in the evening of the same day we departed again and began to make way towards our sampling area on Gakkel Ridge. Early during this week we finally saw some sun again; under the influence of meteorological high light north-easterly winds transported relatively dry air into the study area. However, from the middle of the week winds changed to a south-westerly direction resulting in occasional fog patches. During the time at the North Pole we experienced snowfall.

The geophysics working group started another long-term experiment with the deployment of seismological and magnetotelluric stations on the sea ice over the Gakkel Ridge at approx. 85°E. This was very close to locations where in 1999 earth quake swarms had been detected, suggesting the occurrence of ongoing volcanic eruptions in the central rift valley of the Gakkel Ridge. Hopefully, measurements of the electric susceptibility will resolve the distribution of

various rock types. The main task of this group for this week was to establish a 200 N.M. long seismic reflection profile from the Gakkel to the Lomonosov Ridge; it will help to resolve the opening and history of the Eurasian Basin and of the magmatic-tectonic evolution of the Gakkel Ridge.

The petrologists used the time span of these geophysical investigations to sort the samples received from HEALY. Many of the investigated volcanites were covered by a rim of rock glass, which evolves when the hot lava gets in contact with the cold seawater. Glass was separated from any samples and numerous thin sections have been produced.

The morphology of the Gakkel Ridge has been illustrated in the meantime in a detailed map of 4,5 m length, which allows seeing details in unprecedented detail. Besides processing of the depth measurements we collected several CTD measurements, which provided information on temperature, salinity and pressure in the water column. Also the CTD profile on the North Pole was devoted to checking the automatic calibration of the HYDROSWEEP multiswath system.

With the beginning of the Arctic fall the "landscape" had changed into a homogenous white. The albedo measurements of the sea ice working group over the melt water ponds were near their end, because the melt water ponds were hardly recognizable any more. During summer time these ponds are relatively dark absorbing most of the insolation and thus contributing considerably to the melting of the ice. The deteriorating ice conditions also gave some more importance to the recovery and processing of satellite imagery. The presently available satellite images indicated that substantial regions of open waters were only found much further to the South. The working group on polar ecology continued their regular sampling program on the ice as well as experiments on the feeding behaviour of worms in the ice (Rotatoria). The study, using bacteria or bacteria-like particles, was aiming at a better understanding of the food web in the ice.

In the afternoon of September 6 we reached 90°N (Fig. 5), the "northern end" of this Earth. POLARSTERN's cook conducted a wonderful barbecue on the working deck and a pole-position-party was organised afterwards. POLARSTERN reached the Northpole for a second time, exactly 10 years after ODEN and POLARSTERN reached the Northpole as the first conventionally driven icebreakers. News about this event and many greetings went out despite our limited communication means.

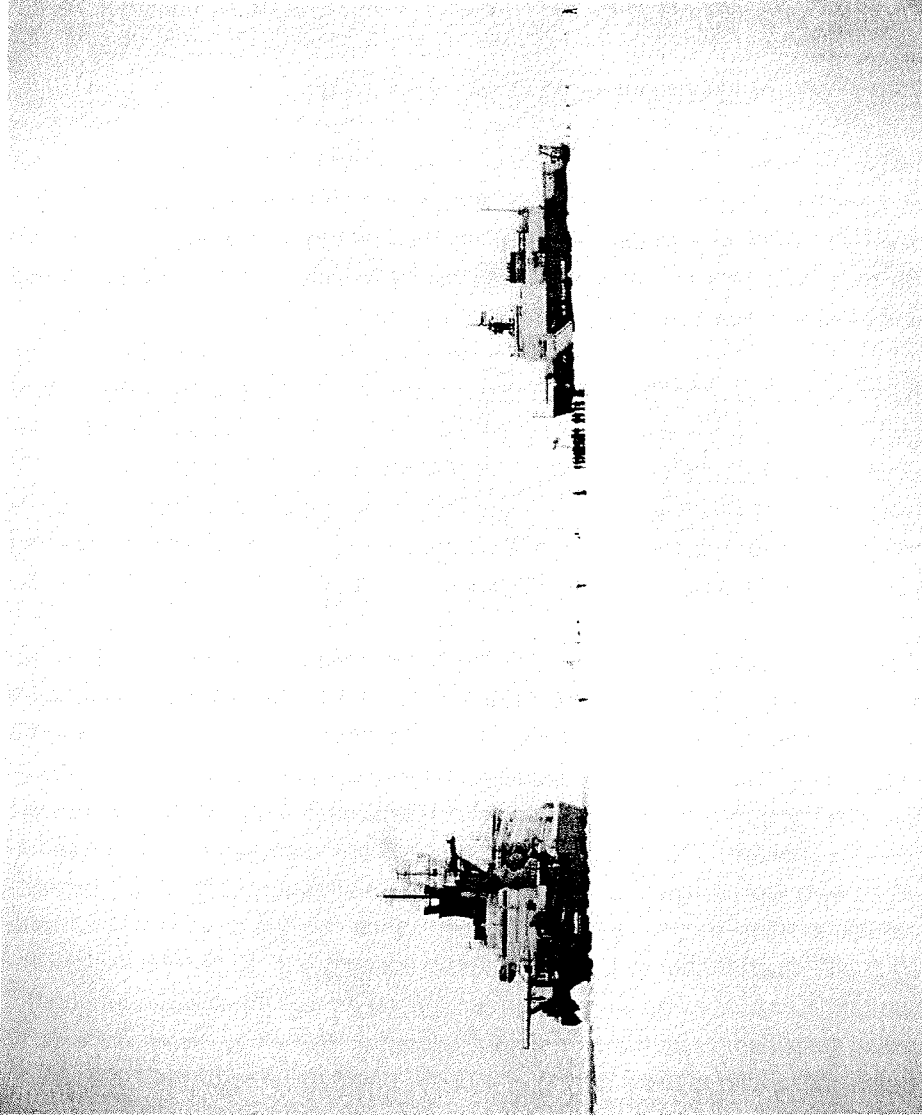


Fig. 5: POLARSTERN (left) and HEALY at the Northpole on September 6, 2001.

Week 37 (September 9-16, 2001)

With another 3 weeks of the expedition to go, this Sunday, September 16, found us over the Gakkel Ridge at 86°54'N and 058°29'E. The weather of the week was highly variable. Until mid-week it was controlled by an influx of mild air masses from the Southwest with frequent fog formation. On Wednesday a meteorologic low resulted on the influx of cold air and the weather station reported the coldest temperatures of the entire expedition up to now, -11,7° with wind chill of -30°C. The poor weather conditions caused reductions in the scientific activities of all working groups.

The petrologists resumed their dredging program after we reached the Gakkel Ridge again; they recovered mostly basalt or sediments, however. They also used this week to promote the exchange of scientists with the HEALY and they established a plan of sample locations to be visited during the remaining time span of the expedition. Combining the bathymetric and lithologic discoveries made it possible to sketch some of the main results of the expedition. The Gakkel Ridge can be subdivided into 4 major morphotectonic segments, which differ in their morphologic trades as well as in the distribution of rock types. Peridotites are found in deep valleys and along steep slopes. Volcanites have been recovered from shallow valleys and step-like slopes; the active magmatic regions consist of thousands of small volcanic edifices.

The geophysics working groups had one of their major successes when they recovered the seismological array and the magnetotelluric station over a distance of 130 km, after these had been deployed approx. 2 weeks ago at 85°E over the Gakkel Ridge. The data logger demonstrated that the instruments had been functioning over the entire period, with an excellent data quality. Towards the end of the week we were also able to continue the HELI-MAG-flights across the axis of the Gakkel Ridge.

The return trip from the North Pole to the Gakkel Ridge was also used to conduct a series of heat flow measurements. As expected the heat flow rises with the decreasing age of the ocean crust and the values tripled from the cold and old central Amundsen Basin towards the hot and central Gakkel Ridge. At the same time the paleoceanology working group was able to collect a number of sediment cores. Ice rafted debris found in glacial deposits of these cores proved that the Siberian ice sheets produced large numbers of icebergs during older glacial ages, when these icebergs floated from the border of the ice sheet into

the open Arctic Ocean and when their melt water influenced ocean circulation and climate.

The sea ice physicists deployed three buoys on the drifting sea ice at the eastern end of the investigated area to collect data on air pressure and temperature as well as on the drift of the ice for the next 3 years. This is part of the AWI contribution to the International Arctic Buoy Program, which maintains a network of approx. 20 continuously measuring buoys.

Tuesday evening news reached us about the terrible terrorist attacks in the USA. They caused horror and grief onboard both ships. Crew and scientists from POLARSTERN passed a resolution to express their anger and their sympathy with our American partners on HEALY and with the entire American people. At this time we were contributing to the peaceful exploration of the Arctic together with our American partner ship HEALY and deeply deplored these horrible cruel terrorist attacks on innocent civilians.

RV POLARSTERN

Captain Jürgen Keil

Chief Scientist Prof. Jörn Thiede

Message to

Captain David Visneski, Commanding Officer

Chief Scientist Prof. Peter Michael

USCGC HEALY

Resolution of Crew and Scientists on RV POLARSTERN:

On this September 11, 2001 crew and scientists of RV POLARSTERN have learned of the horrible terrorist attacks in your home country.

We are all terribly shocked and we wish to convey our condolences to you as well as to the entire American people.

We deeply regret these incidents and out of our hearts we hope that peace may return to your country as soon as possible.

Being engaged in the peaceful exploration of the Arctic together with our partner USCGC HEALY we deeply condemn these terrible acts of terrorism.

Week 38 (September 16-23, 2001)

On Sunday, September 23 POLARSTERN was on position 85°50'N 21°10'E proceeding further E along the axis of the Gakkel Ridge. We expected also to reach the easternmost sampling location from where while sampling en-route we would leave for the meeting point with HEALY. The probably shallowest point of the deep Arctic Ocean was reached at 86°42'N 60°45'E; the large seamount was mapped and its shallowest top was found at 566 m water depth (contrary to approx. 800 m marked on available maps). This depth was also confirmed by HEALY. We were discussing to propose a name for this feature (eventually Karasik Seamount); this proposal will have to await formal procedures.

The weather of this week was unstable and variable. While providing for clear skies and some sunshine early in the week large cloud fields, fog banks and snowfall developed during the later part. We also experienced the sun going below the horizon for the first time for a few minutes; in the meantime the sun was gone for many hours, we were experiencing dark nights and the ship had to proceed while using its powerful ice search lights. Temperature fluctuations between -3° to -13°C corresponded to the expected seasonal averages. The favourable weather windows were also used to continue the exchange of scientific personal between HEALY and POLARSTERN; local "icing conditions" close to HEALY suddenly forced the senior scientists from HEALY to stay on POLARSTERN for the night from Saturday to Sunday.

The weather allowed the continuation of our experiments on ice flows. This included the collection of snow samples for studying atmospheric transfer mechanisms of materials to the Arctic. The concentrations of suspended materials in the surface waters was determined by means of the Secchi-disc; this is white, has a diameter of 30 cm and is lowered into the water until it is not visible anymore. This is so-called Secchi-depth and reflects the amount of suspended material in the water column. We measured Secchi-depths between 18 and 28 m; last week very clear water was crossed with Secchi-depths of 30 m.

The petrologists hunting for peridotites experienced a relatively frustrating week. Theoretically this type of mantle rocks should occur frequently in this segment

of Gakkel Ridge but they were not found except at the end of the week when we reached 33°E, to the chagrin of the petrologists. After collecting an empty pipe dredge we repeated the station and used the giant chain dredge, this time with astounding success. The large dredge ("the white shark") recovered over 1000 kg of peridotites and associated lithologies. We hoped for similar successes for the remainder of the expedition; Sunday morning we recovered a 1 m in diameter large pillow of basalt with its glassy rim entirely intact.

For the geophysicists this week was rather quiet. They evaluated the collected data, and were able to put in some flights for the HELI-MAG-program to map the axial magnetic anomalies of the Gakkel Ridge. Also the program of heat flow measurements was continued, but had sometimes problems because of the lack of a sediment cover on the young volcanics in the centre of the rift valley. Towards the end of the week a new magnetotelluric station was deployed on the ice close to 25°E over the central Gakkel Ridge.

Weeks 39 and 40 (September 23-October 7, 2001)

During the middle of the week POLARSTERN and HEALY left the Gakkel Ridge in convoy to do geophysics whenever the ice would permit. At the end of week 39 we had taken our course towards Bergen/ Norway. On Saturday the geophysics working groups terminated their scientific measurements close to the continental slope north of Svalbard. On Sunday, September 30 POLARSTERN passed Bear Island at a distance of approx. 3 N.M., enjoying quiet weather, fast sailing and a magnificent view of the island's eastern shores.

The beginning of week 39 was sunny and cold, but we were caught by a real Arctic storm with force 9, a meteorological low with a lot of snowdrift and low freezing temperatures. Pressure on the ice and zero visibility due to the storm brought both ships to a halt for approx. 12 hours. Since the middle of the week the weather improved again and after reaching the ice margin zone we enjoyed a mix of clouds, snow showers and sunny intervals with generally relatively mild temperatures with modest north-easterly winds. After leaving the ice we were met by quiet weather and waters which helped with the progress of the voyage and with the stowing activities onboard. Since Sunday, September 30, both water and air temperatures were above zero.

The sea ice physicists used the last week in the Arctic Ocean to measure the decreasing ice thickness when approaching the ice edge. It is here where rela-

tively warm Atlantic waters meet the ice with the consequence that ice thickness rapidly decreases. Average ice thickness at the Gakkel Ridge was about 2 m, but at 84°N only 80 cm. South of 85°N we observed again dirty ice due to sediment inclusions, which meant source regions for the ice different from those on the Gakkel Ridge, where virtually no sediment inclusions have been observed. The sediment inclusions can usually be traced back to specific regions of ice formation over the Siberian shelf.

The petrologists were delighted about the conclusion of a highly successful sampling program. The last station was run on Tuesday, and the totals of the expedition were 64 dredges and 40 TV-grabs. The summed weight of all rock samples is approx. 11 t, but it is not the weight, but rather the diversity of rocks which counts towards an understanding of the evolution of the Gakkel Ridge. All major tectonic features of the region investigated during this expedition have been sampled at least once. The rocks collected during this expedition cover a majority of these aspects of the geology and petrology of the entire ridge and can be considered a treasure, which will have to be exploited by generations of geoscientists.

Early during this week when good flight conditions persisted, we deployed another magnetotelluric/seismological station on an ice flow. The deployment lasted for four days and we successfully recovered the station without any problems. After solving some minor technical difficulties last week we were able to conclude successfully our program of HELI-MAG-flights. The continuation of the seismic reflection survey met some problems because the ice situation had deteriorated early in the week, also under the influence of the major storm mentioned above, so that the seismic profile had to be moved further to west than originally planned. Hence we came very close to positions where we had entered the Nansen Basin in early August at the beginning of this expedition. It was only South of 83°30'N and after crossing very heavy ice that HEALY and POLARSTERN were able to approach the planned profile and to recover a 250 km long seismic reflection line up to the continental slope N off Svalbård.

After more than 7 weeks of joint work and after a highly successful AMORE-2001 expedition the members of the teams of both ships parted from each other. For a last time HEALY and POLARSTERN docked at a large ice flow when suddenly a mother polar bear with 2 cubs appeared off the bow of the HEALY on the same flow. HEALY successfully engaged its typhoon and the animals moved off, but their known presence lead to high alert and vigilance of

the polar bear watch. HEALY invited the POLARSTERN scientists and crew for lunch with hamburgers and other goodies in their hangar, the senior scientists conducted a lengthy and complicated last meeting, and some beer and punch on the deck of POLARSTERN enlightened the mood of all members of the AMORE-2001 expedition. After departing we operated again in convoy for some hours while conducting a seismic survey. We had contact with HEALY the last time next morning, after the convoy operations had been stopped due to loose ice, which allowed us to continue by ourselves. HEALY then turned slowly to starboard because she wanted to remain in the calm waters of the ice for some more time to conclude measurements on vibration sensitive instrumentation and to prepare for her return voyage, which brought her on October 2, 2001 to Tromsø again, but this time observing the strictest precautionary safety measurements for the protection of the ship, its crew and scientists. She was going to leave Tromsø again after a few days port call with another scientific assignment in Svalbard waters.

The scientific program of the AMORE-2001 expedition and of the scientific team on POLARSTERN was concluded after entering the shallow waters of the Barents Sea. The remainder of the return trip to Bremerhaven (Oct. 7 early in the morning) was used to evaluate the collected samples and data as well as to draft the cruise report. Large volumes of samples and equipment had to be readied for unloading and shipment. The return trip was also interrupted for 2 days in the fjords off Bergen and Stavanger/ Norway because the acoustic properties of POLARSTERN and her seismic systems had to be determined, both through active signals as well as through passive listening; the collected measurements will help to evaluate the potential influence of POLARSTERN's research activities in the Southern Ocean on the social behaviour of marine mammals.

On Saturday evening scientists and crew assembled for a final grill party on deck. On Sunday, September 30, we invited also all of them for a final and more formal reception into POLARSTERN's Blue Saloon where words of thanks were exchanged, where the guest book was signed, where the North Pole certificates were distributed and where a poem was read for the first time by the poet himself who had also transcribed it into the guest book. All members of the Science party on POLARSTERN thanked the entire crew under Capt. Keil, the helicopter- and weather teams for a never-tiring co-operation and for their help with finding solutions of many small and sometimes larger problems.

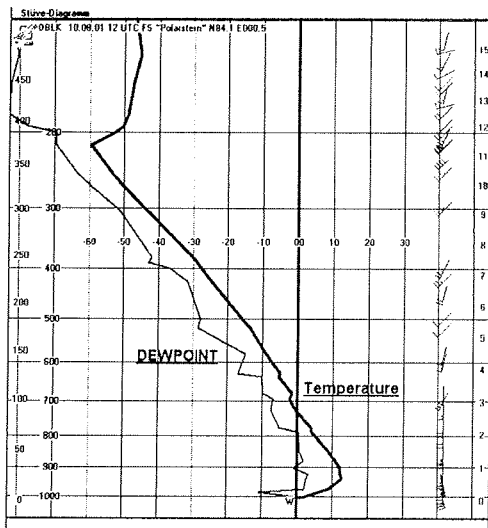
3. Meteorological Conditions

(H. Erdmann)

After leaving Tromsø on July 31st. 2001, a gale centre with minimum pressure below 980 hPa north of Nordkapp caused north-westerly gales force Bft. 8 to 9 with severe storm gusts. The characteristic wave height was about 6 m. Heavy rolling and pitching was noticed on board POLARSTERN. Further on the wind turned northwest to north while decreasing slowly. On August 3rd, the anticyclonic influence became dominant with only light northerly winds and mostly sunny periods. The temperature decreased slowly. After passing 80°N the wind turned from south to north, with moderate speed due to a low, which passed south of vessel's position. Due to incoming cold air from the sea-ice region the temperature dropped below 0°C for the first time during this cruise. Also the first freezing fog patches were noticed, but without any negative influence to helicopter operations. POLARSTERN and HEALY approached the Gakkel Ridge without any time lost due to the light to moderate sea-ice conditions.

On August 5th a large anticyclone developed over the eastern part of Greenland and moved northeast towards Svalbard. Strong warm air advection was noticed by the analysis of POLARSTERN's radiosonde. As a result the air temperature increased up to plus 7°C early on the 6th of August in the lower levels of the troposphere near 1000 m above ground. Fog patches with changing intensity were noticed near the ship. Most helicopter operations had to be cancelled due to bad visibility conditions. The anticyclonic influence of more than 1025 hPa over Svalbard and the Barents Sea remained stable during the next 2 days. The wind thus remained southerly with moderate speed and the fog became more frequent. Due to increasing south-easterly winds at the eastern edge of a small low slightly northeast of Greenland, the weather conditions changed rapidly on the 09. Aug.: the fog dissolved and sunny weather was noticed throughout the day with excellent visibility.

Later warm air advection continued and the zero degree- level was measured by radiosonde on the 10. Aug. at 3000 m. The maximum positive temperature (13.4°C) was noticed near 800 m above ground (see also Fig. 6).



Due to the large amount of moisture and the small spread between dew point and dry bulb temperature, within all layers of the troposphere, strong fog was noticed in the operation area. Additionally, the cooling of the air mass over cold water (-1.8°C) and sea-ice promoted the development of fog.

Figure 6: Analysis of radiosonde POLARSTERN, 10.08.2001, 12 UTC.

On the 11th of August, a small low passed the POLARSTERN's position near 83°N 06°W from south to north. It thus started to rain for several hours at the front of this low. The next low, causing snowfall for nearly 2 days, was noticed in the operation area on the 13. Aug.. All helicopter flights had to be cancelled because of heavy whiteout conditions.

Strong cyclonic activity took place after mid August over the Barents Sea. The minimum pressure was 985 hPa on the 17th of August. Therefore the wind increased up to 11 m/s (Bft. 5 to 6) with some gusts Bft. 7 from northwest. The wind-chill-temperature dropped below minus 20°C.

Increasing cold air advection at all tropospheric layers at the rear of this low was noticed on 18. August, while the cyclonic centre started to disappear near Franz-Joseph-Land. Wind decreased and the dry bulb temperature dropped below minus 5°C for some hours. Further on, the surface pressure increased between central Scandinavia and Svalbard producing an anticyclone with centre near Svalbard on the 20th of August. The expedition area was influenced by warm air advection and also a sinking of the air mass due to the anticyclonic effect, which produced a strong temperature inversion near sea level. Consequently the wind at POLARSTERN was moderate south-westerly. The high rate of moisture coming out of the sea-surface and sea-ice advanced the development of freezing shallow fog. By the way, the air temperature at POLAR-

STERN's deck (abt. 20 m above sea level) was positive, but directly over ice was still negative. This dominant anticyclone kept position for several days, while the research vessels operated northwest of this high. Consequently the weather situation did not change for a few days: mostly foggy and only occasionally the sun could be seen shining through the thin bottom layer of the fog. The top of fog was noticed between 50 m and about 400 m.

On the 25th of August the wind turned right for some hours, bringing up more dry air from ice-covered areas. Therefore the weather became clear for more than 24 hours. Most scientific flight activities were successfully concluded. Subsequently the wind shifted towards southwest to south again, increasing up to Bft. 6 and the visibility became poor. Increasing pressure over the northern part of Greenland took place on the 29th of August, forming a new anticyclone, which moved northeast slowly. Additionally, an upper-level vortex over the northern part of the Beaufort Sea moved west, approaching the operation area near 86° N 40° E. The air became unstable above 850 hPa-level and the fog disappeared rapidly. Also the surface temperature dropped to near minus 5°C.



September began with fog, snow, rain and snow again, caused by a small trough belonging to a strong low opposite the North Pole, which moved towards the Laptev Sea. The trough passed POLARSTERN from west to east with a small belt of moist and warm air. At the rear, cold air advection was responsible for heavy snowfall combined with gusty northerly winds and decreasing temperatures. The low became dominant for most parts of the polar region (Fig. 7) for some time.

Figure 7: Satellite picture (vis) from 01.09.2001.

Due to the corresponding cold anticyclone, which entered the operation area near 86° N 60 °E in 02.Sept., the wind became light and variable and the flight conditions remained good for a further 2 days.

A new anticyclone developed at 05.09. over the Beaufort Sea moved towards 85N 170E within 24 hours. Therefore the wind turned southeast to south at the surface again with the beginning of warm air advection between 1 and 3 km above ground. POLARSTERN, which moved towards the North Pole, was influenced by incoming strong cloud fields with low-layered stratus and some fog patches.

One day later both vessels had a meeting directly at the North Pole. The increasing pressure gradient between the previously mentioned high and a small low north of Greenland caused southerly wind force Bft. 4 to 5. Some snowfall, even freezing rain in places, was noticed but there was no sunshine all through the day. By the reason of stronger wind, the wind-chill- temperature dropped near minus 14°C, while the dry bulb temperature increased from minus 6°C to minus 2°C. The historical launch of radiosonde from the North Pole in 06.09.2001, 12 UTC showed only small spread between dew point-temperature and dry bulb temperature, indicating several stocks of cloud fields over the Pole (Fig. 8).

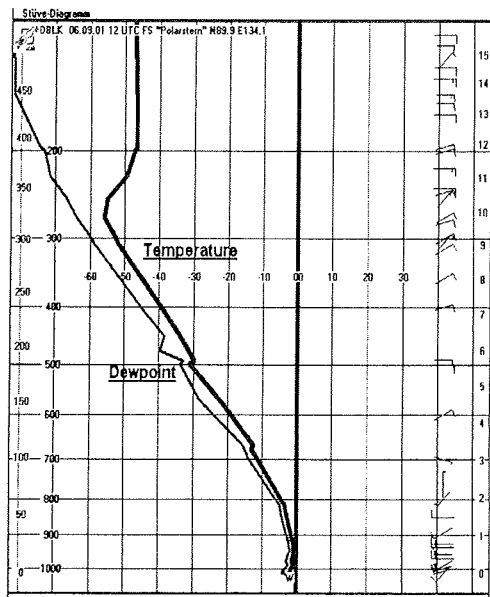


Figure 8: Analysis of the historical radiosonde by the German Marine Weather Service on board POLARSTERN in 06.09.2001, 12 UTC.

The anticyclone was recreated on 07.09. over the North Pole area, when POLARSTERN proceeded towards a position near 87° N 75° E at the Gakkel Ridge again. During the vessels transit the axis of the anticyclone passed from east to west and the wind turned from southwest to northwest with light to moderate force. Consequently the fog disappeared and cloudy conditions with sunny periods and excellent visibility occurred in the operation area on 08. Sept. One day later moist air approached the operation area, again causing dense fog. Further on, the anticyclone intensified more than 1030 hPa while moving south and passing the Barents Sea on September 10th. In the meantime a small low formed over north-eastern part of Greenland, which moved north towards the North Pole area in September 11th. The warm air advection increased at the operation area and entailed the production of dense fog. Due to temperatures remaining below 0°C, white frost was noticed throughout the day.

The general synoptic situation changed on September, 11th: the anticyclonic influence over the Barents Sea decreased, while cyclonic activity started north of Greenland and over the Fram Strait. Therefore the pressure gradient became stronger in the operation area near 86° N 075° E and POLARSTERN noticed south-westerly winds up to Bft. 6 with fog and snowfall. On late September 12th, the low started moving from the northern part of the Fram Strait towards our operation area while deepening below 990 hPa. Therefore the wind turned south increasing up to Bft. 6 to 7 with incoming strong freezing rain. Falling pressure was noticed on board with a rate more than 5 hPa within 3 hours. Next day the low passed a little north of our position with minimum pressure below 990 hPa. Incoming cold air advection was noticed by POLARSTERN's radiosonde analysis. The wind turned northwest Bft. 6 with increasing gusts for a time and the fog disappeared abruptly. In the evening of September 13th, the weather became fair, while the air temperature dropped below minus 9°C. The absolute minimum temperature during this cruise, minus 11.7°C, was noticed at POLARSTERN on early September 14th. The day remained sunny and very cold.

The synoptic situation changed on September 16th again, when the warm front of a low near Svalbard approached our area. As a consequence of strong warm air advection, the dry bulb temperature ascended above freezing point near 1000 m level and the snowfall changed into freezing rain. Further on the low passed south of the operation area (~87° N 055° E) while dissipating. The intermediate strong easterly wind therefore decreased while shifting north. The

following cold anticyclone caused decreasing north-westerly winds on September 17th and also fair weather, the temperature dropping below minus 10°C.

The first sunset of the incoming Arctic winter season was observed on POLARSTERN on September 17th near 86.40° N 47.20° E. A strong low developed at Svalbard, including warm air of subtropical origin from ex-hurricane ERIN. Widespread belts of Altostratus and Cirrostratus covered the sky on September 18th. The surface pressure decreased rapidly and the weather conditions became bad, with incoming snow and fog. This low, with its minimum pressure below 990 hPa on September 19th near 86° N 030° E, influenced the weather in the operation area during the next 24 hours. As a consequence of very strong warm air advection, the snow became freezing rain for some hours and all scheduled helicopter flights had to be cancelled.

On late September 20th, cold air began to flow from the North Pole region into our operation area. The wind turned northerly increasing Bft. 6 to 7 by a time, but low stratus clouds with a ceiling near 300 ft remained in the operation area until morning of September, 21st. Nevertheless weather conditions did not change better in the daytime, because the cooling of the air below minus 10°C at the surface near the sea ice produced fog patches. The absolute minimum temperature during this cruise, minus 12.7°C, was noticed at POLARSTERN on early September 22nd. In the meantime, a large anticyclone had developed over Greenland and the northeastern part of the Beaufort Sea spreading east very slowly. During the transit along the ridge to about 21°E longitude the anticyclonic influence increased. Some light snow showers from low stratus clouds were observed but also some short sunny periods. The wind was only weak to moderate in force coming from northwest. In the strong south-westerly upper air flow crossing the northern part of Greenland a surface cyclone started to develop over the Fram Strait on September 23rd. The minimum pressure, 978 hPa, was analyzed on September 25th little north of Svalbard.

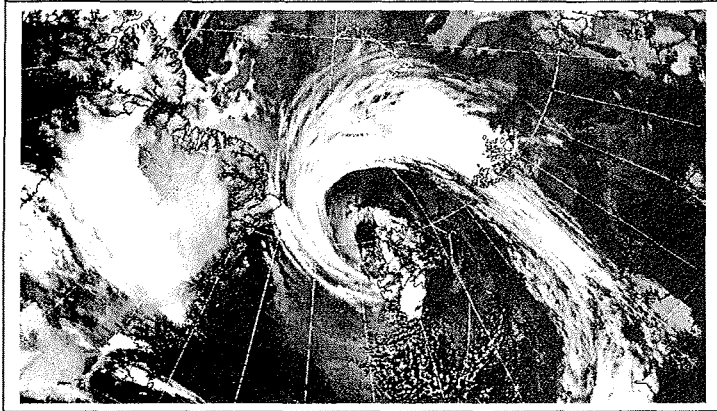


Figure 9: NOAA 12 IR- 25.09.2001, 10.33 UTC.

The cyclone entered the operation area of POLARSTERN on early Sept. 25th with north-eastern storm Bft. 9, snowfall, heavy blowing snow and severe ice pressing. The dry bulb temperature remained near minus 5°C. Figure 9 shows the satellite picture from the adult cyclone. Due to an upper level vortex with vertical axis this low remained stable little southeast of Svalbard for nearly two days. Both vessels got stuck in the pressing ice for several hours.

On early Sept. 26th POLARSTERN and HEALY started their transit from the Gakkel Ridge in south-easterly direction for shooting a seismic profile. Underway the weather conditions became better: due to the filling low little south of Svalbard the north-easterly winds decreased Bft. 5 to 6, while the visibility increased more than 10 km.

Both vessels approached the polar ice edge on Sept. 28th near position 82.30° N 030° E again. During the homeward cruise of POLARSTERN from east of Svalbard to Bergen moderate north-easterly winds (Bft. 3 to 5) and easterly swell 1 to 1.5 m were noticed at the rear of a large low system over the Barents Sea. On Sept. 30th an anticyclone moved from Svalbard to northern Norway and Baltic States while weakening. Therefore the wind turned easterly increasing Bft. 6 near of the Isles of Lofoten on late Oct. 1st. A large gale centre formed west of British Isles on Oct. 1st, which moved towards the Norwegian Sea. The minimum pressure was below 960 hPa. Therefore the wind increased gale force Bft. 8 near Cape Svinøy on Oct. 3rd with seas up to 5 m. After the acoustic testing of POLARSTERN near Bergen and Stavanger on Oct. 4th and 5th the vessel proceeded for Bremerhaven without any time lost due to meteorological or sea wave influences.

Remark: The weather conditions during this cruise in sea-ice were dominated by fog, as shown in Figure 10 below. There were only 2 days registered without any hazard. The activity of fog and freezing rain is much larger in the eastern part of the Arctic Ocean as in the western part, because there is no influence of dry air coming from the Greenland ice.

The table indicates also the most common meteorological problem in the Arctic summer and autumn: all weather-dependent activities like helicopter flights have to be planned carefully by forecasting and should be carried out within shortest time slots.

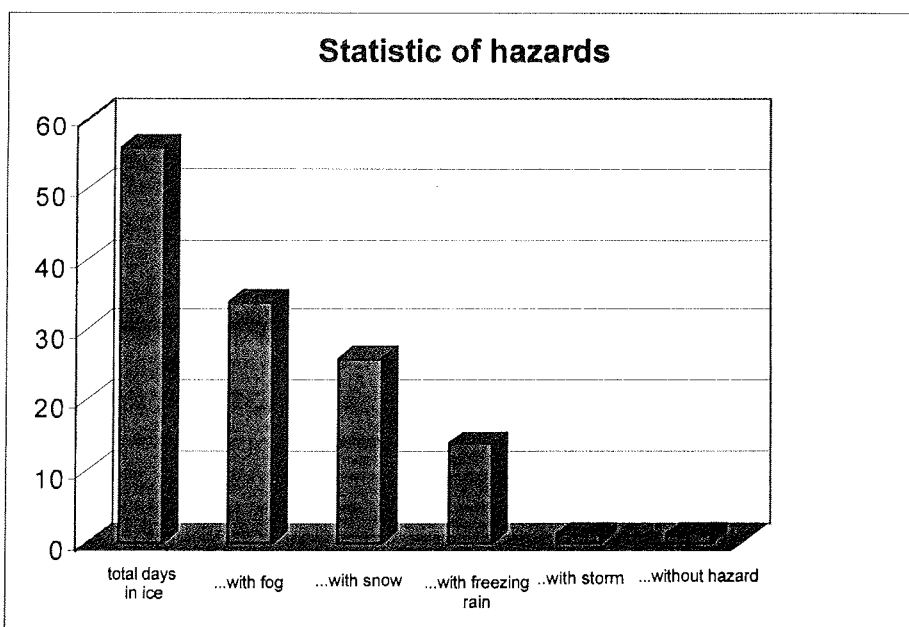


Figure 10: Frequency of hazards during cruise ARK XVII/2 in ice.

Wind statistics

During the expedition in the Arctic ice from 04.08.2001 to 29.09.2001 light to moderate winds were prevailing. The most frequently wind speed was Bft. 3 (3.5 to 5 m/s). For that reason the wind-chill temperature also kept moderate. The main wind direction was the sector between south and west (more than 50% frequency).

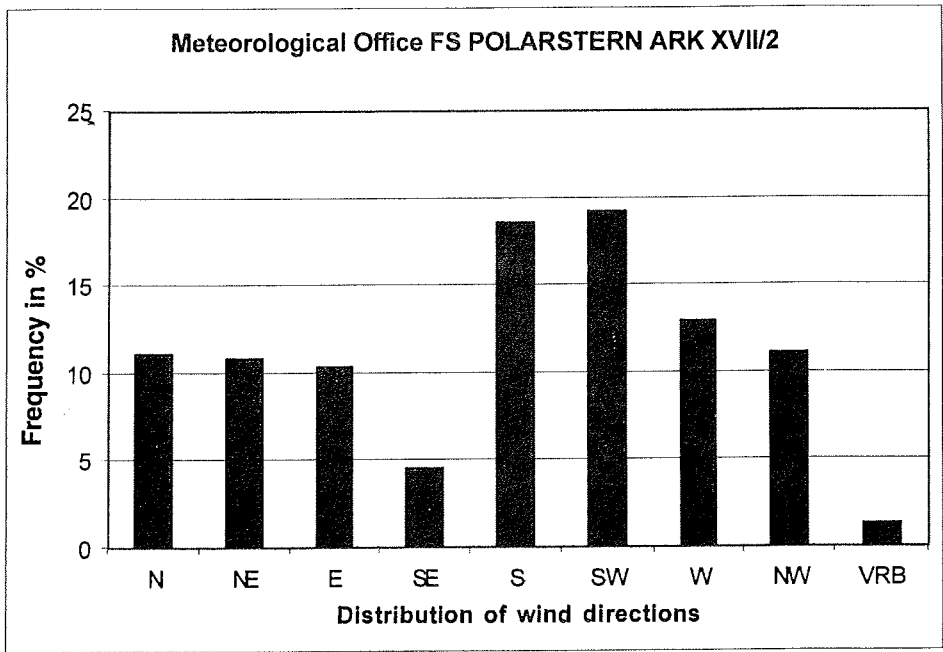


Figure 11: Distribution of wind forces in the time period from 04.08 – 28.09.2001.

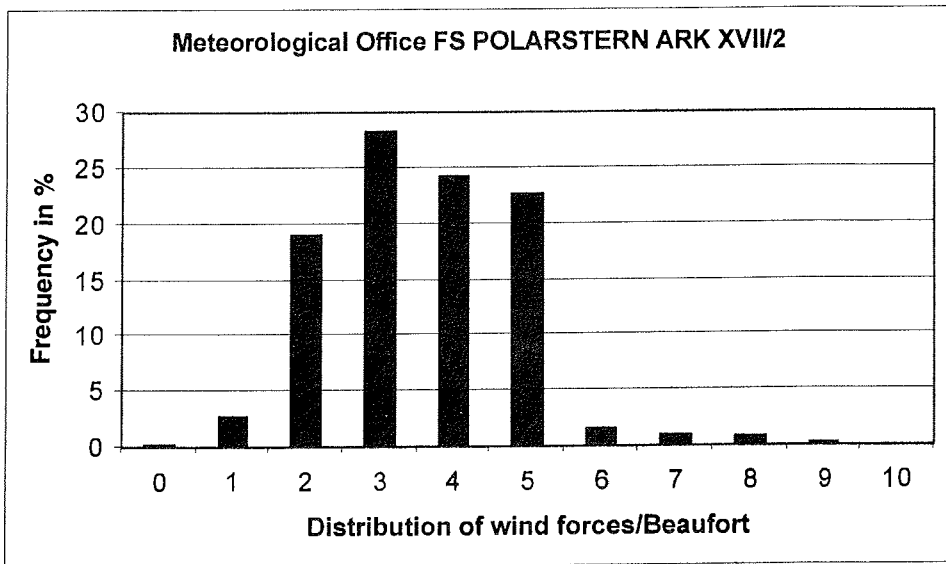


Figure 12: Distribution of wind direction in the time period from 04.08 – 28.09.2001.

4. Sea Ice Measurements and Sampling

(C. Haas)

The goal of the sea ice program was to study geophysical, biological, geological and chemical aspects of the ice in the Transpolar Drift. The sea ice group consisted of three groups from AWI, Institute for Polar Ecology (IPÖ, Kiel), and P.P.Shirshov Institute of Oceanology (Moscow). As no ship time was assigned to sea ice work, almost all floes had to be entered by helicopter, requiring one to three flights to carry all material and personnel to the station floe. Despite partially difficult weather conditions and the occupation of helicopters by other groups, 54 floes could be sampled. Additionally, airborne measurements were performed. All sampling locations and flight tracks are shown in Figure 13.

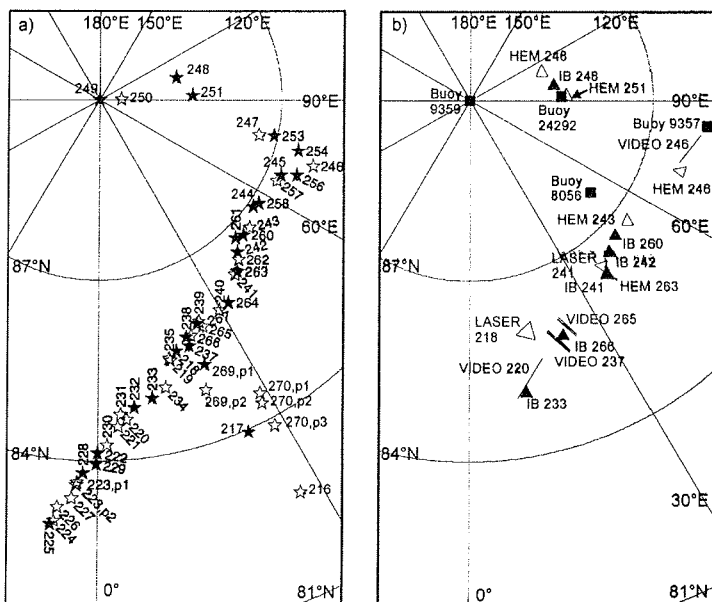


Fig. 13: Map of the study area, showing (a) the positions of the sampled floes and station numbers (filled symbols: ice coring and thickness profiling; open symbols: just thickness profiling) and (b) flight tracks as well as the locations of sampled icebergs and buoy deployments.

4.1 Ice Conditions along the Cruise Track

(C. Haas, J. Lieser, J. Bareiss, G. Kubas, B. Mackowiak, A. Scheltz, H. Schünemann, S. Schuster, V. Shevchenko)

While steaming in the ice, standardized visual ice observations were performed every hour from the ships bridge. Variables like ice concentration, ice thickness, floe and lead size, melt-pond coverage, ridge frequency, as well as the occurrence of dirty ice and icebergs were recorded, representing ice conditions in an area of 500 to 1000 m around the ship. In total 528 observations were carried out. Note that these observations could be highly biased by the partially poor visibility.

Figure 14 shows ice concentration versus longitude, roughly representing a profile along the Transpolar Drift. It can be seen that the cruise track could be subdivided into two distinctly different sections. Westwards of about 45°E, ice concentration was only between 60 and 90%. There, between floes with typical diameters between 100 to 2000 m leads or polynjas had dimensions from 0 up to 1000 m (Fig. 14 b). These large polynjas are generated by divergent winds and are typical for summer conditions in the Central Arctic. Only eastward of 45°E ice concentration increased to 90% and more. At the North Pole ice concentration was 95%, with 2-m thick floes of 300 to 1000 m in diameter and narrow leads with less than 50-m width, covered with new ice. After September 13., when air temperatures decreased significantly below -5°C for most of the expedition period, ice concentration was mostly close to 100%, because all leads were covered by nilas or grey ice. In the eastern region, most leads were 50 to 100 m wide (Fig. 14 b). However, at many locations the leads were covered with small thick floes, such that ice breaking became more difficult.

In Figure 14 c a time series of melt pond coverage is shown. Melt ponds were well developed at the time when we entered the study region. The water surface of most ponds was at sea level, indicating that ponds were well drained. Typical pond depths ranged between 0.2 and 0.4 m. It should be noted however, that most ponds were already covered by a thin ice rind when we entered the ice on August 4. Upon leaving the ice on September 28, the pond ice cover had a thickness of 0.3 to 0.4 m. The decreases in pond coverage around observations 75, 130, and 340 were due to recently fallen snow making the identification of frozen ponds impossible. Later on, the bigger frozen ponds became visible again because the floes were partially blown snow-free by strong winds. Interestingly, dirty ice was observed almost only in the western and southern study

areas. This is also represented in the distribution of samples of dirty ice (Section 4.8). Figure 15 shows the spatial distribution of icebergs. There were mainly two regions where icebergs were observed, partially in quite high numbers. Many icebergs had diameters of more than 100 m and were sediment covered. Some big rocks were found on some of them, too. Some icebergs had a very rough pinnacled surface with melt ponds located in the troughs.

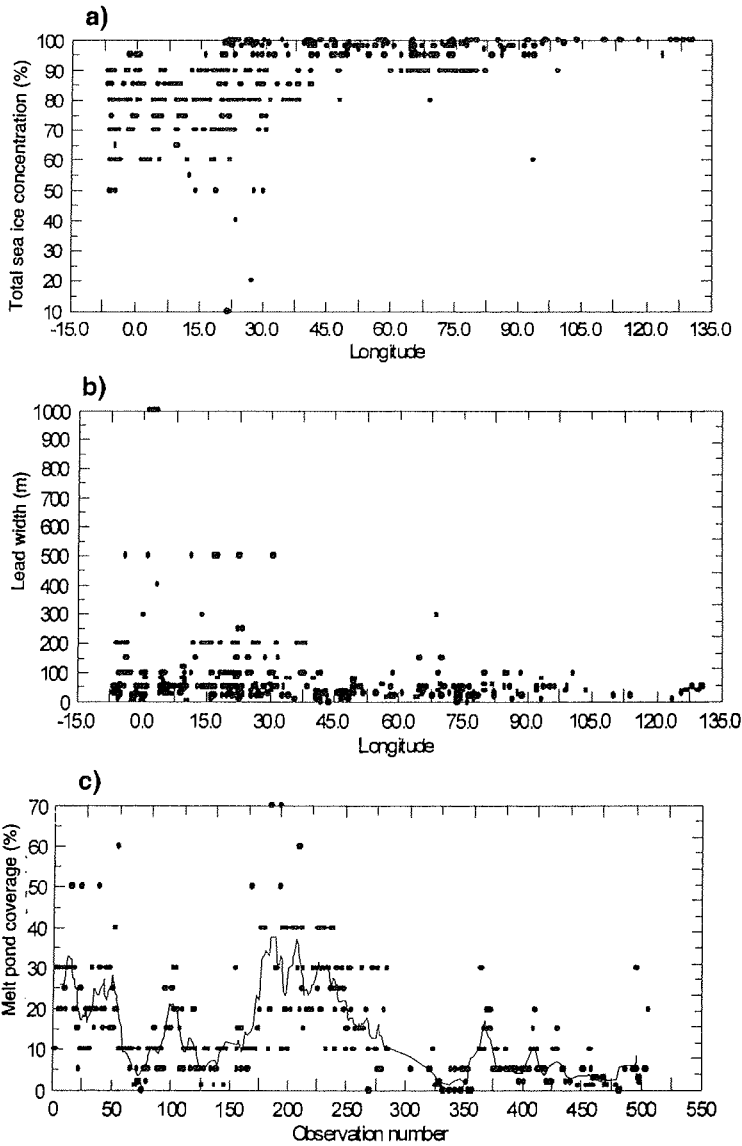


Fig. 14: a,b) Ice concentrations and leads width along the Transpolar Drift. c) Time series of melt pond coverage from the first until the last day in the ice. The solid line is a 9 point running average. Data are from visual observations of ice conditions.

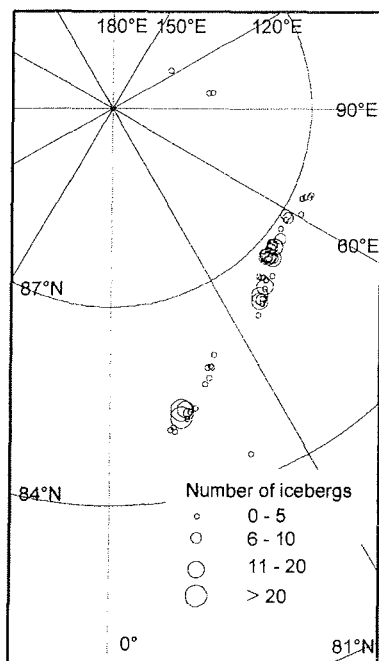


Fig. 15: Spatial distribution of numbers of icebergs per observation.

4.2 NOAA-AVHRR Imagery

(J. Lieser, C. Haas)

Onboard of POLARSTERN a satellite receiving system is installed to receive data from the polar orbiting NOAA-Satellites (National Oceanographic and Atmospheric Administration, USA) NOAA-12, NOAA-14, and NOAA-16. These satellites operate at a height of about 850-km in a near-polar sunsynchronous orbit. During ARKXVII/2 more than 2000 passes of the three satellites have been captured and post-processed. The HRPT-Telemetry (High Resolution Picture Transmission) includes the scans of the AVHRR-Sensor (Advanced Very High Resolution Radiometer) as well as information collected by the DCS-Platform (Data Collection and Positioning System). AVHRR is a five-channel radiometer operating in the visible (two channels) and infrared (three channels) wavelength range with a nadir resolution of about 1.1 km. The DCS system receives environmental data and GPS (Global Positioning System) positions of either stationary or moving platforms, like the four ARGOS-buoys deployed on ice floes during this expedition (Section 4.11).

Over 400 passes have been archived for further post-processing. This will include an exact geolocation of the image data and a comparison of albedo measurements performed on the ice stations (Section 4.5) and albedo seen by the AVHRR for validation. Because visible and infrared sensors are not capable of looking through atmospheric water vapour, online satellite data provided information on the ship surrounding sea ice condition only in cloud free scenes. Nonetheless, the bridge has been supported with sea ice information on a regular basis. One of the geophysical long-term stations installed on an ice floe was equipped with one of the AWI ARGOS-buoys to be easily tracked for 11 days until recovery.

Figure 16 shows an AVHRR image received on August 09, 2001 at 10:27 UTC, when POLARSTERN reached the ice edge just some days ago. The white cross denotes the position of POLARSTERN at that time. In the lower left corner of the image the north-eastern part of Greenland is visible. Ice floes of different size are clearly detectable southwards of 85°N in the cloud free part of the image. Northwards of 85°N most of the scene is cloudy with opaque and thin clouds at different levels.

Figure 17 shows part of an overpass that was received on September 14, 2001, at 07:03 UTC. The black track shows the course plot of POLARSTERN until that time. The white cross gives the position again. The ice regime had changed significantly compared to August (Fig. 16). The differently sized sea ice floes have been compacted by a low-pressure system and some shear zones are clearly visible more or less perpendicular to each other. Ice conditions around the ship were relatively hard.

Figure 18 displays part of a pass received on September 11, 2001, at 05:56 UTC and shows part of the Laptev and East Siberian Seas. The Lena Delta is in the lower left corner. Between 130°E and 160°E a relatively loose ice cover with open water in lee of larger ice sheets can be seen northwards of 76°N. Whereas a cyclone with its centre at about 75°N and 120°E compacted the ice cover between 110°E and 130°E just north-eastwardly to the Taimyr Peninsula, forming the so-called Taimyr Ice Massive.

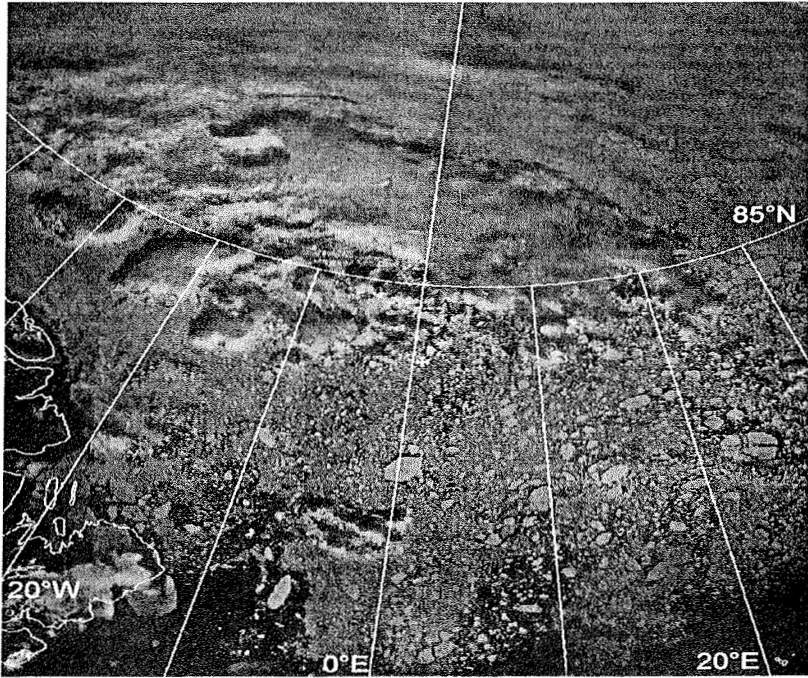


Fig. 16: NOAA-AVHRR image received on August 09, 2001, 10:27 UTC.

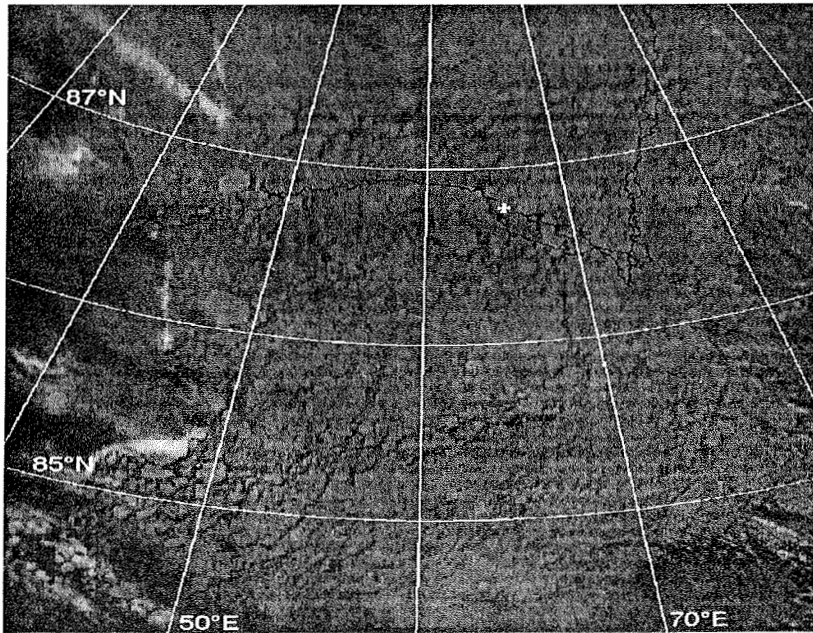


Fig. 17: NOAA-AVHRR image received on September 14, 2001, 07:03 UTC.

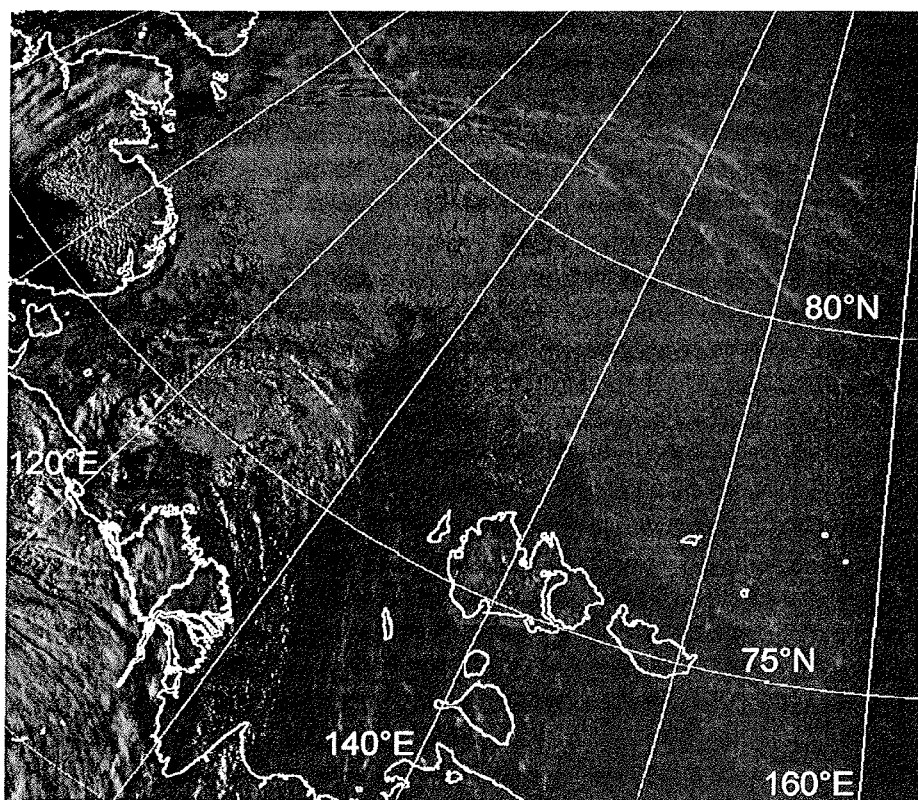


Fig. 18: NOAA-AVHRR image received on September 11, 2001, at 05:56 UTC.

4.3 Ice Thickness Measurements

(C. Haas, J. Bareiss, G. Kubas, J. Lieser, S. Schuster)

The main goal of ice thickness measurements was to gain high-resolution data to describe surface morphology, and to determine a status quo of Transpolar Drift ice thickness. Particular with respect to reports on recent changes in Arctic ice volume, these measurements together with comparable data from 1991, 1996, and 1998 provide a unique independent data set to judge whether the Arctic's sea ice is thinning or thickening. During ARK XVII/2, extensive ice thickness profiling was carried out by means of electromagnetic (EM) induction sounding. The technique allows continuous high accuracy measurements, performed either directly from the ice surface or from above, e.g. by means of the ship or helicopters.

With EM sounding, a low-frequency EM field is generated by a transmitter coil. This field induces eddy currents in the water, which in turn result in a secondary EM field. The strength of this field is measured by a receiver coil. As the strength of any EM field decreases with distance to the source, the secondary field strength decreases with increasing distance between the EM instrument and the water underneath the ice. Thus, the thicker the ice is, the lower the secondary field becomes. Here, we deployed a hierarchy of different means of EM soundings: ground-based measurements have proven to provide very accurate data. Their calibration is evaluated by means of accompanying drill-hole measurements. However, ground based measurements are only possible on single, thick floes, and the profile lengths are very limited. Another possibility is to perform continuous shipborne measurements along the ships track. These provide the most extensive data en-route without any extra requirement for shiptime. However, ice thickness along a ships track is never representative for an ice regime, as the ship usually follows leads with open water or new ice. At floe contacts, where the icebreaker has to break thicker ice, the ice is often deformed. The ultimate way of gathering representative mesoscale thickness data is from aircraft's. During ARK XVII/2 a helicopter EM probe was operated for the first time in the high Arctic.

Ground-based Floe Profiling

Along a 200 m baseline, drill-hole measurements of ice thickness, snow thickness, and draft have been performed every 20 m. These provide a means of evaluating the validity of the EM instruments calibration. Along the baseline the surface elevation was also determined by means of surveying. The measurements were performed with a point spacing of 1 m, to obtain high resolution data for the characterisation of surface morphology, which is very rough due to the presence of melt ponds. Figure 19 shows a typical baseline profile, including drill-hole results as well as the freeboard and surface elevation obtained from snow thickness measurements and surveying. The data sets are particularly important for the interpretation of remote sensing data, e.g. from SAR or Radar Altimeters. Furthermore, the probability distribution of surface elevations provides a means of gathering the state of an ice surface with respect to melt-pond development.

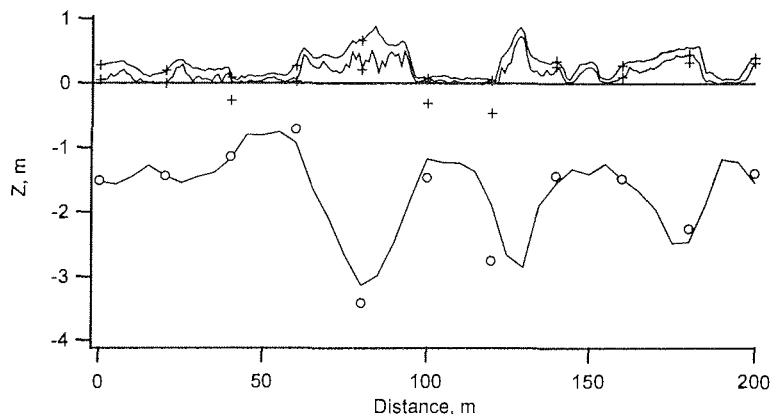


Fig. 19: Typical example for a baseline profile (Station 245). The elevation of the snow and ice surface obtained from surveying is shown, as well as the electromagnetically derived ice draft (lines). The crosses and circles indicate the respective data from drill-hole measurements. Snow-covered melt-ponds are present at 50, 100, 145, 155, and 190 m. Z = Distance of ice surface and underside with respect to the water level ($Z=0$ m).

Ground-based measurements have been performed on a daily basis on single ice floes using a Geonics EM31 instrument. This operates at a frequency of 9.8 kHz with a coil spacing of 3.66 m. The EM31 provides high accuracy data and the procedures are well established (Haas et al., 1997; Haas and Eicken, 2001). The EM31 was placed into a Prijon kayak serving as amphibie sledge, to enable measurements over melt ponds and to shelter the instrument. EM soundings were performed at a lateral spacing of 5 m, extending the baseline profile as far as possible within the time available. The profiles were laid along straight lines, including level and deformed ice. When a floe edge was met, the profile either turned into some other direction, or was continued on a neighbouring floe. As an example, Figure 20 shows the longest ground-based profile ever surveyed in the Arctic with a total length of 4.6 km. In Figure 21 the corresponding thickness distribution is presented. As expected, it possesses a clear mode (at 1.95 m) representing the level ice and a long tail towards thicker ice representing pressure ridges. Due to sufficient profile lengths the thickness distributions of all profiled floes had similar distributions.

Along the EM profiles, the location of melt ponds was recorded to investigate the role of ponds in changing the ice thickness distribution. The profile in Figure 20 also shows the locations of ponds. In Figure 22 the thickness distributions of ponded and pond-free ice are compared. As expected, ponds mostly contribute to the thinnest thickness classes. However, the mode of the pond-free thickness

distribution is much narrower, indicating the contribution of melt ponds to roughening of the ice morphology.

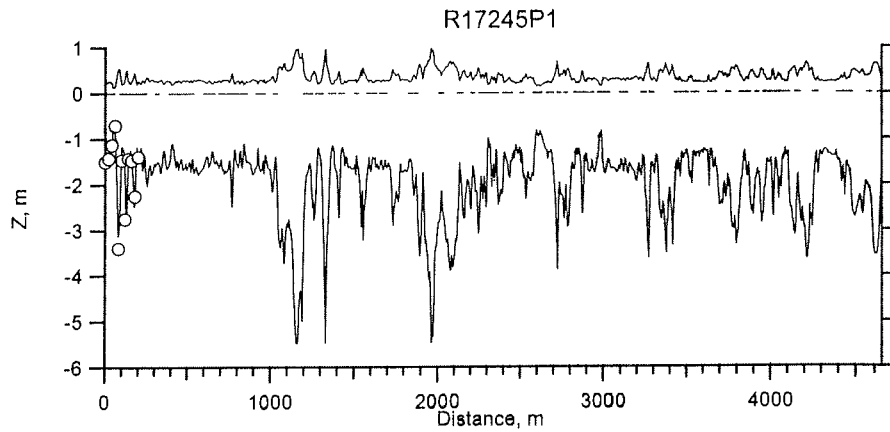


Fig. 20: The longest ground-based thickness profile ever surveyed on an Arctic ice floe. Surface elevation and draft are shown. These were calculated from ice thickness assuming an ice density of 880 kg/m^3 . The ticks and lines at $Z = 0 \text{ m}$ demarcate the location of melt ponds. See Fig.19 for Z .

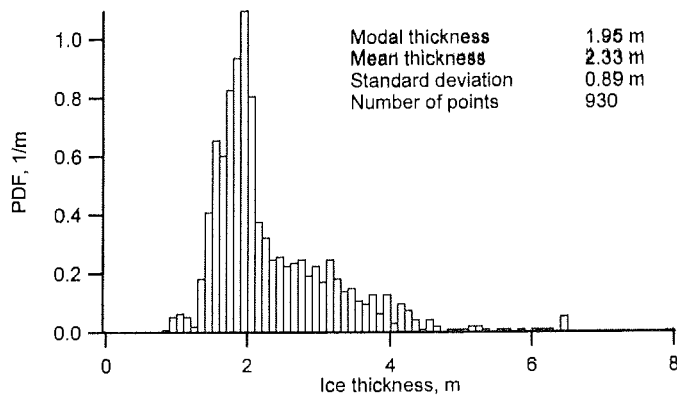


Fig. 21: Thickness distribution of the profile shown in Fig. 20. PDF= Probability-Density-Function.

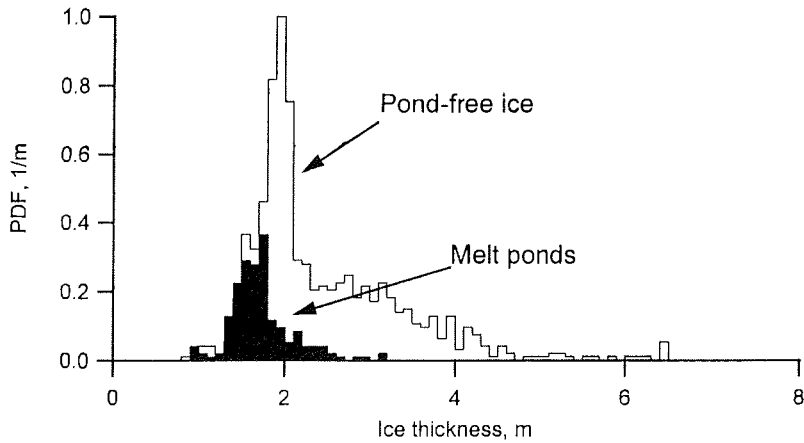


Fig. 22: Comparison of the thickness distributions of melt ponds and pond-free ice along the profile of Figure 20.

In total 113.7 km of thickness data were collected on 54 floes (Fig. 13 a), with an average profile length of 2.1 km. Apart from our approach to the Gakkel Ridge between 82 and 85°N and 25°E there were almost no significant differences in the modal thicknesses of ice floes along the Transpolar Drift. Therefore, all data were pooled to obtain the following preliminary results: The mean ice thickness calculated from the mean floe thicknesses was 2.36 ± 0.46 m, with a mode of the distribution of 1.91 m. The mean surface layer thickness (weathered ice and/or snow) was 0.1 ± 0.04 m. Figure 23 shows the thickness distribution of all EM-measurements. Compared to comparable measurements in the same region of the Transpolar Drift this is 0.50 m thinner than in 1991 and 0.30 m thinner than in 1998. The reason for this thinning is unclear, and can only be identified after careful investigation of this years ice dynamics and meteorological and oceanographical boundary conditions.

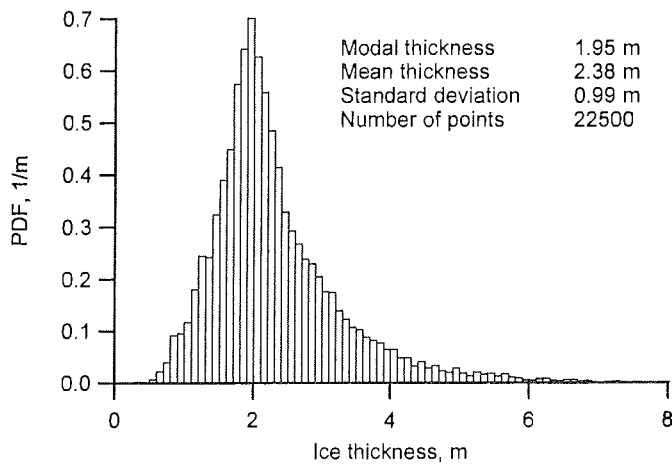


Fig. 23: Thickness distribution of all ground-based EM measurements.
PDF = Probability-Density-Function.

Shipborne Surveys

Since 1994, continuous ship-based ice thickness measurements have been performed during several POLARSTERN expeditions (Haas, 1998). The results obtained during those cruises and the gathered experience justified the fixed installation of a shipborne thickness sensor for routine along-track measurements. There are two main goals of these measurements: When the ship passes through floe ice along straight cruise tracks, the data yield representative thickness distributions for a certain ice regime. These are required for model validation and ice thickness monitoring with respect to an assessment of possible climate changes. However, in thick multiyear ice like in the Arctic this goal is not achievable because the ship mostly follows leads. Second, the data can be used as navigational information. Comparing ice thickness and concentration with e.g. ship speed and delivered power, one could develop trafficability models for transit-time predictions. For POLARSTERN, a third goal is to obtain information on ice thickness with respect to assessing ice damage at the ships hull. Only if a relation between different ice properties and corresponding damage is known, icebreakers can properly be designed and built.

During ARK XVII/2, for the first time the Sea Ice Monitoring System (SIMS) was operated. The idea of SIMS is to provide real-time along-track thickness data directly into PODAS, the POLARSTERN Data Acquisition System. SIMS consists of a Geonics EM31 EM device (see above) and a Riegel laser altimeter, mounted into a GFK housing to protect the instruments and support suspen-

sion. It was suspended from the ship's bow crane at a height of 4 m above the ice surface. Thus it can measure the ice thickness at a distance of about 8-m in front of the ship. SIMS was connected to PODAS through cables leading from the bow to the bridge, where the PODAS interface is. Unfortunately, a fixed installation using a rig on the bow crane, which is remotely controlled from the bridge, could not be completed in due time before the ship left Bremerhaven. Due to the short preparation time, data storage within PODAS could not be achieved either. However, SIMS data were displayable at all information terminals on the ship, and through PODAS the data were provided to a serial link. From there, the data could be stored with a PC notebook on the bridge. With the PC on the bridge, it was also possible to directly read the original SIMS data on the bridge circumventing PODAS.

Calibrations were performed by rising and lowering SIMS above open water (Haas, 1998). Figure 24 shows a typical half-hour section of a SIMS profile, obtained on September 14 when POLARSTERN was steaming alone through closed pack ice, which required some ramming. The laser shows the profile of the ice surface, while the EM31 measures the ice underside. Thus, the presence of ice and its thickness can easily be monitored. The section shows a period of ramming cycles, with backing in-between. After the speed reduces to 0 knots, the ship accelerates backwards or forwards. When ramming, after SIMS sees some thick ice the ship's speed decreases rapidly until the ship comes to a stop again. Only after 25800 seconds, some progress is made.

Figure 25 shows the thickness distribution of all data gathered during September 14. The two modes indicate open water and the typical level ice thickness. The shift of the main mode to 0.20 m is due to the presence of nilas covering the leads. It is noteworthy that a preliminary analysis of all SIMS data showed typical ice thicknesses of 1.2 to 1.6 m, which disagree with the typical thickness of 1.95 m obtained from the ground-based measurements. Currently, there are three major hypotheses for this: The disagreement might be due to a wrong dynamic behaviour of the EM31's conductivity-to-thickness transformation, which was derived during a calibration under bad geophysical conditions. A careful concluding calibration measurement has not been analysed yet. Second, the smaller thicknesses might be due to the small fragmented floes with much water in-between. The presence of water in the footprint area of the measurement causes an underestimate of the true thicknesses. Third, the smaller thicknesses might in fact be true and might show that the small floes in leads are really thinner than the ice of large floes. This could possibly be ex-

plained by the fact that the ice in leads could be younger first-year ice, or that bottom melting of small floes is higher due to the absorption of solar radiation in the leads. More insight will be possible after processing the final calibration, and after comparison with the airborne measurements, which profile both large floes as well as small floes in leads (see below).

In total 244 hours of SIMS data were recorded and will be analysed. They were chosen when POLARSTERN steamed alone through closed pack ice, without following in the broken channel of HEALY or following large lead systems with little ice in-between. After some modifications of the software SIMS will provide valuable real-time ice thickness data available for navigation and sea-ice studies.

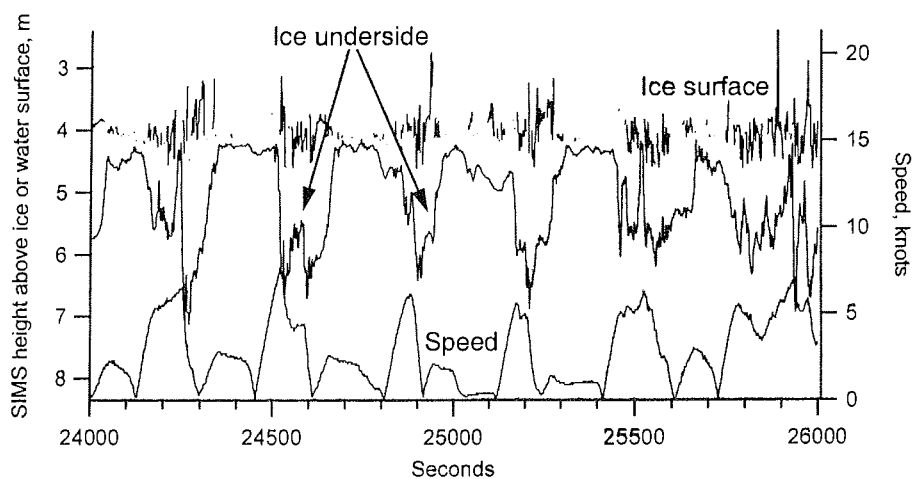


Fig. 24: Half-hour section of SIMS profile from September 14, showing laser and EM-data as well as ship's speed.

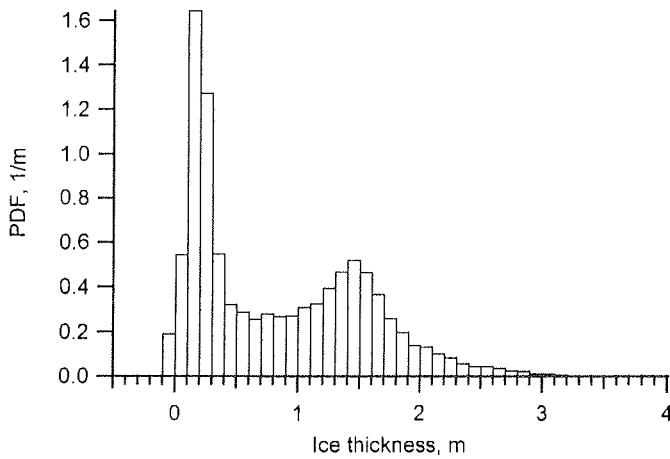


Fig. 25: Typical thickness distribution derived with the Sea Ice Monitoring System. PDF = Probability Density Function.

Evaluation of Airborne EM-Sensor

For the first time, a new helicopterborne EM ice thickness sensor (HEM-bird) was tested and operated with the POLARSTERN BO-105 helicopters. The bird is 3.5 m long, has a diameter of 0.35 m, and weighs about 100 kg. It is towed 20 m below the helicopter, at a height of about 10 to 15 m above the ice surface. Take-off and landing were conducted from the helicopter deck without any operational problems.

The bird operates at 3.68 and 112 kHz, with coil spacings of 2.77 and 2.05 m, respectively. A GPS antenna and a laser altimeter are also included. As an example, Figure 26 a shows a 5 km-long section from a profile measured on August 31 (day 243) at 86°42'N, 51°E. The bird height above the ice surface as measured with the laser and the bird height above the ice/water interface determined from the inphase signal of the low frequency are presented. The low frequency undulations are caused by changes of bird and helicopter altitude. Superimposed are the high frequency signals of the ice surface and bottom topography. For a first data analysis, the inphase signal in PPM is transformed into a height estimate by means of laser/EM data over open water, where ice thickness is zero. Actually, to increase the accuracy of this transformation, the flight track was chosen to connect open water patches where this was possible without deviating too much from a straight profile line. Ice thickness is calculated by subtracting the laser from the EM-data, as shown in Figure 26 b. Figure 27 presents the respective thickness histogram, given as probability density

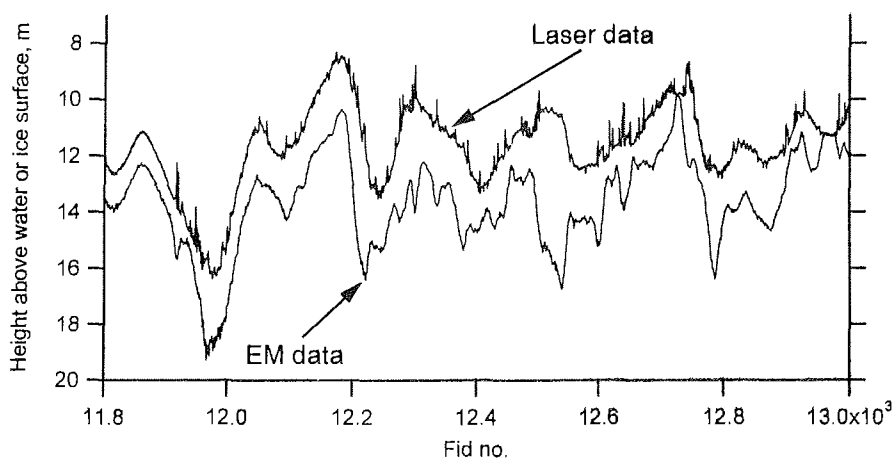
function (PDF). The main mode of 2 m agrees well with the results from the ground-based measurements in the region of the flight. However, note that several other modes appear in the thickness distribution indicating the presence of floes of different age and deformation history. The mode at 0 m results from the presence of open water in leads, as indicated in Figure 26 b.

Flights were performed along triangles with 20 km side length. At each turning point, the helicopter ascended to an altitude of 100 m to allow for internal calibration and nulling of the bird. In total 5 flights were performed on days 243, 246, 248, 251, and 263 (Fig. 13).

The profile flights were complemented by two validation flights. During these, we profiled a floe, which was measured on the ground before. Figure 28 presents a comparison of ground-based and airborne profiles. Both data sets differ by less than 0.2 m, both in their mean and modal thickness. This difference might be caused by the presence of new ice on leads, which were used to calibrate the bird for this preliminary analysis. The HEM bird is well capable of distinguishing between different ice thicknesses on short spatial scales.

In conclusion, the new HEM bird proved to be a very powerful tool for extended ice thickness surveys, which could easily be handled from POLARSTERN. With this bird, the performance of systematic long-range thickness surveys will be possible very soon. However, there were also serious technical problems during take-off leading to many crashes of the bird computer. These problems were probably related to static discharge. This is a challenge for future changes on the instrument.

a)



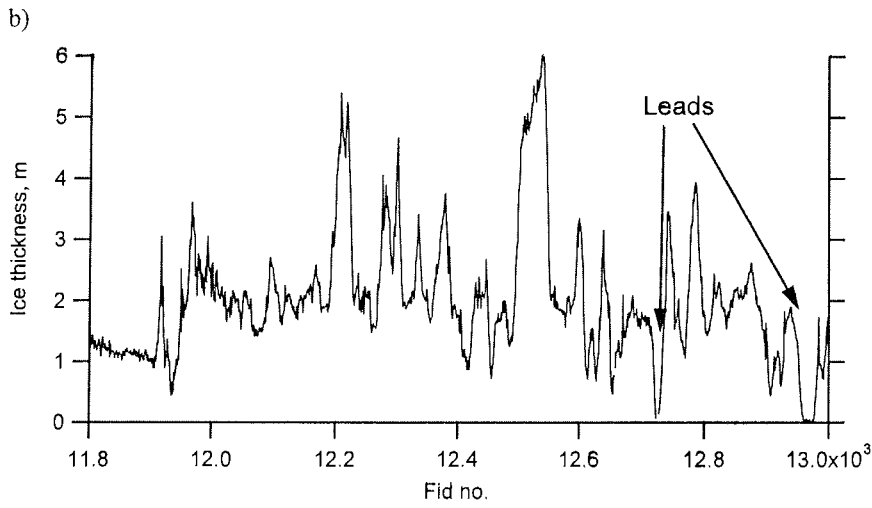


Fig. 26a+b: Typical section of a HEM profile, showing a) the height above the ice or water surface as determined by means of laser altimetry and EM induction, and b) the resulting ice thickness.

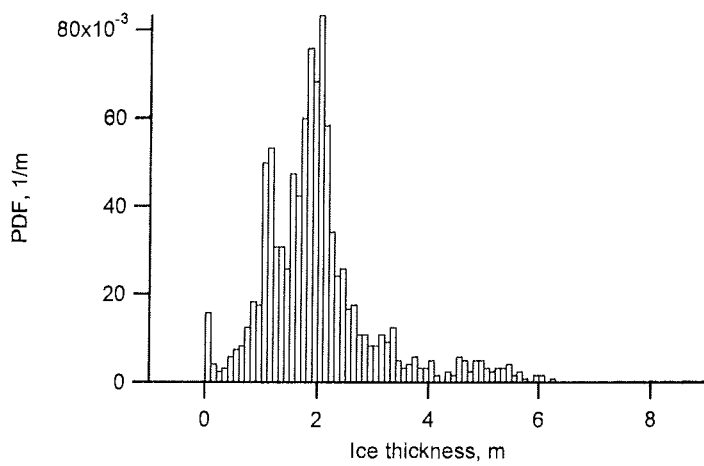


Fig. 27: Thickness distribution for the profile in Fig. 26.

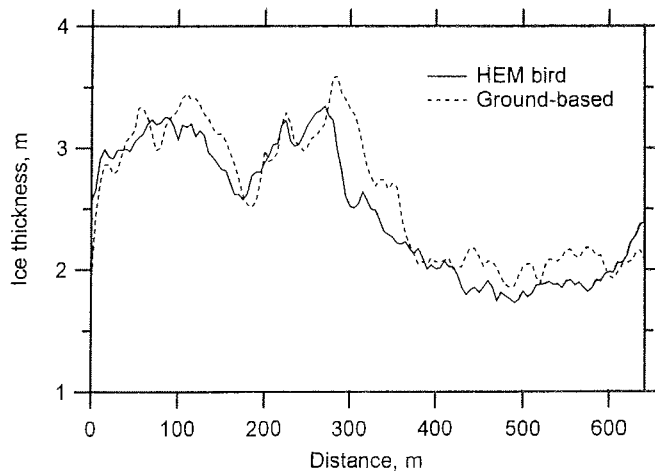


Fig. 28: Comparison of HEM and ground-based thickness profile.

4.4 Laser Profiling of Pressure Ridges

(S. Schuster, C. Haas)

During ARK XVII/2 it was possible for the first time to conduct measurements of sea ice roughness with a laser altimeter that worked parallel to the EM ice thickness sensor (HEM-bird) described in section 4.3. This will improve the understanding of the thickness and surface elevation of pressure ridges, which are the main roughness feature of sea ice. Sea ice roughness plays an important role for the interaction between ice and atmosphere and is therefore an important parameter for state-of-the-art climate models. We conducted a total of seven flights of which two were performed with only a laser altimeter mounted on a helicopter and five with the EM bird. The area reached over 86°03'N, 13°43'E for the southernmost flight (day 218), up to 86°25'N, 71°07'E to the east (day 246) and 88°46'E, 113°23'E to the north (day 248). The laser measured the height above the sea ice surface and relative echo amplitude with a frequency of 100 Hz, resulting in point spacings between 0.2 to 0.4 m.

Flights were performed at heights of 10 – 40 m above ground. Most flights were divided into three legs of equal sides, forming a triangle. Surface profiles with a total length of 400 km were sampled in those seven flights, ranging from 40 km to 68 km. It can be seen from Figure 13 that we did not have a chance to conduct flights closer to the North Pole region and closer to the Greenlandic coast in the west. This would have given results with higher variability due to different

sea ice regimes in those regions. Because of unfortunate weather conditions it was not possible to perform flights at the time we sailed in those regions.

Due to the helicopter motion (unstable vertical motion as well as rolling and pitching) the raw data needed to be processed to obtain a profile of the surface and the pressure ridge height and their spacing, the number of ridges per km as well as the mean width and number of leads. It is also possible to estimate ice concentration and the mean diameter of ice floes.

A raw data example is presented in Figure 29, where the upper Figure shows the movement of the helicopter (upper smoothed curve) as well as the laser altimeter data. The lower figure shows the resulting surface elevation in m. The number of floes per flight per kilometer varied from 9 at day 248 to 55 on the last flight, day 263. The floe size was also very variable and ranged from a mean floe size of 17 m on the first flight at day 218 to 120 m on day 248. Accordingly the sea ice concentration increased from 74% on day 218 to 99% on day 248.

Figure 30 shows the distribution of the pressure ridge density per km against longitude. It can be easily seen that ridge density increases from the smoother central Arctic Ocean towards the heavier ridged region around 13°43'E, where the ice is stronger deformed and older. The higher ridge density also results in a bigger standard deviation, which shows a great variability in this area furthest east on the cruise. Remarkably good is the repeatability of two flights in the region around 40°E. We believe that the sea ice didn't change in that region where we were able to perform a flight on the way to and on the way back from the North Pole three weeks later.

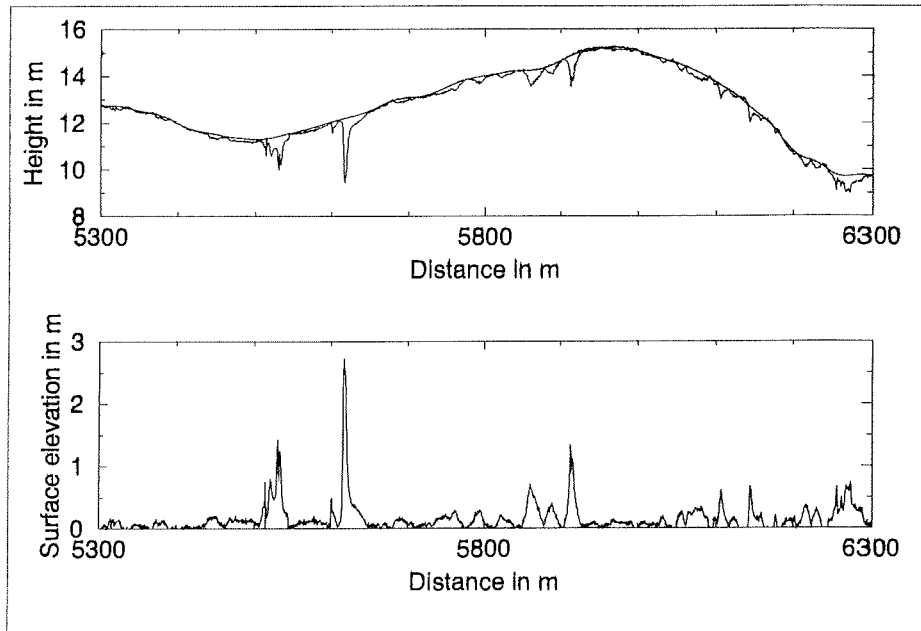


Figure 29: One-kilometer section of a laser profile. The raw data and the helicopter motion derived from it are shown (top) as well as the resulting profile of surface height (bottom).

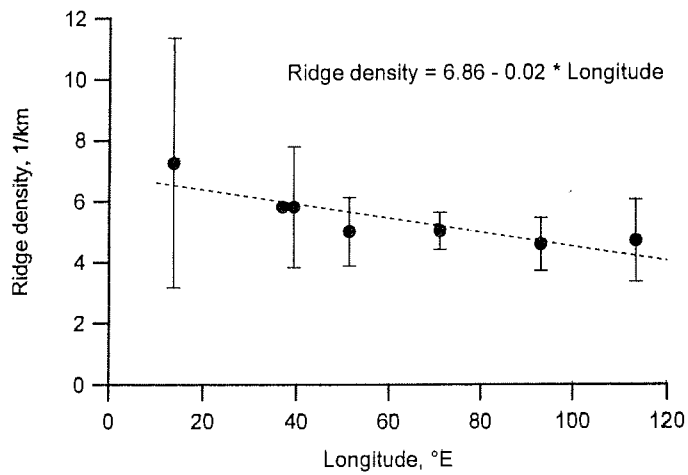


Fig. 30: Mean ridge density versus longitude from the seven laser flights. Error bars indicate one standard deviation. The stippled line is a linear fit given in the graph.

4.5 Spectral Albedo and Areal Coverage of Various Surface Types

(J. Bareiss, C. Haas)

Spectral albedo was measured with a Spectron Engineering SE 590 spectroradiometer consisting of a CE 500 data analyzer and a CE 390 spectral detector, which uses a diffraction grating with a photodiode array (Fig. 31a,b). The detector was used with a calibrated remote cosine receptor with 180° hemispherical field of view (FOV) at 256 wavelengths from 396 nm to 1075 nm. Detector noise (dark current) was removed from each spectral scan. The spectrum is stored binary on tape until it is transmitted through the RS-232C port. The fore-optics were mounted on a tripod with a 1.6-m-long arm, leveled about 0.80 m above the surface. An entire set of 3 incident (upward looking sensor) and reflected (downward looking sensor) scans took a few minutes to complete. Bulk albedos were derived by integrating spectral albedos from 400 to 1000 nm.



Fig. 31a: Spectron Engineering SE 590 spectroradiometer with 180° hemispherical field of view.

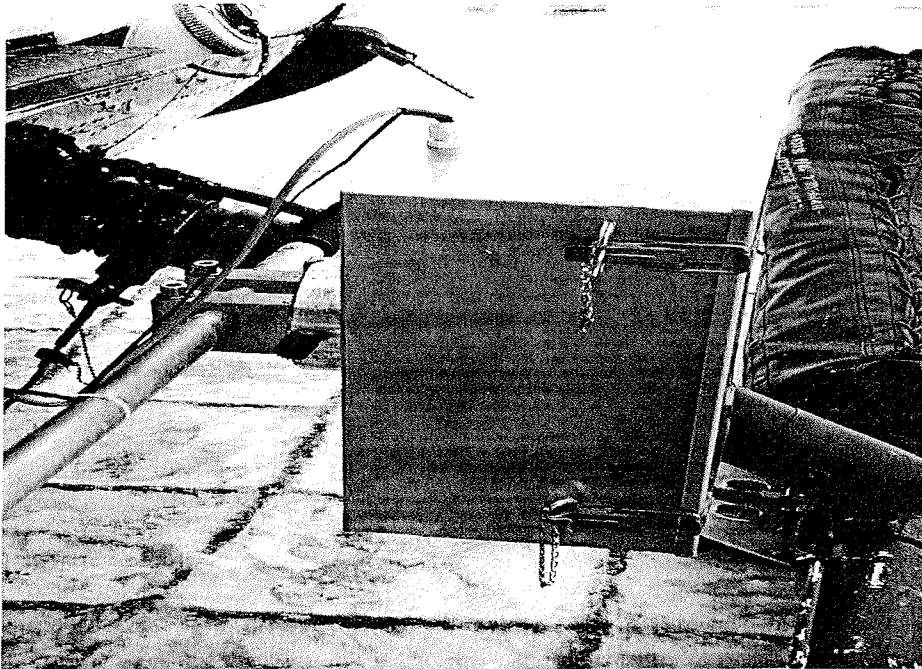


Fig. 31b: Digital video camera mounted „near-to-vertical“ on the BO-105 helicopter.

Surveys of the areal coverage of melt ponds were made using the BO-105 helicopter. A Sony VX-2000 Digital Camcorder was mounted in a weather-protected box attached to an array outside of the helicopter. Five horizontal flights along 100-km transects were made at about 30 m, 100 m and 165 m above ground level (AGL) at a speed of 150 km h⁻¹. Photographs from these digital video data will be digitized using an automated routine that separates the continuous flight record into adjacent frames of 24-bit color images dependent on helicopter speed. Approximately, each frame represents an area of 23x18 m (30 m AGL), 80x60 m (100 m AGL), and 130x100 m (100 km AGL). The photographs are processed using digital image analysis techniques to obtain melt pond size and areal coverage. Most flights were performed during geophysical surveys without requiring any extra time.

Spectral albedos of various surface types

Spectral albedos of various surface types were collected at 32 different sites along the cruise track. While surface albedo measurements show a depend-

ence on wavelength, solar zenith angle, grain size, liquid water content, snow pack thickness, impurities (sediments, algae) and cloud cover, the data is systematically arranged in the categories according to the physical surface properties, cloud cover and the elevation of the sun.

The optical properties of arctic surfaces show large spatial, temporal and spectral variability in late summer and the beginning of fall. Figure 32 summarizes some spectral albedos for important arctic surface types.

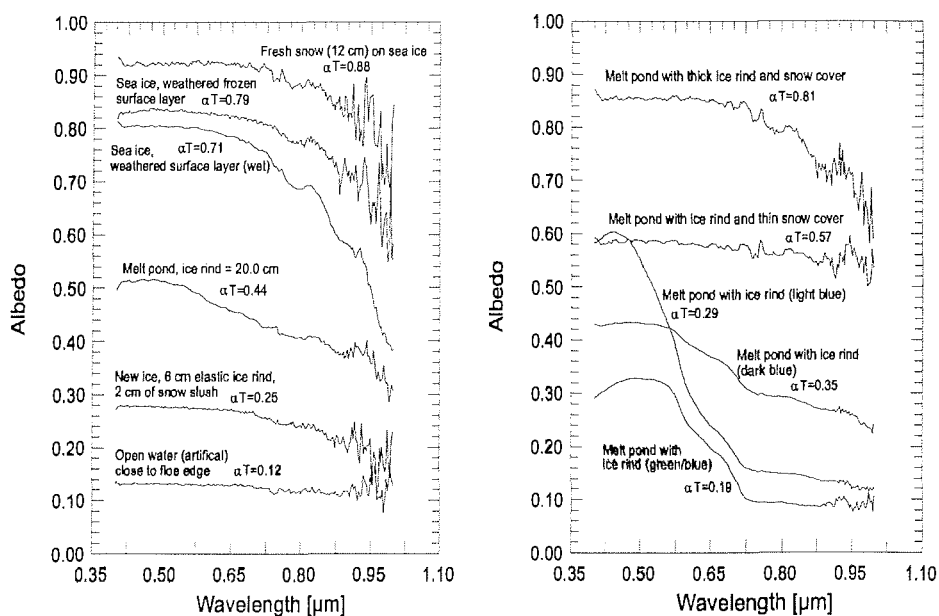


Fig. 32: Spectral albedos of various surface types obtained from ice floes in August and September 2001 along the Gakkel Ridge from 10°W to 80°E. All curves were obtained at overcast conditions. Wavelength-integrated albedo is denoted by α_T .

In general, snow and ice albedos are high in the visible and low in the near-infrared. Cloud cover causes an increase in the spectrally integrated albedo (spectral shift) as a result of the depletion of radiation in the near-infrared. Clouds absorb the same near-infrared radiation that snow and ice would absorb, leaving the shorter wavelengths to penetrate to the surface. From measurements and theoretical calculations (Grenfell and Maykut, 1977; Warren, 1982) overcast albedos are some percent higher than clear-sky albedos. The albedo of snow and ice is found to increase with increasing solar zenith angle.

For snow-covered first-year and multi-year ice albedos are high ($\alpha_T = 0.88$) and spatially uniform. Thin snowpacks (< 2.0 cm) cause a decrease in snow albedo. Some horizontal variability, primarily on clear-sky days, was due to surface topography and the consequently different incidence angles and shadowed surfaces, causing a decrease in albedo.

The surface of ice floes without any snow cover was covered with weathered ice, consisting mainly of granular shaped material that was transformed from columnar ice during summer by melting processes. As grain size increases, albedo drops at all wavelengths. The albedo is relatively high in the visible wavelength and lower in the near-infrared. This effect is caused by the fact, that single photons have a better chance to be scattered with decreasing grain sizes. With increasing grain sizes the path length through the weathered surface layer increases, causing an increase in absorption and hence a decrease in reflectance.

As freeze-up progresses, new ice starts to form in leads. Typical integral new ice albedos vary from $\alpha_T = 0.15$ (frazil ice) to $\alpha_T = 0.30$ (light nilas). Open water close to the floe has integrated albedos of about $\alpha_T = 0.10 - 0.15$. During spring and summer melting decreases the surface albedo, leading to more melting of the snowpack and the formation of numerous melt ponds. On our transect from 85°N to 90°N the number of melt ponds was decreasing. In late summer most of the melt ponds were covered by an ice rind of variable thickness. From the middle of September most ponds were covered by fresh snow. The temporal changes in the optical properties of melt ponds during fall freeze-up are obvious in Figure 32 (right).

The high degree of horizontal variability in surface conditions results in a wide range of integrated albedos. Table 2 summarizes wavelength-integrated albedos (400 to 1000 nm) sampled in-situ over common surfaces under clear-sky and overcast conditions for various solar zenith angles ($> 68^\circ$). Bulk albedos range from 0.14 for open water close to the ice floe edge to 0.87 for fresh dry snow. Ice containing visible sediment ("dirty ice") is common for the Eurasian Arctic. The bulk albedo of sediment-laden ice floes vary from 0.31 to 0.49.

Table 2: Measurements of wavelength-integrated albedo (400 to 1000 nm) over various surfaces in the Transpolar Drift west of 90°E in August and September under clear-sky (CS) and overcast (OC) conditions for various solar zenith angles.

Surface type	Integrated albedo (CS)	Solar zenith angle	Integrated albedo (OC)	Solar zenith angle
Open water	–	–	0.14	76.6°
New ice (1.0 cm)	–	–	0.14	82.8°
New ice (12.0 cm, light nilas)	0.30	83.6°	0.34	84.0°
Melt ponds (artificial)				
Depth = 45 cm	0.24	68.6°	0.29	74.5°
Frozen melt ponds				
Depth = 40 cm, ice rind = 1.5 cm	–	–	0.36	68.8°
Depth = 30 cm, ice rind = 1.5 cm	–	–	0.35	68.8°
Depth = 45 (32) cm, ice rind = 5.0 cm	0.35	68.6°	0.43	68.2°
Depth = 35 cm, ice rind = 4.0 cm	–	–	0.31	71.9°
Depth = 40 cm, ice rind = 3.0 cm	–	–	0.39	78.7°
Depth = – , ice rind = 20 cm, no snow	–	–	0.44	81.9°
Depth = – , ice rind = 20 cm, snow	–	–	0.73	81.9°
Sea ice (weathered surface layer)				
Melting	–	–	0.71	69.2°
Frozen	0.77	76.9°	0.78	71.9°
High sediment concentration	–	–	0.31	70.5°
Low sediment concentration	–	–	0.49	70.5°
Fresh snow				
Depth = 1.0 cm	–	–	0.77	67.0°
Depth = 1.0 cm	–	–	0.81	87.0°
Depth = 50.0 cm	–	–	0.80	70.5°
Depth = 8.0 cm	0.82	80.1°	0.87	80.4°

Nadir aerial photography

Because melt ponds are a common feature of Arctic sea ice in summer and their albedos are a critical component of the surface energy balance, melt-pond size and distribution will be investigated in more detail. The aerial photography presented in Figure 33 shows an example of the spatial distribution of sea ice, melt ponds, new ice and open water. First results from photography and ship-based visual observations reveal that north of 86°N the number of melt ponds decreased. Open and frozen melt ponds at various depths that are not covered by snow can clearly be distinguished. Frozen melt ponds dominate the study area. In August melt ponds had on average a 0 – 0.05 m ice rind, later in the

season and north of 86°N ice rinds exceeded in most areas 0.15 m. With the beginning of snowfall in September the identification of melt ponds by aerial photography and visual observations became difficult or impossible.



Fig. 33: Examples of aerial photography showing the distribution and areal fraction of sea ice, melt ponds and open water on August 9, day 220, (85°N, 15°E) at about 165 m above ground level (at the bottom) and September 3, day 246, (87°N, 75°E) at about 100 m above ground level (at the foot).

4.6 Salinity, Density and Texture of Ice Cores

(C. Haas, H. Schünemann, G. Kubas, A. Scheltz, J. Bareiss)

On most biology stations (Section 4.7), two additional ice cores were drilled for analysis of physical and chemical properties. One core from each station was stored frozen for later radionuclide analysis by American colleagues. From the other cores, vertical thick sections were sawed for analysis of crystal texture in the mobile cold laboratory (-30 °C). In total, the 17 cores were composed of 83.7% of columnar ice, relatively much compared with earlier studies. Of the remaining ice, 10% consisted of retextured columnar, and 4% of orbicular granular ice. On one occasion, after a day of strong rainfall we observed a 4 cm thick layer of superimposed ice. Probably there was more superimposed ice in later cores, too, but this was difficult to observe due to its brittleness and loss during sampling.

The remaining ice was used for density measurements. Cubes of about 25 to 50 cm³ were sawed and their side lengths measured with a ruler. Then, the cubes were weighted. Density was calculated from the ratio of mass and volume. Figure 34 b shows the resulting normalized density profile. The mean density of 15 cores amounts to 862 kg/m³. The profile does not show a significant decrease of density towards the top, as shown by other studies. However, this might be due to the often impermeable ice, where melt water had percolated into the pores and frozen in place. This can also be seen from the mean salinity profile (Fig. 34 a) obtained from the biology cores (Section 4.7). The profile has a shape typical for summer ice, with very low salinities of 0.4 ppt at the top due to melt water flushing. Below a relative depth of about 15%, they rise almost linearly to between 2.7 to 3.1 ppt at a depth of 60%. Salinities decrease also at the bottom, which might indicate the presence of melt water underneath the ice. The mean salinity of 17 cores amounts to 2.16 ppt, very similar to earlier studies. It might indicate a summer season with strong ablation.

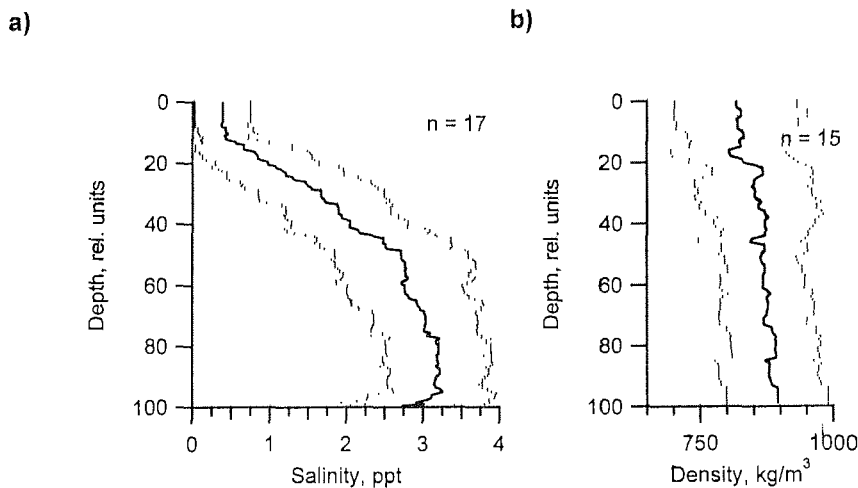


Fig. 34: Mean normalized salinity and density profiles obtained from ice cores. The marks on both sides of the curves indicates ± 1 standard deviation.

4.7 The Role of Sea Ice on the Transport of Radionuclides in the Arctic Ocean

(J.K. Cochran¹, P. Masqué, D.J. Hirschberg)

Sea ice has been shown as a relevant transport mechanism of chemicals over long distances in the Arctic Ocean on the basis of two considerations (Pfirman *et al.*, 1997; Rigor and Colony, 1997, Dethleff *et al.*, 2000). First, these elements can become incorporated to sea-ice in the formation areas. Secondly, sea ice might intercept atmospheric fluxes during its transit. These species might become associated to sediments contained in sea ice. Radionuclides, both from natural (i.e. ^7Be , ^{210}Po and ^{210}Pb) and artificial (i.e. ^{137}Cs and Pu isotopes) origin, may become associated with sea-ice via either these two ways (i.e. incorporation with source sediments or atmospheric deposition during transit). Thus the study of radionuclides in sea-ice sediments can be useful as tracers of the transport mechanisms and as indicators of the importance of sea ice as a mechanism of redistribution of pollutants in the Arctic Ocean. In this last sense, the Laptev and, notably, the Kara Seas are potential source areas of anthropogenic radionuclides to the Arctic Ocean through releases from weapons productions

¹ Marine Sciences Research Center, Stony Brook University. Stony Brook, NY 11794-5000. USA

an nuclear fuel reprocessing facilities. Moreover, nuclear weapons tests were conducted in the past in the Novaya Zemlya archipelago, which also served as a dumping site for nuclear wastes from the former Soviet Union (Bradley and Jenquin, 1995; Baskaran *et al.*, 1996; Smith *et al.*, 1995). Bottom sediments may be affected as well to different extent by the release of the sediments and associated species during melting of sea ice. In this sense, results from a study carried out in the Fram Strait area based on the analyses of samples collected during the ARK XV/3 cruise of the POLARSTERN revealed that input plutonium from a source other than atmospheric fallout has reached the area (Masqué *et al.*, in preparation).

Different types of samples were kindly collected for us during the ARK XVII/2 cruise of the POLARSTERN by several participants in the cruise: Dr. C. Haas (AWI-Bremerhaven) (sea ice cores), Dr. R. Spielhagen (GEOMAR, Kiel) (bottom sediment cores) and Dr. V. Shevchenko (P.P. Shirshov Institute of Oceanology, Moscow) (dirty ice). Preparation of the samples for analyses in the laboratory at the MSRC was conducted at the AWI (Bremerhaven) during the following two weeks after the cruise. Analyses will include:

- Sea ice cores (18 stations): ^7Be , ^{210}Po and ^{210}Pb
- Sea-ice and iceberg sediments (13 stations): ^7Be , ^{137}Cs , ^{210}Pb , ^{226}Ra , ^{239}Pu and ^{240}Pu .
- Bottom sediment cores (6 stations): ^7Be , ^{137}Cs , ^{210}Pb , ^{234}Th , ^{239}Pu and ^{240}Pu .

Determination of sand/silt/clay percentages, silt grain size distribution and clay mineral assemblages will be also carried out.

The main objectives of the current study can be synthesized as follows:

1. Investigate the usefulness of the $^{210}\text{Po}/^{210}\text{Pb}$ ratio in sea ice cores as a chronometer of the sea ice formation and evolution during transit.
2. Determination of the extent to which the radionuclide contents of sea ice depend upon its incorporation into the ice at formation as well as by interception of atmospheric fluxes during transport from coastal regions through the Arctic Ocean.
3. Determination of the origin of the artificial radionuclides transported by sea-ice sediments.
4. Determination of mixing and sedimentation rates in bottom sediments.

5. Evaluation of the role of sea-ice sediments in enhancing both sedimentation and radionuclide inventories.

4.8 Biological Studies

(H. Schünemann, A. Scheltz)

Despite the extreme environmental conditions of temperature, salinity and light, a highly specialised so-called sympagic community has developed and adapted to live within the brine channel system of sea ice. Algae, bacteria, protozoans and metazoans build up a complex food web within this system, which is so far poorly understood. During this expedition physical and biological properties of ice floes were studied. The biological investigations concentrated on the qualitative and quantitative acquisition of the meiofaunal community (here: metazoans > 20µm) and are set into relation to other parameters like salinity, temperature, chlorophyll content and volume of the brine channel system. Furthermore, feeding experiments were conducted to identify and quantify trophic interactions within the sea ice food web.

During ARK XVII/2 a total of 138 ice cores were drilled at 28 stations for biological investigations (see map in Fig. 13 a). At 16 stations samples of brine and the water column directly beneath the ice were taken. The analyses conducted onboard included measurements of temperature, salinity, chlorophyll a and phaeopigment concentrations. Additionally experiments for the determination of ingestion rates of Arctic rotifers were carried out. In the home laboratories abundances and biomasses of sympagic meiofauna organisms will be determined and the experimental work will be proceeded. Ice cores were taken with a SPIRE ice corer (7.5 cm diameter) and temperatures were measured every 10 to 15 cm with a digital thermometer inside the cores immediately after drilling. The same cores were then cut into 1 to 20 cm segments and, after melting in a dark room at 4 °C, analysed for salinity, chlorophyll a and phaeopigment concentrations.

Representing the summer situation the temperature profiles showed highest temperatures with values near 0 °C at the upper side and decreasing temperatures to roughly – 2 °C at the lower surface. (Fig. 35). Many of the sampled ice floes were characterised by under-ice melt ponds, which is also reflected by the salinity data (i.e. Fig. 36). The profiles of these ice cores show "s" shape with decreasing salinity values to the lower surface. Under ice melt ponds form dur-

ing the summer by melting ice and snow on the upper side of the ice. A main part of this melting water accumulates at the underside of the ice floes and freezes. Due to its lower porosity and salinity, under ice melt ponds build up a barrier for settlements by organisms in the ice.

Highest algal biomasses were always found in the bottom parts of the ice floes with maximum values of 97 $\mu\text{g} / \text{l}$ (St. 256). For investigations on sea ice biota three cores were drilled at the same site and cut into 1 to 20 cm segments. These segments were melted in an excess of 0.2 μm filtered sea water to avoid osmotic stress to the organisms. After complete melting, the samples were concentrated over a 20 μm sieve and fixed with Bouin's solution (1% final concentration). They will be used for meiofauna investigations (abundances, biomasses) and taxonomic studies in the home laboratories.

In order to improve the general knowledge of sympagic organisms and the food web existing within the ice, feeding experiments with rotifers were conducted. These organisms represent one of the main taxa within the sympagic community. At 16 locations additional bottom segments of two to three ice cores were taken and melted under same conditions as described for the cores used for investigations on sea ice biota. After melting the meiofauna were concentrated over a 20 μm sieve and rotifers were sorted alive under a binocular. To get information about the grazing rates of sympagic rotifers, fluorescently labelled bacteria (FLB) and bacterium-sized particles (Fluoresbrites) were added to the sorted rotifers and the short-term uptake of both kinds of particles was measured as time-course experiments. Subsamples were taken after 0, 10, 20, 40, 80, 160 and 320 minutes and fixed with Bouin's solution (1% final concentration). In order to estimate the bacterial concentration, in the beginning of the experiments additional subsamples were taken and stained with DAPI. All subsamples were filtered on polycarbonate filters and frozen at $-80\text{ }^{\circ}\text{C}$. The increase of uptaken particles in the rotifers will be determined in the home laboratories using epifluorescence microscopical techniques.

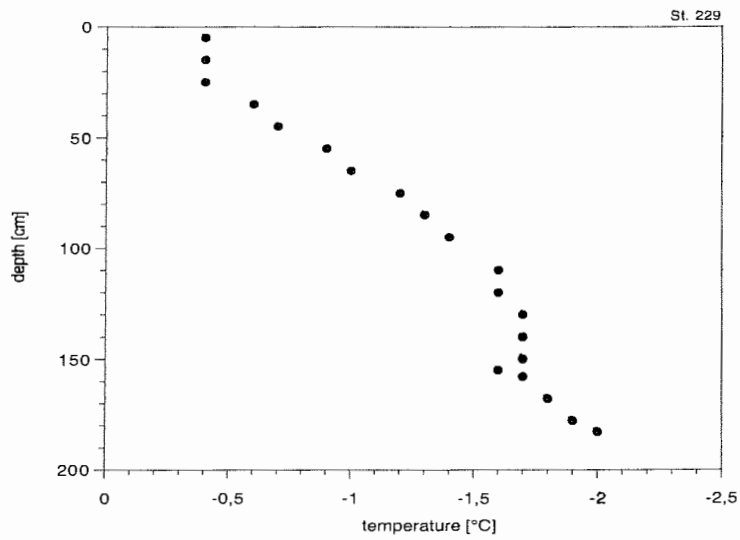


Fig. 35: Typical temperature profile of summer sea ice, with higher temperatures at the top than at the bottom.

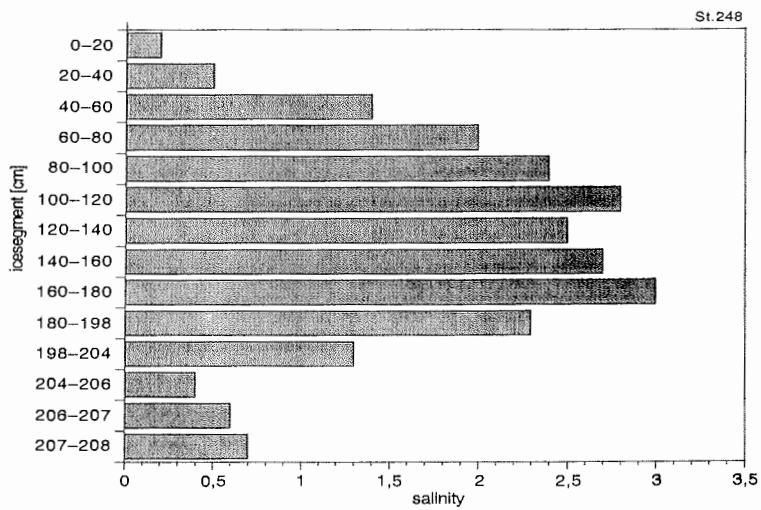


Fig. 36: Typical salinity profile of an ice core containing part of an under-ice melt pond. Note low bottom salinities.

4.9 Particulate Matter in Snow and Ice

(V. Shevchenko, C. Haas, H. Schünemann, A. Scheltz, J. Bareiss)

Aeolian transport of particulate matter onto Arctic sea ice is one of the sources of sedimentary material in the Arctic (Shevchenko *et al.*, 2000). Its role in sedimentation in the Arctic Ocean has been studied insufficiently. The drifting ice in the Arctic is a giant natural accumulator of the aeolian material and attendant pollutants, which first are deposited on the ice and are transformed into cryosols. When the ice melts, often many thousand kilometres away from the places of their fallout, they are released into the water (mostly in Fram Strait and the Greenland Sea).

Snow and ice core samples were collected for chemical composition studies. Sampling was carried out using helicopter. The list of samples is given in the Table 3. Positions of stations are shown in Figure 13. On ice-floes samples of fresh (upper 1–2 cm layer after snowfall) and old, aged snow were collected in clean plastic bags using a plastic shovel. Ice cores were obtained together with colleagues from IPÖ (Kiel) using their ice-drilling equipment. Samples of snow and ice were stored in the refrigerator room at -30 °C. After melting at AWI Bremerhaven, ion chromatography will be carried out. Other subsamples will be filtered through pre-weighed Whatman GF/F and Nucleopore (pores of 0.45 µm) filters to determine concentrations of total particulate matter, particulate organic carbon, black carbon, particulate organic nitrogen, and content and composition of mineral and biogenic particles. It is also planned to study stable carbon isotopes and Pb isotopes in fresh snow. The obtained data will be used for an estimation of the deposition of particulate matter and chemical components from the atmosphere to the Arctic Ocean.

Sediment transport via sea ice is expected to contribute significantly to deep-sea sedimentation at least in regions of ice ablation (Pfirman *et al.*, 1990; Nürnberg *et al.*, 1994). Much work has been performed to study the "dirty ice" in the Arctic but the transport of sedimentary material by icebergs has been studied only occasionally. So, it is important to study the role of different sources of ice-rafted sediments in supplying the Arctic, especially the Gakkel Ridge area. Thus, "dirty sea ice" has been sampled at numerous locations during the ARK XVII/2 expedition; 17 samples have been obtained (Tab. 3). Study of particulate matter transported by icebergs is described in the Chapter 4.9. At AWI the "dirty ice" samples will be melted. After that grain size, mineral and elemental composition, contents of organic compounds, and carbon isotope composition will be

studied at IORAS and AWI, radionuclides will be studied in Marine Sciences Research Center, New York, USA. Using the obtained data we try to estimate the input of matter from different source regions delivered by the drifting ice to the study area.

Table 3. Time and locations of sampling of snow, dirty ice and ice cores.

Ice station	Date	Samples				
		snow			dirty ice	ice cores
		NN	cm	age	NN	
216	04.08.2001				1	
217	05.08.2001	1	0-2	old	2	
218	06.08.2001	2	0-2	old	3	*
220	08.08.2001	3	0-2	old	4	*
		3-a	2-14	old		
221	09.08.2001				5	
222	10.08.2001	4	0-2	old	6	*
		4-a	2-7	old		
223	11.08.2001				7	
					8	
224	12.08.2001				9	
225	13.08.2001	5	0-5	fresh		*
		5-a	5-11	old		
226	14.08.2001	6	0-5	fresh		
		6-a	5-13	old		
228	16.08.2001	7	0,8	old	10	*
		8	1 - 10	old		
		9	10 - 22	old		
		9-a	22-26	old		
229	17.08.2001				11	
232	20.08.2001	10	0-1	fresh		*
		11	1-5	old		
		12	5-8	old		
233	21.08.2001	13	0-1	old	12	*
iceberg 1	21.08.2001					*
234	22.08.2001	14	1-7	old		
					13	
					14	
237	25.08.2001	15	0-2	old		*
		16	2-7	old		
238	26.08.2001	17	0-2	old		*
		18	2-5	old		
		19	5-8	old		
241	29.08.2001	20	0-4	old		*
242	30.08.2001	21	0-4	old		
244	01.09.2001	22	0-1	fresh		*
		23	1-6	old		
245	02.09.2001	24	0-2	fresh		
		25	2-6	old		
		26	6-22	old		
248	05.09.2001	27	0-2	fresh		*

		28	2-10	old		
249	06.09.2001	29	0-2	fresh		*
		30	2-7	old		
		31	7-13	old		
251	08.09.2001	32	0-2	old		
		33	2-5	old		
		34	5-9	old		
253	10.09.2001	35	0-2	fresh		
		36	2-4	old		
		37	4-12	old		
		38	12-20	old		
254	11.09.2001	39	0-2	fresh		
		40	2-6	old		
		41	6-11	old		
256	13.09.2001	42	0-0.3	old		
		43	0.3-10	old		
		44	10-14	old		
258	15.09.2001	45	0-1	old		
		46	2-3	old		
		47	3-12	old		
260	17.09.2001	48	0-1	old		
		49	1-4	old		
261	18.09.2001	50	0-1	old		
		51	1-4	old		
262	19.09.2001	52	0-2	fresh		
		53	2-4	old		
		54	4-7	old		
264	21.09.2001	55	0-2	fresh		
		56	2-5	old		
267	24.09.2001	57	0-2	fresh		
269	26.09.2001	58	0-2	old		
270-2	27.09.2001				15	
270-3					16	
270-4		59	0-2	old	17	
Ice station	Date	Samples				
		snow			dirty ice	ice cores
		NN	cm	age	NN	

4.10 Icebergs: Types and Sediment Content

(V. Shevchenko, C. Haas, R. Spielhagen)

Icebergs are rarely observed in the central part of the Arctic Ocean. Only on the eastern coast of the Severnaja Zemlja Islands are a number of glaciers calving

into the Laptev Sea. Therefore, icebergs provide a unique tracer for the origin and drift trajectory of a certain ice field. However, the interpretation of iceberg observations is complicated by the fact that they might drift for some months through open water until they are eventually enclosed into the pack ice of the Transpolar Drift, and that neither the location nor time of enclosure are known. In three different regions high numbers of icebergs were observed (see Fig. 15), although this seems only natural for a cruise track along the Transpolar Drift. Six of these icebergs were sampled (Fig. 13). Their ice and sediments will be analysed to estimate their origin.

4.11 Deployment of Drifting Meteorological Buoys

(C. Haas)

The main goal of the International Arctic Buoy Programme (IABP; <http://iabp.apl.washington.edu>) is the establishment and maintenance of a network of drifting buoys in the Arctic Ocean to monitor synoptic-scale fields of surface pressure and temperature as well as ice motion. As a main partner of the IABP, the AWI contributes and deploys two to four buoys every year. ARK XVII/2, reaching far upstream of the Transpolar Drift, offered the opportunity to deploy an array of four buoys on ice floes close to the North Pole. All buoys measure air temperature and surface pressure, and their GPS position to derive ice drift trajectories. The data are transmitted to Europe via the ARGOS satellite communication system. The buoys will operate for a time period of 2 to 3 years, during which the ice floes will drift through Fram Strait into the North Atlantic. The deployment dates and positions are given in Figure 13 b and Table 4, respectively. One buoy (ARGOS ID 8056) was actually transferred to HEALY and deployed with their helicopter at the site of a drift camp of the North Pole Environmental Observatory (NPEO), which was set-up close to the North Pole in April 2001. The NPEO measures additional meteorological variables, as well as water temperature and salinity down to 500 m depth. Our buoy replaced the old temperature and pressure sensor, which stopped functioning one month before. One buoy (ARGOS ID 9357) was also used as a tracer for the recovery of the seismologic and MT station deployed during ARK XVII/2 (see geophysics: 9.8 and 9.9). Typical buoy tracks with the tide-induced ice drift superimposed onto the larger-scale wind drift are shown in Appendix 15, Figure App. 5.

Table 4: Dates and position of Argos buoy deployments.

Argos ID	Date	Position	Contributor
9357	03.09.2001	86°05'N, 83°34'E	AWI
9359	06.09.2001	90°00'N, 120°00'E	AWI
24292	08.09.2001	88°27'N, 92°54'E	National Ice Center, USA
8056	16.09.2001	87°29'N, 52°20'E	AWI

4.12 A "Fishermans Camp"

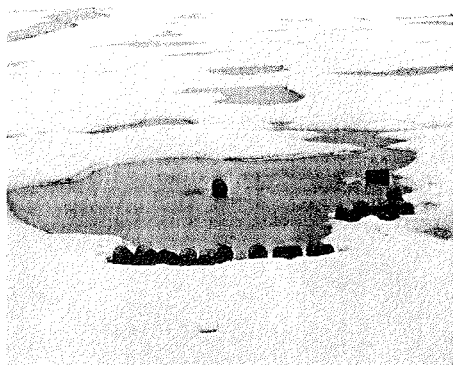
(C. Haas)

Station on 25.08.2001 (day 237) at 85° 37.09' N, 19° 18.82'E, 14:47 UTC:

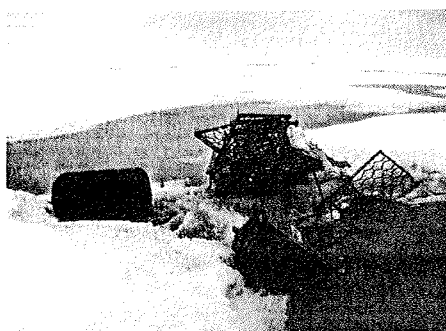
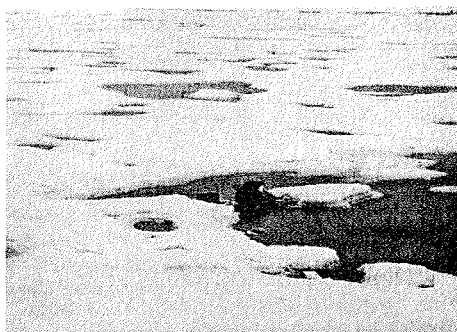
On a flat, ponded floe of approx. 500 m diameter, with no prominent ridges, a depot of drums was observed from the ship and then visited. Close to one floe edge, two groups of about 30 drums in total were lying on the ice, separated by a pile of mattresses and bedsteads inbetween. There, also remnants of burned firewood, ash, PE and glass bottles were found, frozen into the ice cover of a melt pond. Some styrofoam plates of 100x50 cm, partially broken, were scattered around, as far as 50 m away from the main site.

The empty barrels were labelled as containing soya oil, imported into the USSR from Italy in 1991. However, almost certainly they were used for something else, most likely diesel oil, when they were placed onto the ice. The content of one barrel had leaked into one small puddle. This was a yellow/orangish liquid, degraded into flakes. Two water samples were taken, one for later chemistry analysis (V. Shevchenko). One was viewed under the microscope, showing an emulsion-like appearance, typical for oil.

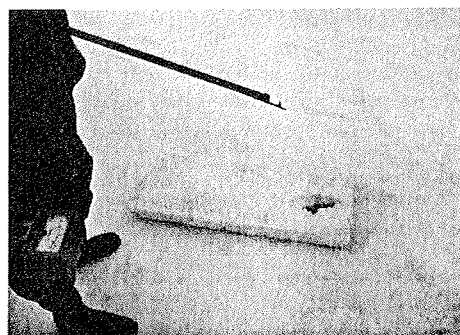
Speculations are that this drum depot was a remnant of a helicopter depot out on the ice, to support long range flights, or of an ice camp for ice fishing. From the appearance of melt ponds, it is unlikely that the ice is broken-off coastal fast ice. The deployment was probably not very old, as melting around the drums and other rubbish was not very extensive.



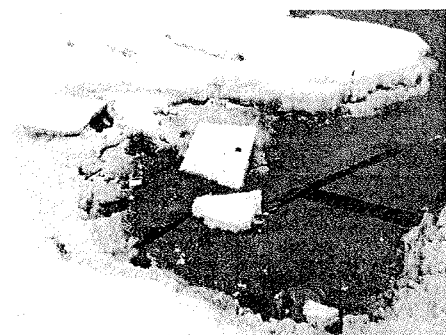
One of two groups of barrels.



The pile of mattresses and bedsteads. The black pond bottom to the right is caused by ash. The red box is an oven.

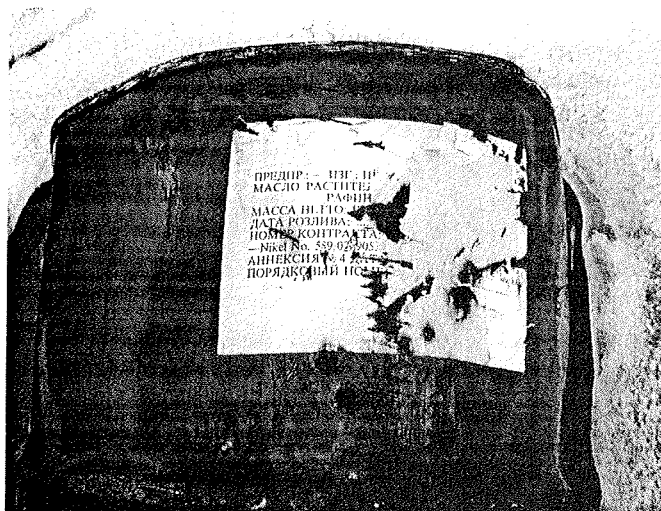


Styrofoam plate.



Burned firewood, styrofoam, and bottles.

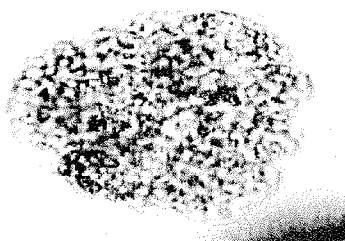
Fig. 37: Various impressions of the "Fishermans Camp".



Russian writing, indicating vegetable oil.



English writing, indicating soya oil exported from Italy to USSR in 1991.



Microscope image of the liquid sampled from a pond under a leaked barrel (120x ampl).

Fig. 38: Various details from the "Fishermans Camp".

5. Hydrography

5.1 Secchi Depth Measurements

(V. Shevchenko)

The Secchi-disc was used for qualitative estimation of the concentration of suspended particulate matter (turbidity). It is a flat circular plate, 30 cm in diameter, all white. It is lowered through the water column in a horizontal attitude until it is observed just to disappear. The depth, at which this happens, is called the Secchi depth, and it depends on the turbidity of the water. The Secchi-disc is both cheap and easily made, and it has been used by oceanographers for over a century as a rapid means of assessing water clarity (Seawater, 1995). In our expedition 32 measurements of the Secchi depth were carried out (Tab. 5). It varied from 16 to 30 m, making on the average 21 m. It shows that the concentration of suspended matter in water is very low. For example in the Kara Sea the 5-m transparency isoline shows the borders of the main area of influence of the fresh turbid waters from Ob, Yenisey and other rivers (Lisitzin *et al.*, 2000). Only in outer part of the Kara Sea, where the concentration of suspended matter is <0.5 mg/l, the Secchi depth increases up to 15 m.

Table 5. Time, locations and results of Secchi depth measurements.

Station	Date	Time (UTC)	Coordinates		Secchi depths, m
			Latitude (N)	Longitude	
59-199	06.08.01	22.40	85°33.3'N	16°06.1'E	22
59-203	07.08.01	21.18	84°57.9'	9°26.2'E	16
59-207	09.08.01	02.05	84°38.7'	5°10.9'E	21
59-214	11.08.01	09.40	83°36.2'	3°06.6'W	22
59-216	12.08.01	16,25	85°05.2'	6°05.1'W	24
59-228	16.08.01	22.46	83°53.5'	1°05.7'W	20
59-229	17.08.01	07.39	83°56.8'	0°15.7'W	19
59-233	18.08.01	08.00	84°16.0'	1°24.9'E	23
59-234	19.08.01	00.10	84°34.3'	3°06.4'E	23
59-236	19.08.01	15.21	84°43.8'	4°32.7'E	21
59-245	21.08.01	19.48	85°05.5'	10°44.8'E	19
59-252	25.08.01	17.22	85°37.2'	18°12.4'E	18
59-255	26.08.01	10.27	85°47.2'	20°20.6'E	19
59-257	26.08.01	21.39	85°57.7'	23°37.6'E	20
59-271	31.08.01	20.21	86°50.4'	47°43.1'E	19
59-274	02.09.01	09.55	86°43.7'	66°45.2'E	24
59-275	02.09.01	20.20	86°35.5'	69°00.7'E	23
59-276	03.09.01	03.14	86°36.6'	70°28.8'E	28
59-279	05.09.01	17.25	89°00.8'	130°06.1'E	17
59-280	06.09.01	18.57	89°59.2'	108°03.3'E	18
59-281	08.09.01	09.43	88°23.5'	93°30.3'E	19
59-282	09.09.01	03.35	87°38.0'	81°56.3'E	25

Station	Date	Time (UTC)	Coordinates		Secchi depths, m
			Latitude (N)	Longitude	
59-283	10.09.01	08.19	87°03.3'	76°38.4'E	25
59-284	10.09.01	22.06	86°43.3'	74°31.4'E	24
59-285	11.09.01	01.28	86°41.8'	74°12.8'E	26
59-287	11.09.01	19.05	86°28.9'	73°55.5'E	19
59-288	12.09.01	08.08	86°20.9'	73°35.4'E	30
59-290	13.09.01	06.20	86°33.7'	69°25.2'E	20
59-292	14.09.01	04.23	86°47.1'	65°27.7'E	24
59-308	20.09.01	08.47	86°20.2'	38°39.4'E	21
59-310	21.09.01	09.50	85°59.9'	32°21.4'E	22
59-316	23.09.01	09.28	85°50.3'	21°22.0'E	26

5.2 Evidence for Hydrothermal Activity, Gakkel Ridge

(J.E. Snow, M. Bock, H. Feldmann)

Hydrothermal activity on mid-ocean ridges has been known for about the last 20 years. It was long suspected because of the metamorphic ores bodies found in ophiolites such as the Troodos massif on Cyprus. However, it was not until actual hydrothermal vents were found on the ocean floor (so-called black smokers) that the study of present day seafloor hydrothermal activity really began. During the AMORE expedition, hydrothermal activity was traced using MAPR (Miniature Autonomous Plume Recorder) devices attached to the main wire during sampling operations. This device records a continuous set of pressure, temperature and light scattering measurements, and is very useful in assessing the level of hydrothermal activity present on a mid-ocean ridge.

The Arctic Water Column

The major feature of the temperature structure of the Arctic Ocean is a positive thermal anomaly of around 3°C (Nansen, 1906). This is clearly visible in Figure 39, as in all water column plots from the central Arctic Ocean. At a depth of about 2500m, the Nansen anomaly is no longer significant, and there is even a slight temperature increase (about .0001° / m) caused by the adiabatic pressure-temperature relationship. These features are observable in all MAPR and CTD profiles from this expedition.

The first order features of the light scattering sensor (LSS) are also clear from Figure 39 – there is a large positive scattering anomaly in the first few meters, where all the biological activity takes place, and then the profile is relatively flat all the way to the bottom.

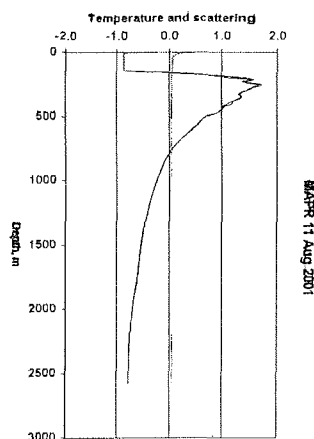


Figure 39: Temperature and LSS profile, 11.8.2001.

Near-bottom MAPR Anomalies

If the data are examined in more detail, however, a fine structure emerges that in other ocean basins has been unambiguously linked to the presence of hydrothermal activity (Baker, *et al.*, 1997). Figure 40 shows a detailed view of a clear anomaly in the LSS

record from a lowering on September 2, 2001. The large spike at about 2300m water depth is probably not significant, as it is only observable on the way down and not the way up. The much broader anomaly centered around 2700m depth however is much more likely

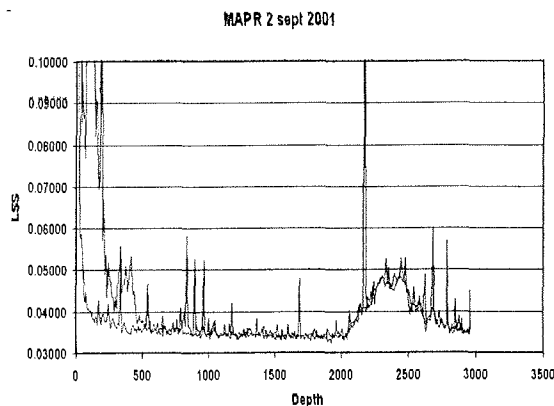


Figure 40: LSS Detail plot.

to be significant, since it is well beyond the background noise of the instrument, is visible in many adjacent records and is observable both on the down and up segments of the record. Unambiguous LSS anomalies are identifiable in 5 of the 30 MAPR records from this cruise, 12 are less developed (see Appendix 14.10).

Because of the Nansen temperature anomaly, the temperature profiles measured by the MAPR are much more difficult to interpret than the scattering pro-

files. In some cases, anomalies are so large that they can easily be seen. In other cases they are much subtler, but are there nonetheless. Figure 41a illustrates this situation from a MAPR profile from 29 August. In this MAPR profile there is a small but recognizable LSS anomaly centered at 3200m. The temperature profile is shown in detail in Figure 41b, in which there does not appear to be an anomaly. However, if the linear trend is removed from the data, as in Figure 41c, there is an anomaly of amplitude 0.003 degrees, still far beyond the background noise of the instrument, and reproducible on both up and down trips.

Because of the Nansen thermal anomaly, however, it is difficult to unambiguously recognize temperature anomalies in the water column above about 2500m depth. Still unambiguous temperature anomalies are identifiable in 4 of 30 MAPR records and 13 are less developed. In all, 3 MAPR records have both temperature and scattering anomalies at the same level, 5 records have scattering anomalies only, 6 records have only temperature anomalies, and 1 shows no significant sign of hydrothermal activity.

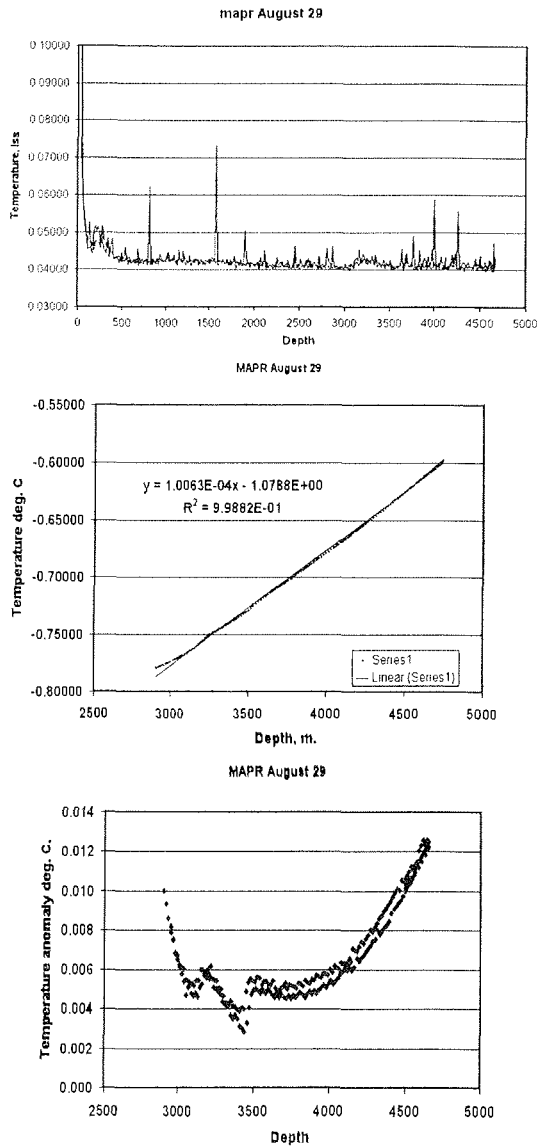


Figure 41: LSS and temperature profiles from 28 August, 2001. a) LSS profile. b) Pure temperature profile of the lower 3000m showing linear fit to data. c) Profile with linear component removed.

This rate of hydrothermal activity is much higher than the 75% reported by the scientific party aboard HEALY. This may be due to the fact that we did not deploy the MAPR on dredge hauls, but only on TV-grab deployments on identifiable, morphologically young volcanoes. Still this is a remarkably high proportion of active hydrothermal activity, considering that this ridge was predicted to have a very low degree of heat transfer because of the slow spreading rate.

AURORA Hydrothermal Field

The Aurora hydrothermal field was discovered on the 12th of August (Dredge haul D8) by HEALY. When dredging a volcanic high in the central graben of the northern end of Lena Trough, fresh hydrothermal sulfide was recovered in the dredge. These samples consisted mainly of chimney pieces, and chinks of massive hydrothermal sulphide. The MAPR attached to the dredge showed a substantial anomaly. POLARSTERN arrived at the site a few hours later and ran an OFOS tow over the site. Figure 42 shows the dredge track and the OFOS track, which intersect near the top of the hill. Unfortunately, none of the still pictures from OFOS were useable. The video material, however, shows possible evidence of hydrothermal vent activity. These sightings are sketched in on Figure 42.

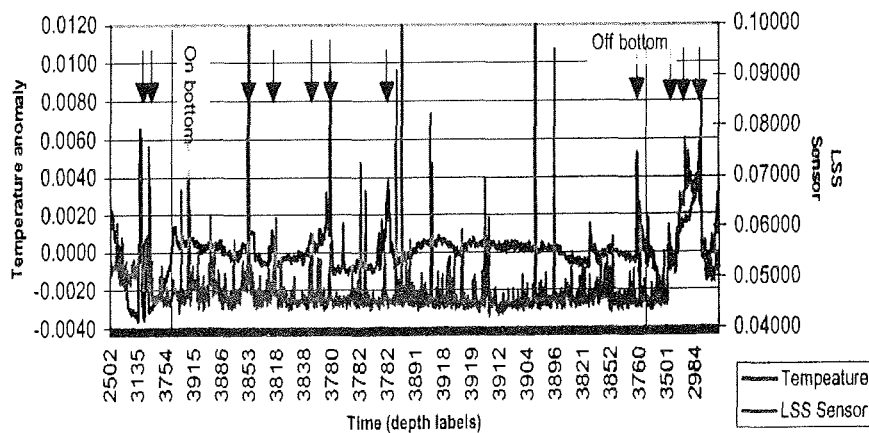


Figure 42: MAPR trace from the Aurora field showing locations of double anomalies.

The MAPR data from the OFOS show multiple small double anomalies and at the final raising, a huge double anomaly.

6. Bathymetry

(S. Gauger, J. Hatzky, T.Hartmann)

The objective of the bathymetric working group on this cruise was a systematic high-resolution survey of the Gakkel Ridge in co-operation with the HEALY using multibeam sonar systems.

The main characteristic of the used deep-water sounding system HYDROSWEEP DS2 on the POLARSTERN is the 90° coverage angle in which the seafloor is depicted with 59 specific values for water depths (Preformed beams PFB) perpendicular to the ship's long axis. The accuracy of this measurement is ~ 0.5% of waterdepth. For the correction of the slant sonar beams the automatic self-calibration process of HYDROSWEEP was used. The multibeam sonar system in the partnership was the SEABEAM SYSTEM 2112, a deep water echosounding system similar to the HYDROSWEEP, but with a 120° coverage angle, subdivided into 121 several PFBs. That means SEABEAM provides a greater coverage of the seafloor with higher resolution than the HYDROSWEEP system. The accuracy of the SEABEAM measurement is also ~ 0.5% of the waterdepth.

On heat flow stations conductivity, temperature and density (CTD) measurements were performed in order to get information about the water properties. Altogether 19 CTD stations were recorded. From this data sound velocity profiles of the water were calculated to compare the results obtained from the automatic HYDROSWEEP cross-fan calibration with the direct measured parameters. Immediately after the start of the expedition a data link between the two ships was established to exchange digital files up to a maximum distance of 8 km. This connection was used every day or as soon as possible in order to supply both ships with the same bathymetric data sets.

The major part of the work was the operation of HYDROSWEEP. Because of the ice-operation the mostly automatically working multibeam sonar system had to be observed continuously in order to intervene in case of faulty or abnormal functioning. Ice conditions made post-processing the depth data difficult. Erroneous measurements were caused by hydroacoustic disturbances and the changing of the ship's speed and direction, as these factors have a large influence on the measurements. Therefore it was mandatory to check the positions, depths and the ship's attitude data for outliers or blunders, and to correct them

when necessary. This part of data processing was done by using the interactive software HDCS (Hydrographic Data Cleaning System).

The ship's operation in high geographic latitudes ($> 85^{\circ}$ N) was heavily impeded through a limited functionality of the navigation system NACOS (ATLAS Electronics). The navigation problems were not caused by environmental conditions in the Arctic waters or by the configuration of the GPS satellites. The problems were only generated by the NACOS system's software, which is not designed for navigation controlling north of 85° N. The major difficulties generated by this lapse was that the main research systems like HYDROSWEEP, PARASOUND (an echosounding system to detect sediments) and the data acquisition system PODAS were not supplied with navigational data by NACOS in regions north of 85° N. In this situation positions (generated by LEICA GPS-Receivers and later extracted from the PODAS database) were combined with the multibeam depths using an on-board developed program. The results of this procedure, which was used 3 days, were checked with the position editor of the HYDRO-MAP-OFFLINE software. When crossing latitude 85° N for the second time, NACOS was working already with a new navigation telegram.

The main objective of work was the analysis of multibeam data and the compilation of preliminary bathymetric charts (Fig. 43 and 44). For the preparation of quick-look maps the software CONTOUR was used, which creates multibeam swath plots in correct planimetric position. Further presentations of the sea bottom topography were made by using the Generic Mapping Tool (GMT) software. With GMT grids were calculated out of the edited data. Based on the grid, contour line maps with colour coded depth ranges were produced, which gave a vivid display of the oceanic ridge topography. Conclusions about the history and characteristics of the ridge were drawn using the detailed maps of the seafloor topography. The complete survey covers an area of 8890 km length and a varying width between 18 and 46 km. Two topographic anomalies were discovered which separate the ridge in areas with different sediment characteristics. Based on the bathymetric maps, the localization of places which show great promise for the petrological sampling program (dredges, TV-grabs) was accomplished. Bathymetry has been proven as being important for seismic investigations and magnetic measurements in order to interpret and geolocate the collected data.

Additionally an important aspect of this cruise was to utilize and analyse the SCICEX (Scientific Ice Expeditions) data of the Gakkel Ridge. These datasets

were collected using the SCAMP system (Seafloor Characterization And Mapping Pods) system of the nuclear submarine USS Hawkbill in 1998 and 1999. Based on this information, geological sampling locations were selected. Because of the position errors of the SCICEX data, which were caused by the submarine's navigation system under the sea ice, the selected sampling locations were not correct. With the help of a light table, it was possible to determine the navigation shifts for the SCICEX data graphically by overlaying the new maps and the SCICEX maps. Improved coordinates for the geological sampling stations were achieved by applying these shifts to the SCICEX coordinates. The calculated shifts were not of the same size over the survey areas and varied from 2 km to 6 km. For this reason it was not possible to correct the entire SCICEX navigation in one step, but just for small areas.

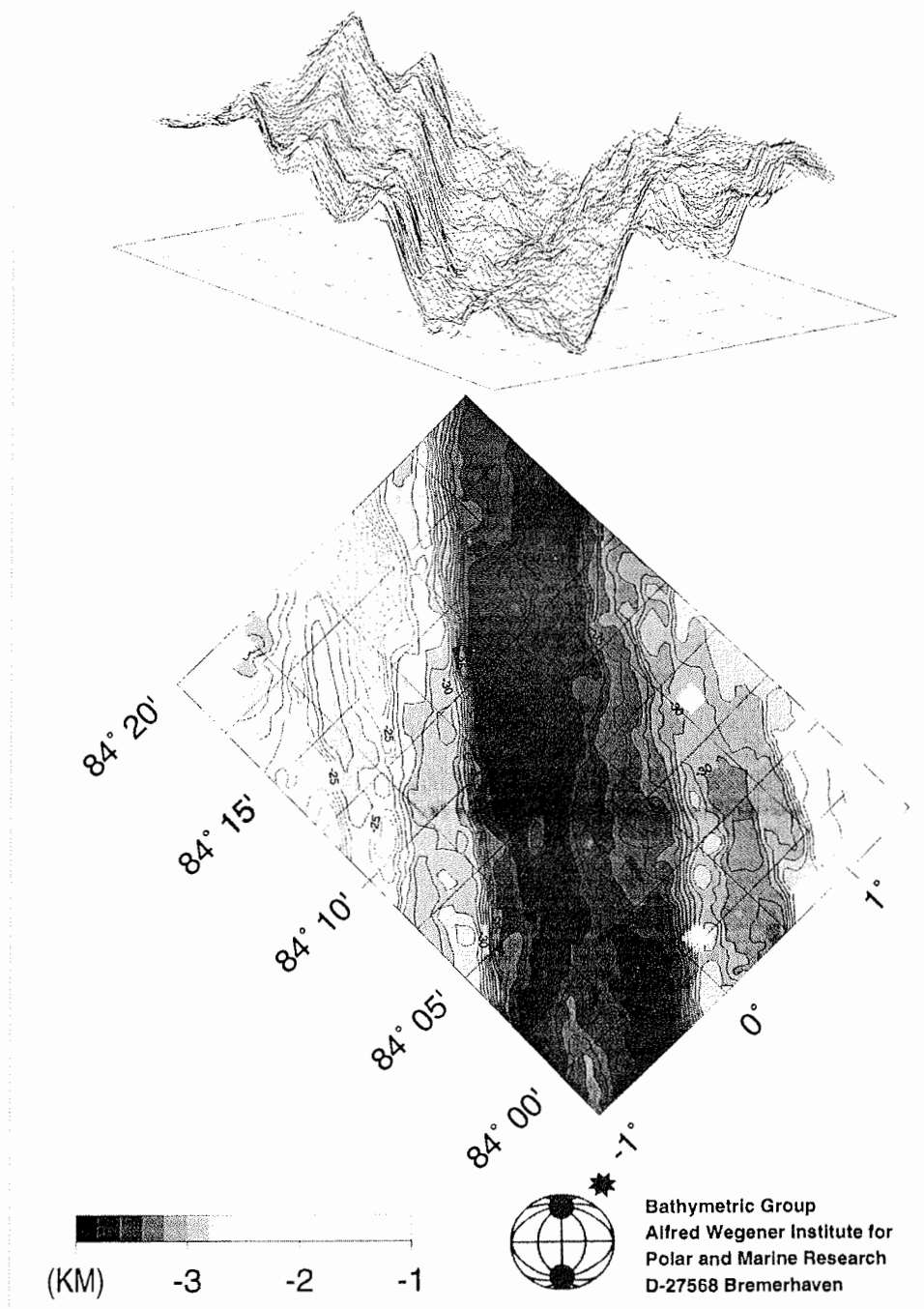
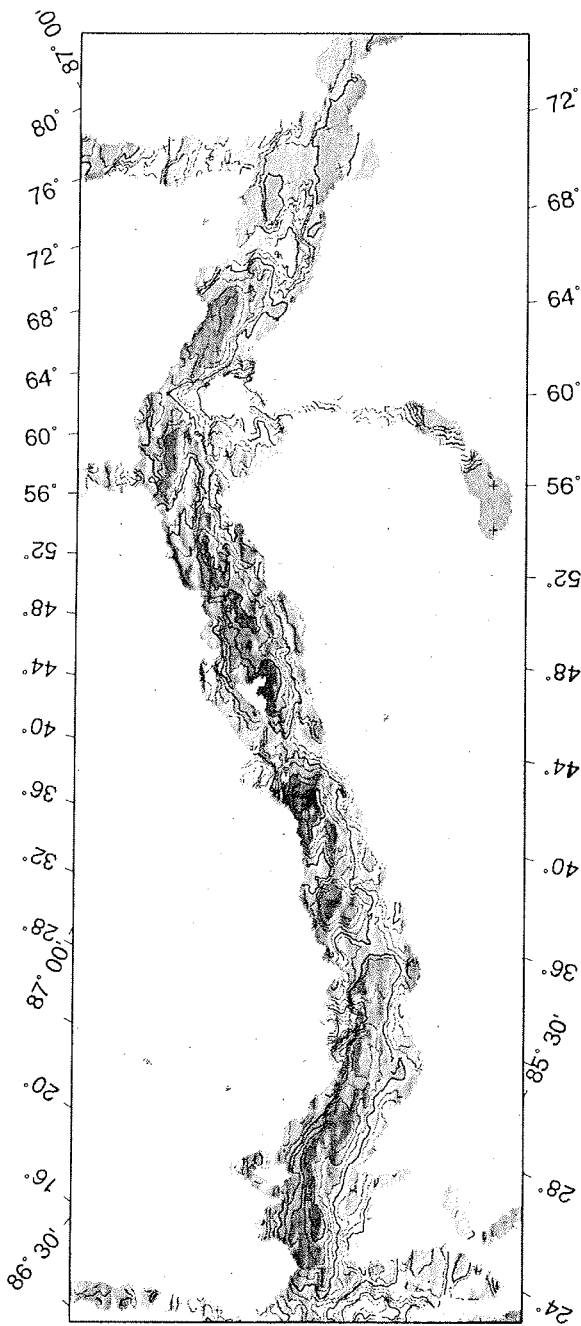
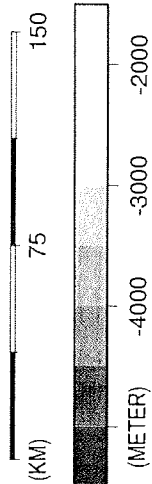


Figure 43: The 3-D picture represents a typical part of the western Gakkel Ridge, with the impressive flanks on both sides and the little ridge on the valley basement.



Eastern Gakkel Ridge
 Hydrosweep / Seabeam Bathymetry of AMORE 2001
 Background Bathymetry of IBCAO Vol.1
 Map Projection: Polar Stereographic
 Scale 1 : 1 700 000
 Contour Interval: 250 m



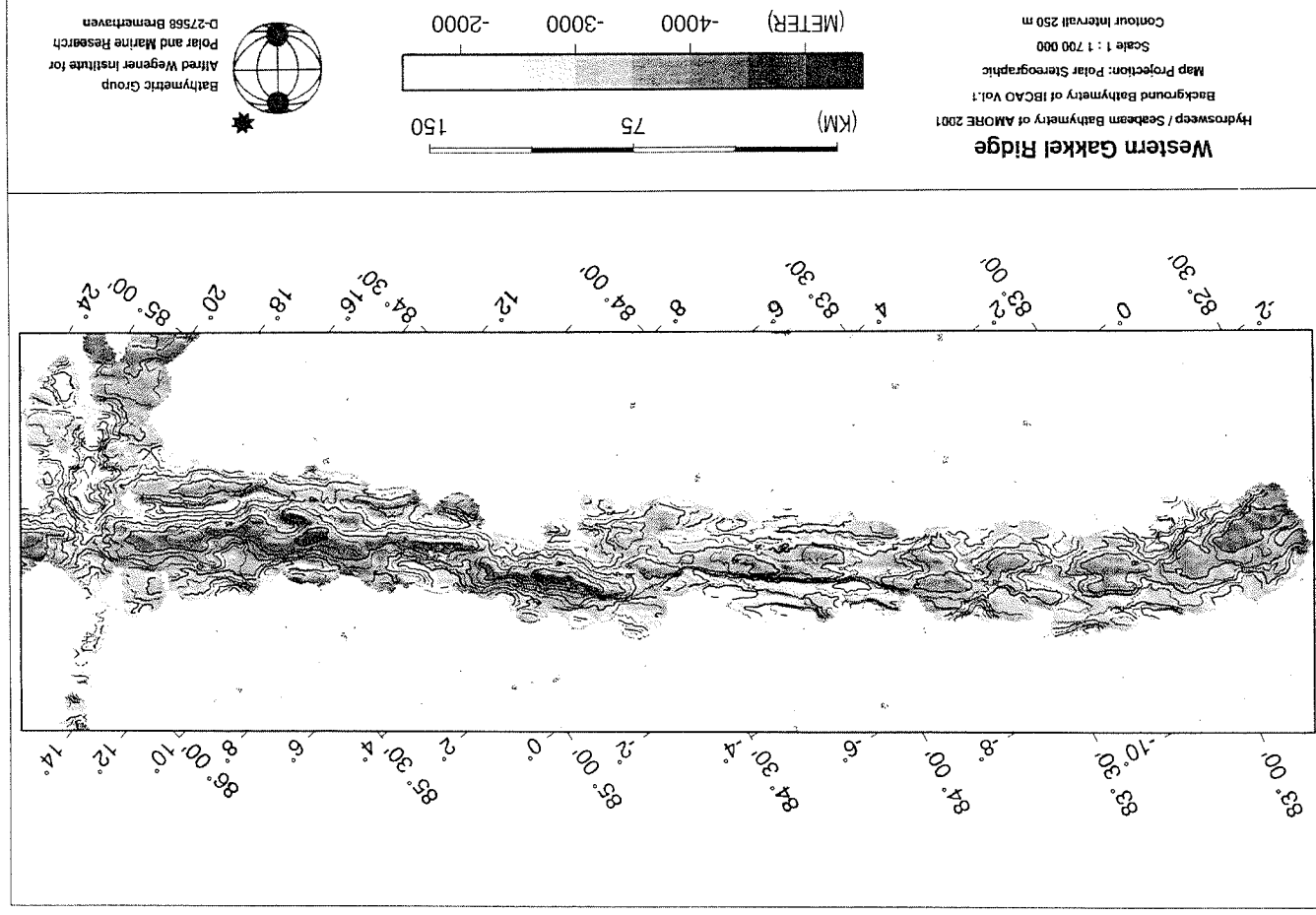


Fig. 44 a+b: The graphical overview shows the area of the bathymetric survey of Gakkel Ridge, which covers nearly 33 000 km² (comparable with the area of Nordrhein-Westfalen). At the position 86:42.44 N / 61:08.22 E we discovered the shallowest place in the Arctic basin with a water depth of 566 m on the top of a huge seamount // (Ch. Appendix 18, this volume). The largest measured depth on this cruise was 5673 m in the central valley of Gakkel Ridge.

7. Sediment Distribution

7.1. Parasound High Resolution Acoustic Profiling

(S. Drachev)

The PARASOUND device designed by Krupp Atlas Electronics GmbH (Bremen, Germany) is among the numerous echosounder devices, which utilize a high frequency (3.5-12.5 kHz) acoustic signal for imaging of sediments down up to 200 m sub bottom. Obtained acoustic records can be interpreted in structural and seismic stratigraphic terms, especially successfully when combining with the coring. According to the research program of the ARK XVII/2 expedition, the PARASOUND along-track survey was mainly aimed to:

- Study distribution of the sediments along ship track, their facial and structural appearance;
- Revealing appropriate locations for sediment sampling by gravity and box corers, as well as for the heat flow measurements.

The PARASOUND was set into 24-hours operational mode as we entered the ice-edge at the Barents Sea continental slope (81°52' N, 29°13' E) and started cruising towards the Gakkel Ridge on 04.09.01 at 09:00 GMT. We kept PARASOUND under a continuous working regime till 13.09.01, when it was turned into a sporadic activity because of several reasons described below. It was then set back into the continuous operation mode on 25.09.01 when POLARSTERN, convoyed by HEALY, left the working area heading towards the Barents Sea. The PARASOUND survey ended on 28.09.01 as soon as ship reached the shelf break at 81°25' N, 32°13' E north of Spitsbergen.

Data acquisition system and data description

The PARASOUND echosounder and its peripheral devices are exhaustively described previously (Thiede, 1988; Fütterer, 1992; Rachor, 1997; Jokat, 1999). In 2001 both the hardware and PARADIGMA software were slightly modified. The main changes were made concerning the data storage. The old-fashioned tape recorder, which was used to dump the data onto DAT-tape storage, was replaced with five removable hard disks of 1.2 Gb capacities each. As the hard disks have been becoming full, they were replaced with the blank ones, and then the data were dumped onto a CD. The settings of the PARADIGMA system for digitizing recorded seismograms were as follows: sampling rate 40 ms, trace length 266 ms, block size 10640 bytes, format PS3.

As it was recognized during the first expedition into the High Arctic (Thiede, 1988) and confirmed later (Fütterer, 1992; Jokat, 1999), the ship operation in the heavy ice conditions produces a noise in range 3.5-4.5 kHz. This ice-breaking noise disturbs the PARASOUND data significantly. Especially strong disturbances are generated during astern ship movements, which have been happening rather frequently during the ice ramming. The latter has also been often resulted in a specific PARASOUND record dominated by a periodically repeated reflection pattern due to back-and-forth ship movements above the same sea-bottom feature (Fig. 45).

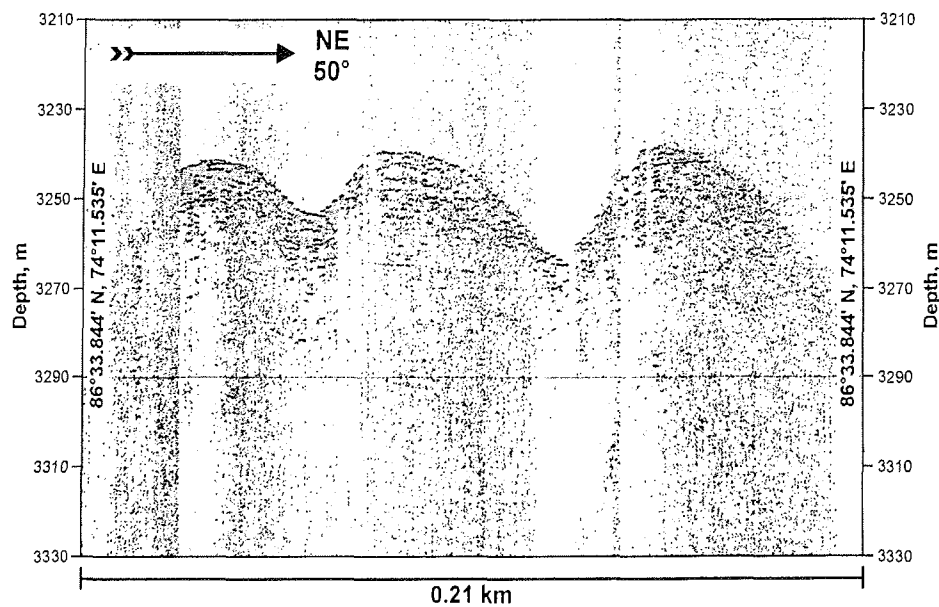


Fig. 45 An example of the PARASOUND DESO record with periodically repeated reflection pattern due to ice ramming above the same sea-bottom feature. Although the time interval recorded is about 20 min, the distance of the total ship movement is 0.21 km only.

The sea-bottom topography represents another factor limiting the quality of the acoustic PARASOUND record. While the data quality is rather good from terrains with a flat and smooth sea-bottom, the steep slopes and rough floor with variable morphology disturb the return echo drastically. Obtained from those areas, the record either is strongly influenced by side reflections (Fig. 46) or exhibits no reflections at all. Since a significant part of the cruise has been devoted to petrologic sampling of the ridge by dredging the walls of the spreading rift valley, acquisition of any reliable PARASOUND data was lowered almost to a zero above the rift sides.

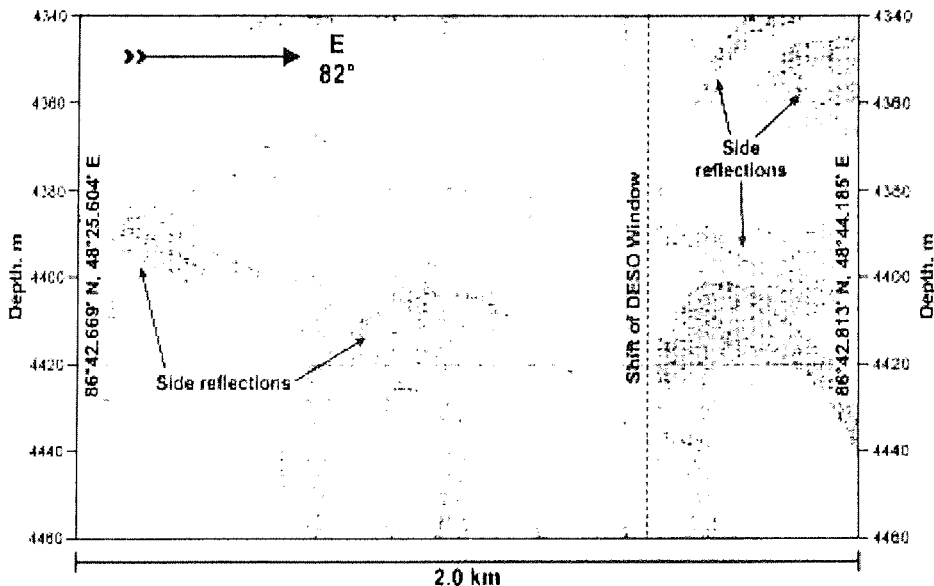


Fig. 46 An example of a poor acoustic PARASOUND record affected by side reflections. Central part of the rift valley.

Especially unfavorable combination of these factors has occurred between 13 and 25 September, when the expedition came into a phase of an intense sampling of the rift walls in the eastern part of the working area. This caused impossibility to record the reflected echoes for the most of the operational time. Since this part of the ridge has already been surveyed during the first part of the expedition, it was decided to turn the PARASOUND into a discontinuous mode of operation. During this period the PARASOUND was switched on 18 times for short periods (1-4 hrs), mostly when the ship has been steaming across the rift valley or when it was requested to search for an appropriate station for heat flow measurements. But only in a few cases we succeed to collect reliable data.

The last cause, which made operator's work more difficult and led to data losses, was unstable work of the PARADIGMA software. This caused two malfunctions, which have been occurring independently but obviously were the result of software failures. The main problem was created by the unexpected and rather frequent system crashes followed by rebooting the computer. The total number of the noted software crashes is 239, but there were more, as some of them have not been reported in the PARASOUND Log. The second problem, assumed to be software-related, was malfunction of the Online Profile printer, manifested in permanent leaking of the ink while the printer has been waiting for the data (printer cartridge in the rightmost position). We have tried to solve this problem by changing

of the printer but it did not help. Ink leaking caused a high consuming of the printer cartridges.

Table 6. The main characteristics of the PARASOUND data.

Morpho-tectonic Province	Start of Record		End of Record		Range of Penetration (m)	DESO Roll, #	Data Files, *.ps3	Data Quality
	Date/Time GMT	Coordinate	Date/Time GMT	Coordinate				
Barents continental margin I	04.08.01 09:00	81°52' N 29°13' E	05.08.01 00:00	83°11' N 26°25' E	5-35	1, 2	08040855- 08042355	Very good
Nansen Basin I	05.08.01 00:00	83°11' N 26°25' E	05.08.01 23:44	84°58' N 21°32' E	15-65	2	08050000- 08052347	Very good and good
Gakkel Ridge I	05.08.01 23:44	84°58' N 21°32' E	04.09.01 04:46	87°11' N 78°03' E	0-40	2-11	08052347- 09040446	Poor and very poor
Amundsen Basin	04.09.01 04:46	87°11' N 78°03' E	09.09.01 15:04	87°09' N 78°13' E	15-90	11-13	09040446- 09091501	Very good
Gakkel Ridge II	09.09.01 15:04	87°09' N 78°13' E	26.09.01 18:50	84°44' N 21°48' E	0-40	13-16	09091501- 09261850	Very poor
Nansen Basin II	26.09.01 18:50	84°44' N 21°48' E	28.09.01 04:40	83°11' N 29°51' E	20-55	16	09261850- 09280435	Very good
Barents continental margin II	28.09.01 04:40	83°11' N 29°51' E	28.09.01 21:46	81°25' N 32°13' E	0-30	16	09280435- 09282143	Very good and good

To give an impression about the reliability of the PARASOUND data, a visual control of the quality of analogue DESO record has been applied using a four-level quality scale (Tab. 6):

- Very good quality denotes a continuous and readable record slightly disturbed by ice-breaking produced noise;
- Good quality denotes an almost continuous and readable record disturbed by ice-breaking related noise and short intervals of signal losses;
- Poor quality denotes a discontinuous and almost unreadable record containing short and rarefied intervals with the recorded reflections;
- Very poor quality denotes a record containing almost no readable intervals.

Regional description

In a course of the ARK-XVII/2 expedition we have surveyed three main morpho-tectonic elements (provinces) of the Eurasia Basin, namely: the Nansen Basin, as well as the Barents Continental Margin bordering the basin from the south, Gakkel Ridge and the Amundsen Basin. All these provinces display considerable differ-

ences in the PARASOUND acoustic imagery, as well as in data quality. In this section we consider some general peculiarities of the morphology and sediment pattern of these provinces as consistent with the DESO analogue record and the PARADIGMA online printed profiles.

Barents Continental Margin

The Barents Continental Margin was crossed twice: at the beginning and at the end of the expedition (Table 6). The PARASOUND data of good and very good quality characterize morphological and sedimentary peculiarities of its slope and rise.

The shelf break is located at about 81°26' N, 32°12' E at 200 m of water depth. The upper slope is relative gentle up to water depths of 1200 m. There is a sequence of well-layered sediments, which covers this part of the slope revealing penetration from 0 to 25 m below the sea-bottom. The middle slope extends from 1200 to 2950 m. It is rather steep causing the signal losses. The lower slope and the continental rise down to 4050 m reveal a pile of overlapping sedimentary slumps and turbidite levees, imaged acoustically downward to 30 m subbottom. These deposits demonstrate no internal stratification and the most of the slump bodies are high reflective at the upper part and acoustically transparent inside (Fig. 47).

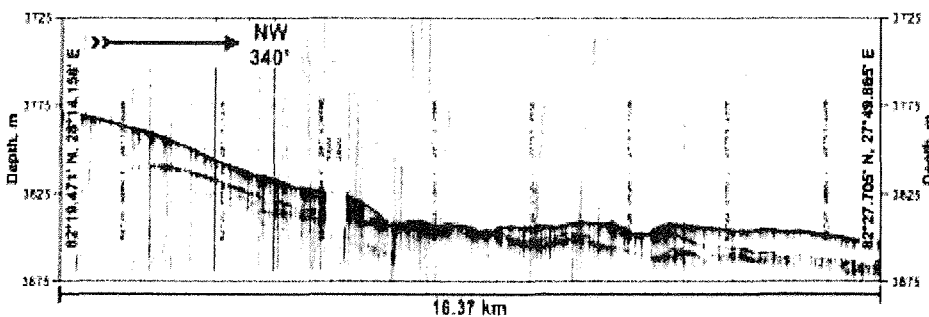


Fig. 47. A pile of overlapping sediment slumps and turbidite levees at the foot of the Barents Sea continental slope (PARADIGMA online printout).

Nansen Basin

As known from the previous geophysical investigations, the Nansen Basin contains a continuous cover of the Cenozoic sediments with a variable thickness up to 1.5 km (Kristoffersen and Husebye 1985; Jokat *et al.*, 1995 etc.). With the

PARASOUND we surveyed the uppermost part of this cover within 60 m of the subbottom interval.

The sediments in the Barents-faced part of the basin exhibit high reflective seismic pattern and clear absence of the stratification. This may be a consequence of abundance of the relative coarse turbidite and debris flow facies, which spread down from the Barents Continental Rise onto the nearest parts of the Nansen Basin's seafloor.

The acoustic pattern is gradually changed towards the Gakkel Ridge as the sediments become stratified. This change is followed by the increase of sound penetration. We assume this facially different section containing mainly distal turbidites. This layered sedimentary succession is rarely disturbed by low-amplitude normal faulting (Fig. 48a), which may be a result of both different rates of compaction and small movements of the basement blocks.

In the vicinity of the southern flank of the Gakkel Ridge we have surveyed two positive diapir-like features, which tower above the seafloor for some 15-25 meters (Fig. 48b,c). The similar features were reported in 1998 as the mud diapirs (Jokat, 1999). During ARK XVII/2 expedition we had an opportunity to verify this earlier suggestion, as the multichannel seismic reflection survey has been accomplished along the same track. The seismic data clearly show that these features represent the uppermost parts of the buried blocks of the oceanic basement outcropped above the seafloor.

Gakkel Ridge

The Gakkel Ridge and especially its axial rift valley were the main targets of the expedition, and the most of the ship operations have been taking place above either its rift valley or the steep walls bordering the spreading axis. The PARASOUND record, as the most, is of poor and very poor quality due to the causes, described above. Nevertheless, we succeed to receive good data along some portions of the ship track. These data, when combined with the bathymetric ones, provide a good basis to decipher the morphotectonic peculiarities of this slowest spreading center.

As revealed by the bathymetric observations, the Gakkel Ridge is pronouncedly segmented along its strike. From the west to east it is consisted at least of three segments in frame of our survey area.

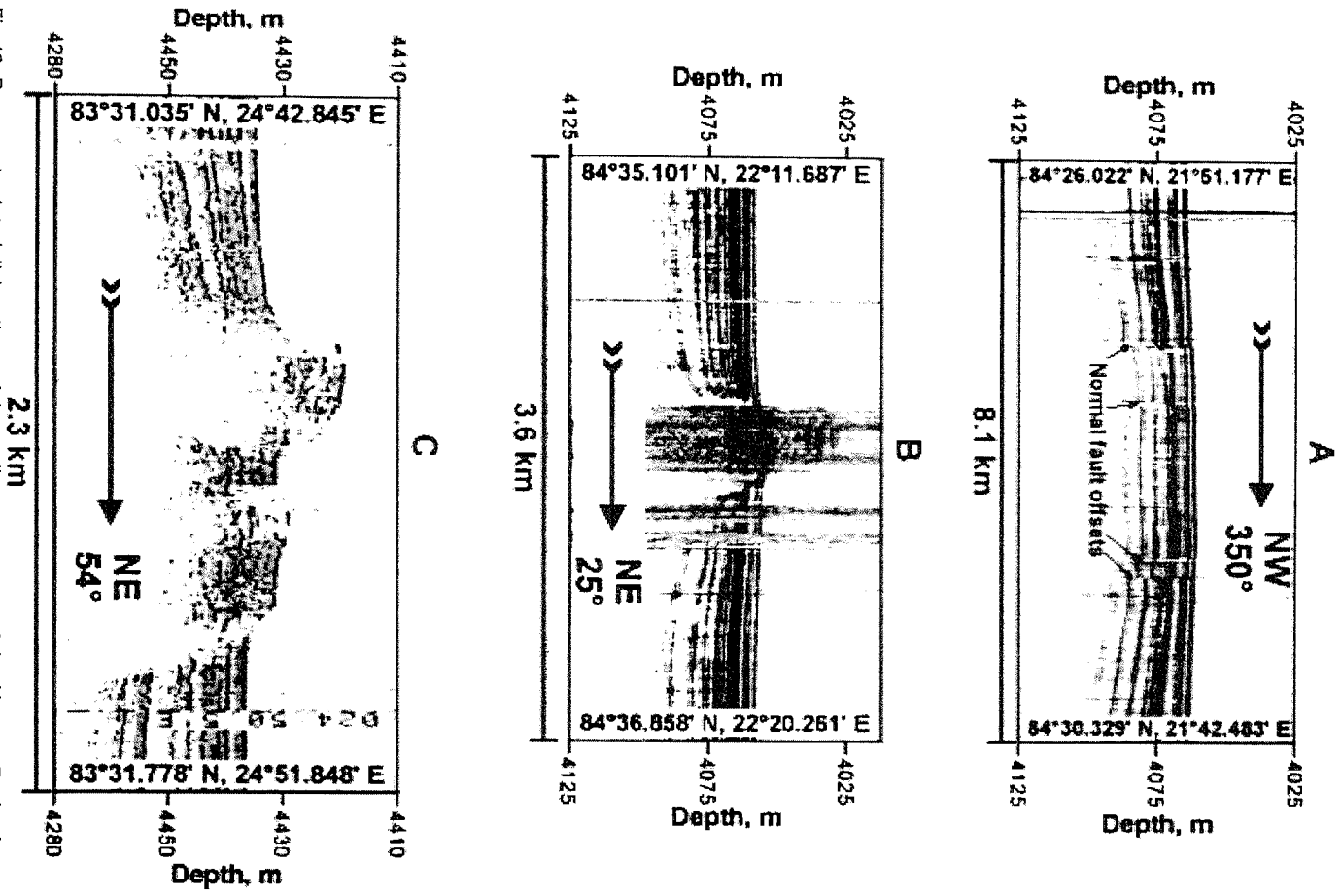


Fig.48. Basement-related dislocations of the sedimentary cover of the Nansen Basin. A – well-layered sedimentary succession disturbed by low-amplitude normal faulting; B and C - the diapir-like dislocations of the sediments, which are caused by outcropping of the uppermost parts of the buried oceanic basement ridges.

The Western Segment between 82°35' N, 06°45' W and 84°32' N, 02°30' E can be considered as magmatically robust. A well-pronounced linear rift valley bounded here by sharp fault-related escarpments (Fig. 49), has the water depths about 4-4.2 km and consists of a well-localized axial volcanic high.

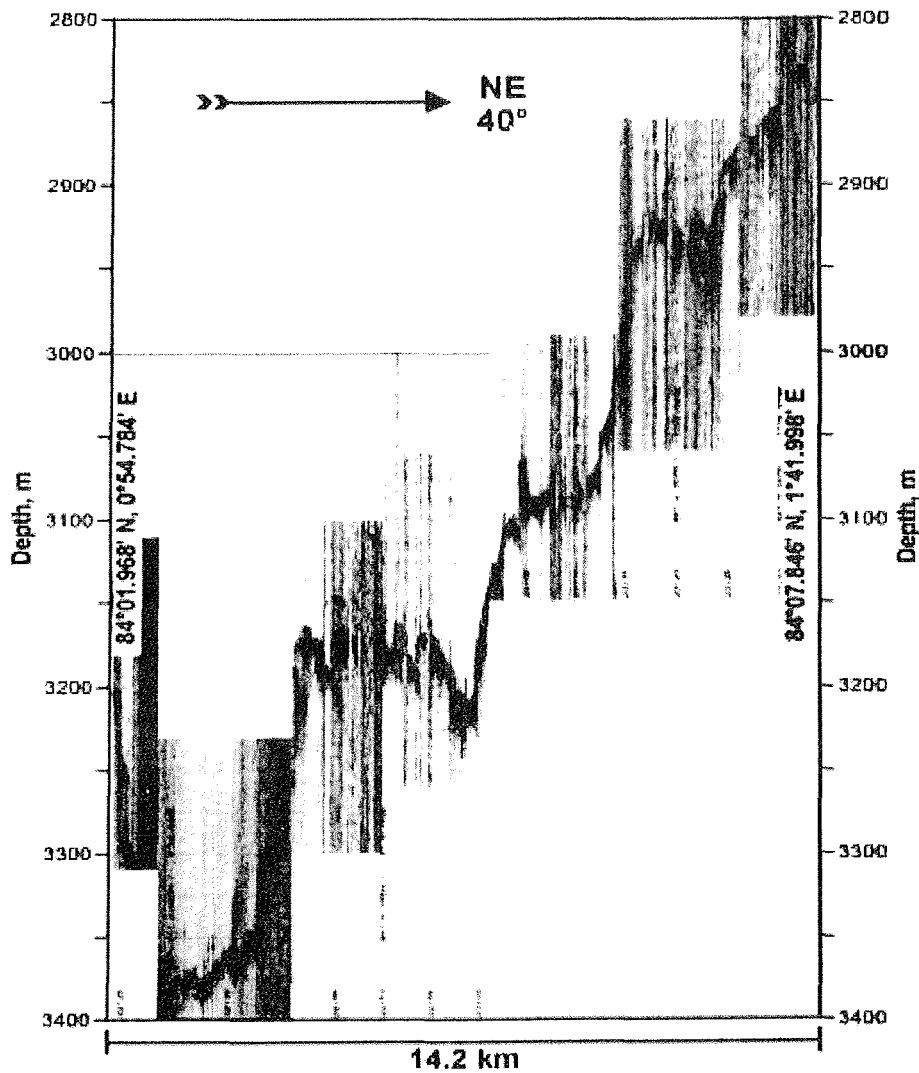


Fig. 49. Steep normal faulted morphology of the southern shoulder of the rift valley, Western Segment of the Gakkel Ridge (PARADIGMA online printout).

The Central Segment is surveyed between 84°32' N, 02°30' E and 86°35' N, 69°00' E. It differs drastically from the Western one by in morphology of the rift valley and in the greatest water depths about 5.2-5.4 km. The rift valley is rather curved and consists of several arched subsegments divided by linear volcanic

ridges extending orthogonal to the spreading axis and obviously consistent with the spreading flow lines. The largest of these transverse ridges, which strikes along 61° E, was crossed at its shallowest part with the water depth of 566 m recorded by both multibeam sonar systems HYDROSWEEP D-2 onboard RV POLARSTERN and SEABEAM 2100 onboard USCGC HEALY. This feature, which represents so far the shallowest part of the Eurasia Basin, has been proposed to be named after a well-known Soviet geophysicist Arkady Karasik (see Appendix 18 for the draft of the proposal).

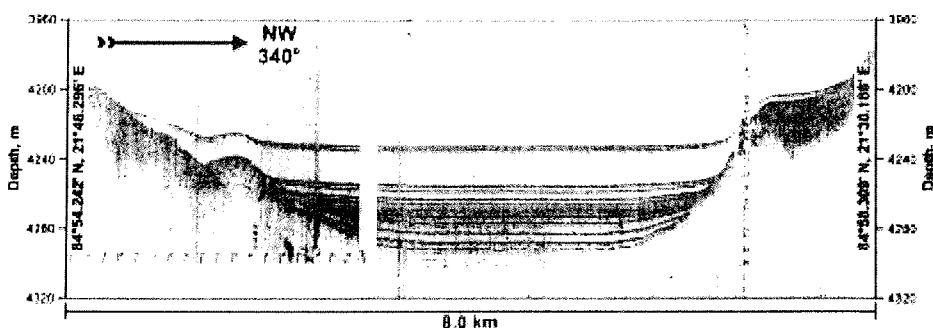


Fig. 50. PARASOUND DESO record showing a local occurrence of the sediments within a trough between two basement ridges, southern flank of the Gakkel Ridge.

The Eastern Segment was surveyed between 86°35' N, 69°00' E and 85°30' N, 86°00' E and it obviously extends further eastward out of our working area. The main feature of this segment is that the ridge here, including the rift valley, is strongly sedimented and has due to this a smooth topography.

The sediments within the ridge distributed irregularly. The most of the sediment occurrences are established on the ridge shoulders between the basement highs elongated parallel to the rift valley (Fig. 50). The rift valley itself consists of almost no sediments within the Western and Central segments, being floored with the very fresh basalts erupted from numerous small volcanic cones. Figure 51 shows a typical PARASOUND record from one of those sediment-lacking parts of the rift valley. And in turn, the sediments are abundant within the Eastern Segment covering the rift shoulders and partly filling the rift valley (Fig. 52, see also Kristoffersen, 2000).

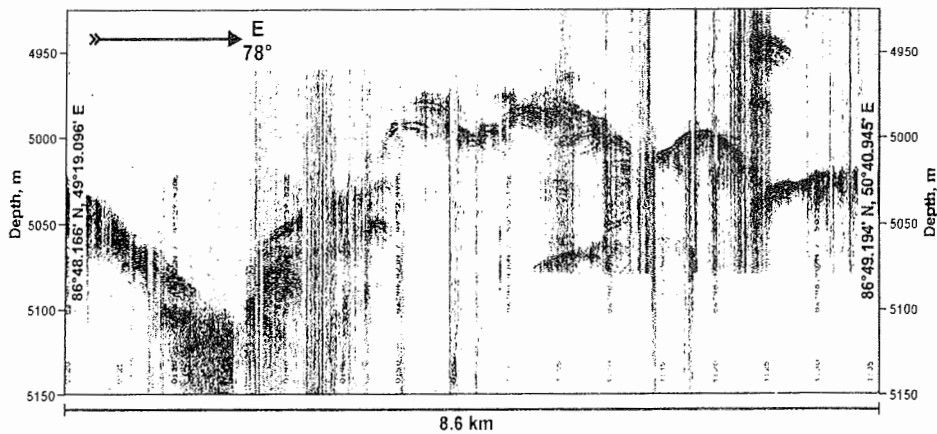


Fig. 51. PARASOUND record from sediment-lacking rift valley of the central segment of the Gakkel Ridge (PARADIGMA online printout). Note presence of the side echoes and very rough topography of the floor, which is considered as a result of recent volcanic activity.

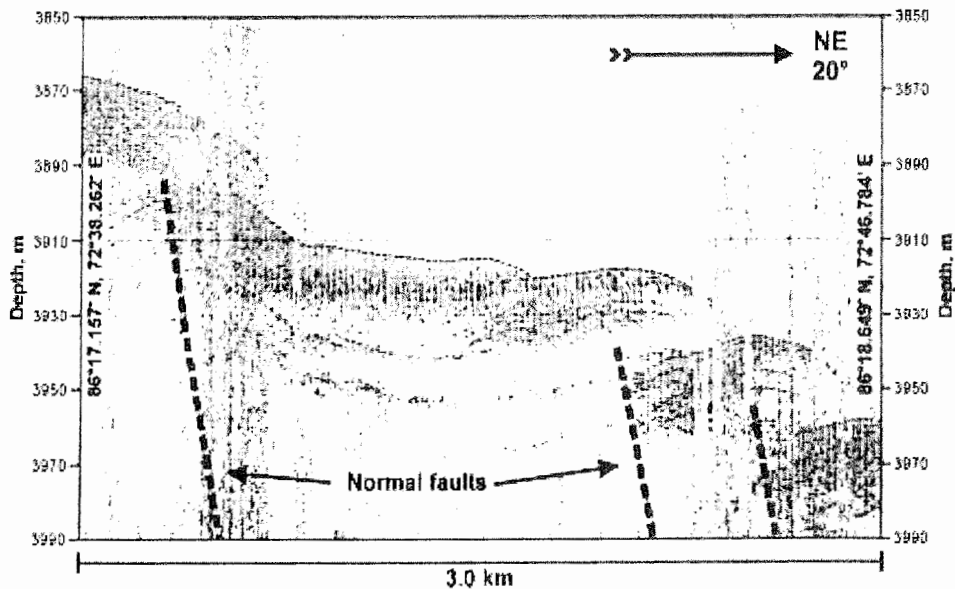


Fig. 52. PARASOUND DESO record across the southern normal faulted flank of the sedimented rift valley, Eastern segment of the Gakkel Ridge.

Amundsen Basin

The Amundsen Basin was crossed twice between 04.09.01 and 09.09.01 along the very closely spaced tracks. According to the seismic reflection data obtained during our expedition, this basin, as the Nansen one, contains a thick cover of Cenozoic sediments. Its flat floor lies between 4400 and 4425 m near the Gakkel Ridge and about 4300-4350 m in its near-pole part. The PARASOUND record is

considered to be of very good quality and exhibits the greatest penetration up to 90 m and predominance of the well-layered sediments, which are supposed to be represented by distal turbidites (Fig. 53). We find these characteristics of the sediments to be rather different from what was observed in 1998 along a ship track in the western Amundsen Basin, where sediments are less penetrable and poorly stratified (Jokat, 1999). This difference may reflect different sedimentary conditions in western, (European) and eastern, (Siberian) parts of the basin. Probably the abundance of the distal turbidites within the latter one is related to increased sedimentary supply by the large Siberian rivers.

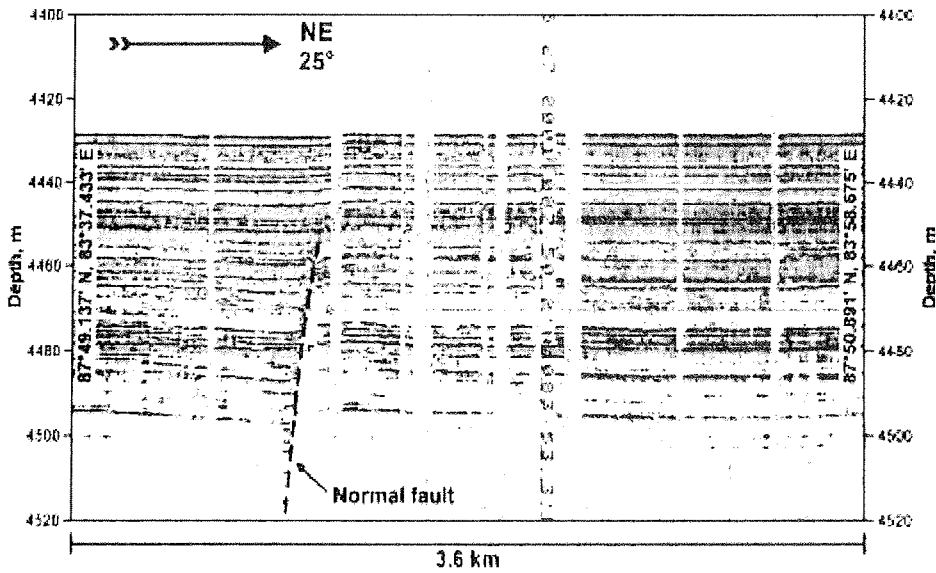


Fig. 53. An example of the PARASOUND DESO record showing stratified sediments in the Amundsen Basin, which are considered to represent distal turbidites. Note high penetration of the acoustic signal reaching about 90 m subbottom. The sediments are disturbed by a low-amplitude normal fault.

7.2 Sea Floor Sediments

(R. Spielhagen)

Sediment sampling, description, and measurements

Surface sediments were sampled at stations PS59/208, /217, /219, /237, /280, and /287 (Fig. 54) using a giant box corer (GKG, 50x50x60 cm).

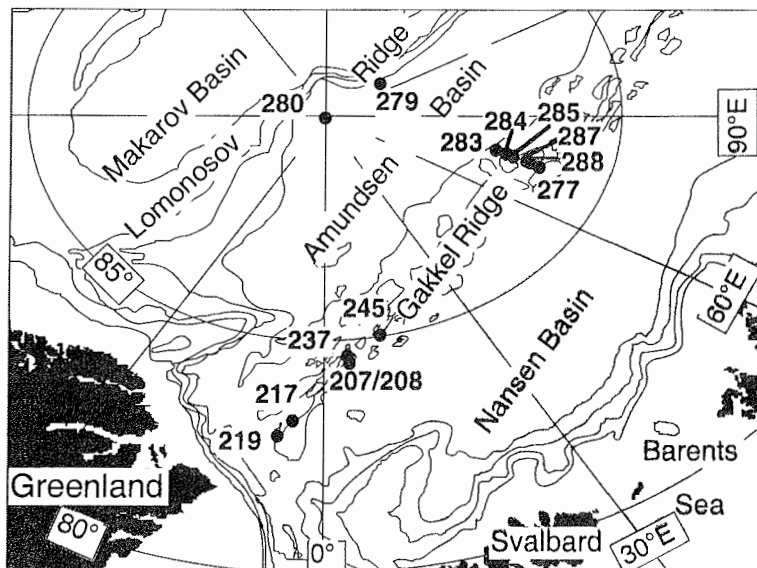


Fig. 54: General bathymetric map of the eastern Arctic Ocean. Coring sites are indicated.

GKG operation at station PS59/230 did not recover sediments, but volcanic rocks and is not considered here. Sediments were usually undisturbed, except at station PS59/280, where the GKG touched the sea floor twice and contained sediments that were tilted and disturbed. GKG surfaces sediments were photographed and sampled for stable isotope measurements of foraminifers and for sedimentological, geochemical, and micropaleontological investigations. At least three plastic tubes (12 cm diameter) and one plastic box (8x15 cm cross section) were taken to archive sediments for future work. Additional samples were taken downcore for X-ray analyses, dry bulk density determinations and onboard determinations of planktic foraminifer contents (Fig. 55). All box cores were opened, photographed and visually described (see App. 14), except PS59/280-1 (core PS2190-2 from the same location is archived at AWI).

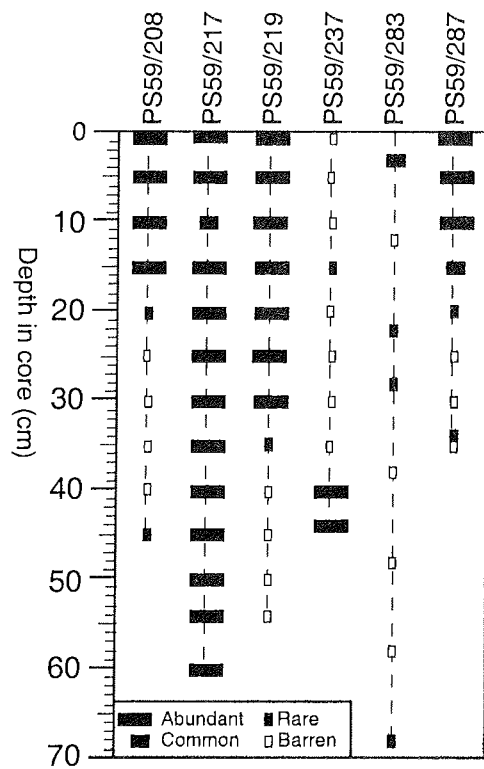


Fig. 55: Relative abundance of planktic foraminifers in the upper sediments from selected coring sites.

To obtain long sediment cores and to perform heat flow measurements by attached sensors (see chapter 9.7), a gravity corer (SL) of 5 or 10 m length and 12 cm diameter was used. The penetration weight was 1.5 t. At stations PS59/285 and /287 the core barrel was bent, and operation at PS59/288 failed because the corer did not penetrate and fell over. Operation at site PS59/212 recovered volcanic glass. Otherwise, core recovery varied from 0.69 to 6.60 m (Fig. 56).

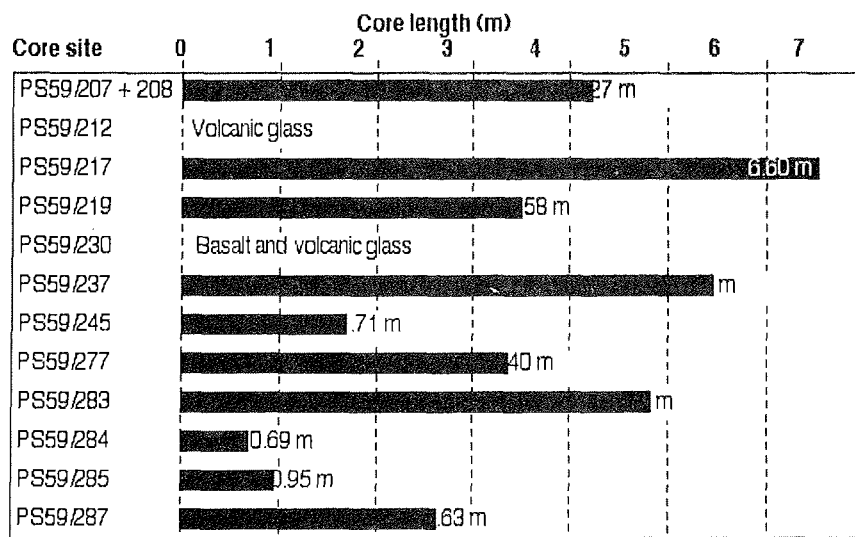


Fig. 56: Sediment recovery (core length) at sites where a gravity corer was used for combined heat flow measurements and coring operations.

Four cores were opened on board (PS59/217, /277, /283, /287), photographed, visually described (see App. 14), and sampled for X-ray analyses and dry bulk density determinations. In addition to the visual description, the sediment color was determined at 1 cm intervals using a Minolta CM-2002 spectrophotometer.

Sediments from the western Gakkel Ridge (007° W to 006° E)

The uppermost sediments from the western Gakkel Ridge, recovered by box cores, consisted of silty clay (sandy silty clay at site PS59/208) and were very homogeneous, which is indicative of a high degree of bioturbation. Sediment colors were dark brown to dark yellowish brown. On the sediment surfaces, planktic foraminifers were abundant in the coarse fraction and other microfossils like benthic foraminifers and ostracods were common. Only at site PS59/237 from the deepest part of the central Gakkel Ridge valley (5364 m), the surficial sediments down to 10 cm core depth were barren of microfossils. While the microfossil content at sites PS59/208 and /219 decreased to zero at 20 and 35 cm, respectively, planktic foraminifers were present in high amounts in the coarse fraction continuously down to about 60 cm at site PS59/217. The latter site is situated in a small sub-basin east of a sheltering SSE-NNW trending ridge, which probably allows the settlement of fine-grained particles in a leeward position of contour currents along the Lena Trough valley escarpments. The existence of such a NNW flowing current is indicated by several known high-

deposition sites along the western Spitsbergen margin and the western Yermak Plateau, visited during previous expeditions of POLARSTERN. Sediments at site PS59/217 below 60 cm depth are silty to sandy clays, often strongly bioturbated, and of brownish or olive colors. The higher sand content between ca. 2 and 5 m core depth may be indicative of a stronger current activity and/or a higher supply of coarse ice-rafted debris. However, no dropstones were found in the sediments, which would support ice-rafting as a major sediment transport process.

Sediments from the eastern Gakkel Ridge (073° to 076° E)

Only one box core (PS59/287-1) was obtained from the eastern area. The surface sediment was dark brown soft silty clay and the upper 10-15 cm contained abundant planktic foraminifers in the coarse fraction. Further downcore, the sediments mostly consisted of sandy silty clay of various colors. Grayish brown colors dominate in the uppermost part below the foraminifer-rich surficial sediments. Further below, in all three opened long cores (sites PS59/277, /283, /287) the same typical succession can be found, but in different depth resolution. It starts with medium light olive and sometimes brownish colors and is underlain by darker olive sediments, which then grade into a distinct dark gray layer. These dark gray sandy silty clays are in most cases very homogeneous and may contain single dropstones. The dark gray layer always has a very sharp lower boundary to the top of the next succession of medium light olive sediments. Core PS59/283-1 is 4.80 m long and contains six full and mostly well-developed successions (one dark gray layer is only 3 cm thick; others are 15-40 cm). Only two successions were found in the 2.63 m long sequence from site PS59/287, but in higher depth resolution. Core PS59/277-1 contains only one full succession, because the lower two thirds of the 3.40 long core consist of dark gray silty clays which most probably were deposited from a gravity-driven sedimentation process. The cyclic deposition of sediments with a typical color succession is obvious also in the gray scale records, which allow a detailed core-to-core correlation (Fig. 57).

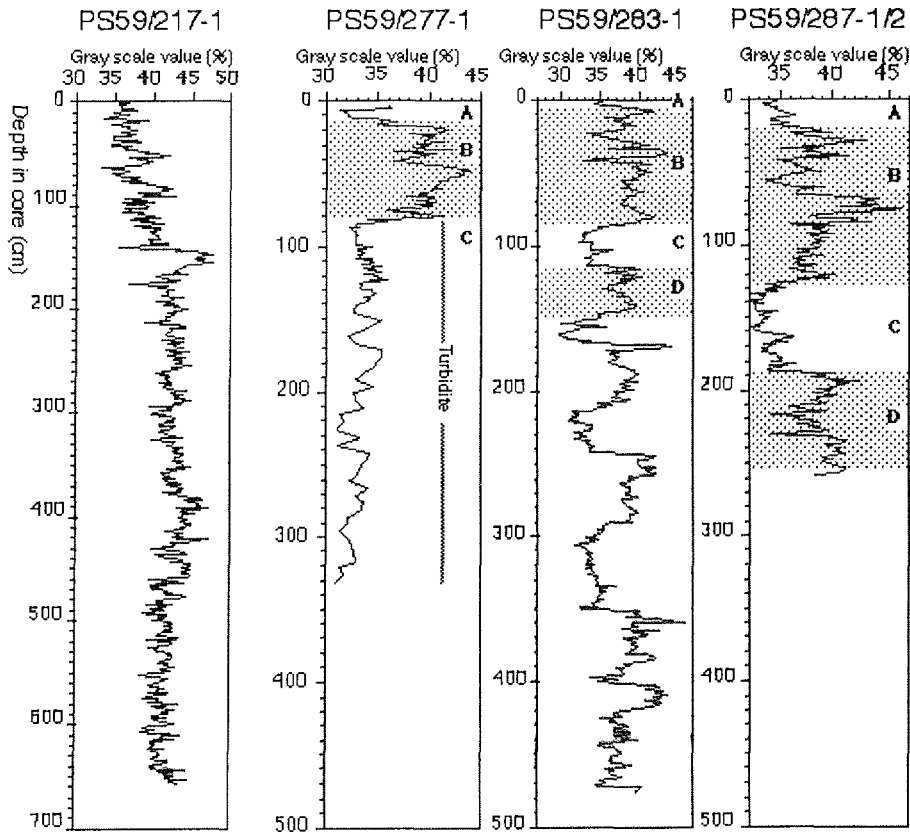
W. Gakkel R. (5°W)**Eastern Gakkel Ridge (ca. 75°E)**

Fig. 57: Results of gray scale measurements on selected sediment cores. Low values represent darker sediment colors, high values represent lighter sediment colors. Note different depth scales. A preliminary correlation of individual segments in three of the cores is indicated by shading and labelling.

The generally higher degree of bioturbation in the brownish and olive layers, if compared to the dark gray deposits, allows the conclusion that they were deposited during times of well-ventilated bottom waters in the eastern Arctic Ocean. Because benthic life in the Arctic Ocean (as elsewhere) depends strongly on the biologic production in the uppermost water column, which was higher in interglacials than in glacials (Spielhagen et al., 1997), a preliminary interpretation of the sedimentary sequence assigns the colorful deposits to environmentally favorable, relatively "warm" phases of the Late Quaternary, while the dark gray layers probably represent cold phases of glacials or stadials and the following deglaciation phases. The latter conclusion is supported by the occurrence of ice-rafted debris in these sediments, which also indicate continental glaciations in the source areas, probably in northern Eurasia.

7.3. Sediment Geochemistry

(V. Shevchenko, J. Snow, R. Mühle)

The chemical composition of bottom sediments is an important tracer of their origin and history. One of important tasks of geochemical work in oceanic rift zones is study metal-enriched sedimentary deposits. Metal-enriched sedimentary deposits (metalliferous sediments) are closely associated with actively spreading mid-ocean ridges. These sediments are enriched in iron, manganese, copper, chromium, lead, and other metals in areas of high heat flow near the ridge crest, and their genesis is closely linked with the generation of new ocean floor (Kennett, 1982), Metalliferous sediments are relatively well studied in the Pacific, Atlantic and Indian Oceans (Kennett, 1982; Lisitzin, 1996), but we didn't find any publication, devoted to such studies in the Arctic. Using box-corer samples we plan to study the historical trend in accumulation of different chemical elements (absolute mass approach) and diagenesis processes.

During the whole expedition bottom sediments were collected from box-corers, dredges and TV-grabs for geochemical studies. Totally, the sediments were obtained at 6 box core stations (Tab. 7), 49 dredge stations and 17 TV-grab stations (Tab. 8).

The geochemical studies will be done in the P.P. Shirshov Institute of Oceanology, Moscow (smear-slides description, X-ray fluorescence, organic carbon determination, instrumental neutron activation analysis, atomic spectroscopy), and at AWI-Bremerhaven (clay mineralogy, organic geochemistry).

Table 7. Box core samples for geochemical studies.

Station	Date	Time (UTC)	Coordinates		Depth, (m)	Collected material
			Latitude (N)	Longitude		
208	09.09	04.12	84°38.87'	5°14.41'E	2776	38 cm core
217	12.08	22.03	83°08.73'	4°51.17'W	3662	56 cm core
219	13.08	20.31	82°54.71'	6°19.24'W	4098	54 cm core
237	19.08	17.30	84°43.9'	4°27.21'E	5326	43.5 cm core
280	06.09	18.52	90°		4240	upper 2 cm
287	11.09	18.00	86°28.93'	73°53.91'E	3781	46 cm core

Table 8. Sediment samples for geochemical studies, collected together with petrology group.

Station	Sampling device
199	TV-grab
204	frame dredge
206	frame dredge
214-2	TV-grab
216	TV-grab
218	frame dredge
219/1	OFOS
220	TV-grab
221	TV-grab
222	dredge
223	pipe dredge
224	pipe dredge
225	pipe dredge
228	TV-grab
229	pipe dredge
235	pipe dredge
236	TV-grab
238	pipe dredge
239	TV-grab
240	pipe dredge
241	pipe dredge
242	pipe dredge
243	pipe dredge
244	pipe dredge
246	pipe dredge
247	pipe dredge
248	pipe dredge
249	pipe dredge
250	pipe dredge
251	pipe dredge
252	TV-grab
257	pipe dredge
262	TV-grab
266	pipe dredge
268	TV-grab
270	pipe dredge

Station	Sampling device
271	pipe dredge
272	pipe dredge
275	TV-grab
276	pipe dredge
291	pipe dredge
292	TV-grab
293	pipe dredge
294	pipe dredge
295	pipe dredge
296	pipe dredge
299	pipe dredge
300	pipe dredge
301	pipe dredge
302	TV-grab
303	TV-grab
305	pipe dredge
306	pipe dredge
307	pipe dredge
309	pipe dredge
310	pipe dredge
311	pipe dredge
312	pipe dredge
313	pipe dredge
313-2	frame dredge
314	pipe dredge
315	TV-grab
317	pipe dredge
318	pipe dredge
319	pipe dredge
320	pipe dredge

8. Petrogenesis of Crustal Rocks

8.1 Introduction

(J.E. Snow)

At mid-ocean ridges, solid mantle is melted to form mid-ocean ridge basalt. In this way, new oceanic basement is formed to accommodate the drift of the tectonic plates. The partial melting reaction involved is one of the most important chemical reactions on Earth, producing yearly about 20 km^3 of oceanic crust -- approx. 5.2×10^{10} tons of basaltic rock. This accounts for over 90% of the active volcanism on Earth. The oceanic crust is generally divided into seismically defined layers whose physical properties correspond generally to the rock types that can be sampled at mid-ocean ridges. Very slowly spreading mid-ocean ridges are important because they are thought to form involving lower degrees of partial melting. This line of reasoning has two main arguments. First, theoretical models of melt generation and the thermal structure beneath mid-ocean ridge spreading centres all predict some kind of relationship of crustal thickness (and thus degree of partial melting) and spreading rate. Figures 58 and 59 show a compilation of different crustal thickness determinations made by both seismic and by geochemical methods, and compared with theoretical mid-ocean ridge melting models. At very slow spreading rates, most models predict a significant decline in melt production. This is because of the lithospheric cap effect. That is, the conductive vertical cooling of the lithosphere is sufficient at very slow spreading rates to put a brake on the degree of partial melting at the ridge.

Crustal thickness can be estimated seismically via well-established refraction techniques. It can also be guessed by using gravimetric techniques. However, geochemical estimates are also possible. One means of doing this is a global inversion of the rare Earth elements (MacKenzie and O'Nions, 1990), another means is to invert the chrome numbers of residual peridotite spinels ($= \text{Cr}/(\text{Cr}+\text{Al})$) for the crustal thickness (Hellebrand et al., 2001). This is based on the finding that the melting degree of abyssal peridotite chrome numbers can be calibrated, and thus for each spinel measured, a degree of melting and thus a crustal thickness can be determined.

All of the theoretical models predict a steep decline in crustal thickness as a function of spreading rate. Seismic results and geochemical results seem to confirm this supposition. It was thus an accepted assumption that the crust on Gakkel Ridge would be significantly thinner than on ridges elsewhere. Secondly, it was expected that the decreasing spreading rate along the ridge would be a major control on the lithologies and morphologies encountered.

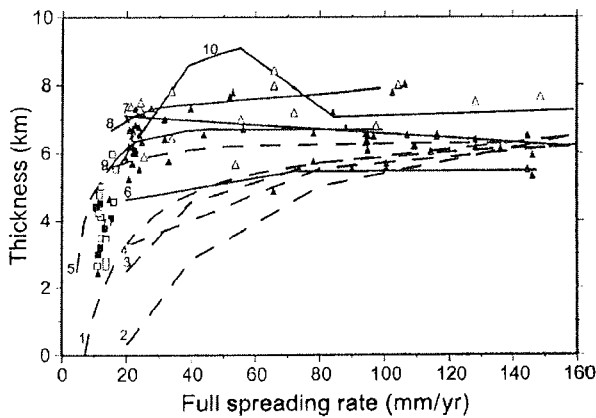


Figure 58: Theoretical crustal thickness variations with spreading rate after White et al., 2001.

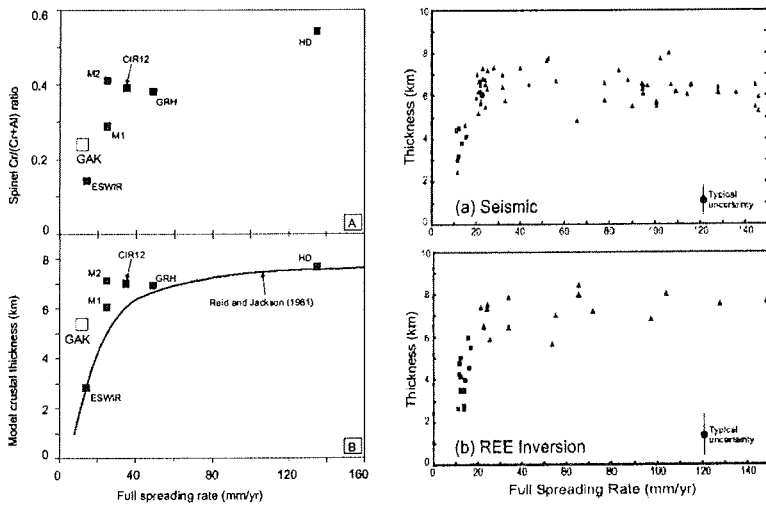


Figure 59: Geochemical and seismic estimations of crustal thickness as a function of spreading rate. After Hellebrand et al., 2001; White et al., 2001.

This document reports on the petrology sampling operations on POLARSTERN and their principal results. Results from HEALY are only shown where they have a direct bearing on the POLARSTERN results.

8.2 Planning and Operations

(J.E. Snow)

Pre-Expedition

This cruise was planned from the beginning to have a substantial sampling program. The Memorandum of Understanding, drafted in October 2000 in Bremerhaven called for approximately equal time for geophysics and for petrology in a 58 day program. This was later expanded to 63 days plus 1 week of transit to Bremerhaven.

Two kinds of sampling program were planned. First, a shared transit, during which a seismic profile of 20-30 nautical miles was shot between sampling intervals. These could consist of one or more dredge or TV-grab stations by either or both ships. It was intended that most parts of the ridge would be covered twice, once on the way there during shared transit, and once on the way back, during detailed sampling. Because of the light ice conditions, the two ships were able to operate independently during detailed sampling. One ship always surveyed and sampled the northern flank of the ridge, while the other ship surveyed and sampled the southern flank of the ridge. This optimized the bathymetric and sampling coverage.

The overall structure of the cruise was to be as follows: entry to the ridge at 18° E by a seismic traverse starting to the east of Spitzbergen. It was assumed that three knots would be possible in all ice conditions and that the two ships would have to support each other during sampling operations. Shared transit to the west for 6 days, followed by 15 days of detailed sampling on the return to 18 degrees east was suggested, then shared transit to the west until 85° E, followed by detailed sampling on the volcanic field there, and a transit across the Amundsen Basin to Lomonosov Ridge. On the return from Lomonosov Ridge, HEALY was to further sample the 85° E region, while POLARSTERN conducted

a heat flow survey back long the track of the seismic transect. Then both ships would conduct detailed sampling back along the ridge as far as time would allow until the planned exit from the ridge at 30° E.

Organization Underway

Several meetings were held on POLARSTERN and HEALY to establish / coordinate the locations of sampling targets, and plan the dual ship tracks. The POLARSTERN petrology staff was divided into three groups, dredging (6), curation (7) and technical (4). The dredging staff rotated three 8-hour shifts consisting of a dredger and a watchstander. A. Büchl was responsible for leading the curation and description staff that rotated on two eight-hour shifts, avoiding the hours from 0200-0600. It has been shown that more accidents occur on the night shift than on other shifts, and since there is no direct need for rock curation to proceed at 3 am, it was decided to dispense with it. This had the advantage of a happier and better rested curation staff, but the disadvantage that the night dredging staff sometimes had to deal with full dredges alone.

Operational Results

The excellent ice conditions during the cruise resulted in significantly more sampling stations being taken than was initially expected, resulting in a relatively large amount of sample material.

The transit to the ridge was conducted as a geophysical traverse, with HEALY breaking ice for POLARSTERN. After entry to the ridge on 6.8.2001, we conducted our first two sampling stations, then commenced seismic transit to the west. In these, HEALY broke ice for POLARSTERN for short transits that were interspersed with sampling stations. In 13 such transits of 20-30 nm we covered 350 km of ridge axis and took 10 sampling stations. This phase of the project ended on 13.8.2001. Following a short bathymetric survey of the intersection of Gakkel Ridge with Lena Trough south of 83° N, we investigated a potential hydrothermal field discovered by HEALY via dredging. On 14.8.2001 we commenced detailed sampling of the western end of Gakkel Ridge, following a plan whereby POLARSTERN stuck to the southern wall of the rift and HEALY to the northern wall, both entering the axial valley to sample the ridge axis. This stra-

tegy proved quite successful at characterizing the ridge petrologically. At the end of this transect, on 23 August, both ships met with the Swedish icebreaker ODEN. This culminated the western detailed sampling transect.

The program continued with shared seismic transit to the east of 15° E. In 15 transits we covered 500 km of ridge out to 73° E, taking 21 sample stations. More difficult ice conditions encountered during this part of the cruise made sampling operations somewhat less efficient. At 73° E, the transit to Lomonosov Ridge began. This seismic and heat flow program lasted 4 days and included a visit to the North Pole on 6. September. Afterwards we resumed detailed sampling operations in the eastern end of Gakkel Ridge. Difficult ice conditions prevented us from carrying out one portion of the program – a series of sampling stations and camera tows on a suspected active volcanic field at 85° E on the ridge.

After resuming detailed sampling at 73° E on 13 September, we turned west rather than east, and sampled the southern wall of the ridge, then crossed over to the northern wall for a few days before returning to the southern wall. HEALY followed a complementary program. On the westward detailed sampling transit we were able to cover nearly the entire ridge once again, before meeting HEALY on September 25. for the transit out of the ice. In all, 106 petrologic sampling operations were carried out returning 11 tons of rock. This includes basalt glass returned from one box core and one gravity core as well. This result in 44 days total sampling time is only slightly worse than what one would expect sampling in open water.

Sampling technologies

Dredging

We used two different types of dredges during this cruise. The first was a simple pipe or barrel dredge constructed by EISEN- und STAHLBAU KIEL, GmbH. These dredges, in diameters ranging from 50 to 70 cm, proved to be extremely robust sampling tools. The frame dredges provided by AWI consisted of a steel frame with teeth and a solid steel bridle, underneath which hangs a steel chain-

bag. A very large frame dredge nicknamed "Der Weiße Hai" completed the sampling tool set.

Dredging in ice is of necessity quite different from dredging in open water. The easiest situation, in loose ice, is quite comparable to the open water situation. The danger in such situations is always when the dredge is stuck. If the ice does not allow the ship to back up, the loss of the dredge, its contents or even the wire can be the result. In pack ice, positioning the ship with respect to a lead and the slope/volcano to be sampled is the critical factor. This positioning time can often last several hours as a suitable lead is sought. Once the lead is found, the stretch to be traversed has to be driven once, to be sure it is open enough for the operation. This requires a close cooperation between the dredging scientist and the helmsman, and is usually done on the bridge. In compressive ice conditions, dredging may not be possible at many desired localities. It was frequently the case during the course of this cruise that dredging of some or all targets in a region was impossible because of unsuitable ice conditions. Therefore, it is extremely important in Arctic sampling missions to have alternative sampling tools available.

The dredge operates by being pulled along the sea bottom on the end of a wire. The problem is to avoid situations that could endanger the ship (like getting wire in the propellers) or the wire (by getting stuck on the sea floor) or the personnel on deck (if the cable breaks with 18 tons of tension on it). Some of the major components of the dredging system are shown in Figure 60. The wire carries the dredge and weak link system at its end, but is also usually equipped with a 3.5 KHz pinger and a MAPR. The properties and purpose of these devices will be explained below.

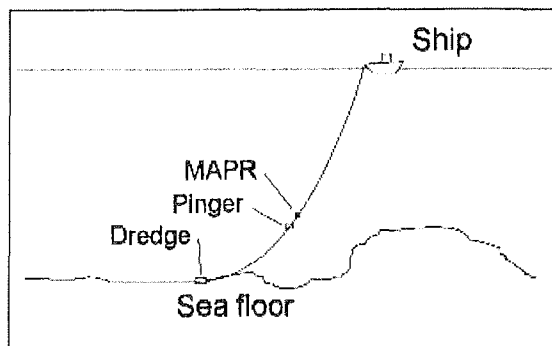


Figure 60: General arrangement during dredging.

The Wire

For ARK XVII/2, the main working winches were equipped with one 8000m roll of 18.2mm coaxial conducting cable for TV-grab operations and one 10000m roll of 18mm Starlift wire rope from CASAR Drahtseilwerk GmbH as the main dredging cable. In reserve are a further 4000m of older coaxial cable and another 10000m of new Starlift cable. Starlift is a general purpose oceanographic deep sea cable which is rotation balanced, internally lubricated and intended for heavy duty use in extreme environments.

This cable has a certified minimum breaking strength of 25 metric tons. Of this 25 tons, it is only safe to use 75% or 18.75 tons of pull without causing damage to the internal structure of the wire. Including a safety factor of another 15% we are allowed to pull at a maximum of 15 metric tons. This value becomes critical, because of the eventuality that the dredge becomes stuck on the ocean floor. If that happens there is a great danger that the wire may break on deck (the point of maximum stress) and that flying ends of it may injure deck personnel. Even if the wire is not lost, if it is stretched beyond its elastic limit in the course of retrieving a dredge, it can be damaged beyond repair. In order to prevent this, weak links are used to insure a controlled separation of the wire from a stuck dredge.

Rigging

A dredge is rigged with two or three weak links as shown in Figure 61. The last, strongest one is set so that the maximum pull on deck never exceeds 15 tons given the water depth. The next is set 500kg weaker and the next 1000-kg weaker.

All the links are secured to the dredge with 7/8" marine shackles and 22mm cable with reinforced loops fastened by metal clamps. These parts must be able to withstand a tension of at least

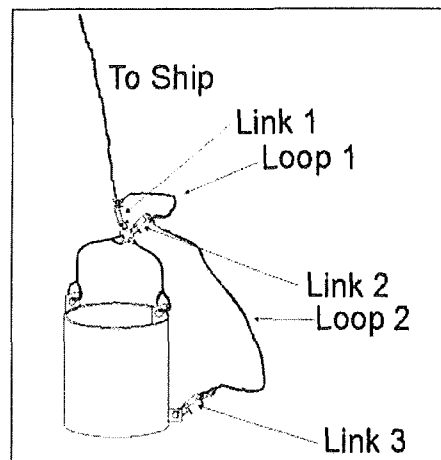


Figure 61: Rigged dredge.

30T without breaking, giving a safety factor of 2.

Breaking the first link gives a powerful jerk on the dredge that often breaks it free. Breaking the second link gives another mighty jerk on the dredge, this time from the back. This should in principle pull the dredge up off the bottom from another angle. The third link lets go of the dredge altogether.

TV-Grab

The TV-Grab (Fig. 62) is a hydraulic-electronic device for retrieving samples from the sea floor. It consists of a video camera in a watertight housing looking down (Fig. 63) between the jaws of a remotely controlled hydraulic grab. Depending on what is visible in the TV-picture, the grab is set down with open jaws on the sea floor, and the jaws are closed. This can be done several times with a single battery charge. This device thus allows visual monitoring of the sea floor and the controlled selection of the samples, as well as the collection of data about the sea floor and biology in the working area. Therefore, in contrast to dredging operations, the samples collected have a defined location, depth and geologic context on the sea floor.

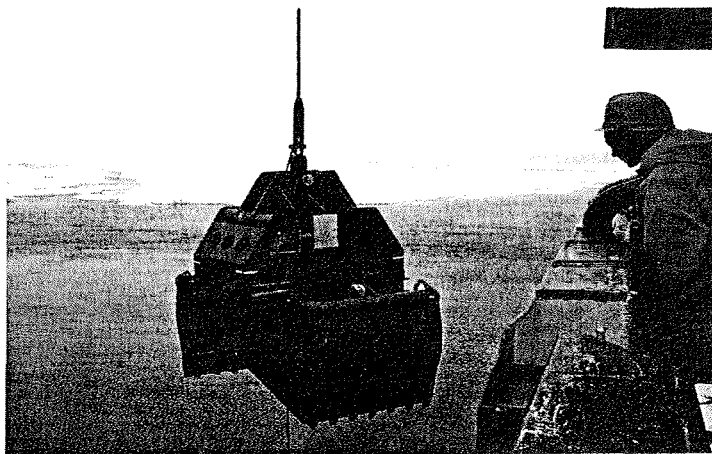


Figure 62: TV-Grab.

The TV-Grab consists of two different units, one on board and one operating in the sea. The onboard unit controls the camera and the four spotlights and gives information about depth, battery voltage and if the TV-Grab is open or closed. The onboard unit also contains an "altimeter", which shows the last 100 m above ground. The deep-sea unit is attached to a standard 18.2mm coaxial cable, which also provides the data link to the ship. The unit consists of a massive galvanized steel housing that supports the hydraulic jaws. The measurements of the deep-sea unit are 220 x 210 x 140 cm (H x W x D) with a weight of 2,8 tons and a payload up to 3 tons. The maximum working depth is 6000m. The housing contains an integrated hydraulic pump unit, a telemetry unit, a camera, four spotlights of 150 W each, and a power supply. The power is provided by two deep-sea batteries (12V, 230Ah). The voltage for data and image transfer (screen refreshing) is max 24 V, which provides additional security, as the other telemetry units use a voltage of 1000V, requiring special handling on deck. The TV-Grab can be lowered or raised with up to 1m/s (60 m/min). Greater winch speeds are not allowed due to hydrodynamic drag on the internal connecting cables. The maximum ship speed during grabbing operations is 0,5 knots. This is because drag on the main cable tends to lift the grab up off the sea floor, making it difficult to control the height off bottom.

Typically, the TV-grab was used to sample volcanoes. These were frequently as small as 100-200m in diameter. This required careful positioning which took into account the ice drift and the necessity of having relatively flat terrain to set the grab on. The biggest problem encountered was sediment, which covered the samples, making it impossible to know when the grab was over outcrop or a sediment pond. In that case, drifting with the ice or even moving the ship generally was enough to bring outcrop into view.

Normally, when a target is identified, the grab is set down on the sea floor completely, and 10m or so of additional cable are reeled out. In the relatively rough topography of Gakkel Ridge, this caused problems, because the grab nearly always fell over and rolled down the slope. Because there is no swell in the ice and consequently no heave, this technique was modified by simply unloading the wire by 1-2 tons before grabbing. If there had been a swell this would have

resulted in slamming the grab into the seafloor repeatedly, but in the ice, this meant that the grab remained upright even on slopes.

In the course of this expedition we carried out 32 TV-Grab operations, which collected a total of 4,2 tons of rock. Due to the power supply the maximum running time of one operation was about four hours, with the possibility of 3 to 4 grabbing attempts as necessary. Generally though a single grab was all that was necessary. The bottom time was generally less on this cruise than is usually the case with TV-grab operations. This is because in unsedimented areas nearly all of the bottom can be sampled. Where sediment is present, typically the ship is allowed to drift or is actually driven in order to an outcrop. In one or two cases even then no outcrop could be found, but in most cases good outcrops were located. The range of grabbing times was generally between 1 h 35 min and 10 sec. In more than twenty of the grabbing operations the bottom time was less than 10 min.

OFOS

The OFOS device is a towed camera platform that was used on station 219-1 to attempt to document hydrothermal activity in the axial valley of Lena trough at its intersection with Gakkel Ridge. This was to have resulted in a video and still camera documentation of the sea floor. One of the plugs did not remain water tight on lowering however, and none of the exposures actually showed anything. This result was disappointing, leaving us with a relatively low-quality video picture as the only visual documentation of the hydrothermal activity at this site.

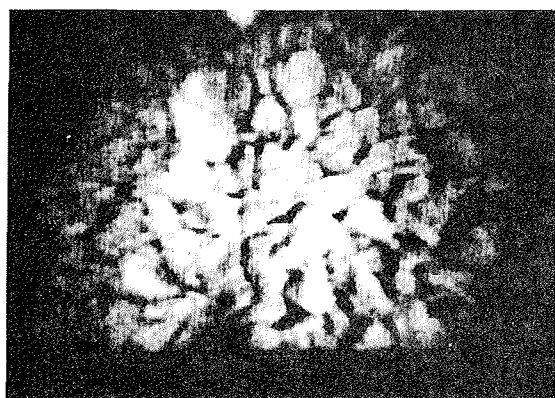
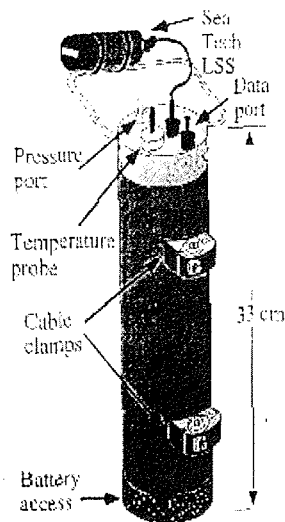


Figure 63: TV-Grab Screen.

MAPR

The MAPR (Miniature Autonomous Plume Recorder cf. Ch. 7 for data and results) is a compact device that is attached to the sampling wire like a CTD and records pressure, temperature and light scattering. Figure 64 shows a schematic view of a standard MAPR device. The MAPRs for this cruise are a hardened new design especially created for use in ice conditions, with no external sensors.

The data are extracted from the device using a standard PC with parallel port, using software supplied by NOAA. Further processing is then done using an excel spreadsheet.



A Miniature Autonomous Plume Recorder

Figure 64. Schematic view of a MAPR device.

8.3 Samples

Rock Curation

(A. Büchl, A. von der Handt)

During AMORE 2001 along Gakkel Ridge almost 11 tons of rocks were brought aboard by 64 dredge operations and 32 TV-Grab operations. Among these were 2323 kg of peridotites, 435 kg gabbros and 7259 kg basalt. The range in weight of a single sample was from a few grams up to approximately one ton (large pillow basalt). In accordance with the MOU, all samples brought on board were catalogued, described and divided between the 2 ships.

Once on board, the rocks were washed, cut and allowed to dry. They were then roughly sorted into different lithologies and their subtypes. The samples were given numbers in the following way: Ship name - Cruise number – station number – sample number. Example: PS 59 – 210 – 1. Some of the station numbers have extensions due to several operations on the same location e.g. PS 59 – 210 – 1 – 1. The weight of each subtype was noted to determine the weight distribution of the different lithologies. Out of the peridotites all samples of sufficient size (>5cm diameter) were cut, grouped and described in their subtypes. Nearly all peridotites were defined as working samples. Out of the basalts approximately 40% were cut and defined as working samples and described in their subtypes. If available from one to two working samples glass was chipped and microprobe mounts were produced. The gabbros were usually all cut, grouped and described. Thin section blocks were cut of every basalt and gabbro group, except the peridotites, where more thin sections were produced. Altogether 351 thin sections were made.

Glass Processing

(A. Ksienzyk, M. Amini)

First of all a few glass chips were removed from each basalt sample with enough glass, using a hammer and a screwdriver as a chisel. The glass chips were wrapped in aluminum or plastic foil and crushed with a hammer. All glass samples were put into small polyethylene bottles, labeled and listed. The crushed glass was washed by repeated shaking (by hand) in fresh water until the wastewater was clear. After drying, some samples were selected to be picked for microprobe chips or chemical analysis. A few microprobe disks were made. Picked samples and samples with microprobe chips are marked in the

glass sample list. All glass samples go to the University of Bremen (Prof. C. W. Devey) for further processing.

Thin Section Preparation

(J. Michel)

The rock samples are cut into chips of 40x20x11 mm. The side of the chip, of which the thin-section will be made, is ground on an abrasive grinding machine until the side is one flat surface. This side is then ground successively with coarse to fine grinding-powder and cleaned in an ultrasonic bath to remove the grinding powder. The glass-slides (27x46 mm) on which the chips will be glued are ground a little bit, to give them a rough surface. After grinding, the slides are labelled and their thickness measured with a micrometer. The chip and the glass slides are then cleaned with Ethanol and glued together with a two component epoxy resin. This has to be done carefully, in order not to leave any air-bubbles between glass and chip. When glass slide and chip are glued together, they are put in a vacuum oven and stored overnight to let the resin harden.

The next day, the bulk of the chip is cut from the glass slide so that only a 0.5mm layer of rock remains on the glass-slide. This is done with a Struers-Discoplan-TS cut-off-machine, which integrates a saw and a grinding wheel. The thin section is then ground down with the grinding wheel to a thickness of 0.08 mm. Using the grinding-powder from coarse (320) to fine (1000), the thin-section is then ground down by hand to a thickness of 0.025 mm. The thickness can be measured approximately during grinding by using the micrometer-screw. A more precise thickness determination can be made using a microscope. In the microscope, the interference colour of known minerals under crossed polarized light indicates the correct thickness.

Since the thin-sections are not polished on the ship, they are sealed with Buehler Metcoat Specimen Protective Lacquer, which can be easily removed with methyl acetate. After lacquering the thin sections are ready to be viewed under a microscope. All thin sections and chips are catalogued and will reside in Mainz.

Microscopy

(R. Mühe)

Overall 351 thin sections were fabricated and subjected to microscopic investigation. About 40 more thin sections were begun but could not be completed.

Microscopic work was done with a Zeiss microscope and transmitted light was used. In order to allow an overview of the thin section, 1.5x and 2.5x objectives resulting in ca. 15 and 25 times magnification were used. For detailed study of minerals and textures 12x, 25x and 40x objectives gave magnifications of ca. 120, 250 and 400 times the original size. Thin section photography was accomplished using a Fuji Finepix Digital camera with a ca. 6 Megapixel recording chip. Photos were stored subsequently to CD-ROM for further use.

Thin sections were numbered TS 1 ...TS 391. Working sample numbers are listed in a thin section log file (Appendix 9). Where the origin of samples or thin slide numbers were unclear question marks have been added to this log. Two thin sections of the same working sample are discriminated by 'a' and 'b' following the working sample number. Repetition of the thin slide due to bad quality is indicated by either 'TS1 –TS 3' or 'A – D' following the sample number in the log. No sample number or both no number and rock short name indicate that no thin section exists.

Disposition of samples

All POLARSTERN samples are deposited at the AWI. Samples for direct scientific examination were transferred to the relevant institutions. Half of all POLARSTERN samples were sent to HEALY and are divided there for analysis to WHOI, LDEO Institute and the University of Tulsa. The other half of the POLARSTERN samples and half of all HEALY samples are divided after lithologies for Mainz, Bremen, Bremerhaven and Kiel. The destination for all peridotites and gabbros is Mainz. All basalts, which are working samples, were sent to Bremen. The destination for the gravel and all non-working sample basalts is Bremerhaven and for the greenstones Kiel. Table 9 provides an overview.

The samples for the most part are stored in 10-liter plastic buckets. Samples too large for the buckets are stored in metal pallets. Nearly all of these oversized samples are basalts recovered by the TV-grab and are to be kept in Bremen.

Table 9: Final disposition of rocks by type.

Samples	USA	Germany
Basalt	LDEO, Tulsa, OSU	Bremen
Gabbro	WHOI	Mainz
Peridotite	WHOI	Mainz
Greenstones and sulfides	WHOI	Kiel
Non-working and gravel	depending on the Lithology, LDEO, WHOI	Bremerhaven

8.4 Observations

Rock Descriptions

(A. Büchl, A. von der Handt, R. Mühe, J.E. Snow)

The rock description for this cruise was made using a scheme worked out with the curatorial staff of HEALY, so that the sample descriptions could be applied uniformly as much as possible. Thus a sparsely ol-pl phyric basalt should mean the same thing whether described on HEALY or on POLARSTERN. The major difference between the two data sets is that on HEALY each individual sample was described, while on POLARSTERN groups of identical samples were described. Sometimes this amounted to the same thing, such as when a particular subgroup consisted of a single sample.

This cruise strictly follows the IUGS naming system for mafic plutonic rocks (Tab. 10). Figure 65 shows the IUGS naming system for mafic plutonic rocks. The triangle shown represents the mineral content of mafic plutonic rocks as a folded out tetrahedron, with vertices for each of the four major minerals olivine orthopyroxene, clinopyroxene and olivine. For example, a rock containing only olivine would plot at the olivine vertex of the tetrahedron, which is at the midpoint of the lower edge of the triangle. Major oceanic rock types are marked as shaded areas in Figure 65: Peridotites are labelled A, troctolites B and gabbros C.

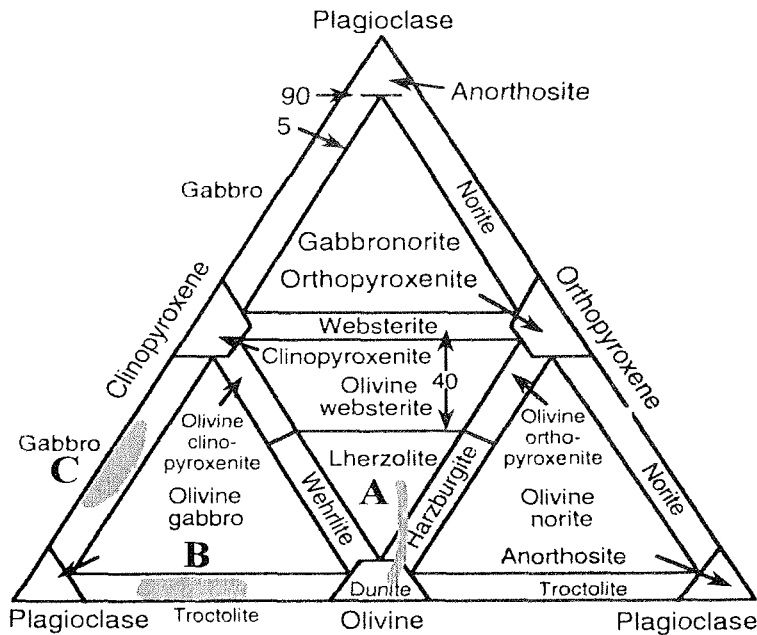


Figure 65: IUGS Classification for mafic rocks. The most common oceanic rock types are shown as shaded areas: A) Residual mantle rocks B) and C) Crustal gabbroic rocks.

Most of the rocks encountered fell into a small subset of rock types: Basalts occurred with recognizable plagioclase and olivine phenocrysts and were named by their phenocryst content. It was not attempted to identify pyroxenes in volcanic rocks in hand sample, as these are generally very difficult to reliably distinguish from olivine, much less from each other. Even in thin section, the identification of pyroxenes can be difficult, as the cleavages are often poorly developed making both the distinction from olivine and the determination of the extinction angle quite difficult. The gabbros seen were mostly oxide gabbros, gabbros *sensu stricto*, olivine gabbros and troctolites (shaded fields B and C in Figure 65). Once again, no attempt was made to distinguish clinopyroxene from orthopyroxene in hand sample. In any event no orthopyroxene was observed in thin section (see section on plutonic rocks), so no norites or gabbronorites were observed.

Among the ultramafic rocks, lherzolites, harzburgites and dunites were observed (shaded field A in Fig. 65). The IUGS nomenclature specifies 5% cpx as the dividing line between harzburgite and lherzolite, however many petrologists consider any amount of cpx to indicate a lherzolite. Typically harzburgites can also be recognized on the basis that they are also generally poor in pyroxenes and in spinel. Though it is possible to distinguish clinopyroxene from orthopy-

roxene in hand sample, it is difficult to do consistently. Dunites are generally easy to spot because of their complete lack of pyroxenes. Where thin sections were cut, the rock type descriptions determined in thin section were applied to the hand sample description.

Table 10: Rock description terms.

Basalts

With glass: Pillow Basalt or sheet flow (tabular), no glass: basalt

Phenocrysts or microphenocrysts: marked with abbreviations in front of the rock name in order of abundance, e.g. pl-ol-phyric basalt.

Igneous Texture

Aphyric:	no phenocrysts or microphenocrysts
Sparsely phyric:	< 2 % phenocrysts or microphenocrysts
Phyric:	2 % to 10% total phenocrysts or microphenocrysts
Highly phyric:	10% to 25% total phenocrysts
Porphyritic:	>25% total phenocrysts

Grain size

G:	glassy – consists mostly of glass.
A:	aphanitic – individual grains cannot be seen even in hand lens.
VF:	very fine – individual grains can barely be seen.
F:	fine (<1mm)
M:	medium (1 to 5mm)
C:	coarse (5-30mm)
P:	pegmatoidal (>30mm) usually accompanied by pegmatite textures.

Igneous fabrics

1:	weak – little alignment of crystals.
2:	moderate – crystal alignment obvious, but not pervasive.
3:	strong – nearly every crystal is aligned.

Crystal plastic deformation

0:	not visible in hand specimen
1:	deformation evident, but no well developed foliation and abundant relict igneous texture
2:	clearly foliated, little primary igneous fabric left
3:	(protomylonite) no igneous fabric, strongly foliated, generally medium grained
4:	(mylonite) strongly laminated, most primary mineral recrystallised to fine-grained, the rest is porphyroclasts
5:	(ultramylonite) some porphyroclasts, but grain size reduction to the point where there is no visible foliation present

Abysal peridotite deformation

0:	Protogranular
0.5:	Protogranular and porphyroclastic present
1:	Porphyroclastic 1
2:	Porphyroclastic 2

- 3: Protomylonite
- 4: Mylonite
- 5: Ultramylonite

Cataclastic deformation

- 0: only cracks around grains with no visible movement on them
- 1: a few cracks with clear movement on them
- 2: brecciated by numerous cracks, but no significant clast rotation
- 3: brecciated with clast rotation
- 4: clasts floating in fine grained matrix
- 5: basically compacted rock flour

Alteration

- F: fresh, no visible alteration
- L: most of the primary mineralogy is preserved
- M: moderate- a majority of the primary mineralogy is preserved
- H: heavy- some primary mineralogy is preserved
- VH: very heavy- complete alteration of all primary phases

Lithologic Overview POLARSTERN and HEALY

(N. Augustin, B. Schramm)

During the ARK XVII/2 Cruise, POLARSTERN carried out 63 dredge hauls and 32 TV-Grabs at the Gakkel Ridge, additionally 2 sediment cores returned fresh basalt glass. The total sample weight from these stations was 10.9 tons. HEALY carried out 101 dredges and 20 rock cores. An overview of the rock types by dredge is given in Table 11.

Table 11: Sampling statistics from AMORE 2001. Note that more than one rock type can be represented in a given dredge – that means the columns do not add up to the total indicated at the top.

	HEALY			POLARSTERN		
	101 Dredges	20 Rock cores	Summary	63 Dredges	32 TV-Grabs	Summary
Basalt (incl. greenstones, glass fragments and breccias)	72	15	87	43	24	67
Peridotite (incl. breccias)	15	0	15	17	3	20
Gabbro	3	0	3	3	2	5
Hydrothermal (inc. sulfides)	2	0	2	0	0	0
Others	6	0	6	31	4	35
Empty (empty or just mud)	7	1	7	8	4	12
Lost	2	0	2	0	0	0

Collected rocks included basalts, diabases, peridotites, gabbros, greenstones, breccias and dropstones. An overview of all dredged rock types for both cruises in percentages is shown in Figure 66. For HEALY only 40 dredges with a total

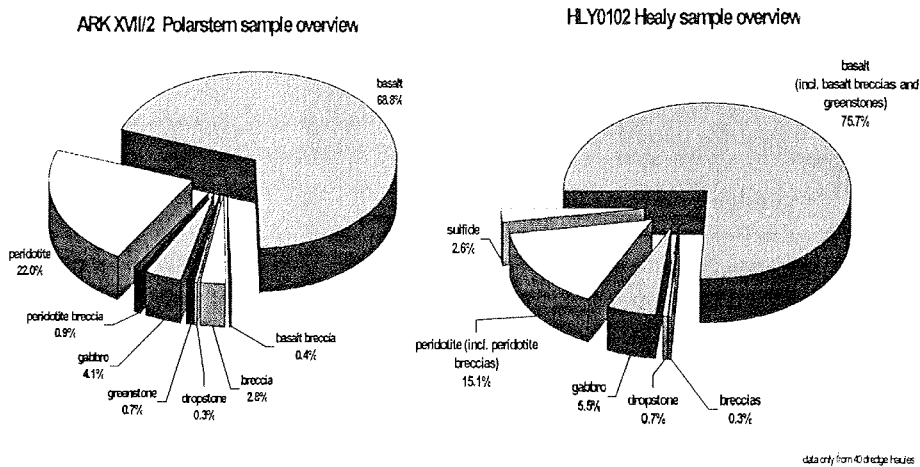


Figure 66: Lithologic overview by weight from HEALY and POLARSTERN.

weight of 2 tons are included, because the rock descriptions for this cruise are as yet incomplete. As is obvious from the figure, the proportions are pretty much the same for both cruises. However, HEALY collected some sulfides and the overview contained less rock types because peridotites and peridotite breccias are taken together. The same is true of the basalt group; basalt and basalt breccia are included together in the HEALY description forms. Figure 66 gives an overview of the rock types recovered by each ship by weight.

Basalts are the main dredged rock type, making up about 2/3 of the rocks sampled, followed by peridotites. Already this is a somewhat unexpected result. Preliminary planning estimates assumed approximately equal amounts of peridotite and basalt or even a predominance of peridotite. This is because of the ultra slow spreading rate and the low degree of partial melting predicted theoretically (White et al., 2001).

POLARSTERN collected relatively more peridotite than HEALY and less basalt, while HEALY sampled more basalt than POLARSTERN and less peridotite.

This relationship is surprising in view of the different sampling technologies employed. Both ships used alternative sampling technologies in place of dredges on axial volcanoes: HEALY used rock coring, which retrieved only at most a few grams of material per station. The equivalent axial volcano technology on POLARSTERN was the TV-grab, which often retrieved boulders of many hundreds of kg. Therefore one might expect that POLARSTERN should have sampled more basalt by weight than HEALY and not the other way around.

Thus, it is clear that the overall sampling program of POLARSTERN was more oriented toward peridotite recovery than was that of HEALY. The relative predominance of basalt on HEALY in comparison to POLARSTERN may also be explained by the operational limitations on HEALY. Between dredge D9, when the dredging wire was lost for the second time, and, when HEALY rigged their coaxial cable for dredging, HEALY was unable to dredge the deep wall sites that typically yielded peridotite. In order to balance the overall science program, these sites were taken by POLARSTERN. The deeper dredging thus may be responsible for the differing rock recovery patterns on the two ships.

Full descriptions of all samples taken from the POLARSTERN and the 40 HEALY dredges that they had described by the end of the cruise is given on the data CD (see Appendix). The data sheets contain the most important rock specifications such as primary lithology, average grain size, texture, minerals, deformation, alteration and other sample characteristics. The POLARSTERN sample description database contains an optimized print sheet for DIN A3.

Thin Section Overview (R. Mühe, J.E. Snow)

351 thin sections were microscopically examined by transmitted light microscopy. An overview can be seen in Appendices 14.9 and 14.10. Six main rock types were found in the sample set, including Basalt, greenstone, gabbro, peridotite, serpentinite and dropstones (see Table 12). The ca. 10 breccias seen in thin slides were added to those rock types of which the majority of breccia clasts are made of all of the breccias were monomict. The majority of the thin sections (148) consist of peridotites in all stages of alteration, i.e. mainly serpentinitization (Table 12).

Table 12: Number of thin sections discriminated by rock type.

Basalt*	Greenstones	Gabbros	Peridotites#	Serpentinities	Dropstones
134	12	15	148	39	3

*including a few dolerites and breccias

#including all serpentinised and mylonitic peridotites

Next come basalts including a few breccias and dolerites (134). Serpentinities as a 100 percent alteration product of peridotites are third. Rocks were classified as serpentinities only if no relict phases could be identified in the thin section. Otherwise they were given the name serpentinized peridotite. 12 thin slides were greenstones, 15 were gabbros and finally 3 were dropstones (one sandstone and two claystones were determined).

OFOS and TV-Grab Video

(A. von der Handt, B. Schramm)

OFOS-Observations

This tape was recorded on the 13.08.2001 at station number PS59/219 by the OFOS in the potential hydrothermal field in the western segment of the Gakkel Ridge. It is a black and white recording with voice comments on VHS-tape in PAL-system. The whole duration of the record is 3h 19 min. During the recording, the flashing of strobe lights can be seen because of the shooting of slides. Unfortunately the slides were unusable for observations as they were underexposed, or perhaps not exposed at all. This was clearly due to the jamming of the shutter on the camera. The details of the observations are shown in Table 13.

Table 13: OFOS Observations, Aurora Hydrothermal Field.

PS59/219-1	start: 13:10 / on bottom: 14:25 / off bottom: 17:45
13.08.2001	latitude (N): 82°93'17 / longitude: 6°16'45 W / depth: 3991 m
times	observations
0:01:47	on bottom, thick sediment cover
0:19:45	pillows, biology (shrimps, sessile organisms), steep wall
0:22:30	sediment cover
0:27:10	sediment cover, higher scattering
0:33:20	pillows, biology (sessile organisms), steep wall, less scattering
0:34:50	sediment, flattening topography, higher scattering
0:56:54	few sedimented rocks
1:00:25	few sedimented rocks, biology (sessile organism)
1:03:45	few sedimented rocks, biology (sessile organism)
1:04:17	sedimented rocks, biology (sessile organism), steeper topography
1:04:34	sediment, flattening topography
1:08:10	sediment, biology (sessile organism)
1:08:55	sedimented rocks, biology (sessile organism), steeper topography
1:09:51	sediment, flattening topography
1:10:30	sedimented rocks, biology (shrimps, sessile organism)
1:11:20	sediment
1:12:30	sedimented rocks, biology (sessile organism), steep wall
1:21:13	few sedimented rocks, sediment, flattening topography
1:36:00	sediment, biology (sessile organism), higher scattering
1:38:30	few sedimented rocks, biology (sessile organism)
1:59:00	large rock with biology (sessile organism)
1:59:28	black sessile organism
2:03:33	cloudy suspension (maybe due to bottom contact of OFOS) with many shrimps
2:10:00	sedimented rocks, biology (sessile organism), steeper topography, steep wall
2:19:09	thick sediments, higher scattering, swarm of shrimps
2:24:32	few sedimented rocks, biology (sessile organism)
2:26:14	cloudy suspension, followed by a swarm of shrimps
2:29:40	less scattering
2:29:58	few sedimented rocks
2:30:30	cloudy suspension, with many shrimps
2:30:53	less scattering, Sediments
2:31:05	sedimented rocks, biology (sessile organism)
2:32:51	sediments
2:36:12	elongated structures in the sediment (rocks?)
2:37:57	cloudy suspension (maybe due to bottom contact of OFOS)
2:38:29	sedimented rocks, biology (sessile organism, swarm of shrimps), steeper topography
2:39:29	few sedimented rocks, biology (sessile organisms) flattening topography

PS59/219-1	start: 13:10 / on bottom: 14:25 / off bottom: 17:45
13.08.2001	latitude (N): 82°93'17 / longitude: 6°16'45 W / depth: 3991 m
times	observations
2:41:14	sedimented rocks, biology (sessile organism, swarm of shrimps), steeper topography
2:42:23	sediments, flattening topography
2:48:31	cloudy suspension (maybe due to bottom contact of OFOS)
2:49:55	few sedimented rocks, biology (sessile organisms) flattening topography
2:50:00	cloudy suspension (maybe due to bottom contact of OFOS), swarms of shrimp
2:50:24	few sedimented rocks, biology (sessile organisms) flattening topography
2:51:31	higher scattering, few sedimented rocks, sediments
3:04:10	cloudy suspension (due to bottom contact of OFOS), swarms of shrimp
3:04:45	sediments, sedimented rocks, biology (sessile organisms, shrimps), less scattering
3:09:04	sedimented rocks, biology (sessile organism, swarm of shrimps), steep topography
3:10:30	cloudy suspension (due to bottom contact of OFOS), swarms of shrimp
3:11:25	sedimented rocks, sediment, biology (sessile organisms, shrimps), higher scattering
3:12:15	few sedimented rocks, sediment, flattening topography, less scattering
3:16:45	higher scattering, few sedimented rocks, sediments, biology (shrimps)
3:19:24	Finis

TV-Grab Observations

The observations are based on 5 videocassettes, which were recorded during the 32 TV-Grab operations along the Gakkel Ridge. Recordings were made in black and white on VHS-tape in the European PAL format. Some recordings also have voice comments. The picture quality is variable on the recordings due to the autofocus of the camera, which causes disturbances of the picture. The pictures show an image of the seafloor where, for example, sediment, biology and different varieties of rocks, e.g. pillows can be seen. For an estimation about height above the seafloor, there is a weight attached on a 4m long rope under the TV-Grab. The observations are shown in Table 14, for greater detail, including locations see Appendix 12.

Table 14: TV-Grab bottom observations.

station	date	location	begin [UTC]	on bottom [UTC]	off bottom [UTC]	latitude N	longitude	depth [m]	tape #	begin	on bottom	grab	end	observation	grabs	results
PS59/199-1	06/08/01	volcano	16:47	18:21	19:41	85° 33,3'	016° 07,4' E	4627	1	0:00:00	0:06:33	1:33:20	2:26:27	sparsely sed't d pillows, biology (sponges, shrimps), steep walls	4	15,668 kg basalt + glass
PS59/210	09/08/01	central valley	22:34	0:04	0:22	84° 07,8'	000° 19,4' E	3907	2	0:00:00	0:20:30	0:35:35	0:39:12	sparsely sed't d rocks, biology (shrimps), steep wall	2	empty
PS59/211	10/08/01	central valley	2:04	3:17	3:28	84° 08,0'	000° 25,7' E	3882	2	0:39:14	0:52:31	1:00:21	1:06:00	sed't d pillows, mud on lens after grabbing	2	0,685 kg basalt
PS59/212-1	10/08/01	sm volc axial valley	5:05	6:21	6:27	84° 07,9'	000° 27,7' E	3812						no video record		34,5 kg basalt
PS59/214-1	11/08/01	Volc high ax valley	4:45	5:38	6:01	83° 36,5'	003° 05,5' W	2725	2	1:06:01	1:22:26	1:45:15	2:00:00	sediment, sed't d rocks, biology (shrimps, ?), steep wall	2	41,3 kg gabbro
PS59/214-2	11/08/01	volc high in ax valley	7:04	8:04	8:05	83° 36,2'	003° 06,1' W	2680	2	2:00:02	2:07:42	2:08:28	2:11:05	large unsed't d rocks	1	250 kg gabbro
PS59/216-1	12/08/01	axial volcano (crater)	12:07	13:20	14:30	83° 05,2'	006° 05,9' W	3559	2	2:08:29	2:14:12	3:21:39	3:53:32	sediment, small sed't d rocks, biology (shrimps)	1	796,5 kg basalt
PS59/220	14/08/01	axial volcano (crater)	7:21	8:45	9:34	83° 12,2'	005° 31,2' W	4255	3	0:00:01	0:02:49	0:45:30	1:00:00	sediment, sed't d pillows, biology (shrimps, sessile organisms)	1	250 kg basalt
PS59/221	14/08/01	axial volcano (crater)	12:14	13:30	14:00	83° 15,9'	005° 32,9' W	4146	3	1:00:00	1:00:00	1:11:40	1:16:37	sediment, sed't d pillows, biology (shrimps, sessile organisms)	1	51,25 kg basalt
PS59/227-1	16/08/01	axial volcano (crater)	9:46	10:55	10:58	83° 47,5'	002° 07,6' W	2960	3	1:16:37	1:16:38	1:16:55	1:18:53	unsed't d pillows	1	0,2 kg basalt
PS59/227-2	16/08/01	axial volcano (crater)	13:47	15:15	15:35	83° 46,7'	002° 08,6' W	3123	3	1:18:54	1:27:48	1:45:57	1:47:47	thin sed't d pillows, steep wall	4	0,14 kg basalt
PS59/228-1	16/08/01		8:38	23:42	23:47	83° 52,6'	001° 01,8' W	3303	3	1:47:48	1:47:48	1:49:50	1:52:51	sed't d rocks, biology (shrimps)	1	170 kg basalt
PS59/233-1	18/08/01	axial volcano	7:43	9:10	9:13	84° 15,6'	001° 25,6' E	3768						no video record		empty
PS59/233-3	18/08/01	axial volcano slope	11:45	13:16	13:18	84° 15,4'	001° 31,5' E	3849	3	1:52:52	1:55:11	1:55:46	1:59:12	thin sed't d rocks	1	6,2 kg basalt
PS59/236-1	19/08/01	potential volcano	12:46	14:25	14:30	84° 43,8'	004° 34,4' E	5348	3	1:59:13	2:06:53	2:12:49	2:15:12	thick sediments	1	0,016 kg peridotite
PS59/239	20/08/01	septum	7:54	9:20	9:46	84° 51,4'	006° 33,6' E	4188	3	2:12:13	2:19:30	2:42:31	2:46:00	thick sediments, little rocks, biology (shrimps, algae?), steeper topog. at end	1	8 kg peridotite
PS59/252-1	25/08/01		17:15	18:40	18:42	85° 37,4'	018° 13,7' E	4018						no video record		1,402 kg basalt + glass
PS59/253	25/08/01	axial valley	7:55	23:51	23:54	85° 42,9'	018° 19,3' E	3773	3	2:46:01	2:52:50	2:53:03	2:58:28	unsed't d rocks	1	600 kg basalt
PS59/254	26/08/01		2:31	4:50	4:53	85° 44,1'	019° 33,1' E	4135	3	2:58:29	3:03:23	3:03:36	3:06:24	unsed't d pillows, steep wall	1	11 kg basalt
PS59/255-1	26/08/01		7:00	8:30	8:35	85° 47,2'	020° 21,3' E	4387	3	3:06:25	3:10:17	3:10:37	3:12:20	thin sed't d rocks, biology (sponges)	1	717,4 kg basalt
PS59/260	28/08/01		0:56	2:29	2:31	85° 57,8'	029° 12,2' E	4473	3	3:12:21	3:14:04	3:15:12	3:19:23	sed't d pillows, biology (sessile organisms, sponges), steep topography	1	137,206 kg basalt + glass
PS59/261	28/08/01	axial volcano	6:10	7:45	7:48	85° 58,5'	030° 10,6' E	4145	3	3:19:24	3:23:30	3:23:55	3:28:32	sed't d rocks, biology (sessile organisms), steep wall	1	95 kg basalt
PS59/262	28/08/01	volcano	10:40	12:05	12:10	85° 58,0'	030° 07,2' E	4088	3	3:28:33	3:31:42	3:36:59	3:40:16	sediment, few sed't d rocks, biology (sessile organisms)	1	0,258 kg basalt + others
PS59/265	29/08/01	axis	8:34	10:02	11:41	86° 19,5'	037° 45,7' E	4826	3	3:40:17	3:42:21	3:42:27	3:45:15	thin sed't d rocks	1	26 kg basalt + others
PS59/268	30/08/01	axis	10:32	11:52	13:27	86° 36,1'	042° 16,3' E	3780	3/4	3:45:16	3:49:06	1:17:01	1:19:24	sediment, biology (sessile organisms, shrimps)	1	1,832 kg basalt, peridotite + others
PS59/275-1	02/09/01		17:38	18:37	18:39	86° 35,4'	069° 00,7' E	3068	4	1:19:24	1:22:21	1:22:48	1:25:25	unsed't d pillows	1	21 kg basalt
PS59/292	14/09/01	sheet flow axis	3:32	5:06	6:00	86° 46,4'	065° 29,1' E	5022	4	1:25:26	1:31:09	2:24:49	2:27:49	sediment	1	mud only
PS59/302	18/09/01	seamount/wall	18:41	19:27	19:35	86° 39,9'	040° 31,6' E	2346	4	2:27:50	2:33:34	2:39:31	2:42:31	sediment, biology (shrimps)	1	9,45 kg basalt + others
PS59/303	19/09/01		0:50	2:05	2:08	86° 32,5'	040° 09,3' E	4264	4	2:42:32	2:46:04	2:47:49	2:49:43	sediment, few thin sed't d rocks, biology (shrimps)	1	39 kg basalt
PS59/304	19/09/01	volcanic high	6:43	8:02	8:08	86° 29,0'	040° 58,0' E	4496	4	2:49:44	2:50:03	2:50:10	2:53:42	unsed't d rocks, biology (sessile organisms)	1	210 kg basalt
PS59/315	23/09/01	seamount	2:15	3:46	3:56	85° 48,5'	020° 26,2' E	4766	4	2:53:43	2:57:03	3:06:13	3:12:56	sed't d rocks, biology (sessile organisms), mud on lens after grabbing	3	701,85 kg basalt + glass
PS59/321	24/09/01		23:42	0:59	2:00	85° 56,1'	023° 12,9' E	4545	4/5	3:12:57	3:16:52	no grab	0:10:44	sediment, few biology (sessile organisms), high drift speed, camera lens damaged	0	empty

8.5 Discussion

(J. E. Snow)

When this expedition was planned, the fundamental assumption was that magmatic activity and spreading rate would be strongly correlated, and that seafloor morphology would allow precise sampling of the different rock types of interest. Both of these assumptions were proven to be false in the context of Gakkel Ridge. It was not possible to directly relate spreading rate with crustal thickness along the ridge in any simple petrologic way, despite the nearly 50% variation in predicted crustal thickness from west to east.

More important for daily operations was the assumption that morphologic lessons learned from other ridges could be applied to Gakkel Ridge in selecting sample sites. This turned out to be false. Morphologically classic volcanoes turned out to be constructed of peridotite, and clearly tectonic wall sites that must have been millions of years old (given the spreading rate) sometimes produced fresh glassy basalt. The assumption that hydrothermal activity must be significantly lessened at these low spreading rates also turned out to be false, as nearly all MAPR records turned out to have hydrothermal plume-related anomalies.

What follows is a schematic representation of some of the principal scientific results that will be developed over the course of the next months as immediate results of this cruise.

Morphotectonic Segmentation of the Gakkel Ridge

(J.E. Snow)

The study area of AMORE 2001 can be separated into four morphologically distinct regions based on HYDROSWEEP and SEABEAM bathymetry. The characteristics of these regions are governed by the tectonic and magmatic evolution of the ridge, which varies quite strongly along strike. Many of the morphologic features of this unique ridge have quite unfamiliar forms, and it is thus often difficult to draw direct geologic analogies between Gakkel Ridge and other mid-ocean ridges worldwide. The main morphotectonic units are (Fig. 67).

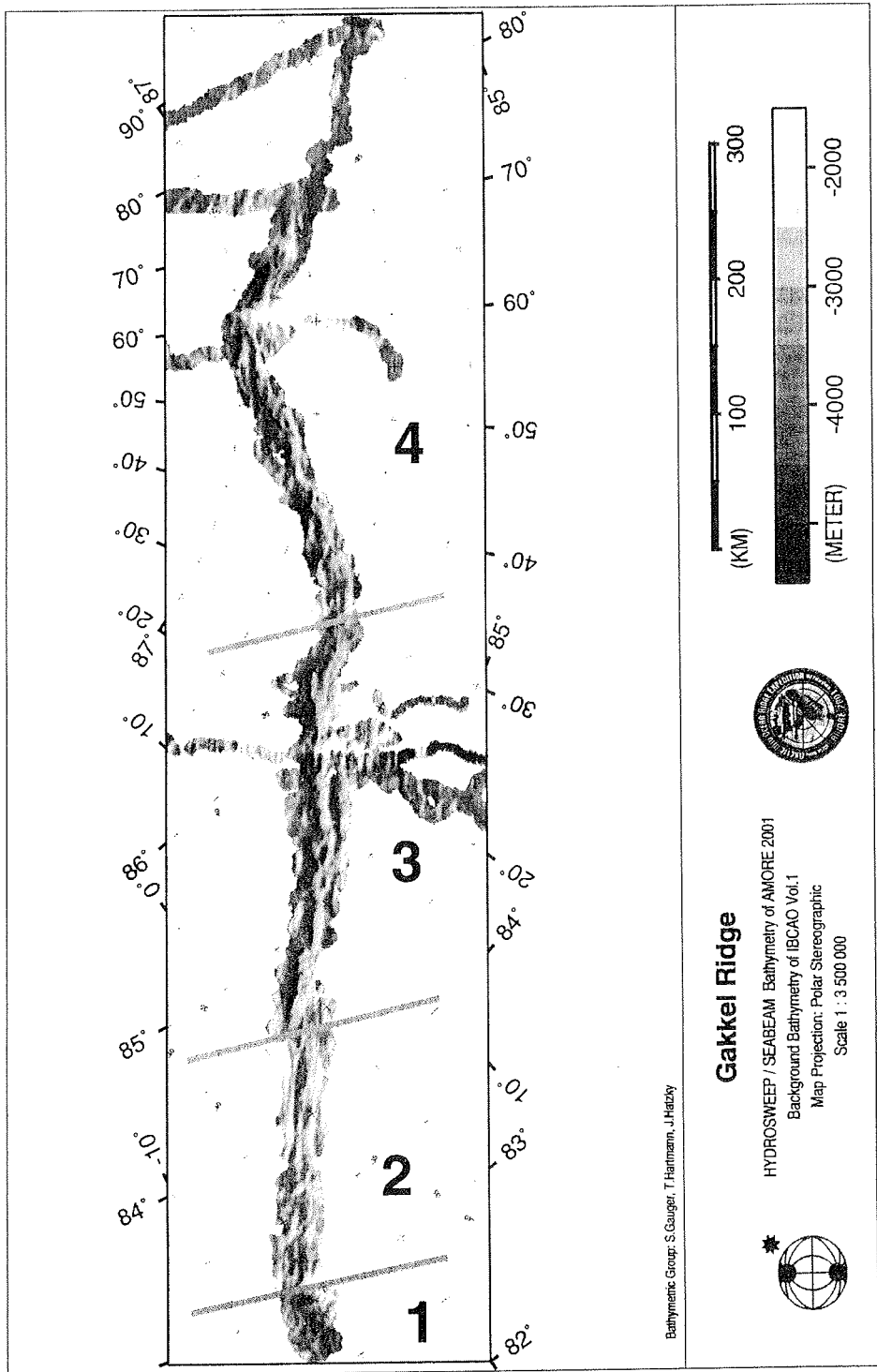


Figure 67: Morphologic segmentation of Gakkel Ridge

- 1) Intersection of Gakkel Ridge with Lena Trough, 7°-6° W. In this region, the ridge shallows and flattens toward the south, before plunging into the deep parallel rift of Lena Trough. Lena Trough's obliquity results in morphology similar to the amagmatic rift segments further east, with high sides and a straight and deep valley floor (~5000m). Dredging results from the central Lena Trough confirm this observation.
- 2) Magmatically robust region 6° W-3° E. This region is characterized by three well-developed axial magmatic swells along the ridge that are obviously constructional in nature, being composed of hundreds of small volcanic cones. In between these magmatic "upwelling" centers there is tectonic exposure of lower crustal rocks. These are places where fracture zones would be if there were any on this ridge. The rift valley walls are composed of widely spaced low stepped benches in which obvious constructional features are still visible. This suggests short-throw steep angle faulting that does not seriously disrupt the underlying crustal structure.
- 3) Magma-starved region 3-30° E. At 3° E the ridge suddenly goes through a transfer structure that appears similar to an overlapping spreading center, but where the eastern limb is purely tectonic. This deep valley plunges to the east to 1000m greater depth than the magmatic ridge adjacent. The ridge continues as a series of lenticular basins interrupted twice by a tectonic septum and twice by volcanically constructed magmatic centers.
- 4) Magmatic regions 30-85° E. Despite the declining spreading rate in this region, both the frequency and magnitude of magmatic constructional features increases in this region. There are magmatic saddles in the rift valley at 31° E, 33° E, 37° E, 42° E, 55° E, 61° E, and enormous volcanic centers at 69° E and 85° E. Very little to no peridotite is found in this region, suggesting that fault throws are short and that magmatism has increased. The shape of the valley is largely unchanged though with steeper rift valley walls than those of the western magmatic region, and less obvious constructional sea-floor morphology.

In the magmatic centers, the crust is shallow and volcanic. The magmatic highs occur at the ridge axis and extend as strips of magmatic crust away from the rift valley, suggesting that they are long-lived features. One of these mapped completely in the course of this expedition ends abruptly 70 km from the ridge (approximately 14 Ma), suggesting that these magmatic centers are not permanent

features, but are born, evolve and die out over the course of time. East of 69° E the ridge is inundated by sediments originating from the northward flowing rivers of Siberia. This can be readily seen in the flatness of the floors of the basins, suggesting sediment cover, and is confirmed by parasound and seismic traverses in the easternmost basins. Volcanism is apparently largely confined to the 2 major volcanic centers along several hundred km of rift axis. Whether the sedimentary burial is accompanied by a change in underlying tectonic style as well is not clear.

Petrographic Segmentation of the Gakkel-Ridge up to 87°N

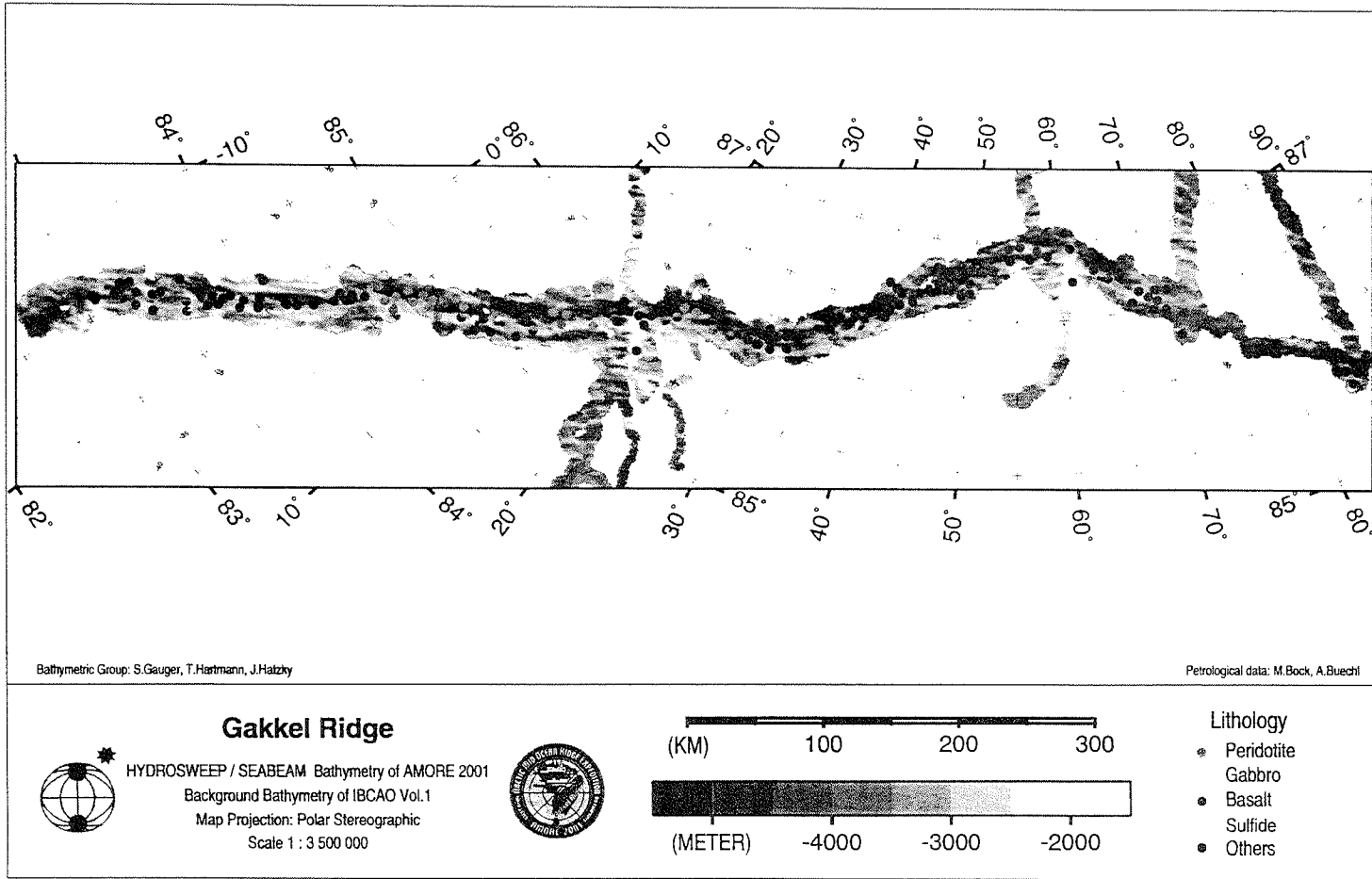
(A. Büchl, M. Bock)

The survey area investigated in the course of ARK XVII/2 can be divided into several petrographic segments (Fig. 68). In the first of these, the northern end of Lena Trough, there is a single dredge haul consisting of basalts and subordinate fresh massive sulfides and sulfide chimney material, which are a result of active hydrothermal venting in this region. On ARK XV/2 in 1999, the central portion of Lena Trough was sampled, 40 miles to the south of our survey area, returning three dredge hauls fresh glassy basalts, massive hydrothermal sulfides and peridotites (Snow *et al.*, 2001). Thus Lena Trough appears to be a hydrothermally active region.

The southern most part of the Gakkel-Ridge (6°W-3°E) is composed of three magmatic swells along the ridge, formed by numerous small volcanic cones 200-300m in diameter and around 100m high. In this whole segment only basalt was dredged and grabbed, except in one area (83°24'N 4°38'W to 83°36'N 2°45'W), where due to tectonic exposure gabbros and peridotites occur. The basalts dredged included the entire range of basalt types found on the ridge in general, from aphyric to highly plagioclase phyric vesicular basalt.

At 3°E the morphology changes suddenly to a deep valley with steep walls composed of a series of lenticular basins. This segment starts with peridotites up to 85°9'N 9°50'E, followed by a larger region, which is composed of basalts (dredged in 18 hauls), gabbros (dredged in 3 hauls) and peridotites (dredged in 12 hauls). This larger region is interrupted by one magmatic high at 15°E to 20°E, where only basalt is exposed and ends at 25°E. The northern part of the Gakkel-Ridge up to 85°2'E also consists of deep valleys with steep walls, but in contrast to the middle part it is only built up by basalts, with one single gabbro and peridotite outcrop (86°19'N 39°25'E) among them.

Figure 68: Petrographic segmentation of Gakkel Ridge



It is quite astonishing that most of the Gakkel Ridge is composed of basalts and not of peridotites. Especially in the eastern part, where the spreading rate is the lowest (~8 mm/yr full rate), more peridotites would have been expected because the crust should be thinner there. The lack of peridotites contradicts the widely accepted model of the correlation between spreading rate and crustal thickness. One possibility to explain this discrepancy might be the lack of fracture zones along the ridge. If fracture zones are required to disrupt the volcanic crust whatever the thickness, then even a very thin crust might suffice to cover up the peridotitic basement completely. However, there are no fracture zones in the central amagmatic segments either, so this explanation seems unlikely. Another idea would be the existence of thermal anomalies below the spreading center. In this case the amount of partial melting would be higher than expected at this spreading rate. Or the composition of the upper mantle in this region differs from the generally assumed depleted mantle composition, which melts below mid-oceanic ridges are believed to form snow.

All peridotite outcrops along the Gakkel-Ridge consist of unusually high percentage of lherzolites. This is a result of the low degree of partial melting due to the ultra-slow spreading rate leading to an unusual fertile mantle for a mid-oceanic ridge. Aside from that dunites only occurred in 6 dredge hauls. This is due to a minor amount of melt percolation as a result of the low amount of partial melting. It is remarkable that the dunites mainly occur where basalts are nearby and not in the part where solely peridotites were dredged. In addition plagioclase bearing peridotites are rare compared with Molloy Deep, further south in the Arctic ridge system, where they are plentiful.

There is no recognisable systematic distribution of basalt subtypes along the Gakkel Ridge. In contrast there even exist highly phyric and aphyric basalts in some dredge locations together. This points to the existence of small magma chambers in which different magma batches evolve to different degrees before being juxtaposed against one another by eruption.

Petrography of Volcanic Rocks
(R. Mühe)

134 thin sections of basaltic rocks (including 2 dolerites and 6 basaltic breccias) recovered during cruise AMORE 2001 were studied by means of transmitted light microscopy (Fig. 69-71). Given the number of ca. 160 stations for both

ships that contain basalt samples (90 stations for HEALY and 70 stations for POLARSTERN) of roughly 80 percent of all basalt stations a basalt thin slide has been microscopically investigated.

Prior to this study, only two basalt samples from Gakkel Ridge had been examined by microscopical means (Mühe et al. 1991, 1997). These two basalts have true aphyric textures and display a glassy rim as well as devitrified mesostasis towards their interior parts. Tiny equant to euhedral olivines, rarely occurring in clusters, numerous skeletal olivines, skeletal plagioclases, anhedral to skeletal clinopyroxenes, idiomorphic spinels and minute titanomagnetites constitute the main minerals of these rocks.

AMORE 2001 Basalt-Types

Of 126 basalt samples 10 percent were truly aphyric (Table 15). As a matter of fact 90 percent of all samples were phyric to porphyric. By far the most samples, 61 percent were phyric (they have from 2 – 10 percent phenocrysts) and highly phyric (16 percent; they contain more than 10 – 25 percent phenocrysts). Finally, 7 percent represent porphyric samples (>25 up to >50 percent phenocrysts).

Table 15. Basalt-types discriminated after the amount of phenocrysts (% of samples).

aphyric	sparsely phyric	phyric	highly phyric	porphyric
10	6	61	16	7

Thus, more than 80 percent of the Gakkel Ridge basalt examined display a more or less pronounced texture that results from the existence of fractionation processes in a magma chamber. Even at this very preliminary stage of work done on our samples this figure is surprising if one considers that it was believed that on Gakkel Ridge only very small and ephemeral magma chambers could exist if any.

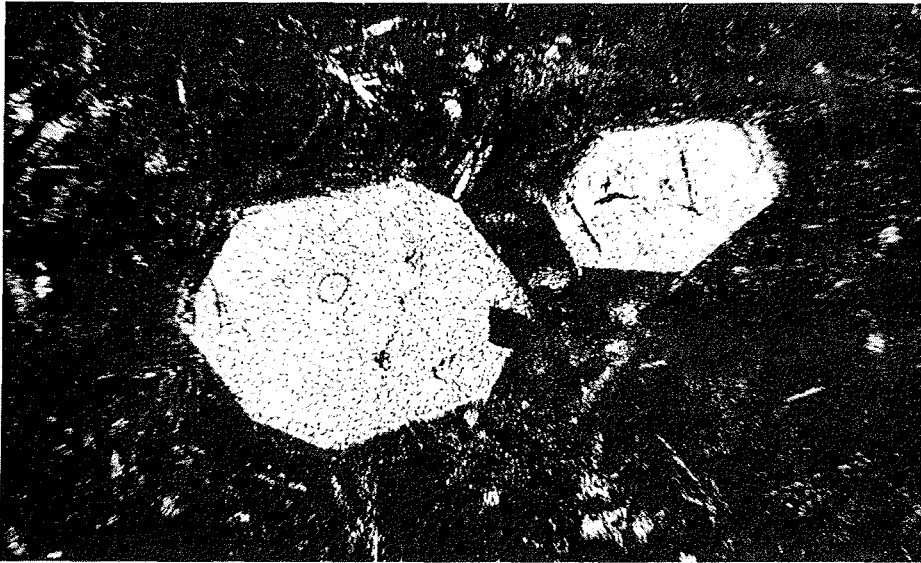


Figure 69: Olivines with glass inclusions and brown spinel (left crystal) set in dark devitrified mesostasis with numerous skeletal plagioclase laths. Mag: 120x, plane polarized light.

Phenocrysts

Olivine is the mineral most frequently seen as pheno- or micro-phenocrysts followed by plagioclase. Very rarely clinopyroxene could be identified as phenocryst mineral due to its similarity in shape and appearance to olivine. Spinel appears in one sample as up to 2 mm large idiomorphic phenocryst together with plagioclase in a porphyritic rock.

Glomerophytic textures of plagioclase and olivine or clinopyroxene are not uncommon, as well as two generations of phenocrysts divided by their size. Olivine phenocrysts are around 2 mm large on average (15 mm maximum size) and make up more than 4 vol.-% (30% maximum) of the rocks. In about half of the olivine bearing rocks olivine displays skeletal growth whereas euhedral shape is prevalent. In quite a few cases olivines are anhedral and rounded as a result of resorption following mixing of chemically distinct magma batches. Also not frequent but observed are glass inclusions within the olivines. In one case fluid inclusions can be seen.

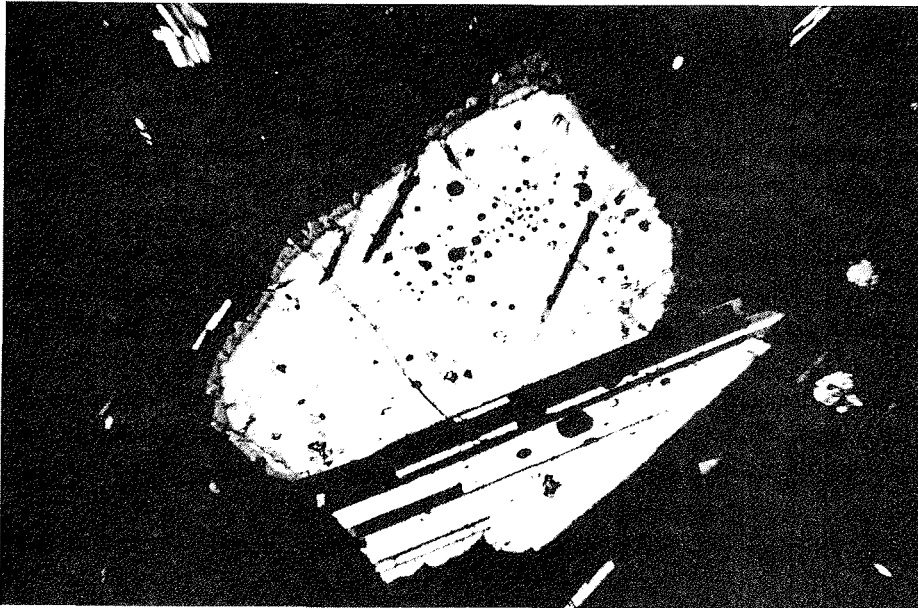


Figure 70: Zoned plagioclase phenocryst with numerous glass inclusions set in a glassy mesostasis with small skeletal plagioclases. Mag: 25 x, crossed Nichols.

Plagioclases are nearly as ubiquitous as olivines, but are generally larger (>6 mm on the average, around 20 mm maximum size). If present as phenocryst they make up 11 vol.-% on average and can have more than 50 vol.-%. Due to their appearance, especially the number of twinning lamellae seen per specimen, an anorthitic composition is estimated. Quite often they display strong zoning pattern and numerous glass inclusions (Fig. 70). However, skeletal growth as well as late skeletal ongrowth on idiomorphic crystals is also seen in some slides. Resorption, due to magma mixing is most often seen on plagioclase xenocrysts, sometimes resulting in ball-shaped relicts of former large idiomorphic crystals.

Clinopyroxenes are identified here by their well-developed cleavage and their octahedral crystal shapes. As pointed out earlier their amount as phenocrysts could be higher, but their proper identification remains a matter of home-lab microprobe analysis. Those clinopyroxenes identified here are on average 3 mm large (5 mm maximum size) and make up 2 vol.-% (3 maximum). As a matter of fact the crystals display idiomorphic contours. No signs of resorption, or glass inclusions are seen.

In entirely glassy basalt with pl-porphyric texture a large (2 mm) phenocryst of spinel is observed. The pale brown-yellowish colour of the crystal points towards low Cr-contents. This is the only example of a spinel as a phenocryst in the entire suite of basalt thin slides.

Types of groundmass of the Gakkel basalts

Generally the basalt's groundmass varies between 5 different types:

1) is a nearly holo-crystalline groundmass (doleritic) of plagioclases, clinopyroxenes and titanomagnetite.

2) intersertal groundmass with idiomorphic to skeletal plagioclases, intergrown with clinopyroxenes. Titanomagnetite crystals may be visible or too small and usually some interstitial glass is preserved,

3) is named micro-crystalline, displaying a nearly opaque mesostasis and/or glass in which plagioclase skeletal laths and olivines are embedded. Clinopyroxenes are seldom well crystallized and dust like titanomagnetites add to the opaqueness of the mesostasis.

4) devitrification zone is that part of the groundmass that borders the glassy rim. Here, nearly opaque spherical or sheaf-like structures are dominant, that preferentially form around minute crystal seeds. Plagioclase seeds form spherical or oval structures, olivine seeds form rhombic opaque fields with rounded edges. Sheaf-like structures can be initiated by both plagioclase or olivine or clinopyroxene crystals. Within this type of groundmass spinifex textures of skeletal olivines (>1 mm) elongated along the c-axis (Donaldson, 1982) can be found quite a few times. Such textures were observed in the first Gakkel Ridge samples examined by Mühe et al. (1991).

5) glassy rim or entirely glassy groundmass (seen only in one thin slide). Glassy rims can be up to 25 mm thick and glasses have dark-brown to light-brown colours.

Most often micro-crystalline and devitrified groundmass is observed followed by glassy rims and intersertal groundmass. Only 5 times doleritic groundmass has been examined.

Some special features should be added: residual glass being pressed into vesicles in the very late course of solidification after eruption of the lava is seen quite a few times as are flow structures typical of highly viscous lava being emplaced on the seafloor. However, quite a few times streaks and bands of groundmass rich in plagioclase laths or devoid of any crystals and thus contrasting starkly to the ambient groundmass is observed. In some other cases phenocrysts or clusters of phenocrysts or parts of groundmass rich in vesicles are surrounded by flow aligned plagioclase or vesicle poor groundmass. These phenomena are interpreted as signs of inhomogeneous mixing of various magma batches in the late stage of magma chamber activity followed by fast lava upflow and eruption.

Alteration

60 percent of the samples appear virtually fresh and unaltered under the microscope. Two thirds of the remaining samples are only lightly altered and the rest is mostly moderately altered. Only 3 samples have been classified to be strongly altered. This in general is also surprising, since this result reflects an unawaited overall degree of freshness, i.e., relatively young age of the Gakkel Ridge basalts under investigation. Given the fact that the recovered dredges contained quite a few very fresh looking glassy basalt samples that appeared to be of Recent age, it should be stated that this again constitutes one of the astonishing outcomes of the sampling campaign and that Gakkel Ridge seems to be more recently volcanically active than predicted by our models.

Smectite is the ubiquitous alteration mineral appearing in the groundmass, filling vesicles and lining cracks. Palagonite, a mineral mixture of mainly also smectite and Fe-oxy-hydroxides replaces glassy rims and comes next after (Fig. 71). Severe cases of alteration are coloured interal zones made up of smectite, mixed layered smectite-chlorite and rarely chlorite and epidote replacing olivines, clinoproxenes, plagioclases and titanomagnetites and filling a few thin cracks. Where the overall amount of alteration of this latter type exceeds a certain volume of the rocks they have to be termed metamorphic, i.e. greenstones and are treated and described separately.

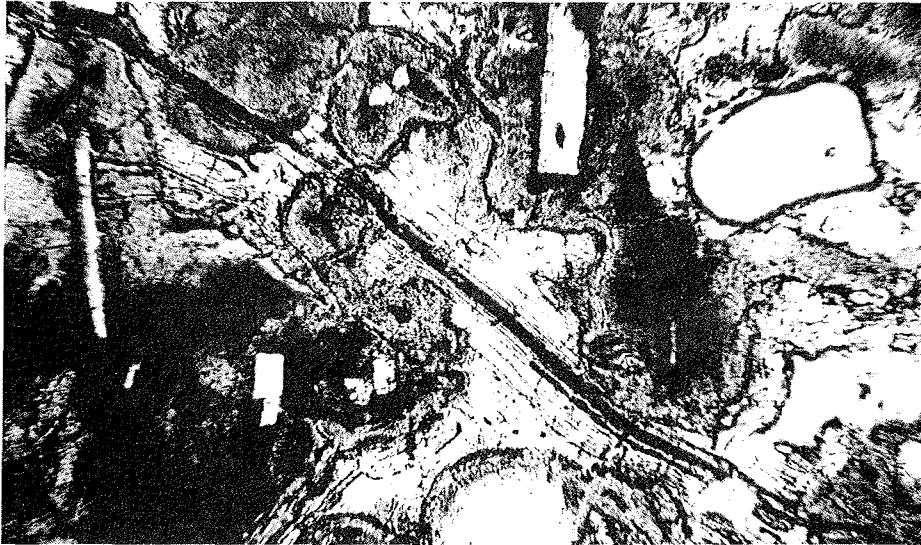


Figure 71: Yellow palagonite replacing glassy groundmass along a crack (upper left to lower right) and showing banded structure. Groundmass is partly devitrified (dark) and contains plagioclases and vesicles. Mag 25 x. Plane polarized light.

Petrography of Plutonic Rocks

(Y. Gao, J.E. Snow)

Gabbros (Fig. 72), which form the oceanic crustal layer 3, are plutonic rocks that have cooled more slowly than basalts, under greater pressure and in the more protracted presence of volatiles. In contrast to the relatively greater recovery of basalt and peridotite, gabbros were only recovered from 6 stations by POLARSTERN (two TV-grabs and four dredges) along Gakkel Ridge, which were exposed by tectonic tearing of the upper lithosphere (see Morphotectonics section in Ch. 8.5). Besides these 6 gabbro stations, several gabbro dropstones were also found from one dredge station (PS 59-218).

Based on the primary mineralogy estimated by the observations on thin-sections, following the standard IUGS nomenclature and the general marine usage established at Hole 735B (Dick, Natland et al., 1999), the recovered gabbros are mainly olivine-bearing gabbro, troctolite and troctolitic gabbro, together with some iron-titanium oxide microgabbro. The different mineralogies probably indicate a difference in the proportion of cumulus to the intercumulus phases. The primary textures of olivine-bearing gabbros which consists of olivine (<5%), plagioclase (60-80%) and clinopyroxene (20-40%), are characterized by poikil-

itic clinopyroxenes that enclose or partially enclose euhedral plagioclase and sometimes olivine. This indicates that olivine and plagioclase crystallized together prior to the crystallization of clinopyroxene. Some plagioclases have obviously continuous zoning patterns with relatively high-Ca cores to high-Na rims. Clinopyroxene usually has (001) exsolution lamellae or exsolution patches.

Troctolite, which consists of olivine (20-25%), plagioclase (70-75%) and clinopyroxene (0-5%), and troctolitic gabbro that consists of olivine (20-25%), plagioclase (60-70%) and clinopyroxene (5-15%) are also characterized by poikilitic textures indicated by the euhedral plagioclase enclosed by poikilitic olivine and clinopyroxene. Zoned plagioclase and exsolution of clinopyroxene exist in some thin sections.

These rocks are medium to coarse grained and contain poikilitic clinopyroxene crystals ranging in size from less than 1 cm to more than 5 cm. In many cases, the clinopyroxene crystals are elongated and aligned in an igneous fabric. The texture relationships in thin sections indicate that these gabbros are orthocumulates that formed in a cooling magma body by rapid crystal settling or by in-situ crystallization on the wall, floor, or roof of the magma chamber.

The iron-titanium microgabbros with an equigranular texture contain more than 10% opaque minerals (magnetite and ilmenite) which crystallized from the intergranular fluids suggested by the fact that they are only restricted to the interstitial areas. They are fine-grained rocks and contain on average 70-80% plagioclase (0.2-2mm), 10-20% clinopyroxene (0.1-1.5mm), and less than 5% olivine (0.1-0.5mm).

Contrary to the well-developed fractures caused by brittle deformation, the poorly foliated texture in some gabbros indicates that that crystal-plastic deformation was only weakly developed in these rocks. The metamorphism and alteration broadly exist in these gabbros, the high-temperature sequences are mainly greenschist mineralization represented by the well-developed replacements of plagioclase, clinopyroxene and olivine by epidote – chlorite - sericite. On the contrary, high-grade metamorphism was only restricted to few samples or absent. At the same time the low temperature alteration indicated by the abundant smectite and carbonate related to the circulating seawater, which filled in the fractures and replaced olivine and clinopyroxene are broadly present, but the high temperature alterations usually manifested by the coronitic alteration halos around olivine are absent.

The orthocumulate character of the main gabbros, the zoning patterns of plagioclase, the broad existence of exsolution lamellae in plagioclase and clinopyroxene, together with the particular patterns of deformation, alteration and metamorphism developed in these gabbros reflect the low temperature nature below the Gakkel Ridge and the relatively fast cooling history of the gabbros caused by the ultra thin crust thickness of this area (Coakley and Cochran, 1998).



Figure 72: Thin section showing poikilitic clinopyroxene enclosing plagioclase in an olivine bearing gabbro. Magnification 12,5 x, crossed nichols.

Petrography of Mantle Rocks

(J. E. Snow, A. Büchl)

One of the main aims of the AMORE expedition to Gakkel Ridge was to investigate the nature of mantle residues of low-degree partial melting. Previous results from a single sample of highly serpentinized Gakkel peridotite were unable to conclusively resolve many of the issues of mantle melting and mantle veining involved. We have made a preliminary examination of 150 thin sections and hundreds of hand samples of mantle peridotites made onboard POLARSTERN

and HEALY in the course of the expedition. There are two differences between this sample set and those commonly observed on mid-ocean ridges that are of particular note. First is the relative abundance of clinopyroxene (Fig. 73). The mean clinopyroxene content and size observed in thin section are both qualitatively greater than is commonly observed in abyssal peridotites. Second, the spinels are more nearly euhedral, more abundant and commonly very pale in color. The pale colour is well known to be a sign of low Cr content (and thus high activity of Al) in the residual system. All of these observations suggest a low degree of partial melting in the Gakkel Ridge mantle, in accordance with theoretical predictions.

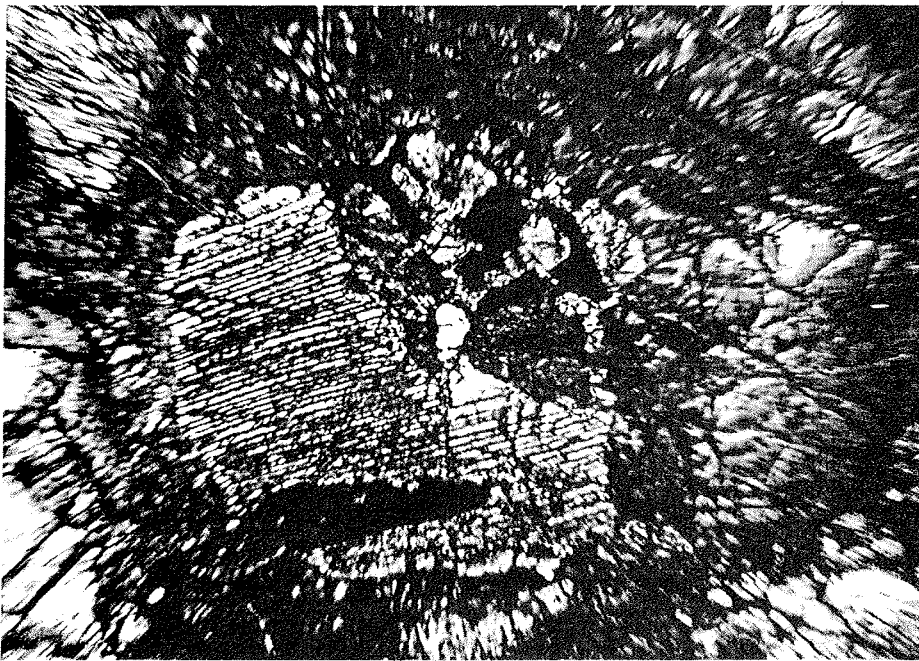


Figure 73: Serpentinized peridotite showing partially intact relict clinopyroxene bordered by relict spinel. Magnification 12.5 x, crossed nichols.



Figure 74: Clinopyroxene in fresh abyssal peridotite showing lack of serpentinization and large grain size (field of view is 4mm).

Most of these peridotites are altered 60-90%, like most abyssal peridotites (Fig. 73). About 62% of these peridotites are weathered to different degrees and only 35% are serpentinized. Serpentinization of peridotites takes place at temperature of approximately 350°C – 400°C. Therefore this observation is a hint that in most of the areas where peridotites were dredged hydrothermal activity was low. Moreover most peridotite dredge holes contained serpentinized and weathered peridotite, suggesting locally restricted hydrothermal activity. However, some peridotites are stunningly fresh, containing no detectable serpentine in thin section (Fig. 74). The distribution of mantle rock types is similar to that from other mid-ocean ridges. Dunites are present but rare, in contrast to the SW Indian Ridge oblique spreading center at 12°E, as are plagioclase peridotites, in contrast to their abundance at Molloy Deep further south on the Arctic ridge system. Some dunites of dredge hole D92 contain spinel schlieren. These spinel schlieren are usually found in ophiolites and have not been observed in abyssal peridotites until now. They could be traces of melt percolation, where melt started to pool and to crystallize chromite. Plagioclase is present in a few of the fresh samples, forming haloes around embayed spinels, and in contact with clinopyroxene forming spectacular symplectic haloes around the spinel.

This suggests that in this case, the low pressure phase transformation $\text{cpx} + \text{spinel} \rightarrow \text{plagioclase} + \text{olivine}$ is responsible for the observed textures rather than impregnation by a basaltic melt (Fig. 75).

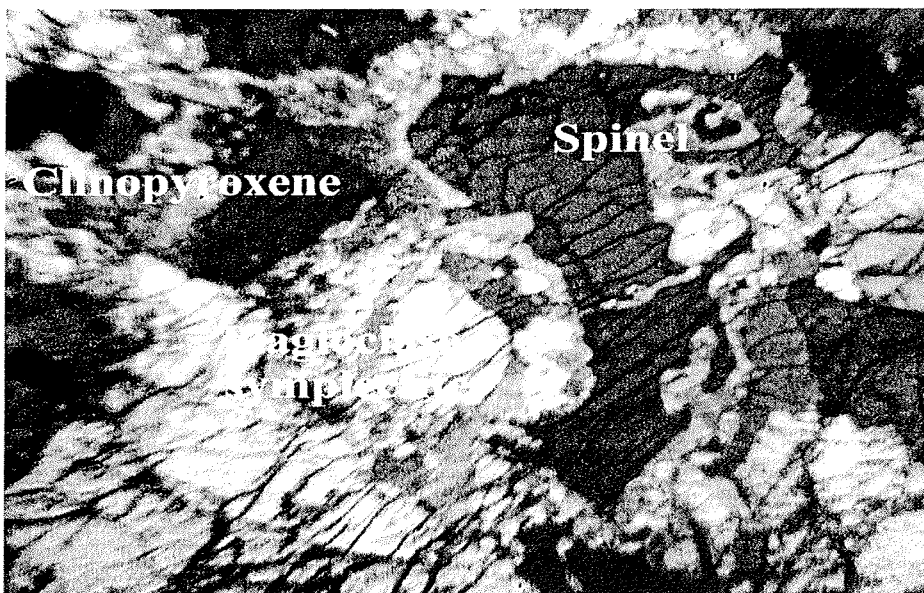


Figure 75: Photomicrograph showing breakdown reactions of spinel and clinopyroxene to plagioclase. Field of view is 2 mm.

Gabbroic veins in the peridotites are not very common and just present in few dredges. Particular in D85 nearly all peridotites are veined with different vein sizes. The lack of abundant veining could be the result of the low degree of partial melting, which leads to an unusual small amount of melt percolating through the peridotite. A few mylonites are also present, which are the results of emplacement of the peridotites from deep in the mantle by high-temperature crystal plastic creep processes.

Petrography of Metamorphic Rocks

(R. Mühe)

Hydrothermally altered basalts when affected by greenschist-facies metamorphic conditions (100 – 400° C and a few hundred bars of pressure) are termed greenstones. Greenstones constitute an overall very important and sometimes

dominant part of the oceanic crust. Considering the fact that every 200 Ma all oceanic crust is subducted into the earth mantle thus forming one important part of the dynamic earth system very little is known about the mineralogy and even less about the chemical composition of greenstones. Only recently their importance in controlling the global flux of various hydrophilic elements has been pointed out (e.g. Hofmann, 1988; Mühe et al., 1997).

In contrary to our expectations awaiting not just a few signs of hydrothermal impregnations on Gakkel Ridge rocks, at least 10 percent of all successful sampling stations (158) contained greenstones. A few dredges were nearly entirely made up of greenstones. The most surprising find are real epidiosites, rocks that were before known only from ophiolites (Fig. 76). This report gives preliminary information on the microscopy of 13 thin slides of greenstones out of 6 dredges recovered during the AMORE 2001 cruise.

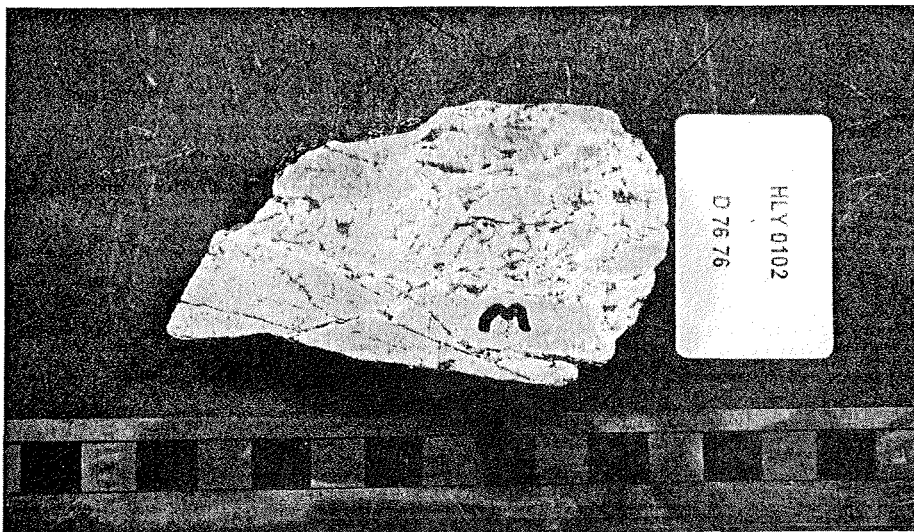


Figure 76: Epidiosite, greenstone with epidote as main secondary mineral. Scale bar is 1cm.

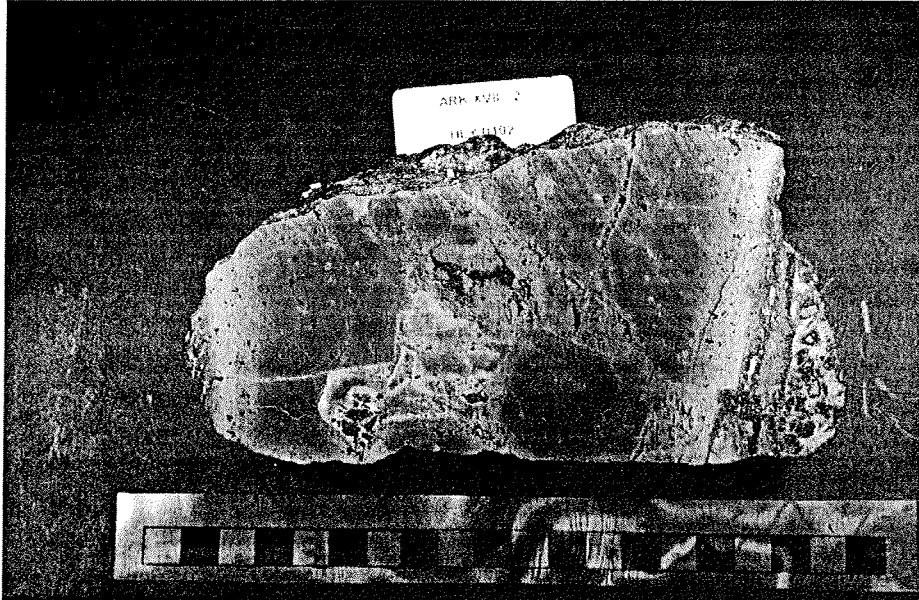


Figure 77: Veined greenstone with chlorite vein-fillings (green to dark-green) and tendency towards auto-brecciation as a result of breakdown of primary minerals. Scale bar is 1 cm. Working sample.

Types of Greenstones

The majority of the greenstones examined (8) are cut by veins (Fig. 77), that are filled with secondary minerals. Five specimens are unveined and also show well preserved primary textures.

Primary textures recognised have been intersertal in 7 cases with or without the presence of phenocrysts and doleritic (6) again with or without the presence of phenocrysts. The presence of veins is not controlled by the primary texture. Five samples display sulfide impregnations in the form of disseminated blebs of pyrite in the groundmass. Only two samples show the presence of sulfides in veins.

Secondary and Tertiary Hydrothermal Minerals

Chlorite

The most crucial mineral in a greenstone can be considered to be chlorite. Chlorite forms out of mafic minerals olivines and clinopyroxenes as well as out of plagioclases and glass. As a Mg-silicate that has build in 8 (OH) groups chlorite formation as no other secondary mineral accounts for the strong increase of H⁺ in the hydrothermal fluid, i.e., the low pH (2-5) necessary to leach base metals out of basalts from the reaction zone above the magma chamber level within the oceanic crust. Thus chlorite formation is a must in order to run hydrothermal convection cells that as a result precipitate metal-sulfides within the crust or as massive sulfides on the sea-floor as happened where Dredge 8 of HEALY grabbed through a hydrothermal smoker field. Chlorite is ubiquitous and is found in veins and in the former groundmass.

Epidote

Epidote is also quite common in the samples studied. It forms mainly out of plagioclase and clinopyroxene as well titanomagnetites through the uptake of (OH) groups into the crystal lattice. Epidote is easily recognized in thin slides through its high relief and unusual birefringence colour under crossed nicols. Epidote occurs both in matrix and in veins.

Albite

Albite is also common. Strong uptake of seawater sodium into the plagioclases and the release of calcium to form epidote, prehnite as well as carbonate give the plagioclases a mottled appearance and some show irregular pattern of albite domains recognisable by their different extinction angles from Ca-rich plagioclase domains.

Prehnite

Similar to epidote but at lower temperatures (below 250° C) prehnite, a water bearing Ca-silicate is formed out of the primary silicates in the basalts. Prehnite is easily recognised by its tendency to form spherical aggregates of bladed crystals with typical birefringence colours of the second order. Prehnite as epidote occurs in matrix and veins.

Leucoxene

Leucoxene formation replaces titanomagnetites and constitutes a fine grained mineral mix of mainly rutile, anatase, Fe-oxides, titanite and epidote. Leucoxene

is ubiquitous though its presence is restricted to the former groundmass titanomagnetites.

Quartz

Quartz forms in the course of the breakdown of primary silicates, since secondary silicates all inhibit much less silica into their crystal lattice. Quartz enriched hydrothermal fluids enhance the amount of base metals solved. Quartz forms mainly in veins and is accompanied by sulfid precipitation in veins.

Sulphides

Under transmitted lights no direct reconnaissance of sulfides is possible. However, the shape of opaque minerals can be determined. Pyrite typically is identified as disseminated blebs spread all over the former groundmass, reaching 1 or more mm in diameter.

Vein mineralogy

Two types of veins are recognised under the microscope. Those filled with one mineral and those showing sequential filling by various minerals. Monomineralic veins can be made up by (in order of abundance) quartz, epidote, chlorite. Polymetallic veins are filled by quartz and chlorite, quartz and epidote, quartz and prehnite, epidote and chlorite, epidote and prehnite. Sulfides as pointed out earlier occur exclusively in quartz-dominated veins.

8.6 Conclusions

(J. E. Snow)

Gakkel Ridge, aside from being the world's slowest spreading mid-ocean ridge, is without a doubt the most enigmatic and interesting mid-ocean ridge in the world as well. With this expedition, Gakkel Ridge has gone from being one of the least studied mid-ocean ridges to being one of the best-studied, that perhaps not yet the best-understood. One reason for this situation is the fact that the expected relationship between morphology and petrology that holds true for other mid-ocean ridges does not function here. The expected and theoretically predicted relationship between crustal thickness and spreading rate is not seen either, as evidenced by the abundant outcrop of basalt in the slowest spreading eastern region of the ridge. In all over two hundred sampling stations conducted by the two ships now reveal the details of this ridge.

In general, the rock types encountered on Gakkel Ridge are comparable to those found on other very slowly spreading mid-ocean ridges. Basalts ranging from aphyric to plagioclase-olivine phyric are similar to those on other ridges, and are unusual only in their vesicle content, which is much higher than normal, in many cases approaching 10% of the rock. Where plagioclase phyric lithologies are present, olivine is always also present, suggesting that the rocks remain primitive, as olivine remains on their liquidus. The abundance of phyric basalts suggests that magma chambers are present, as it is generally accepted that these are required for the formation of basalt phenocrysts.

The presence of greenstones and epidote-quartz-chlorite metamorphic mineral assemblages suggests a robust hydrothermal development of the crust. This is similar to oceanic crust elsewhere, but is somewhat surprising given the expectation that hydrothermal activity should be greatly diminished at ultra slow spreading rates. This observation is borne out by anomalies observed in the water column using the MAPR devices (of Ch. 5). Nearly all of the MAPR recordings show evidence of active hydrothermalism nearby.

The peridotites are generally more fertile than those observed elsewhere on mid-ocean ridges, though a quantitative evaluation of this assertion must await mineral modal and chemical analysis on land. Harzburgite and dunite are in any event rare, and this suggests low degrees of modification of the melts by melt-wallrock interaction prior to eruption. The recovery of extremely fresh abyssal peridotites will allow geochemical analyses that previously could only be dreamed of. Gabbros are nearly non-existent on this ridge compared to basalts and peridotites, implying that magma chambers are small or non-existent. This is somewhat surprising in view of the abundance of phyric basalts, which seem to suggest the opposite, that magma chambers are well developed.

The general picture of the ridge that emerges is that Gakkel Ridge has crust that is petrographically thin (i.e., low degrees of partial melting), and seismically thin, but is nonetheless lithologically robust, that is to say that basalt crops out nearly everywhere. This may perhaps be due to the absence of fracture zones along the ridge. These tend to break up what basaltic crust is present, allowing deeper lithologies to be sampled.

The previous expectation that the crust would be only 2-3 km thick (Coakley and Cochran, 1998) seems not to be borne out by the evidence. However, a slightly thicker crust would be more in line with geochemical indicators of crustal

thickness (White et al., 2001; Hellebrand et al., 2001) that suggest a slightly thicker crust of perhaps only 4-5 km. Extremely thin crust could only be inferred in the central magmatically starved zone of the ridge.

For this reason one can conclude that lithospheric top cooling induced by a low spreading rate is not the most important geological forcing function that determines the magmatic robustness of a ridge. Mantle temperature and fracture zone density undoubtedly also play major roles.

9. Geophysical Investigations

(W. Jokat, H. Bohlmann, S. Drachev, A. Galaktionov, G. Kapinos, B. Lahrmann, N. Lensch, U. Miksch, K. Müller, A. Pignatelli, O. Ritzmann, M. Schmidt-Aursch, T. Schmidt, T. Schmitz, A. Wüstefeld)

9.1 Introduction

The Arctic system of spreading centres extends from the Kolbeinsey Ridge at the northern margin of Iceland to the termination of the Mid-Atlantic Ridge (MAR) spreading system on the Laptev Shelf in the Arctic Ocean. The Gakkel portion of the ridge in the Arctic Ocean is the least explored part of the global ocean ridge system. Almost every segment of the Arctic ridge system is anomalous in some way. The Kolbeinsey Ridge is anomalously shallow and may represent the extreme in mantle temperature for a normal ocean ridge. The Gakkel Ridge, which is an extension of the MAR into the Arctic Ocean, is anomalously deep and is the slowest spreading major ridge segment in the world's oceans. The Gakkel spreading axis is almost completely cut off from normal sediment supply by the permanent covers of sea ice and large ridge-flank highs. The spreading rate diminishes almost to zero as the Gakkel Ridge approaches the pole of rotation and dies out on approaching the Laptev Shelf. It is the slowest spreading ocean ridge, with the full spreading rate declining from 1.3 cm/year at the European end of the ridge near Greenland to 0.6 cm/yr at the eastern end in the Laptev Sea. The Gakkel Ridge also has an exceptionally deep rift valley, and the thinnest known crust for a normal ridge. The two stations from which basalts have been recovered suggest that the crust has end member major and trace element characteristics as well.

The critical issue at the Arctic ridges is how their exceptionally slow spreading rates have influenced melt production in the mantle, melt migration through the lithosphere, crustal genesis and tectonism associated with the seafloor-spreading process. Geophysics provide insights into these issues by generating information about the physical state of the mantle, the thickness and temperature of the crust, and the morphology and segmentation of the actively spreading axis. Crustal thickness, which is a measure of the total melt production rate, is known to be exceptionally thin in the Arctic spreading axes, with a minimum of 3 km being reported for the westernmost Gakkel Ridge. Whether or not crustal thickness

varies systematically - and smoothly - with the spreading rate needs to be established with additional seismic measurements. Both on and off axis measurements should be made, since spreading rates (as determined by magnetic lineations) have varied with time as well as latitude. Seismic investigations also retrieve information about the crustal structure of the active ridge system. Refraction seismic and earthquake studies, using micro-earthquakes, provide critical constraints on the crustal structure and current tectonic activities. Determining the relationship between spreading velocity and crustal thickness is relevant to defining variability along the global ridge system. Geodynamic understanding of the evolution of the spreading system in the Eurasia Basin can be derived from the sedimentation history of the adjacent basins. Here, parameters such as basement topography or topography of the former ridge give insights into how slow spreading ridge systems evolve. Seismic imaging techniques can provide this information in great detail. Knowledge of the sedimentary cover over the ridge and the adjacent areas is a critical parameter for interpretation of other geophysical data such as magnetic, gravity, heat flow and micro-seismicity.

To provide a consistent geophysical/petrological model for the super-slow Gakkel Ridge, sufficient information on the crustal thickness and the composition of the upper mantle beneath the rift valley and its flanks is required. Therefore, a wide range of different geophysical methods was applied to meet these objectives. Both conventional ship-based experiments like seismic reflection experiments as well as measurements located on drifting ice floes were conducted. In this chapter the results will only be briefly reviewed, while details will be described in the subsequent chapters.

Seismic Reflection Experiments

To determine the crustal structure of the Eurasian Basin north and south of Gakkel Ridge, long seismic transects in Amundsen and Nansen basins were acquired. A 24 l airgun cluster in combination with a 300 m long streamer (48 channels, 6.25 m group spacing) was used. In addition sonobuoys were deployed in order to provide information on sediment and crustal velocities for a depth conversion of the seismic data. All three profiles provided excellent data and most of the oceanic basement was clearly imaged after processing. In total, 36 sonobuoys were deployed along the seismic profiles. The sonobuoys provided signals even from deeper levels of

the oceanic crust. On some of the sonobuoy records also signals from the Moho are visible. This allowed a minimum estimate of the crustal thickness. Gravity modelling of the transects will provide more reliable crustal models than in the past.

Seismic Refraction Experiments

To investigate the crustal thickness along the rift valley of Gakkel Ridge both ships had to work together. For this type of reconnaissance survey only a few stations were deployed along each profile. In case of reverse shooting at maximum two seismic data acquisition units were deployed on ice floes to record the airgun signals. During profiling HEALY lead the convoy, while POLARSTERN towed an airgun array (in total 24-l) to generate the acoustic signals. In total the crustal thickness was measured at 18 different locations. Most of the record sections show clear Pn arrivals from the crust/mantle boundaries with velocities between 7.8 and 7.9 km/s. All stations worked without problems. For both types of experiments the icebreaking support of HEALY was essential. Only the joint operation of both ships ensured a certain quality of the seismic data within a reasonable time.

Gravity Measurements

A fixed mounted gravity meter onboard the POLARSTERN gathered gravity data during the entire cruise. The instrument worked without any problems during the entire cruise. Harbour values were taken in Tromsø and Bremerhaven.

Heat Flow Measurements

In addition to the seismic and bathymetric data gathered during the two-ship experiment, 21 heat flow stations (38 measurements) were conducted along the rift valley of Gakkel Ridge, and also along an off-axis seismic transect into the Amundsen Basin. In the Amundsen transect in total 7 stations were conducted. Here good control for the sediment thickness is provided by the seismic reflection data acquired on the way to Lomonosov Ridge. Along this transect three stations were cancelled due to extremely difficult ice conditions, which did not allow the ship to position in a reasonable time. The rest of the stations are located in the rift valley of Gakkel Ridge. In the valley the difficult part was to find sediment patches at a sufficient extent to perform the measurements. The PARASOUND data clearly

showed that small volcanoes covered most of the seafloor with only few sediment pockets in between.

Helicopter-based Magnetics

This programme intended to fly a detailed magnetic survey across the rift valley of Gakkel Ridge. Unfortunately most of the planned survey could not be conducted, due to mainly bad weather conditions. Fog conditions in the western part of the ridge prevented any significant survey activity for almost 9 days. The same happened in the eastern part of the ridge. Here almost 12 days of difficult weather conditions prevented any systematic surveying. Only during 14 days of the cruise helicopter based magnetic measurements were performed. However, in total 56 hours of flight time (4480 nm) could be used to gather magnetic data with a line spacing of 2 km across the ridge. The data has a good quality and have been flown across prominent bathymetric features, so a contribution towards better understanding of spreading processes along the Gakkel Ridge can be expected.

Magnetotelluric Experiments

In total five MT-experiments were conducted along Gakkel Ridge to investigate the conductivity of the earth's crust and the mantle below this mid-ocean ridge. The stations were recovered after 3 - 9 days. Critical to the interpretation of this data is the rotation of the ice floe on which the instruments are located. Although the floes showed significant drift paths, the rotations of the floes was not so strong. So the instruments acquired reasonable data for most of the deployment periods.

Seismological Array

While the crustal thickness along Gakkel Ridge was determined by seismic refraction experiments, seismological data is necessary to probe the upper mantle. For this experiment a mobile network consisting of 3-4 stations was deployed on an ice floe. The deployment of the array was mostly finished in three hours. The RefTek recording units had almost no failures during their deployment on the floes. A first view on the seismological data showed that teleseismic as well as local events were recorded. The most spectacular quakes were recorded from the

Pacific-Antarctic Ridge with sufficient S/N ratio. A careful data analysis will show to which extent local seismicity along the ridge was recorded.

The deployment of the seismological and MT stations faced two problems. At first, the constantly bad flight conditions in the beginning of the cruise in combination with the relatively fast sampling of the petrology programme did not allow us to deploy them in a reasonable distance to the ship. The risk involved in finding the stations after several days of deployment and with flight distances of more than 50 N.M. was too high. That is also a reason why the number of MT stations deployed in a certain area was only two. Secondly, the time of 3 hours plus limited flight windows needed in the beginning to build up one MT station restricted the number of instruments.

In the following chapters the different experiments, problems and technical challenges will be described in greater detail. In summary, the geophysical programme of this cruise was very successful. Most of the problems at the beginning were quickly solved and although a great number of different instruments was used, we had almost no failures. Beside good preparation, the excellent motivation of the geophysical team onboard made this success possible.

9.2 Seismic Reflection Experiments

(W. Jokat, H. Bohlmann, S. Drachev, A. Galaktionov, G. Karpinos, B. Lahrmann, N. Lensch, U. Miksch, K. Müller, A. Pignatelli, O. Ritzmann, M. Schmidt-Aursch, T. Schmidt, T. Schmitz, A. Wüstefeld)

Past seismic experiments from drifting ice stations in the Eurasian Basin reported conflicting data for the crustal thickness in the Nansen and Amundsen basins. The occurrence of normal and thin oceanic crust was directly linked to models describing a general dependence of the crustal thickness on spreading velocity. However, the few widely scattered seismic data did not provide coherent information on this issue. Therefore, one of the main geophysical objectives was to gather a critical amount of new off-axis seismic reflection data to provide better constraints for models of super-slow mid-ocean ridges.

For this three long transects were acquired. Two lines in the Nansen Basin, which start at the northern Svalbård continental margin and terminate at Gakkel Ridge at 17°E and 21°E, respectively (Fig. 78, Table 16). A single profile was acquired in the Amundsen Basin from Gakkel Ridge (70°E) to Lomonosov Ridge (130°E) (Fig. 79). Due to the icebreaking support of HEALY the oceanic basement along all off axis lines is clearly imaged (Fig. 80). The lines in the Nansen and Amundsen basins show striking differences. While in the Nansen Basin a standard subsidence of the oceanic crust is observed, this is not true in the Amundsen Basin. This had been reported earlier (Jokat et al., 1995; Weigelt and Jokat, 2001) for the Amundsen Basin and is now confirmed to be typical for the central part of the Eurasian Basin. Furthermore, the sediment thickness in the Nansen Basin is much greater than in the Amundsen Basin. This is an expected result since the Nansen Basin is much closer to a major sediment source, the Eurasian Shelf. Much to our surprise the surface sediments in the Nansen Basin are much coarser throughout most of the basin, indicating frequent slump activity in the past. In addition 36 sonobuoys were deployed to better constrain the seismic velocities of the sediments and the underlying oceanic basement. Most of them provided reasonable results and we were able to convert the data to depth later on. More important the buoys also recorded clear signals from deeper levels of the oceanic basement, so that a minimum estimate on crustal thickness together with the gravity data will be possible in the subsequent interpretation.

Profiles AWI-20010100/0400/0450/0460 - Sonobuoy-Locations

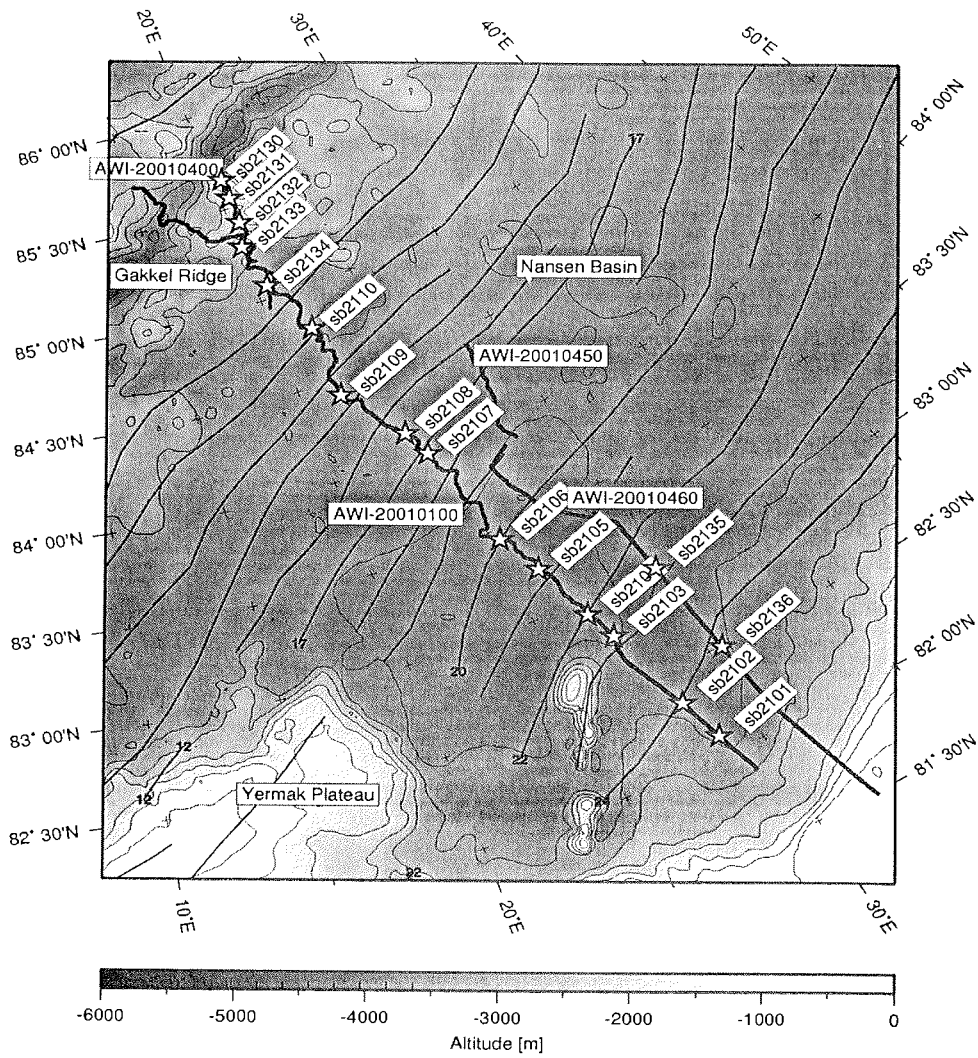


Fig. 78: Location map of the seismic profiles in the Nansen Basin. The stars indicate the positions where sonobuoys were dropped.

Profile AWI-20010300 - Sonobuoy/RefTek-Locations

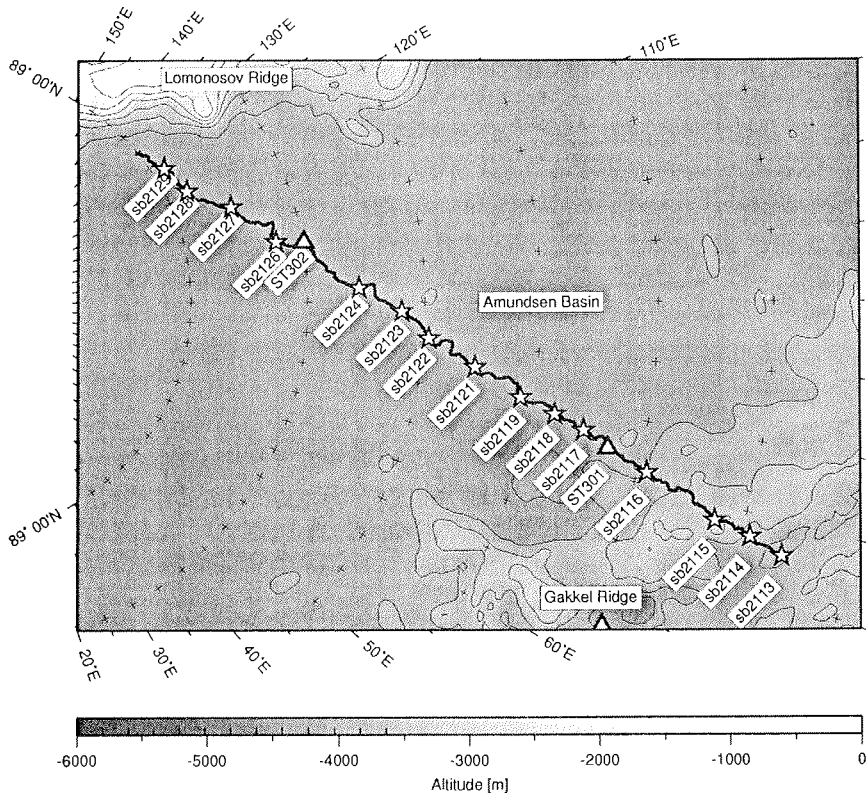


Fig. 79: Location map of the seismic profile in the Amundsen Basin. The stars indicate the positions where sonobuoys were dropped.

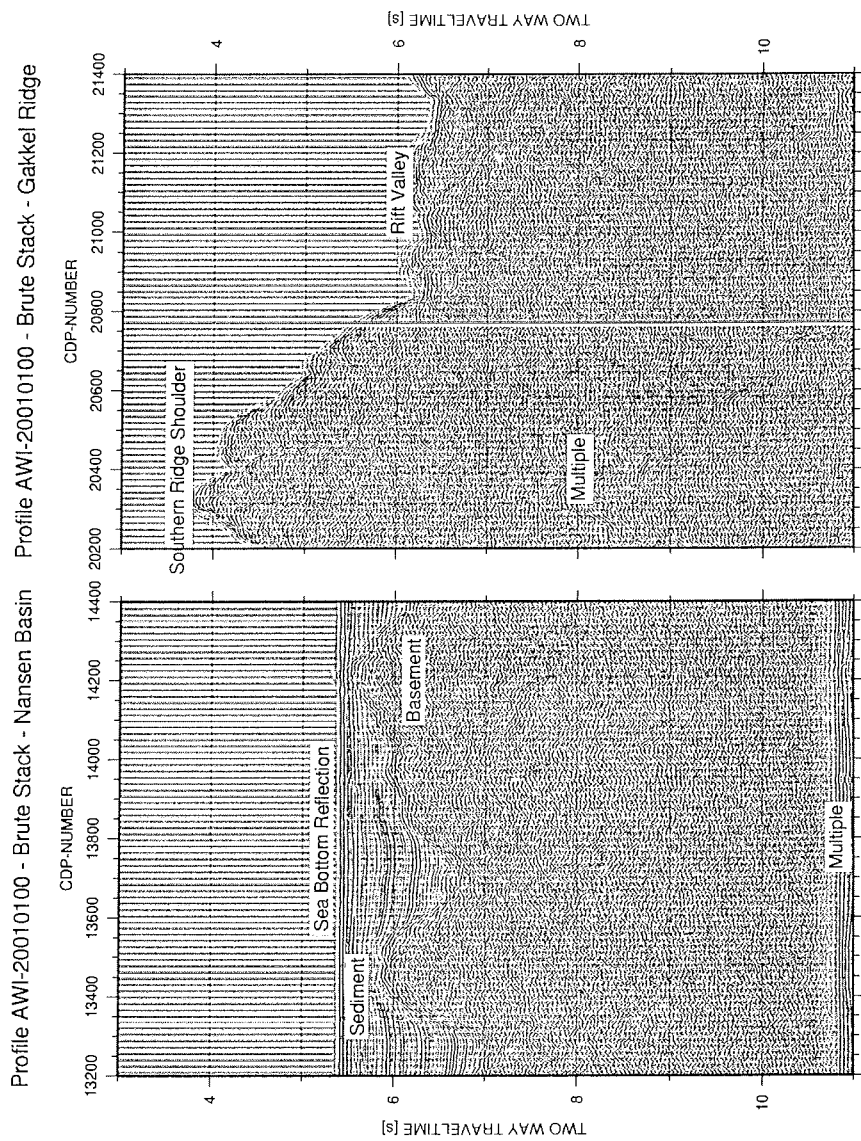


Fig. 80: Data example for the quality of the seismic reflection data.

9.3 Refraction Experiments along Seismic Reflection Transects

(O. Ritzmann, W. Jokat)

Along the seismic reflection profiles (Profiles AWI-20010100(0400)/0300/0460) of the expedition seismic wide-angle data were acquired to resolve the seismic velocity structure of the Nansen and Amundsen basins and the Gakkel Ridge. The main targets of these experiments were to determine:

- (1) Depth of the basement when sediment thickness on the Eurasian Shelf/Lomonosov Ridge edges of the profiles is high and could not be imaged by the acquired seismic reflection data.
- (2) Seismic velocities and thickness of the sedimentary section in the Eurasian Basins as support for a stratigraphic model of the basins.
- (3) Seismic velocities of the basement/upper crust for interpretations to whether it is oceanic/continental or transitional. Petrological interpretation (and crustal age) of the basement derived from seismic velocity.
- (4) Seismic velocities of the entire igneous section of the crust to define the spreading history, i.e. melt production, mantle temperatures, etc. of the slow spreading Gakkel Ridge.
- (5) Seismic velocities of the upper mantle to understand its petrology as the initial member in the petrologic cycle of crustal evolution.

Experimental Set up

In total we used 36 Sonobuoys (2 failed) and 2 RefTek-Stations along the reflection profiles as shown on maps (Figs. 78 and 79). Almost 75 percent of the entire length of the profiles 0100/0300/0400 are covered by sonobuoy-data. The profiles 0100/0400 are covered by 10/5 sonobuoys with spacing between 18-60/11-25 km, respectively. Along profile 0300 wide-angle data was acquired by 13 sonobuoys and 2 additional RefTek-Stations deployed on floes. The mean spacing of receiver stations on Profile 0300 is almost constant at 18 km. Unfortunately two gaps of 40 km are present. Two sonobuoys on profile 0460 were only dropped to get depth and velocity information of the basement close to the continent-ocean transition. Therefore, no continuous coverage is achieved for this line.

Nine stations resolve the seismic velocity structure of the Gakkel Ridge System while the remaining 28 stations provide information on the Eurasian Basins. For detailed information of location, quality, recording length, etc. of the various stations see Table 17.

Acquired Seismic Data

The seismic source consisted of a tuned array of 8 VLF-Airguns with a total volume of 24 l and frequencies between 15-60 Hz. The receivers were single hydrophones (lower cut-off 4.5 Hz) in the case of the sonobuoys and an array of 2x48 geophones (stacked, lower cut-off 4.5 Hz) for the RefTek-Stations on the ice floes. For further processing after demultiplexing we applied a 3/5/20/30 HZ-Band pass-Filter according to the attenuation of higher frequencies at large offsets (> 5 km). Due to a non-straight ship course, dependant on the ice conditions, the direction of the receiving ship antenna deviated partly from the line insight of the sonobuoys. Therefore, signals were sometimes overlain by a high noise. Large drift rates of the sonobuoys (in/decreased acoustic velocities of water, direct wave) due to strong surface currents of seawater were not observed, while the maximum recording length of the receiver was limited to 3 hours (about 28 km at a speed of 5 Knots). According to the drift paths of the RefTek-Stations (see Chapter 9.4: Seismic Refraction Gakkel Ridge) we determined that the range of the drift varied between 0.05 and 0.2 km/h, which can be neglected for this study. For the deployed RefTek-Stations a correction of the drift was calculated and applied from the GPS-positioning of the devices.

The signal range of the receivers varied between 8-26 km. As the water depth was higher than 4000 m, first arrivals from deeper structures occurred at distances greater than 12 km. Therefore, the recordings with a signal range lower than 12 km showed only a wide angle reflection hyperbola pattern, which also provided useful velocity information. Multiples, which travel within the water column at a shot interval of 15 s, are not problematic for sonobuoy-data. In the case of the RefTek-Stations, which record at distances greater than 50 km, we increased the shot interval to 20 s to shift multiples to distances greater than 30 km. A data example is shown on Figure 81.

Preliminary Results Profile AWI-20010100

Sediment thickness in the Nansen Basin varies between 0.4 and 2.5 km. This section can be subdivided by seismic velocity into 3 segments. Outcrops of the oceanic basement increase towards the Gakkel Ridge. The mean velocities in the upper parts of the oceanic basement in the central part of the Nansen Basin are about 5.0 km/s. We observe no velocity gradient in this basement section. The velocity of the oceanic basement decreases in the vicinity of the ridge shoulder to approx. 4.2 km/s. Underneath this 1.2-2.0 km thick portion, the seismic velocity increases rapidly to 7.1 km/s. On some recordings we identified reflection phases from deeper boundaries, which can be interpreted to mark the crust/mantle-boundary. According to these reflections we calculate the depth of the Moho-boundary to approx. 10 km, which result in a total crustal thickness not higher than 4-5 km.

Further Interpretation

During the cruise we picked travel time/distance pairs from the seismic sections for modelling of the data with RAYINVR ray tracing software. The seismic reflection data along the profiles supports the modelling procedure, i.e. fitting the travel times, when basement topography is very rough. As the crust-mantle boundary is partly not imaged by the sonobuoy-data, the p-wave velocity models will be transferred to density-models by published Vp/density relationships. Modelling of the ship borne gravity recorded along the profiles will help for resolving Moho-topography. The derived p-wave velocity and density models as well as the seismic reflection data will finally be used for a joined interpretation of the sedimentary and crustal structure of the Nansen and Amundsen basins.

Sonobuoy 2104 - BP3/5/17/25 - AGC 500

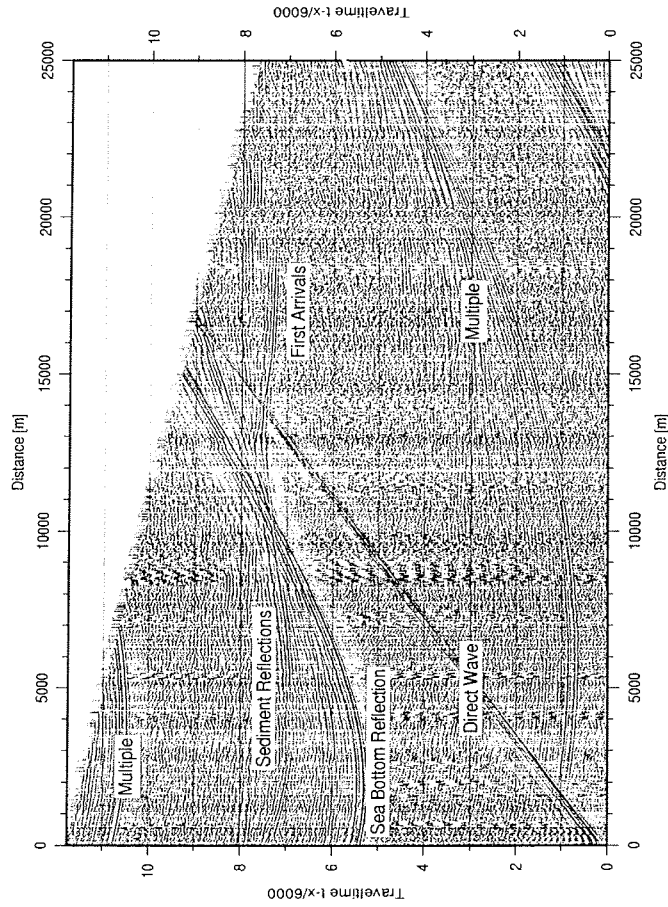


Figure 81: Record section of sonobuoy 2104, clearly shows the reflection of the top of the basement between 5-10 km distance and travel times of 7 s. At distances higher than 11 km refracted waves from deeper layers are faster than the direct wave and give reliable information of crustal velocities. The energy of first arrivals dies out beyond distances of 18 km.

9.4 Seismic Refraction Experiments along the Gakkel Ridge

(W. Jokat, H. Bohlmann, S. Drachev, A. Galaktionov, G. Karpinos, B. Lahrman, N. Lensch, U. Miksch, K. Müller, A. Pignatelli, O. Ritzmann, M. Schmidt-Aursch, T. Schmidt, T. Schmitz, A. Wüstefeld)

The only data on crustal thickness from the Gakkel Ridge were acquired during the FRAM expeditions close to 0° in the late 70's (Kristoffersen et al., 1982). Here, crustal thicknesses of 6-7 km for the oceanic crust at Gakkel Ridge were reported. So far, this single refraction survey was the only crustal thickness determined by seismic refraction methods along the entire ridge. Recently only gravity studies were published on the crustal structure of Gakkel Ridge (Coakley & Cochran, 1998; Weigelt & Jokat, 2001). Both studies indicate that thin crust with thickness between 2-4 km may be present beneath the rift valley, which is regarded to be normal for oceanic crust formed at ultra-slow mid-ocean ridges.

Consequently, one of the main objectives for the geophysical programme was to acquire more seismic data on the crustal thickness along Gakkel Ridge. Practically, RefTek recording instruments were deployed on ice floes, while a 24-l airgun array provided the sound energy (Fig. 82). No large volume airgun was used to generate seismic energy since it would have been difficult to tow it in the ice safely well behind the ship. The problems and set-ups chosen for the data acquisition will be described in a separate chapter and will not be repeated here.

In total seismic refraction data were acquired at 18 different locations and profiles, whenever possible with stations at the start and end of the profile (Tab. 18). Having two stations out on the floes often created problems with the geometry since the ships were not able in some cases to approach the station at the end point below 5 km due to unfavourable ice conditions. Furthermore, the profiles are crooked lines since large floes did not allow us to steam a straight line. All these factors together degrade the quality of the data and will introduce larger errors for the velocities during modelling. The profile lengths varied between 30 and 50 km. The signal to noise ratio on most of the records is close to 1 or even below. However, the shooting interval of 20 s (50 m) provided enough coherent energy to allow a safe identification of the travel time branches in the record sections (Fig. 83). Most of the unreversed record sections clearly show travel time branches with velocities between 6.5 and 7.9 km/s. Fast arrivals from the mantle occur between 6 and 12

km offset from the station and can be followed in some cases up to 35 km. From the modelling it is also obvious that a layer with velocities ranging between 2.5 to 5 km/s has to be introduced in the modelling although only few stations show travel time branches of such velocities. This layer can be interpreted as mainly consisting of pillow lavas and/or altered basalts or peridotites, as along other mid-ocean ridges. Combining all the existing geophysical and petrological information will allow us later on to better constrain the composition of this unit. The transition from this unit to the upper mantle is not abrupt but gradual. No wide-angle reflections of the Moho discontinuity are observed.

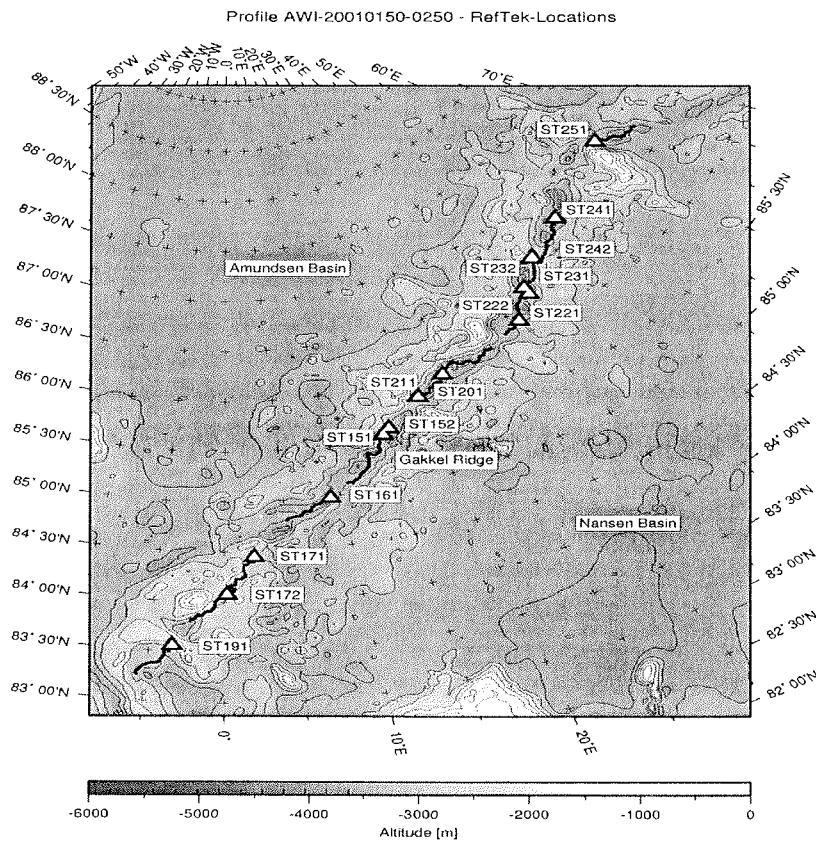


Figure 82: Location map of the seismic refraction profiles along Gakkel Ridge. The stars indicate the positions of the RefTek recording instruments along each profile.

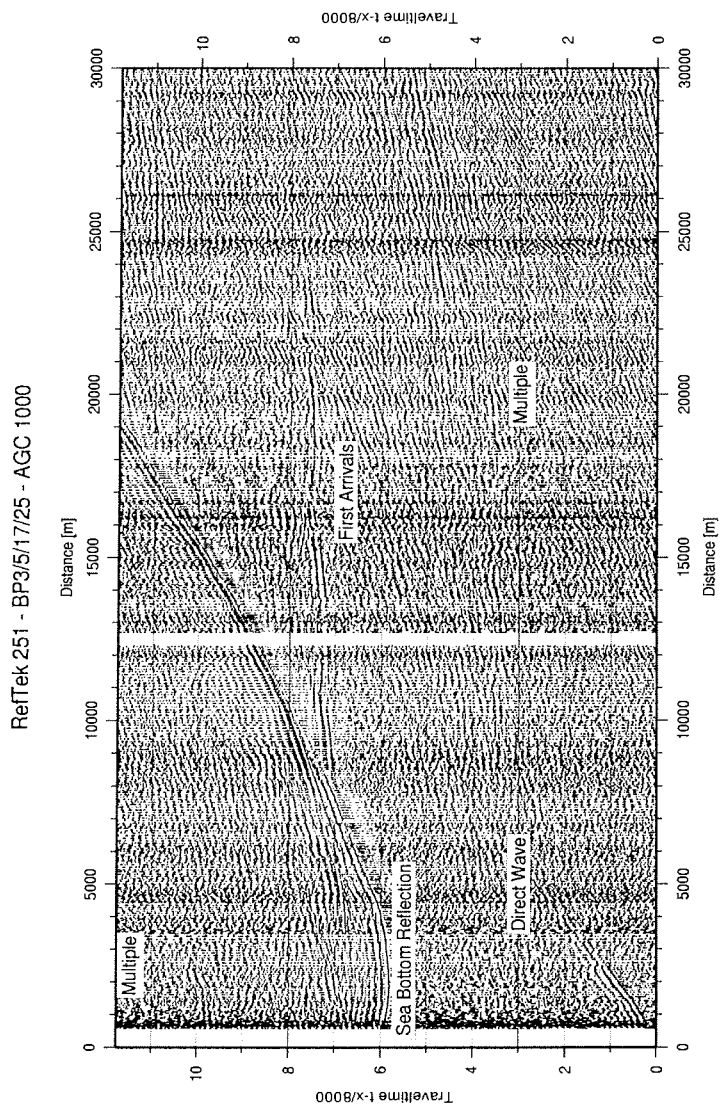


Figure 83: Data example for a RefTek record section. Here, it is station 251 at the very eastern part of our survey.

9.5 Gravimetric Measurements

(W. Jokat)

During the entire cruise gravity data were acquired with a fix-mounted KSS31 gravimeter on POLARSTERN. Harbour values were taken in Tromsø (Norway) and Bremerhaven (Germany). The instrument worked throughout the cruise without any problems. The data quality is reasonable for data being acquired from an icebreaking vessel. Strong accelerations were not avoidable but do not distort the overall picture. On the long transects in the Nansen and Amundsen basins the data quality is better, as HEALY provided icebreaking support during seismic profiling. No processing or interpretation of the data was done onboard of POLARSTERN, so that no results can be reported here.

9.6 Helicopter-based Magnetics

(M. Schmidt-Aursch, W. Jokat)

In a regional sense the Arctic Ocean is well covered by aeromagnetic data. In the past three decades especially Russian and US institutions having long range aircrafts available acquired magnetic data over the entire Arctic Ocean with line spacing of approx. 20 km. These data allowed identifying the major tectonic units. This key information forms the base for any tectonic interpretation in this region. The magnetic programme conducted during the AMORE cruise therefore was designed to address the following issues:

a) Along the Gakkel Ridge denser lines were flown to identify major tectonic units along the rift valley, which cannot be resolved by the existing data. A line spacing of 2 km was chosen as being the best compromise between target depth, available flight time and the expected spatial resolution necessary to distinguish between different tectonic units.

b) Focussing on the rift valley geology profile length of max. 56 km (30 N.M.) are sufficiently long. The width of the rift valley is approx. 20 km. Thus, the survey covered also sea floor spreading anomalies adjacent to the rift valley. However, the lengths of the profiles were optimised to plan efficiently the flight paths for the helicopter borne magnetometer system.

c) The limitation of flight time due to competing programs as well as difficult weather conditions changed our strategy. The available flight times were concentrated now on prominent geological features which are believed to play an important role in the interpretation of the processes along the Gakkel Ridge. Due to the tight time schedule of the helicopters it was not possible to deploy a base station. For some days we could use the data from the MT stations deployed on ice floes during the same time. For the large amount of lines we will use data from magnetic observatories in northern Svalbard. Thus, only a very preliminary processing of the magnetic data onboard of POLARSTERN is done.

Technical Operations

For the magnetic survey with POLARSTERN the commercial available HELIMAG system (SCINTREX, Canada) was used. It consisted of a caesium optical-pump magnetometer towed 30 m beneath the helicopter. The registration unit was coupled with the aircrafts radar altimeter to get reliable altitude information. An internal GPS receiver provided navigation data. Several problems occurred during the cruise. Especially bad weather conditions like fog, snowfall or freezing rain limited the possible flight windows. Clouds at low altitude and thick fog fields prevented a constant flight level, so the flight altitudes varied between 90 m and 450 m. Strong winds were also problematic as during dredging the ship sometimes could not be moved into a direction necessary to ensure a safe start or touch down. Other scientific activities required helicopter flights too (e.g. deployment or recovery from stations on ice floes), so often no helicopter was available. A severe technical problem was the failure of the internal GPS receiver of the HELIMAG system, which led to large data gaps and the premature end of two flights. Using an external GPS instrument allowed us to continue the survey until the receiver was fixed.

Processing and Interpretation

In spite of all these problems during 14 days of flying approx. 56 hours of new magnetic data could be acquired. This corresponds to 8300 km (4480 N.M.) total profile length, assuming a mean flight velocity of 148 km/h (80 knots). Figure 84 shows a map of all flown lines. The grey shade and contour lines show bathymetric depths taken from IBCAO bathymetric data set (Jakobsson et al., 2000). Black lines mark the flight paths, which are annotated with the corresponding dates. The

length of the lines varies between 37 km (20 N.M.) and 56 km (30 N.M.), the line spacing amounts 2 km. See Table 19 for further details. Though it was unfortunately not possible to map large ridge segments, some prominent bathymetric structures were investigated. The data quality is very good with amplitudes up to 2000 nT. Figure 85 shows an example of the eastern part of the Gakkel Ridge. The grey shade and contour lines show the bathymetry acquired by POLARSTERN and HEALY. Black wiggles indicate the negative anomalies along the rift shoulders. Grey wiggles show a prominent positive anomaly in the area of the rift valley. Around 47°E the positive anomaly diminishes and increases again with an offset of roughly 10 km. This correlates very well with bathymetry and will be further interpreted after the final processing. As there was no base station deployed during the cruise, most processing has to be done later when more information about daily variations of the magnetic field is available. Several lines show distinct shifts between adjacent lines flown at different times. All lines have to be adjusted not only for diurnal variation but also for different flight levels. Susceptibility measurements on rock samples later on will lead to a combined interpretation of petrology and magnetic data.

HELIMAG Profiles

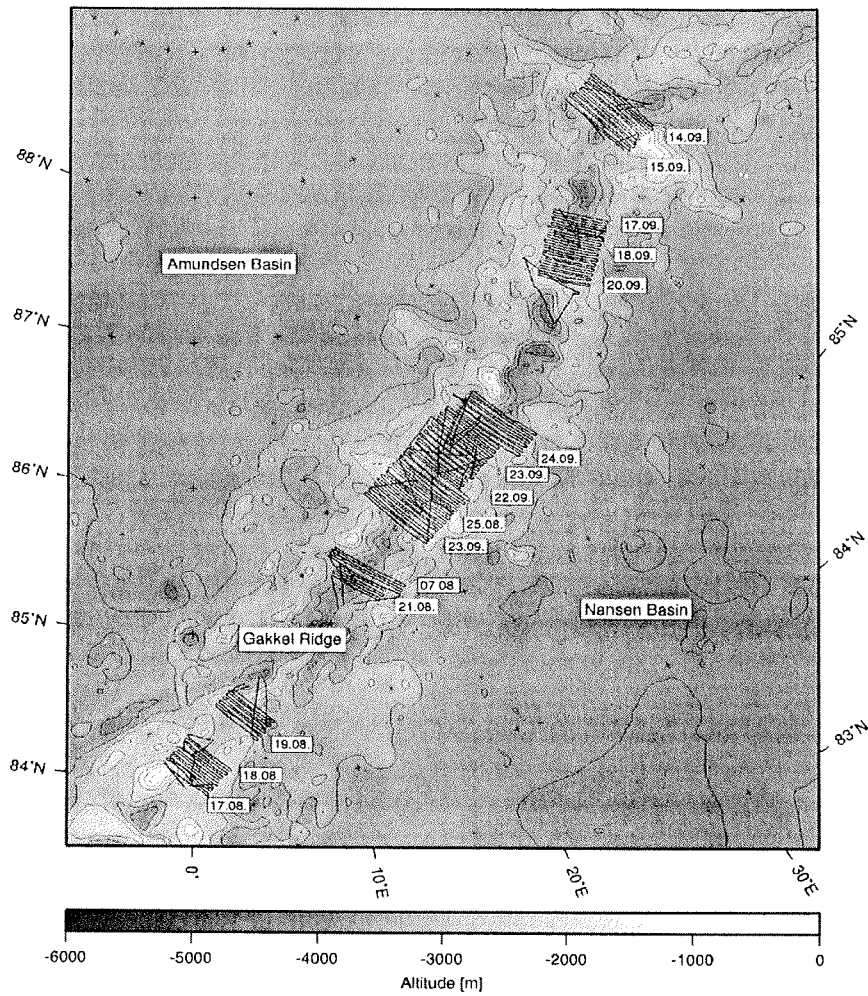


Figure 84: HELIMAG profiles along the Gakkel Ridge. The grey shade and contour lines (500 m interval) show bathymetric depths taken from IBCAO data. Black lines mark the flight paths. Dates of flights are indicated.

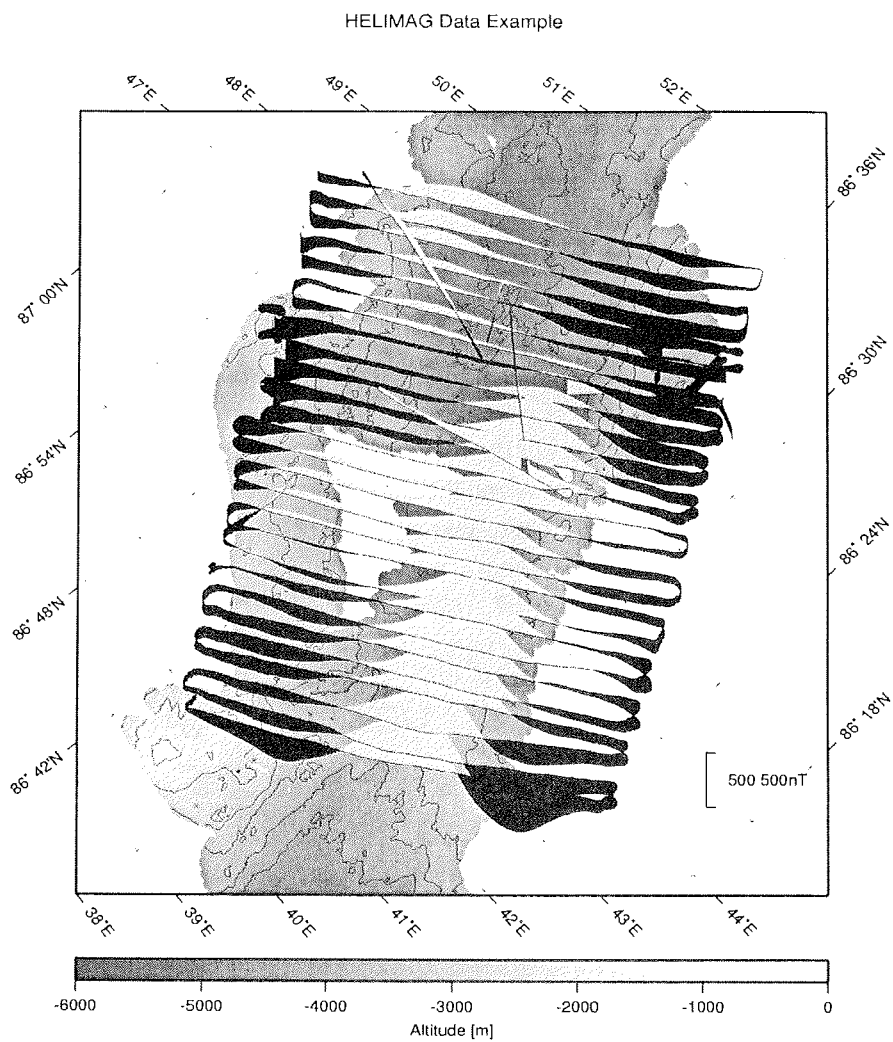


Figure 85: HELIMAG data example. The grey shade and contour lines (500 m interval) show bathymetric depths acquired by POLARSTERN and HEALY. Black wiggles mark negative anomalies of the raw data, grey ones positive values. Note the diminishing and offset of the positive anomaly at 47°E.

9.7 Heat Flow Measurements

(R. Spielhagen, N. Lensch, K. Müller, W. Jokat)

The Gakkel Ridge is one of the few sediment-covered spreading centres of the global mid-ocean ridge system. Such ridges can provide important opportunities for quantitative studies of sea floor spreading and associated hydrothermal systems. Furthermore, the sediment can preserve a stratigraphic record of the magmatic and thermal events along a mid-ocean rift system. Heat flow measurements in the Eurasian Basin and especially along the Gakkel Ridge are rare and widely spaced. A first attempt to gather systematically heat flow data along Gakkel Ridge was made during a POLARSTERN cruise in 1987. Here, extremely high heat flow values up to 1200 mW/m^2 were measured in the rift valley at 23°E . POLARSTERN sampled only a few additional locations in 1998 at the Siberian termination of Gakkel Ridge off the Laptev Sea continental margin. Thus, the reconnaissance type of programme clearly intended to significantly increase the number of heat flow data along the ridge and in the adjacent deep-sea basin to better describe the thermal status of the ridge and the basins. Along the ridge it was planned to deploy sensors whenever a sufficient sediment cover was available (Fig. 86). Off-axis heat flow data were intended to acquire along a seismic transect from Gakkel Ridge to Lomonosov Ridge. (s. Figs. 86 and 87, Table 20).

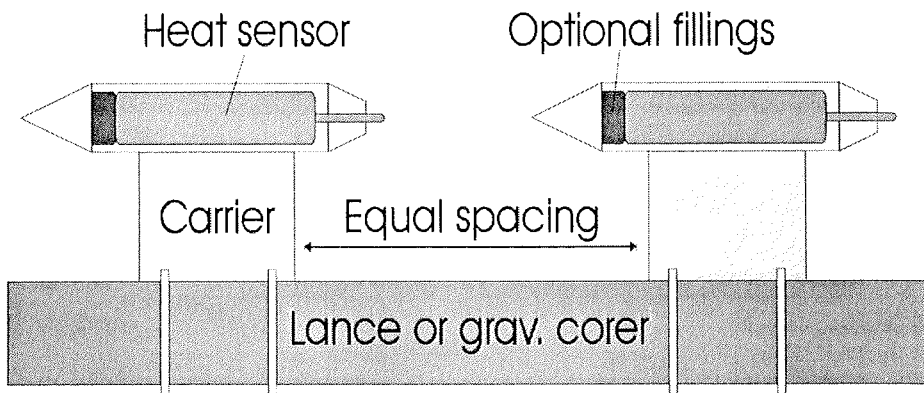


Figure 86: Heat flow set-up.

HEAT FLOW GAKKEL-RIDGE

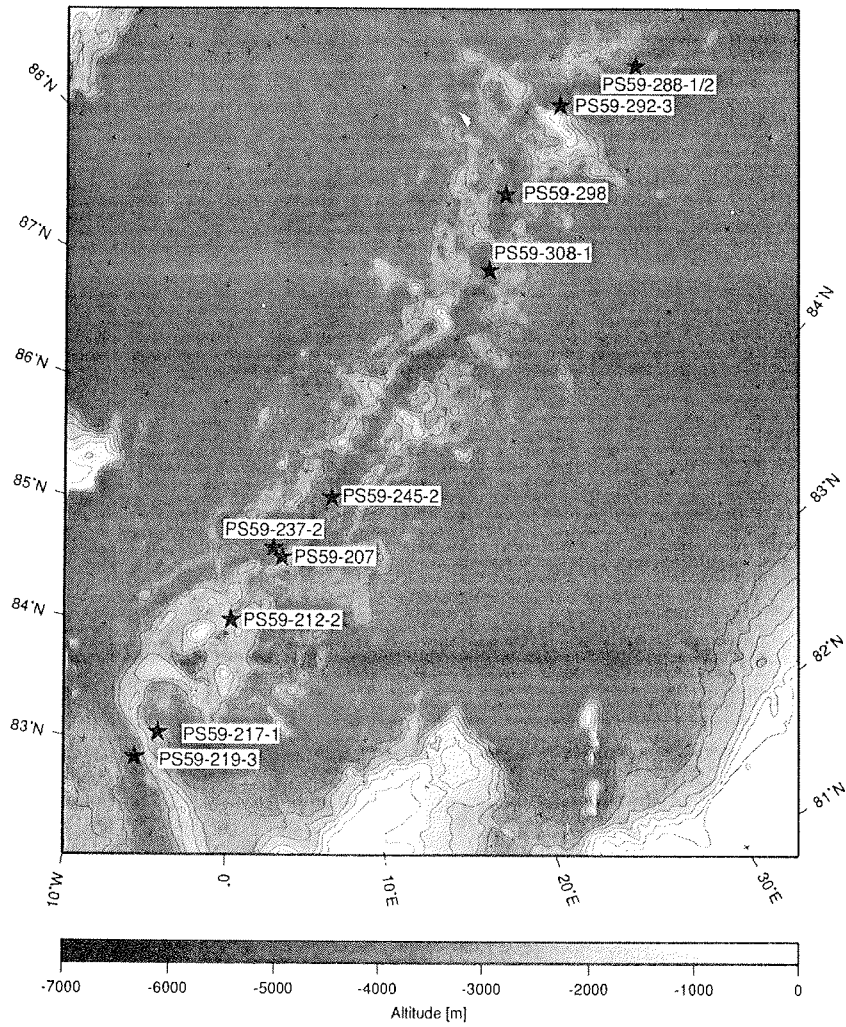


Figure 87: Location of the heat flow stations along the Gakkel Ridge.

HEAT FLOW AMUNDSEN-BASIN

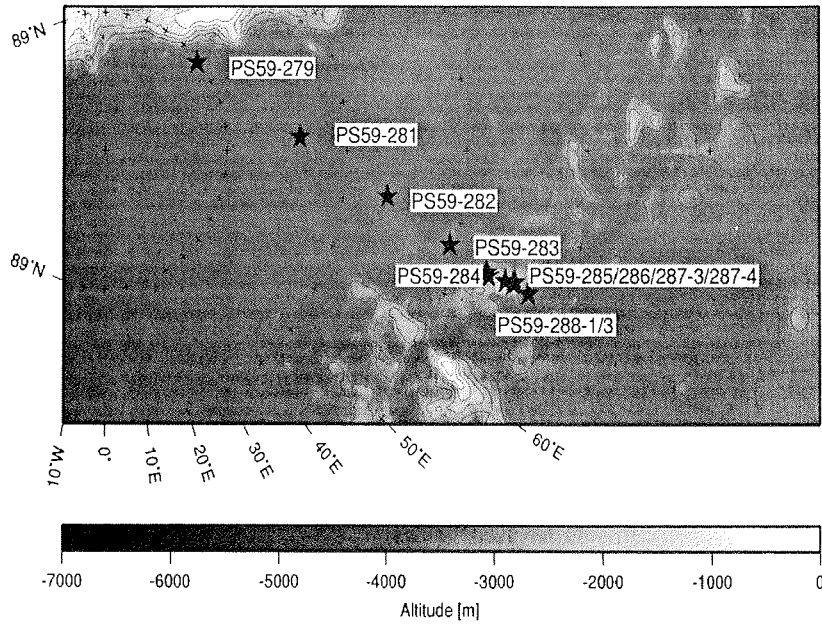


Figure 88: Location of the heat flow stations along a seismic transect from Gakkel Ridge to Lomonosov Ridge.

Here, the sediment and crustal thickness were determined. This information could then be used to correct the heat flow data. The profile may allow identification of any asymmetry in crustal temperature decrease. Furthermore a denser number of stations were conducted across a 20 Myr segment to monitor the temperature field of an ultra-slow spreading system. For retrieving the temperature information autonomous temperature loggers mounted on a gravity corer were used.

Theory of Heat Flow Measurements

To determine the heat flow the following equation has to be solved:

$$Q = k \, dT / dz \text{ [W/m}_2\text{]}$$

Q : heat flow

k : heat conductivity [W/ m K]

dT : temperature difference [K]

dz : distance [m]

(Fowler, 1990)

The heat flow provides the information of the amount of radiated energy per square meter. To derive the heat flow from a discrete measurement, the first equation changes to

$$Q = k \, \Delta T / \Delta Z$$

In case of sediments the heat conductivity k is often close to '1'. To get the true value for k , conductive measurements at sediment cores are necessary. The measurements of the heat conductivity k (see first equation) have been done during the expedition. Due to the irregular movements of the ship during ice breaking reliable data were only achieved in relative smooth movement of POLARSTERN while it was on the station.

Experimental Set-up

Identical sensors were mounted at a gravity corer or a lance (Fig. 86, Tab. 21). The sensors were equally spaced along the gravity corer and /or lance. The closest spacing for the gravity corer was 0,75 m, our largest 2 m. Along the lance the sensors have a fixed spacing of 0,75 m. Using the lance, it is possible to penetrate the sediment at a location while the ship moved with the ice drift. For each measurement the corer/lance stuck in the sediment for 7-10 minutes. Often one or more penetrations failed since the lance could not penetrate into the sediments. To monitor any dips of the corer/lance while penetrating into the sediment, an additional dip sensor was mounted. This information might be used to correct the

distances between the sensors. The sensors themselves operated independently once they were programmed in the lab. Most of the autonomous sensors worked without any problems. Whenever possible we used a gravity corer armed with up to five temperature sensors to perform the measurement in order to retrieve simultaneously information on the sediments. The sites were carefully chosen with the help of the sediment echosounding system Parasound. The data showed that only few sediment patches were present in the ridge segment between 20° and 50° E, so that only a few chances existed to get reliable data.

Results

In total 21 heat flow stations were visited along and off-axis Gakkel Ridge. At several stations at maximum three heat flow values were taken with the lance by offsetting with the drift. So, in total 38 different locations were sampled by the heat flow sensors. Along the rift valley of Gakkel Ridge ten stations are located between 83°N 06°E and 87°N 63.5°W (Fig. 87). Here, one station failed since the small sediment patch seen on the Parasound data could not be hit.

In the Amundsen Basin in total 11 locations were sampled along the seismic line AWI-20010300 between 86°N 73°E and 89°N 130°E (Fig. 88). Here, two gravity corer/lance operations failed to penetrate into the sediments and did not provide reliable data. Most of the available time for heat flow measurements were used for this transect. Difficult ice conditions along the profile prevented us from relocating the ship to an optimal position within a reasonable time. However, the failure of the gravity corer and the lance at the same position was a surprise. Instead of 1.5 days more than 4 days were needed for the transect.

Along the rift valley of Gakkel Ridge a systematic spacing of the heat flow stations could not be achieved due to the difficult ice conditions in the middle segment and partly due to the lack of sediments. Since this programme was carried out as a service for the University of Bremen, the interpretation of the data is very preliminary. The heat flow as well the conductivity data will be checked and interpreted by an experienced person at the University of Bremen. Therefore, no data will be published here.

9.8 Seismological Studies

(T. Schmidt, O. Ritzmann)

Melt production in the mantle is related to mantle temperature through its effect on the depth range of melting. Anomalously low melt production at ultra-slow spreading rates (resulting in the thin crust mentioned above) has alternatively been ascribed either to an anomalously shallow maximum depth of melting (i.e. anomalously cool up welling), or to an anomalously deep minimum depth (i.e. a thick lithosphere). Measurements of upper mantle seismic structure, by either refraction techniques (i.e. Pn velocities) or teleseismics (i.e. P-wave tomography and surface wave dispersion) provide a method of distinguishing between these models, since seismic velocity correlates with temperature and melt fraction. The seismological experiments with detection arrays along the Gakkel Ridge should analyse the following objectives:

- (1) Is there still any indication for increased seismicity especially in the area near 85°N/85°E where a swarm of earthquakes were detected by the global seismological network in 1999 (Müller & Jokat, 2000).
- (2) Detecting local earthquakes and estimations about the distribution of microseismicity along the Gakkel Ridge.
- (3) How does the signal/noise ratio measure seismological events with an 3-component-seismometer on a floe?
- (4) Determination of the detection level for teleseismic events.

Experimental Set-up

The detection array for seismological events was built up on floes at 3 locations along the Gakkel Ridge (Fig. 89):

- (1) GAK-0 was located around 83° 27' N, 04° 20' W during 5 days from August 11.-15., 2001. This location was at the most westerly point of the cruise, near the location where the FRAM-1 experiment was done in 1979 (Kristoffersen et al., 1982).
- (2) GAK-1 was located around 85° 37' N, 16° 20' E during 5 days from August 20.-24., 2001. This location was in a part of the Gakkel Ridge where only very few teleseismic observations had been made before.

(3) GAK-2 was located around $86^{\circ} 00' N$, $85^{\circ} 30' E$ during 12 days from September 02.-13., 2001. This location was at the most easterly point of the cruise. It was placed as near as possible to the area where in 1999 a large swarm of earthquakes occurred. These earthquakes were strong enough to be detected by the global seismological network (ISC/NEIC).

Further on at the end of the cruise, we installed a seismological station GAK-3 at $86^{\circ} 01' N$, $26^{\circ} 40' E$ from September 22. - 25., 2001 (4 days). Due to restricted time and logistical reasons we didn't build up an entire array there, but only one single seismological station.

Locations of SMT-Stations

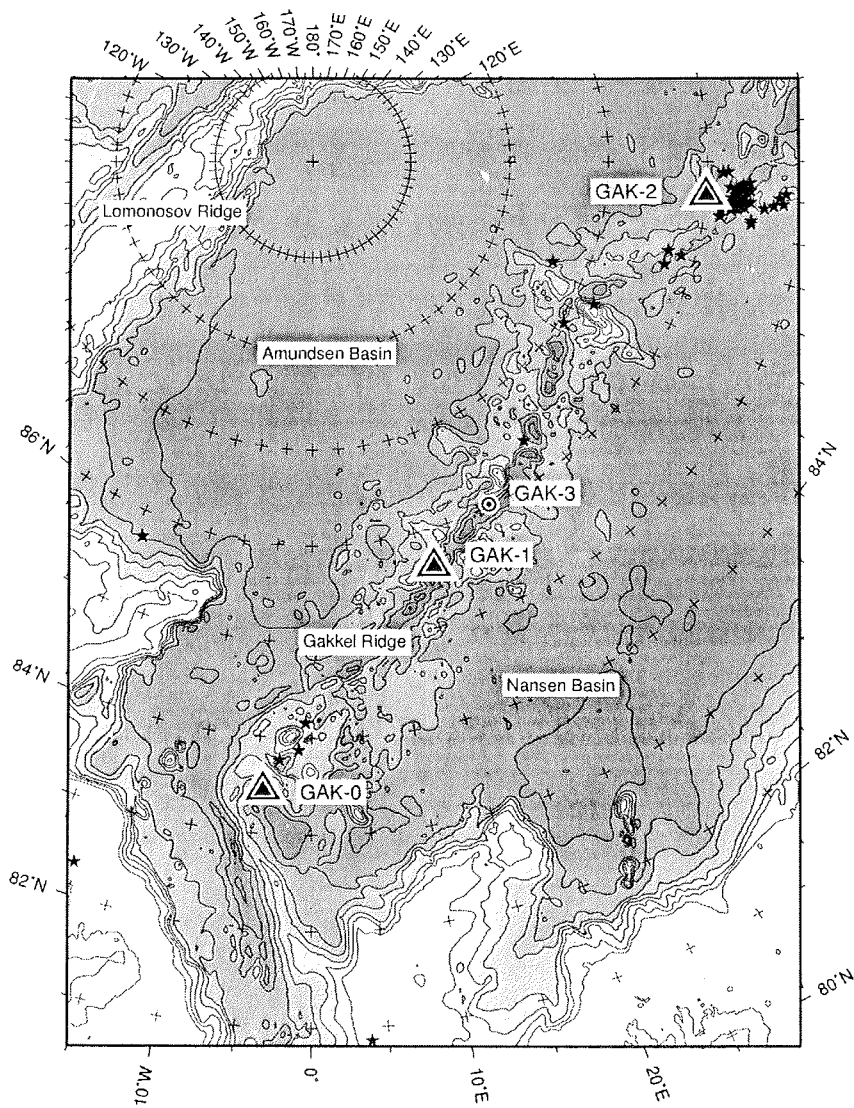


Figure 89: The locations of the SMT-Stations (seismological array + magnetotelluric station) GAK-0, GAK-1, GAK-2 and GAK-3 built up along the Gakkel Ridge. GAK-2 was located quite near to the location where a swarm of earthquakes occurred in 1999.

Due to the fact that the signals of local earthquakes consist of higher frequencies than signals of earthquakes received from greater distance (Fowler, 1990), the arrangement of the array was optimized for processing the recorded data of local and regional events. Therefore, the diameter of the array was less than one kilometer to ensure the coherency of signals up to 50 Hz (see Fig. 90). Conditional to this anti-aliasing characteristic for high frequent signals this arrangement will additionally cause minor resolution to locate epicenters of distant earthquakes. This principal concurrence between aliasing and resolution characteristics of an array cannot be solved in any way. Therefore, we tried to make an optimal compromise, which applied the good experiences derived from 3-years-operation of the seismological array at Neumayer-Station in Antarctica (Eckstaller and Müller, 1998).

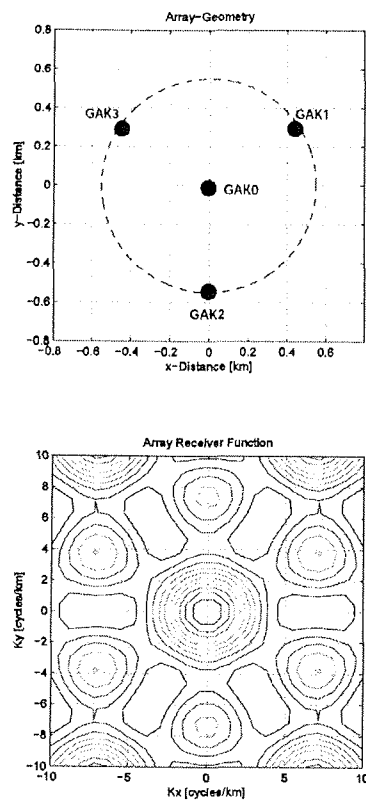


Figure 90: The arrangement of the seismological array and its receiver characteristics.

The array-response function in the wave number domain. The concentric shape of the maximum in the middle represents the wave number range, which can be resolved by the array.

Acquired Seismological Data

The recorded data had been processed with a software packet, which is highly compatible to the data acquisition unit of the RefTek instruments used. This software (PASCALL, Version 1.9, 2001) supports tools to convert the field data to a commonly used SEG-Y format and visualize the data.

As mentioned before, the array was fitted especially to detect local earthquakes from smaller distances. Because there's always water beneath the floe down to the seafloor, only compressional waves (P-waves) can be recorded from an earthquake below. The other type of elastic waves, the transversal waves (S-waves) cannot travel through fluid media. Therefore, the transversal waves cannot be recorded on the horizontal components of the seismometer directly. But it is possible to record transversal waves which had been converted to compression waves at the boundary between the seafloor to the ocean (SP-waves) on the vertical component. Figure 91 shows a typical example of a local earthquake recorded at the array GAK-2.

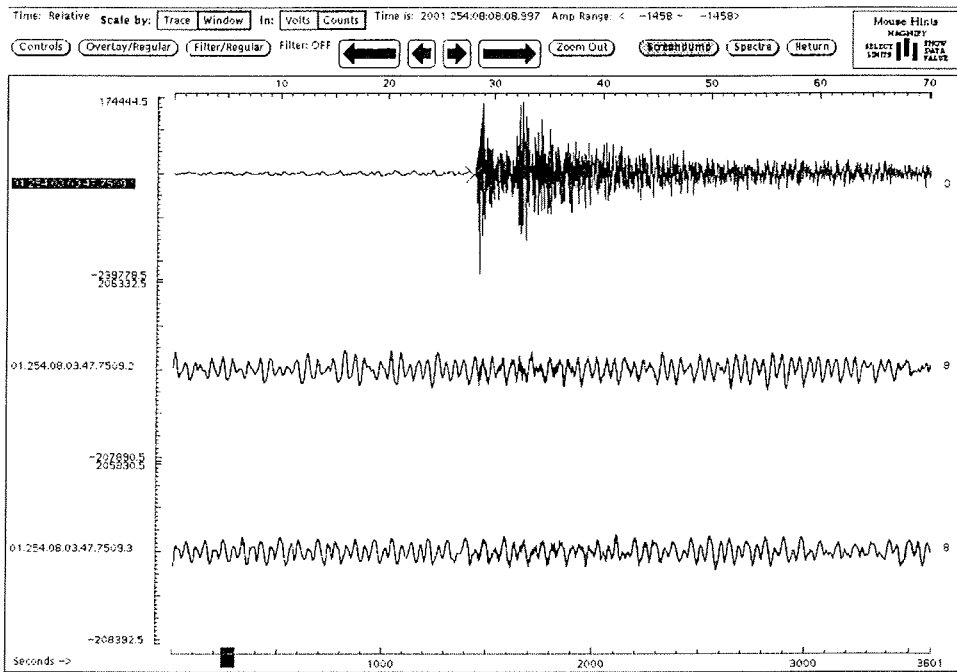


Figure 91: Record of a local earthquake at a single station (GAK21) of array GAK-2: Trace 1 above displays the vertical component, Trace 2 in the middle the horizontal components in NS-direction and trace 3 at the bottom the horizontal component in EW direction of the seismometer. Note the typically high amplitudes on the vertical component compared to the low amplitudes on the horizontal components.

Cross checking the data showed that most of the events recorded on the floe are not the local earthquakes we were looking for. Movements of the internal plates the floe consists of must have caused the events. The signals of these ice-quakes are typically characterized by sharp first-breaks and high amplitudes in the records of the horizontal components (Fig. 92).

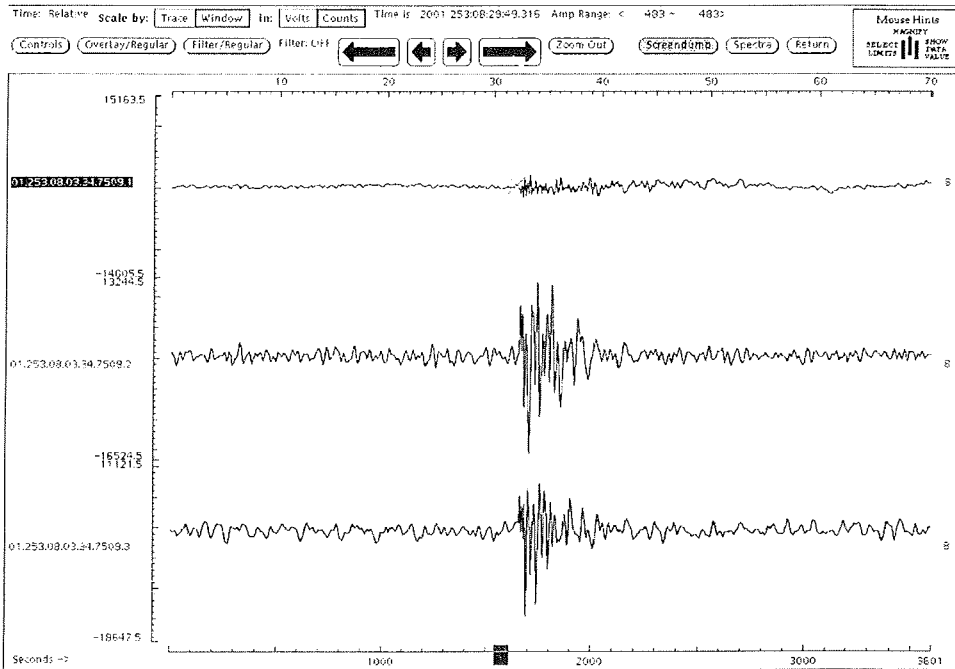


Figure 92: Typical record of an ice-quake at a single station (GAK-21) of array GAK-2. Trace 1 above displays the vertical component, Trace 2 in the middle the horizontal components in NS-direction and Trace 3 at the bottom the horizontal component in EW direction of the seismometer. Note the characteristically high ratio of amplitudes of the horizontal components compared to the amplitudes of the vertical component.

Extensive analyses of hundreds of those events showed that the ratio of the amplitudes of horizontal to vertical components is commonly greater than a value of 4.0. Furthermore the ratio of the amplitudes of the vertical components varied in most cases more than the value 2.0 on the single stations of the array. These typical features of ice-quakes helped us to derive a catalog of criteria to distinguish between ice-quakes and real local earthquakes. Therefore to be acknowledged as a local earthquake, an event had to fulfill the following criteria:

- (1) The signal of the local event must be clearly recorded on all stations of the array.
- (2) The maximum amplitudes (peak to peak) of the vertical components of all stations must be at least 4 times greater than the amplitudes of the horizontal components.
- (3) The maximum amplitudes (peak to peak) of the vertical components of the stations may not differ more than 2 times

Preliminary Results

Applying this catalog of criteria to all the recorded data, we recognized a couple of local events as highly probable earthquakes listed in Table 23 below. The recordings of all these events are summarized in the Appendix (s. Figs. App. 10 - 19).

Table 23: List of events detected during the measuring period. The last two columns "mean peak-to-peak" and "PPmax/PPmin" should give estimation about signal strength:

(a) "mean peak-to-peak" is the average of the difference between minimum and maximum amplitude measured for all stations.

(b) "PPmax/PPmin" is the ratio between the highest peak-to-peak-value of the stations.

Teleseismic events

Event name	first break	received at	mean peak-to-peak	PPmax/PPmin
Hokkaido	01 08 13 20:20:51	GAK-0 1	5500	1.21
Antarc-1	01 09 02 10:26:35	GAK-2	4370	1.87
Antarc-2	01 09 02 11:33:36	GAK-2	2060	1.92
Greenland Sea	01 08 26 18:29:58	151	69500	1.00

Local events:

event name	first break	received at	mean peak-to-peak	PPmax/PPmin
GAK-0-223-1738	01 08 11 17:38:03	GAK-0	9350	1.76
GAK-0-223-1944	01 08 11 19:44:34	GAK-0	17050	1.27
GAK-0-224-1012	01 08 12 10:12:22	GAK-0	8800	1.76
GAK-0-224-1143	01 08 12 11:43:02	GAK-0	16250	1.44
GAK-0-224-2033	01 08 12 20:33:51	GAK-0	10100	1.03

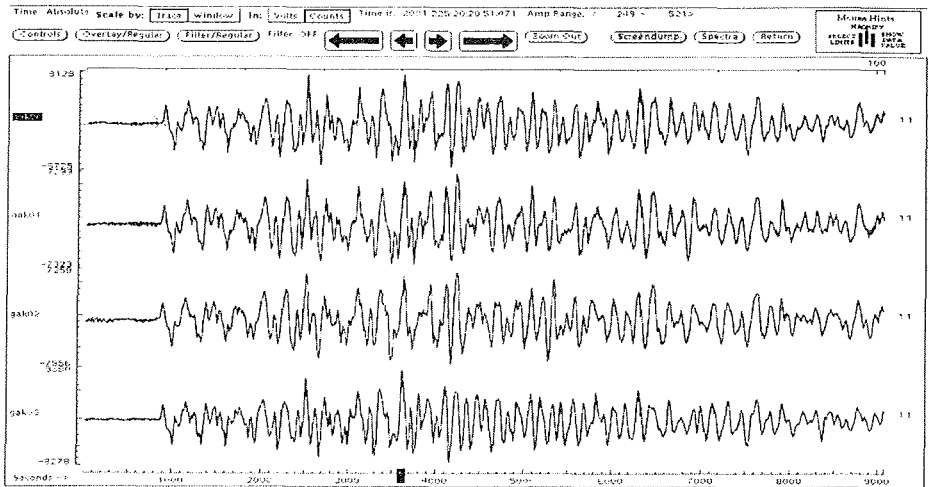
Local events:

event name	first break	received at	mean peak-to-peak PPmax/PPmin	
GAK-0-227-0449	01 08 15 04:49:38	GAK-0	9250	1.22
GAK-1-233-2129	01 08 21 21:29:08	GAK-1	138350	1.14
GAK-2-245-1039	01 09 02 10:39:43	GAK-2	775	1.38
GAK-2-245-2117	01 09 02 21:17:01	GAK-2	530	1.60
GAK-2-247-0821	01 09 04 08:21:54	GAK-2	2850	1.42
GAK-2-247-2223	01 09 04 22:23:24	GAK-2	21750	1.91
GAK-2-247-2255	01 09 04 22:55:30	GAK-2	25400	1.65
GAK-2-248-0120	01 09 05 01:20:10	GAK-2	5550	1.18
GAK-2-253-0956	01 09 10 09:56:59	GAK-2	1430	1.20
GAK-2-253-1623	01 09 10 16:23:43	GAK-2	1130	1.09
GAK-2-254-0808	01 09 11 08:08:09	GAK-2	525800	1.53
GAK-2-254-1628	01 09 11 16:28:04	GAK-2	53200	1.43

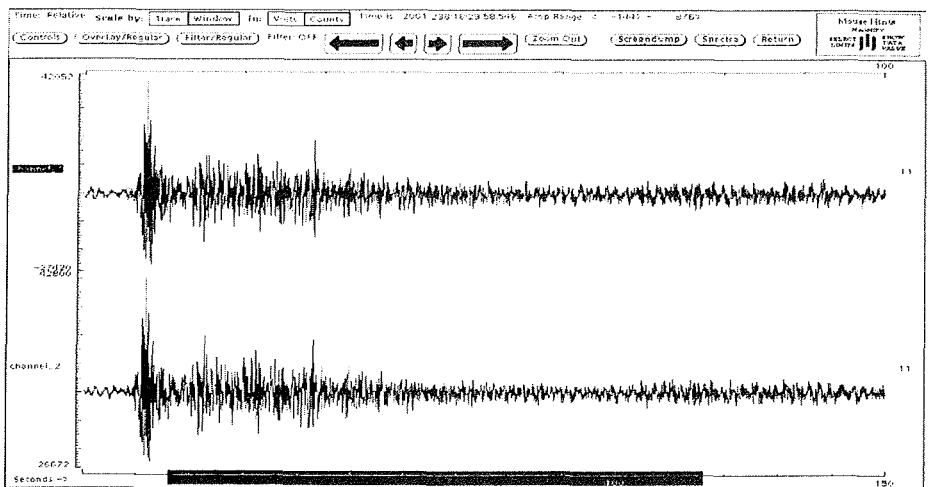
The events listed in Table 23 (Figs. App. 10 to 19). They can be divided into two types of earthquakes: Teleseismic and local events.

The teleseismic events had been determined with the regularly published event lists of the global seismological network (ISC/NEIC). First we detected a large teleseismic event clearly on all stations of the array GAK-0. This earthquake of Magnitude 6.1 (according to ISC list) had its epicenter on the island of Hokkaido, Japan at an equicentral distance of 55° (6100 km) (see Fig. 93a). Furthermore, we detected two large teleseismic events from the Pacific-Antarctic Ridge on all stations of the array GAK-2 at an epicenter distance of 147° (16300 km, Magnitude 6.3 and 5.8) which are shown in the Appendix Figure 10. The signals of all these far distant earthquakes clearly show a lower frequency content than signals of local or regional earthquakes. This was proved in another way too. When the Antarctic earthquake arrived, a refraction station (#251) had recorded incidentally on another floe at the same time. But on this station the event could not be seen, because another geophone type was used which could only detect signals with frequencies higher than 4.5 Hz. On the other hand, we detected a regional earthquake from Greenland Sea (Magnitude 5.1, epicenter distance 6.5° , 715 km) even with this type of geophones on another refraction station (#201) during a time period where no array was build up. This event (see Fig. 93b) shows clearly that local and regional earthquakes consist of higher frequencies than teleseismic events traveling longer through the earth. From these four earthquakes we can conclude,

cautiously that the detection limit for an array on a floe may be at least determined around Magnitudes of 5.1 - probably even lower.



a) Hokkaido



b) Greenland Sea

Fig. 93: Teleseismic events: a) Hokkaido earthquake: vertical components of stations at detection array GAK-0; b) Greenland Sea: vertical components at the refraction station 201; Note the different frequency contents of the two quakes compared to the same timescale (100s).

In addition to the teleseismic events, we extracted a total amount of highly probable local events, which are listed in Table 23 too. On board only a rough processing of all these events was possible. For some of the local events we tried to derive travel time differences between P- and SP-breaks. We determined a range between 4 and 15 seconds, which corresponds with distances between 32 and 120 kilometers. Further processing with special methods dedicated for array analysis in the frequency-wave number domain will give more detailed results about distance and localization of the local events.

9.9 Magnetotellurics on Drifting Ice Floes

(G. Kapinos, B. Lahrmann)

Magnetotelluric (MT) measurements use the natural variations in the Earth's magnetic field to probe the crust and the upper mantle. The periodic and transient fluctuations can be correlated with diurnal variations in the Earth's magnetic fields caused by particles, which are radiated from our sun, the solar wind. Depending on the solar activity the solar wind can strongly affect the shape of the Earth's magnetic field, which is in general visible through the northern lights. However, the interaction of the Earth's magnetic field with the solar wind has direct influence on electrical currents in the ionosphere. The inductive mechanism is an electromagnetic field propagated with slight attenuation over large distances between the ionosphere and the Earth's surface, somehow like a guided wave. These magnetotelluric fields can penetrate the surface to produce the telluric currents. The different electrical conductivity of the surface, crustal and mantle rocks deforms the induced fields in the crust, which can be measured by MT-experiments.

The method provides information about structure, heterogeneity and anisotropy of the upper mantle, the presence of fluids as well as the degree of melting and the connectivity of the melting in the asthenosphere. Especially, hints about the presence of magma chambers beneath mid-oceanic ridges are one important application in marine sciences. Different magnetotelluric experiments along mid-ocean ridges have been conducted during the last years, like the MELT (Mantle Electromagnetic and Tomographic) experiment above the East Pacific Rise (1996) or the RAMESSES (Reykjanes Axial Melt Experiment Structural Synthesis from Electromagnetics and Seismics) Experiment above the Reykjanes Ridge (1998).

All these experiments used ocean bottom instruments to record the telluric currents. In the Arctic Ocean ordinary instruments for onshore experiments can be used avoiding many problems which are inherent in using deep-sea deployments. Another issue is that MT-experiments were previously not performed in the high Arctic; so it was also some kind of test if drifting MT – stations provide reasonable results in high magnetic latitudes.

The purpose for the magnetotelluric experiments on this cruise was to get information on the conductivity of the crust and mantle beneath the rift valley of Gakkel Ridge. This method is sensitive to large-scale distributions of temperature and to the presence and amount of conductive crustal fluids. In combination with seismics it is possible to reveal and to characterize structures within the lithosphere that will enlarge our knowledge about crustal growth and evolution in the area of Gakkel Ridge. It was planned to make a setup with at least 5 Stations approximately 10 km away from each other. The profile should have been oriented perpendicular to Gakkel Ridge and should record for 5 – 8 days on the floe. This would allow a better interpretation of expected 2-D effects due to differences in the distribution of conductivity.

The principal problem for this experiment is that the strength of the natural long-period source signal, which is produced in the earth ionosphere, is significantly attenuated by the high conductivity of the seawater. This effect decreases with increasing wavelength. Therefore long observation times are necessary to achieve good results. Low environmental noise was expected since no man-made electric field or plants are present in the Arctic environment. However, the noise level being produced by the conductive seawater through the earth's magnetic field was unknown. Furthermore, the data can be affected through changes in bathymetry, when the ice floes drift across the rift valley.

Deployment of MT Stations

The basic plan (Fig. 94) was to use the same setup as for onshore measurements. At first the two lines for the electric components (E_x & E_y) had to be measured. Their orientation is vertical to the direction of the main magnetic directions: N – S and E – W. At the intersection of the two lines and on the end of both lines (length

of each line: 100 m) electrodes were dug into the ground and were connected with the amplifier. The magnetic sensor was positioned ca. 10 – 20 m apart from the data acquisition unit and adjusted to the magnetic field. To ensure the power supply two (12V, 65 Ah) batteries were connected to each station (4 to the longtime stations Gak2-1 & Gak2-2). Finally all five components (B_x , B_y , B_z , E_x , E_y) had to be compensated to a mean value of signal strength due to the limited dynamic range of the recording instruments and the GPS receiver had to be switched on.

In the ice, holes for the electrodes were drilled through the ice floe, in order to get a good coupling to the seawater. For this setup after gathering some experience on the work on ice floes approximately 2 hours were needed to build up one station. In order to reduce the time for building up a station and to raise the probability for recovering of the electrodes, the previous setup was changed. In this case only one hole had to be drilled for the base electrode and the other two sensors only were deployed into the water over the edge of the ice floe. Thus, the time for building up a complete station decreased to approximately 75 minutes.

For locations see chapter 9.8: Overview of seismic and magnetotelluric stations.

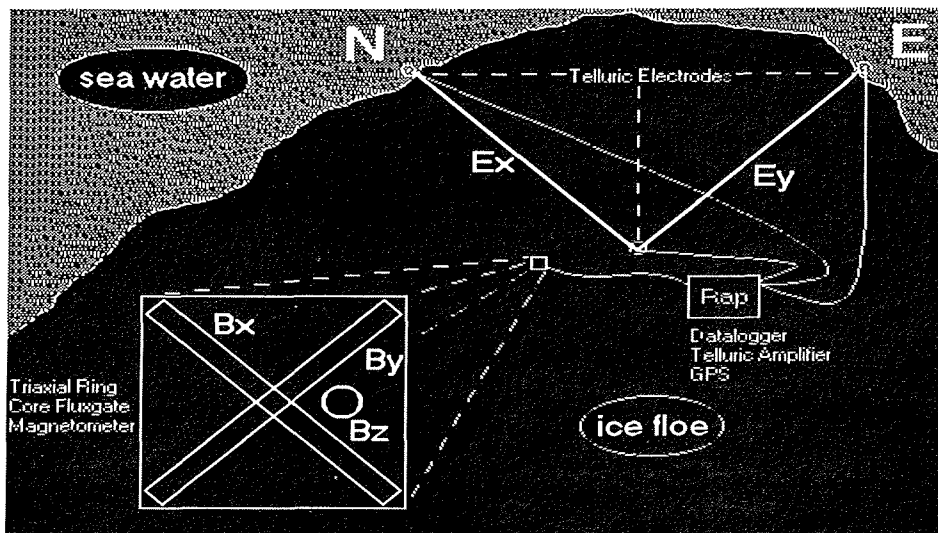


Figure 94: MT-experimental setup.

Problems during the Measurements:

Temperature Drift of the Electrodes

To reduce this drift during onshore measurements the electrodes were dug approximately 1m into the ice floe (Fig. 95). On an ice floe this is no problem at all, because the water has a relative constant temperature beneath the ice floe. However, the electrodes should have a constant temperature of about 0 °C before deploying them. Therefore, on this cruise the electrodes were stored all the time on the working deck in a tub filled with seawater.

Freezing up of the Electrodes

During the first measurement the electrodes were deployed to the bottom of the ice floe (ca. 2m). A covered plastic pipe with a length of 1 m should prevent freezing from above. But after nearly 4 days all 3 electrodes froze completely in their holes and were lost. Reasons for this might be the invasion of fresh water in the drill hole. For all subsequent measurements the electrodes were only deployed to the end of the pipe. The electric contact was ensured, even when freezing occurred, through water-filled channels in the ice.

On station GAK2-1 it wasn't possible to drill through the ice floe, because it was thicker than 4 m. Therefore, the electrode was deployed into a melt pond. A first look at the data showed that even this setup worked fine.

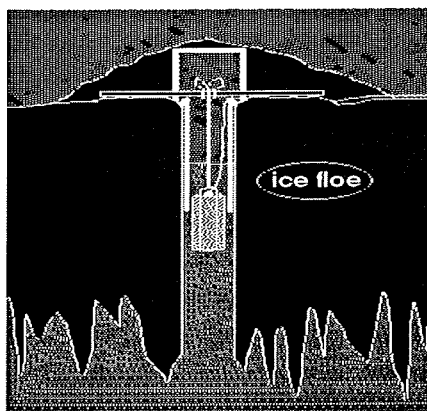


Figure 95: Sketch of the deployment of a MT-sensor.

Rotation of the Ice Floe

Because of the limited dynamic range of the magnetometer rotations are critical to the data quality. For the first station the rotation was so strong that only 16 hours of good data could be recorded. Here, the station was out on the floe for nearly four days. A comparison with the GPS coordinates of the seismology stations on the same ice floe showed a rotation that was hardly recognizable, but obviously too strong for the measurement. To our surprise the problem didn't occur at all during stations GAK2-1 and GAK2-2. They had a very much longer observation time of about 11 days and a drift path of about 50 km. Perhaps winds pressed the ice more together during the later stations and prevented any rotation of the ice floes. The problems with the electric components during stations GAK2-1 & GAK2-2 happened because of a higher electric amplification than during the other stations and had nothing to do with any rotation of the ice floe.

Long Observation Times

Since the MT experiments needed long deployment times (Tab. 23), difficulties with the ship's schedule were unavoidable. The uncertainty of the petrologists time schedule didn't allow us to deploy more stations, because most of the time it was not clear if the POLARSTERN would still be in helicopter range after some days. Therefore the solutions were either to fly 2 days ahead of the ship or to 2 days before arriving at a turning point of the cruise. So the previous plan of a profile across the ridge was absolutely not practicable and the stations were all set up near the main rift valley. An observation period of 11 days was achieved while both ships sailed to the Lomonosov Ridge and afterwards to the North Pole. To ensure the recovery of the stations an ARGOS buoy was deployed on the same floe together with the MT and seismological stations. The buoy transmitted via NOAA satellites every six hours the position of the instruments. All geophysical gear could be recovered without any problems after almost 2 weeks.

The quality of the data seems to be good compared with a model calculated by the RAMESSES – experiment (Figs. 96 and 97). For further results or models some time is needed, since the existing magnetotelluric analysis-programs have to be modified. The codes were written for stations at fixed locations.

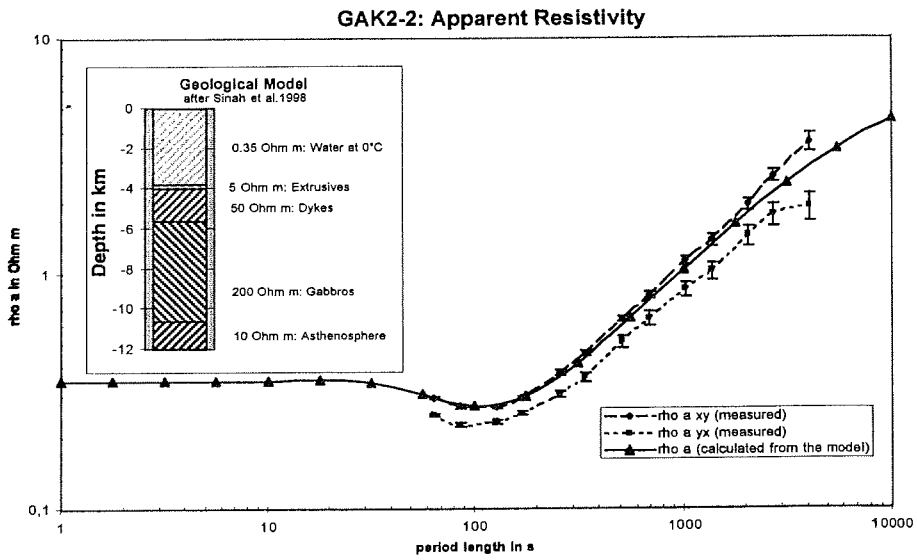


Fig. 96: Data example.

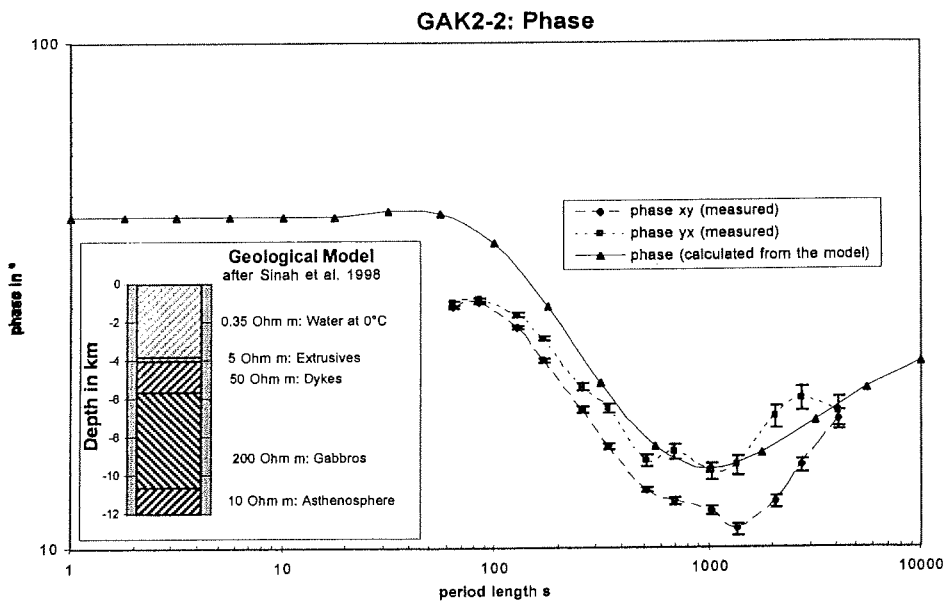


Fig. 97: Data example.

10. Plans for Future Work

Glaciology

ARK XVII/2 has shown that electromagnetic (EM) induction sounding has become an established technique for ice thickness measurements, which can be operated from the ground, from a steaming icebreaker or from a helicopter. As already demonstrated with SIMS (Sea Ice Monitoring System), EM measurements can be performed on a continuous and operational basis. Therefore, and considering the importance of ice thickness measurements for understanding the Arctic climate system, on any POLARSTERN or other ships expedition into closed pack ice SIMS should be operated, and some person should perform ground-based EM measurements at least along short profiles. The observations of a thinning ice cover and the difficulties of interpreting them in terms of Arctic-wide climate changes demonstrate the need for systematic and regular ice thickness surveys. These will be soon possible by means of airborne surveys using the new HEM bird. EM flights should be performed on an annual or even seasonal basis using e.g. long-range helicopters based on Svalbard or northern Greenland. We would also suggest using tourist ships crossing the Arctic Basin to the North Pole as a platform for ground-based, ship- or airborne surveys. Clearly, the region of the Transpolar Drift is of great importance for extending the present ice-thickness time series consisting only of measurements in three summers performed over a period of ten years. However, to estimate and monitor the basin-wide sea-ice mass balance, longer transects across different ice regimes are needed. These transects should be performed as soon as possible but will be finally performed with the planned new icebreaker AURORA BOREALIS.

Geochemistry

During ARK XVII/2 much material and data on the geochemistry of modern sedimentation have been collected. But in future it makes sense to organize these studies more wide, because their results are important both for understanding geological processes and for ecological researches. It will be very useful to organize following studies:

Aerosol studies

Aeolian transport of particulate matter onto Arctic Sea ice is one of the sources of sedimentary material in the Arctic. Its role in sedimentation in the Arctic

Ocean has been studied insufficiently. It would be necessary to study both the aerosol particle size distribution (using different particle counters) and composition of aerosols, collecting samples of aerosols by filtration of air.

Study of Particulate Matter in Snow and Ice

The drifting ice in the Arctic is a giant natural accumulator of the aeolian material and attendant pollutants, which first are deposited on the ice and are transformed into cryosols. When the ice melts, often many thousand kilometres away from the places of their fallout, they are released into the water (mostly in Fram Strait and the Greenland Sea). Sediment transport via sea ice is expected to contribute significantly to deep-sea sedimentation at least in regions of ice ablation. Much work has been performed to study the "dirty ice" in the Arctic but the transport of sedimentary material by icebergs has been studied only occasionally. Snow, dirty ice and ice cores are to be collected for chemical composition studies. In the land laboratories detailed analysis of these samples could be carried out.

Study of Suspended Particulate Matter in the Water Column

The concentration and composition of suspended matter are important characteristic of sedimentary environment. It could be very reliable tracer of the modern hydrothermal activity. It seems most worth studying the optical properties of the water column simultaneously with the distribution and composition of suspended matter, as well as physical, chemical, and biological characteristics. We propose to study water column with Rosette unit with CTD and Niskin bottles. Collected water samples are filtered through Nuclepore and Whatman GF/F filters. Along with suspended matter sampling we recommend to carry out hydrooptical studies, measurements of the turbidity by conventional sensors and Secchi disc.

Vertical Particle Flux Studies

In the Ocean particle fluxes from the surface waters to the bottom represent a significant link in geochemical cycles of carbon and many other elements. In the Central Arctic only few particle flux studies were carried out. Vertical particle fluxes could be measured using short-term deployment of sediment traps.

Geochemistry of Bottom Sediments

The chemical composition of bottom sediments is an important tracer of their origin and history. One of the important tasks of geochemical work in oceanic rift zones is to study metal-enriched sedimentary deposits. Their genesis is

closely linked with the generation of a new ocean floor. Metalliferous sediments are relatively well studied in the Pacific, Atlantic and Indian Oceans, but we didn't find any publication, devoted to such studies in the Arctic. Their studies in the Arctic are of great importance. Bottom sediments are natural records of past particle fluxes.

Geophysics

From a geophysical perspective the next step for investigating the Gakkel Ridge is to move eastwards to the junction of the mid-ocean ridge with the Laptev Sea. To describe the nature of the ridge the same range of the methods will be applied as it was used during this cruise. However, more time will be given to the seismological and magnetotelluric investigations, if they provide reasonable results from this cruise. In terms of geophysical methods the mantle and the crust will be probed equally.

The neo-volcanic area at 85°E, which could not be investigated by the full range of geophysical methods during this cruise, will be one of the major targets for the next expedition to the Gakkel Ridge. We will try to reach both target areas within the next three years.

Petrology

Future work on the Gakkel Ridge will necessarily involve a detailed sampling of particularly interesting geologic and geochemical features. One of these will be certainly the hydrothermal field located at the western end of the Gakkel Ridge. The second one will be the large amagmatic ridge segments in the central Gakkel Ridge. The third one will be certainly a further sampling eastward than was reached during AMORE 2001. Due to the sediment cover this will be necessarily a difficult task. It may be that the most eastern sampling of the Gakkel Ridge will be only possible with the use of a drill ship.

Paleoceanography

Tremendous progress has been achieved within the last years in the understanding of land-ocean interactions along the northern Eurasian margin. However, the impact of glaciations and deglacial events has been studied only from sediment cores taken either along the margins, where the sediments often reflect local developments, or in the area of the Lomonosov Ridge, which is quite

remote from the sources of terrigenous input. To study the several short-term events of glacial advances in northern Eurasia during the Weichselian and the associated discharge of icebergs and meltwater, the area sampled by long sediment cores needs to be extended further to the east of the area visited during the ARK XVII-2 expedition. Our seismic and PARASOUND surveys have demonstrated the existence of a thick sediment cover on the Gakkel Ridge east of 60°E. The obtained cores had undisturbed hemipelagic sequences at least in the area between the ridge valley and the outermost morphologic ridge parts which serve as a protective wall sheltering the inner part from turbidites triggered from the continental slopes off northern Eurasia. This indicates that sediment cores suitable for paleoenvironmental studies can be obtained along the Gakkel Ridge as far east as the ridge is still a morphologic element above the sediment cover in the Nansen and Amundsen basins. It is strongly desirable to visit this area during future expeditions to complement and connect the existing data sets from the Laptev and Kara seas and continental margins with data from the central Arctic and the area west of 60°E to understand the effect of developments in the terrestrial and continent-near environment on the entire Arctic Ocean and the global oceanic circulation and climate.

11. Public Relations

(B. Mackowiak, D.Hans)

Why would two free-lance science journalists go on such a long expedition? Although food and lodging on the ship are free continuing financial expenditures at home are a weighty factor, which cannot be ignored. This frightened away the established mass media and prevented them from sending one of their teams on this journey.

There are three main reasons why we came, all of which out-weighed the financial difficulties. The first reason is the extraordinary region of the planet, which the expedition ARK XVII/ 2 visited. Second, the planned research program; and last but not least, the special research vessel, which transported the crew and scientists to that place. In spite of modern mass tourism, which routinely sends men and women into every last corner of our planet, the Arctic region – especially the North Pole still remains one of the most mysterious and fascinating regions of our planet. The chance to visit this place, is not given to every journalist, even he is a master of his profession.

All this made this expedition an uncontested highlight in the career of a science journalist - whether his interest is in astronomy, geoscience or biology and medicine; more than a professional highlight: This expedition is a personal highpoint of one's life. We could see a well-planned and successful research program, which included various fields of geological and polar research, all working together on the research vessel POLARSTERN. Although she has been in service for almost twenty years, the POLARSTERN is still one of the largest and most modern research and transportation icebreakers in the world. To get used to the everyday life on this ship and to report afterwards to a wide public how such a complex and multi-faceted research machinery works in such an extreme region is the third big reason why we came.

It was a fortunate chance that this expedition could be covered not only by the print and radio media but also by television. Certainly the fruit of our work will be harvested only after the end of the expedition because only a small number of editorial staffs agreed to coverage beforehand; only the "Berliner Morgenpost" and the "Hamburger Abendblatt". In their science pages they reported the destination and preparations of the expedition. Other papers pointed out the interest of our reports after the end of the journey or gave obliging additions, like the science editor staff of the West-German Broadcasting Company.

From the very start of our journey we saw the great difference between theory and practise. In spite of our study of the ship's layout and the expedition program, we found that the ship and the working teams formed a complex unity. During the first week we had no choice but to make a survey according to the principal of try and error and to take photos and interviews at random.

Because of this it was a great help, and also an evidence of trust, to be allowed to participate in the daily meetings of the chief scientists and the crew. They took place in the library or "Blue Saloon" of the POLARSTERN. There were talks about the important daily work, which had to be done and the weekly projects, and also the problems that had come up during the week's work.

The crew and scientists went out of their way to help us, which we appreciated, especially because journalist has a reputation of always disturbing other peoples work. People also think that we don't report the news correctly but we never felt this prejudice. And whenever there was a problem it was easily corrected. This was not only a factor of time, but also of our long time living together. After one week, it was like we weren't journalists any more. We were members of the expedition like everyone else on the ship, except that we carried cameras and recorders all the time.

The crew and scientists were very co-operative, sometimes going to extreme edge of what was permitted for us. We had the chance to look in every part of the ship, and to take part in helicopter flights and excursions to the ice floes. We received answers to all our questions, when the scientists and crew were not too busy. We tried to get a practical insight into the work, which was being done. We ourselves tried to participate in the work by helping out as ice watchers or helping during the ice floe excursions.

Of course we didn't forget that we are working journalists. As soon as we knew the principals of the work and the working methods, we could begin to draw a systematic picture of the everyday science and the progress of the expedition, with interviews, photos and film tapes. We accompanied and documented the two highlights of the expedition, the three-ship meeting of the POLARSTERN, the ODEN and the HEALY on the 23rd of August, and the arrival of POLARSTERN and HEALY at the North Pole on the 6th of September with two extensive press releases. The meeting of the POLARSTERN and the HEALY at the North Pole happened exactly ten years after the historic meeting of POLAR-

STERN and ODEN at this magic place. We distributed our press releases among German and international news agencies and wrote two extensive reports about the conquest of a none-ice free Northpole for the "Berliner Morgenpost" and the "Hamburger Abendblatt" newspaper.

Another important event was the days we spent on the US Coast Guard icebreaker HEALY. At the invitation of the captain we had the chance to observe the everyday life of crew and scientists, the working operation and HEALY's Cupertino with POLARSTERN, seeing the American perspective towards our vessel.

These events were overshadowed by the terrorist attack on 11th of September. Here the difficult communication conditions of the Arctic became evident. But contrary to our initial apprehensions the disaster in New York did not bring to an end or even change the expedition program.

Instead, the expedition went on as planned and the important research continued. And so too did our work. We recorded an enormous amount of impressions, which will last us for days and weeks into the future. With the rich film, photo and sound material we collected, we will be able to document an expedition, which will not be undertaken again for years and years.

12. Acknowledgements

The AMORE-2001 expedition to the central eastern Arctic Ocean was special because of several reasons. It was a demanding expedition of high visibility and international involvement. It was the scientific maiden voyage for the USCGC HEALY, and we are grateful to captain and crews that the 2 ships performed superbly together when operating in convoy and that they were able to share amicably in an exciting scientific program. At the same time both ships were able to reach the North Pole on September 6, 2001, HEALY the first time, POLARSTERN exactly 10 years after its first visit when the Swedish ODEN and POLARSTERN reached the North Pole as the first conventionally powered research vessels ever.

By lucky coincidence HEALY and POLARSTERN met ODEN on August 23 at the Gakkel Ridge, when ODEN passed through the area on her way back from an extended research program close to the North Pole. It was a memorable occasion opening a new age of Arctic marine and polar research when more than 250 crew and scientists from 17 nations on the American, German and Swedish research ice breaker met in the middle of the Arctic Ocean. The occasion was used to direct the following note marking this event and thanking the 3 nations providing the research icebreakers to their heads of state:

*USCGC HEALY, United States of America
Icebreaker ODEN, Sweden
PVFS POLARSTERN, Federal Republic of Germany
85° 30' N 015° 00' E over the Gakkel Ridge in the Arctic Ocean*

*To
His Excellency, the
President of the United States of America
Mr. George W. Bush*

*His Majesty,
King Carl XVI Gustaf of Sweden*

*His Excellency, the
President of the Federal Republic of Germany
Mr. Johannes Rau*

Today, the 23 of August 2001, the polar research vessels CGC HEALY, ODEN and POLARSTERN met in the frozen central Arctic Ocean, one of the most inhospitable and loneliest parts

of our Earth. This meeting at the summit of the world marks a new epoch of systematic and peaceful research of a poorly known ocean that has an enormous impact on the climate and environment of North America and Europe.

ODEN and POLARSTERN were the first conventional research icebreakers to reach the pole in 1991, and can now celebrate 10 years of international polar research since then. ODEN is on her way home from a climate change and environmental research expedition consisting of sub-programs in atmospheric chemistry, biogeochemistry, oceanography, remote sensing and geophysical research near the North Pole.

The new research icebreaker CGC HEALY, together with POLARSTERN, is studying the geological and geophysical characteristics of Gakkel Ridge. This northernmost extension of the worldwide system of mid-ocean ridges is the tectonic plate boundary between the North American and Eurasian continents. Its undersea volcanoes, hot springs and biota are expected to yield a wealth of new information regarding the origins of mid-ocean ridges worldwide.

The scientists and crews of the three ships include over 250 participants from 17 nations (China, Germany, Italy, Norway, Russia, Sweden, Spain, USA, Finland, Brazil, Estonia, Great Britain, the Netherlands, Australia, Canada, Austria and Switzerland). Together they are carrying out internationally recognized programs of peaceful scientific research of this little-known region of our planet.

We are thankful that these three outstanding platforms for the conduct of peaceful scientific research have been made available to the international scientific community by the people of their respective countries.

Captain David Vizneski
Commanding Officer
USCGC HEALY

Commandør Mads Johanson
Captain of ODEN

Kapitän Jürgen Keil
Captain of POLARSTERN

Prof. Dr. Peter Michael
Chief Scientist HEALY

Hr. Ulf Hedman
Chief Scientist ODEN

Prof. Dr. Jörn Thiede
Chief Scientist POLARSTERN

The AMORE 2001 expedition has been launched after several years of preparation. The ships were made available through the US Coast Guard and the Alfred-Wegener-Institute for Polar and Marine Research, but substantial additional funding had been acquired upon individual applications from the US National (NSF) and German (DFG) Science Foundations. Research permits from Denmark for Greenland and Norway granted access to the EEZ of both countries, and the ships were permitted to use port facilities in Tromsø/ Norway.

The AMORE 2001 expedition lasted 69 days. During the entire time span the crew of POLARSTERN under Captain Keil from the shipping company "Reederei F. LAEISZ G.m.b.H." provided excellent seamanship, a comfortable plat-

form for conducting the long expedition and in many occasions helpful solutions to many large and small technical and logistics problems. The activities of the scientific party also benefited from the untiring service of the helicopter crews from "Fa. Helikopter Service WASSERTHAL GmbH". Regular weather forecasts were guaranteed from the POLARSTERN weather station of the German Weather Service (DWD).

The members of the scientific party on POLARSTERN from China, Italy, Russia, USA and Germany gratefully acknowledge the help of many people and institutions who through its activities both before and during the expedition helped to make AMORE 2001 reality. They all share our success of harvesting very exciting and novel research results from a corner of planet Earth that was virtually unknown up to now.

13. References

- Baker, E.T. and Milburn, H. (1997). MAPR: a new instrument for hydrothermal plume mapping. *RIDGE Events*, 7.1.
- Baskaran, M., Asbill, S., Santschi, P., Brooks, J., Champ, M., Adkinson, D., Colmer, M.R. and Makayev, V. (1996). Pu, ^{137}Cs and excess ^{210}Pb in Russian Arctic sediments. *Earth Planet. Sci. Lett.*, 140: 243-257.
- Bradley, D.J. and Jenquin, U.P. (1995). Radioactive inventories and sources for contamination of the Kara Sea by riverine transport. *Report PNWD-2316*, Pacific Northwest Laboratory, Richlin, WA.
- Coakley, B.J. and Cochran, J.R. (1998). Gravity evidence of very thin crust at the Gakkel Ridge (Arctic Ocean), *Earth Planet. Sci. Lett.*, 162: 81-95.
- Dethleff, D., Nies, H., Harms, I.H. and Karcher, M.J.(2000). Transport of radionuclides by sea-ice and dense-water formed in western Kara Sea flaw leads. *J. Mar. Syst.*, 24: 233-248.
- Dick, H.J.B. (1989). Abyssal peridotites, very slow spreading ridges and ocean ridge magmatism. In: A.D. Saunders and M.J. Norry (Editors), *Magmatism in the Ocean Basins. Geol. Soc. Spec. Publ.*, London: 71-105.
- Dick, H. J. B., Natland J.H., et al. (1999). *Proceedings of the Ocean Drilling Program; Initial Reports: Return to Hole 735B*. College Station, TX, United States Washington, DC, United States, Texas A & M University, Ocean Drilling Program American Geophysical Union, vol. 176.
- Donaldson, C.H. (1982). Spinifex-textured komatiites: a review of textures, mineral compositions and layering. In: N.T. Arndt and E.G. Nisbet (Editors), *Komatiites*. Allen and Unwin, London: 213-244.
- Eckstaller, A., Gaw, V., Przybilla, T. and Schmidt, T. (1998). Installation eines seismischen Detektionsarrays. *Ber. Polarforsch.*, 267/98: 98-113.

Fowler, C.M.R (1990). An Introduction to Global Geophysics, Cambridge University Press. In: The Solid Earth: 85-92, 220-224.

Fütterer, D. K. and Shipboard Scientific Party (1992). ARCTIC 91. Expedition ARK-VIII/3 of RV "Polarstern" in 1991.- *Rep. Polar Res.* 107, 267 pp.

Grenfell, T. C. and Maykut G. A. (1977). The optical properties of ice and snow in the Arctic Basin, *J. Glaciol.*, 18: 445-463.

Haas, C. (1998). Evaluation of ship-based electromagnetic-inductive thickness measurements of summer sea-ice in the Bellingshausen and Amundsen Sea, *Cold Reg. Sci. Techn.*, 27(1): 1-16.

Haas, C. and Eicken, H. (2001). Interannual variability of summer sea ice thickness in the Siberian and Central Arctic under different atmospheric circulation regimes, *J. Geoph. Res.*, 106 (C3): 4449-4462.

Haas, C., Gerland, S., Eicken, H. and H. Miller (1997). Comparison of sea-ice thickness measurements under summer and winter conditions in the Arctic using a small electromagnetic induction device, *Geophysics*, 62 (3): 749-757.

Hellebrand, E., Mühe, R. and Snow, J.E. (2001). Mantle melting beneath the Gakkel Ridge (Arctic Ocean): Abyssal peridotite spinel compositions. *Chem. Geol.*, in press.

Hofmann, A.W. (1988). Chemical differentiation of the Earth: the relationship between mantle, continental crust, and oceanic crust, *Earth Planet. Sci. Lett.*, 90: 297-314.

Jakobsson, M., Cherkis, N.Z., Woodward, J., Macnab R. and Coakley, B. (2000). New grid of Arctic bathymetry aids scientists and mapmakers; *EOS, Trans., Amer. Geophys. Union*, 81, No. 9: 89, 93, 96.

Jokat, W. (1999). ARCTIC 98: The Expedition ARK-XIV/1a of RV "Polarstern" in 1998. *Rep. Polar Res.*, 308: 159 pp.

Jokat, W., Weigelt E., Kristoffersen, Y., Rasmussen, T., and Schöne, T. (1995). New geophysical results from south-western Eurasia Basin (Morris Jesup Rise, Gakkel Ridge, Ermak Plateau) and the Fram Strait. *Geophys. J. Intern.*, 123: 601-610.

Kennett J. (1982). *Marine Geology*. Englewood Cliffs, N.J.: Prentice-Hall, 813 pp.

Kristoffersen, Y. (2000). The Eurasia Basin: An Update from a Decade of Geoscientific Research. *Polarforschung*, 68: 11-18.

Kristoffersen, Y. and Husebye, E. S. (1985). Multichannel seismic reflection measurements in the Eurasia Basin, Arctic Ocean, from U.S. ice station Fram-IV. *Tectonophysics*, 114: 103-115.

Kristoffersen, Y., Husebye, E.S., Bungum, H. and Gregersen, S. (1982). Seismic investigations of the Nansen Ridge during the FRAM I experiment, *Tectonophysics*, 82: 57-68.

Lisitzin A.P., Shevchenko V.P. and Burenkov V.I. (2000). Hydrooptics and suspended matter of Arctic seas. *Atmos. Oceanic Opt.*, 13: 61-71.

Lisitzin A.P. (1996). *Oceanic Sedimentation. Lithology and Geochemistry*. American Geophysical Union. Washington, D.C., 400 pp.

Masqué, P., Cochran, J.K., Hebbeln, D., Hirschberg, D.J., Dethleff, D. and Winkler, A. Sea ice and the fate of contaminants in the Arctic Ocean: Plutonium in the Fram Strait. *Nature*, in press.

McKenzie, D. and O'Nions, R.K. (1991). Partial melt distributions from inversion of rare earth element concentrations. *J. Petrol.*, 32: 1021-1091.

Mühe, R., Bohrmann, H., Garbe-Schönberg, D. and Kassens, H. (1997). E-MORB glasses from the Gakkel Ridge (Arctic Ocean) at 87°N: evidence for the Earth's most northerly volcanic activity, *Earth Planet. Sci. Lett.*, 152: 1-4, 1-10.

Mühe, R., Bohrmann, H., Hörmann, P.K., Thiede, J. and Stoffers, P. (1991). Spinifex basalts with komatiite-tholeiite trend from the Nansen-Gakkel-Ridge (Arctic Ocean). *Tectonophysics*, 190: 95-108.

Mühe, R., Devey, C.W., Peucker-Ehrenbrinck, B. and Garbe-Schönberg, D. (1997). On the redistribution of Pb in the oceanic crust during hydrothermal alteration, *Chem. Geol.*, 137, 1-2: 67-77.

Müller, C. and Jokat, W. (2000). Seismic Evidence for Volcanic Activity Discovered in Central Arctic, *EOS, Trans., Amer. Geophys. Union*, 81, No. 24: 265, 269.

Müller, C., Eckstaller, A., Frenzel, A., Graham, G., Otto, A. and Swanevelder, P. (1998). Aufbau einer seismologischen Breitbandstation an der neuen südafrikanischen Überwinterungsstation SANAE IV, Vesleskarvet. *Ber. Polarforsch.*, 267/98: 188-199.

Nürnberg D., Wollenburg I., Dethleff D., Eicken H., Kassens H., Letzig T., Reimnitz E. and Thiede J. (1994). Sediments in Arctic sea ice - entrainment, transport and release. *Mar. Geol.*, 119: 185-214.

PASSCAL Reference Manual, PASSCAL Version 1.9.23, 2001.

Perovich, D. K., Roesler, C. S. and Pegau, W. S. (1998). Variability in Arctic sea ice optical properties, *J. Geophys. Res.*, 103 (C1): 1193-1208.

Pfirman S., Lange, M.A., Wollenburg, I. and Schlosser, P. (1990). Sea ice characteristics and the role of sediment inclusions in deep-sea deposition. In: Arctic and Antarctic comparisons. U. Bleil and Thiede, J. (Editors), Geological History of the Polar Oceans: Arctic versus Antarctic. Kluwer Academic Publishers: 187-211.

Pfirman, S., Colony, R., Nürnberg, D., Eicken, H. and Rigor, I. (1997). Reconstruction the origin and trajectory of drifting Arctic sea-ice. *J. Geophys. Res.*, 102 (C6): 12575-12586.

Rachor, E. (1997). Scientific Cruise Report of the Arctic Expedition ARK-XI/1 of RV "Polarstern" in 1995. *Ber. Polarforsch.* (Rep. Polar Res.), 226: 157, 173 (Annexes).

Rigor, I. and Colony, R. (1997). Sea-ice production and transport of pollutants in the Laptev Sea, 1979-1993. *Sci. Total Environ.*, 202: 89-110.

Seawater: Its Composition, Properties and Behaviour. The Open University in Association with Pergamon. (1995).

Shevchenko V.P., Lisitzin A.P., Vinogradova A.A., Smirnov V.V., Serova V.V. and Stein R., (2000). Arctic aerosols. Results of ten-year investigations. *Atmos. Oceanic Optics*, 13: 510-533.

Shine, K. P. and Henderson-Sellers, A. (1985). The sensitivity of a thermodynamic sea ice model to changes in surface albedo parameterization, *J. Geophys. Res.*, 90 (D1): 2243-2250.

Sinha et al. (1998). RAMESSES - Reykjanes Axial Melt Experiment Structural Synthesis from Electromagnetics and Seismics; *Geophys. J.* 135: 731-745.

Smith, J.N., Ellis, K.M., Naes, K., Dahle, S. and Matishov, D. (1995). Sedimentation and mixing rates of radionuclides in Barents Sea sediments of Novaya Zemlya. *Deep-Sea Res.*, 42:1471-1493.

Snow, J., Hellebrand, E., Jokat, W. and Mühe, R. (2001). Magmatic and Hydrothermal Activity in Lena Trough, Arctic Ocean. *EOS*, 82 (17): 193-198.

Spielhagen, R. F., Bonani, G., Eisenhauer, A., Frank, M., Frederichs, T., Kassens, H., Kubik, P. W., Nørgaard-Pedersen, N., Nowaczyk, N. R., Mangini, A., Schäper, S., Stein, R., Thiede, J., Tiedemann, R. and Wahsner, M., (1997). Arctic Ocean evidence for Late Quaternary initiation of northern Eurasian ice sheets.- *Geology*, 25 (9): 783-786.

Thiede, J. and Shipboard Scientific Party (1988). Scientific Cruise Report of Arctic Expedition ARK IV/3.- *Rep. Polar Res.*, 43: 237 pp.

Warren, S. G. (1982). Optical properties of snow, *Rev. Geophys. Space Sci.*, 20: 67-89.

Weigelt, E. and Jokat, W. (2001). Peculiarities of roughness and thickness of oceanic crust in the Eurasian Basin, Arctic Ocean, *Geophys. J. Int.*, 145: 505-516.

White, R., T. Minshull, M. Bickle and C. Robinson, (2001). Melt generation at very slow spreading oceanic ridges: Constraints from geophysical and geochemical data. *J. Petrol.* 42:1171-1196.

Contents Appendices:

1.	Scientific Party ARK XVII/2.....	224-225
2.	Participating Institutions ARK XVII/2.....	226-227
3.	Ship's Crew ARK XVII/2.....	228-229
4.*	Scientific Party on HEALY.....	230
5.	Station Log POLARSTERN.....	231-234
6.*	Station Log HEALY.....	235-240
7.*	Petrology: Sampling Technologies.....	241-245
8.*	Petrology: Sample Descriptions.....	246-281
9.*	Thin Sections Overview.....	282-288
10.*	Thin Section Descriptions.....	289-335
11.*	MAPR.....	336-341
12.*	TV-Grab Video.....	342
13.*	OFOS Observations.....	343
14.*	Sediment Core Descriptions.....	344-350
15.*	Geophysical Investigations: Experience Report.....	351-387
16.*	Polar University.....	388
17.	List of Abbreviations and Acronyms.....	389-390
18.*	Karasik Seamount.....	391-397

* - *only on CD*

1. FahrtteilnehmerInnen / Scientific Party ARK XVII/2

Tromsø - Bremerhaven

Amini, Marghaleray	MPI
Augustin, Nico	IGK
Bareiss, Jörg	AWI
Bock, Michaela	MPI
Bohlmann, Harald	iSI
Büchl, Anette	MPI
Büchner, Jürgen	HSW
Drachev, Sergej	VNIIO
Erdmann, Hilger	DWD
Feld, Andrew	MPI
Feldmann, Heinrich	MPI
Feldt, Oliver	HSW
Franke, Phillip	FGUB
Galaktionov, Andrey	VNIIO
Gao, Jongjun	MPI
Gauger, Steffen	AWI
Haas, Christian	AWI
Handt, Anette von der	MPI
Hans, Dirk	AWI
Hartmann, Thomas	AWI
Hatzky, Jörn	AWI
Jokat, Wilfried	AWI
Kapinos, Gerhard	IGM
Ksienzyk, Anna	FGUB
Kubas, Guido	AWI
Kulescha, Friedhelm	OKT
Lahrman, Birger	IGM
Lensch, Norbert	AWI
Lieser, Jan Leonhard	AWI
Mackowiak, Bernhard	Journalist
Michel, Jürgen	MPI
Micksch, Uli	AWI
Mühe, Richard	IGK
Müller, Kristian	AWI
Pies, Carmen	MPI
Pignatelli, Alessandro	IGNV

Ritzmann, Oliver	AWI
Scheltz, Annette	IPÖ
Schmidt-Aursch, Mechita	AWI
Schmidt, Thomas	AWI
Schmitz, Thomas	AWI
Schramm, Burkhard	FGUB
Schünemann, Henrike	IPÖ
Schuster, Sandra	AWI
Seidler, Kai	HSW
Shevchenko, Vladimir	SIO
Snow, Jonathan	MPI
Sonnabend, Hartmut	DWD
Spielhagen, Robert	GEO
Strauß, Holger	FGUB
Thiede, Jörn	AWI
Wüstefeld, Andreas	AWI
Zepick, Burkhard	HSW

2. Beteiligte Institutionen /Participating Institutions ARK XVII/2

AWI	Alfred-Wegener-Institut für Polar- und Meeresforschung Columbusstraße D-27568 Bremerhaven
DWD	Deutscher Wetterdienst Geschäftsfeld Seeschifffahrt Jenfelder Allee 70 A D-22043 Hamburg
FGUB	Fachbereich Geowissenschaften der Universität Bremen Klagenfurter Straße D-28334 Bremen
OKT	Firma OKTOPUS Wischhofstr. 1-3 D-24148 Kiel
IGK	Institut für Geowissenschaften der Christian-Albrechts- Universität zu Kiel Ludewig-Meyn-Straße 10 D-24098 Kiel
GEO	GEOMAR Forschungszentrum für marine Geowissenschaften Wischhofstr. 1-3 D-24148 Kiel
HSW	Helicopter-Service Wasserthal GmbH Kätnerweg 43
iSI	iSITEC GmbH Stresemannstraße 46 D-27570 Bremerhaven

- IGM Institut für Geophysik der
Westfälischen Wilhelms-
Universität
Corrensstr. 24
D-48149 Münster
- IPÖ Institut für Polarökologie
Christian-Albrechts
Universität zu Kiel
Wischhofstr. 1-3
D-24148 Kiel
- INGV Istituto Nazionale di Geofisica e Vulcanologia
Via di Vigna Murata, 605
00143 Roma/ Italy
- MPI Max-Planck-Institut für Chemie
Joh.-J.-Becher-Weg 27
Universitätscampus
D-55128 Mainz
- SIO P.P. Shirshov Institute of
Oceanology RAS
Makhimovsky Prosp., 36
Moscow 117851/ Russia
- VNIIO VNI Okeangeologia
1, Angliiskiy Ave.
190121 St. Petersburg/
Russia

3. Schiffsbesatzung / Ship's Crew ARK XVII/2

Master	Keil, Jürgen
1. Offc.	Schwarze, Stefan
Ch. Eng.	Pluder, Andreas
2. Offc.	Spielke, Steffen
2. Offc.	Thieme, Wolfgang
3. Offc.	Hartung, René
Doctor	Schlenker, Wilhelm
R.Offc.	Koch, Georg
1. Eng.	Delff, Wolfgang
2. Eng.	Ziemann, Olaf
3. Eng.	Richter, Frank
Electron	Bretfeld, Holger
Electron	Muhle, Helmut
Electron	Greitemann-Hackl, Andreas
Electron	Roschinsky, Jörg
Elektr.	Muhle, Heiko
Boatsw.	Clasen, Burkhard
Carpenter	Reise, Lutz
A. B.	Gil Iglesias, Luis
A. B.	Pousada Martinez, Sato
A. B.	Kreis, Reinhard
A. B.	Schultz, Ottomar
A. B.	Burzan, G.-Ekkehard
A. B.	Schröder, Norbert
A. B.	Bastigkeit, Kai NN
Storekeeper	Preußner, Jörg
Mot-man	Ipsen, Michael
Mot-man	Voy, Bernd
Mot-man	Elsner, Klaus
Mot-man	Hartmann, Ernst-Uwe
Mot-man	Grafe, Jens
Cook	Haubold, Wolfgang
Cooksmate	Völske, Thomas
Cooksmate	Silinski, Frank
1. Stwdess	Jürgens, Monika
Stwdess/KS	Wöckener, Martina
2. Stwdess	Czyborra, Bärbel

2. Stwdess	Silinski, Carmen
2. Steward	Gaude, Hans-Jürgen
2. Steward	Huang, Wu-Mei
2. Steward	Müller, Wolfgang
Laundrym.	Yu, Kwok Yuen
Apprentice	Gerads, Sebastian
Apprentice	Habermann, Sven

4. Scientific Party on HEALY*: only on CD-ROM.

**with kind permission of Professor Dr. Peter Michael, Chief Scientist HEALY.*

No	Date	Time (UTC)	Start			On Bottom			Off Bottom			End			Equipment used	Comments/Issues
			Latitude (N)	Longitude (E/W)	Water Depth (m)	Latitude (N)	Longitude (E/W)	Water Depth (m)	Date	Time (UTC)	Latitude (N)	Longitude (E/W)	Water Depth (m)			
197	02.08.01	07:00	84° 13.3'	026° 44.9' E	417	83° 32.2'	016° 14.9' E	10.50	08.08.01	10:50	83° 32.2'	016° 14.9' E	417	MS-D32	redfish / redfish + sandeels	
198	04.08.01	08:30	81° 42.1'	027° 12.2' E	3196	83° 32.2'	016° 13.2' E	4687	06.08.01	19:50	83° 33.6'	015° 12.8' E	4713	MS-D32	redfish / redfish + sandeels	
199	06.08.01	16:47	85° 34.8'	016° 13.2' E	4687	83° 32.2'	016° 13.2' E	4687	07.08.01	00:37	85° 33.3'	016° 07.4' E	4484	TV-Gab, MAFR	redfish / redfish + sandeels	
200	08.08.01	22:38	85° 33.3'	016° 06.1' E	4686	83° 32.2'	016° 06.1' E	4686	08.08.01	22:38	85° 33.3'	016° 06.1' E	4686	TV-Gab, MAFR	redfish / redfish + sandeels	
201	09.08.01	00:35	85° 32.6'	016° 06.1' E	4686	83° 32.2'	016° 06.1' E	4686	09.08.01	00:35	85° 32.6'	016° 06.1' E	4686	TV-Gab, MAFR	redfish / redfish + sandeels	
202	07.08.01	09:13	85° 30.1'	015° 35.6' E	4403	85° 30.1'	015° 35.6' E	4403	07.08.01	09:13	85° 30.1'	015° 35.6' E	4403	Firma Dredge	redfish / redfish + sandeels	
203	07.08.01	21:17	84° 57.9'	026° 25.2' E	3538	84° 57.9'	026° 25.2' E	3538	07.08.01	21:17	84° 57.9'	026° 25.2' E	3538	TV-Gab, MAFR	redfish / redfish + sandeels	
204	08.08.01	01:39	85° 00.3'	026° 25.2' E	3538	85° 00.3'	026° 25.2' E	3538	08.08.01	01:39	85° 00.3'	026° 25.2' E	3538	TV-Gab, MAFR	redfish / redfish + sandeels	
205	08.08.01	09:59	84° 38.7'	026° 25.2' E	3538	84° 38.7'	026° 25.2' E	3538	08.08.01	09:59	84° 38.7'	026° 25.2' E	3538	TV-Gab, MAFR	redfish / redfish + sandeels	
206	08.08.01	19:27	84° 38.7'	026° 25.2' E	3538	84° 38.7'	026° 25.2' E	3538	08.08.01	19:27	84° 38.7'	026° 25.2' E	3538	TV-Gab, MAFR	redfish / redfish + sandeels	
207	09.08.01	01:50	84° 38.7'	026° 25.2' E	3538	84° 38.7'	026° 25.2' E	3538	09.08.01	01:50	84° 38.7'	026° 25.2' E	3538	TV-Gab, MAFR	redfish / redfish + sandeels	
208	09.08.01	03:35	84° 38.7'	026° 25.2' E	3538	84° 38.7'	026° 25.2' E	3538	09.08.01	03:35	84° 38.7'	026° 25.2' E	3538	TV-Gab, MAFR	redfish / redfish + sandeels	
209	09.08.01	13:51	84° 25.6'	027° 35.4' E	3743	84° 25.6'	027° 35.4' E	3743	09.08.01	13:51	84° 25.6'	027° 35.4' E	3743	TV-Gab, MAFR	redfish / redfish + sandeels	
210	09.08.01	22:34	84° 07.2'	026° 16.0' E	3796	84° 07.2'	026° 16.0' E	3796	09.08.01	22:34	84° 07.2'	026° 16.0' E	3796	TV-Gab, MAFR	redfish / redfish + sandeels	
211	10.08.01	02:54	84° 07.8'	026° 16.0' E	3796	84° 07.8'	026° 16.0' E	3796	10.08.01	02:54	84° 07.8'	026° 16.0' E	3796	TV-Gab, MAFR	redfish / redfish + sandeels	
212	10.08.01	08:30	84° 08.0'	026° 20.0' E	3874	84° 08.0'	026° 20.0' E	3874	10.08.01	08:30	84° 08.0'	026° 20.0' E	3874	TV-Gab, MAFR	redfish / redfish + sandeels	
213	10.08.01	12:28	84° 09.1'	026° 23.8' E	4023	84° 09.1'	026° 23.8' E	4023	10.08.01	12:28	84° 09.1'	026° 23.8' E	4023	TV-Gab, MAFR	redfish / redfish + sandeels	
214	11.08.01	04:45	83° 36.7'	027° 02.1' W	2633	83° 36.7'	027° 02.1' W	2633	11.08.01	04:45	83° 36.7'	027° 02.1' W	2633	TV-Gab, MAFR	redfish / redfish + sandeels	
215	11.08.01	09:04	83° 36.5'	027° 02.1' W	2633	83° 36.5'	027° 02.1' W	2633	11.08.01	09:04	83° 36.5'	027° 02.1' W	2633	TV-Gab, MAFR	redfish / redfish + sandeels	
216	11.08.01	09:45	83° 36.5'	027° 02.1' W	2633	83° 36.5'	027° 02.1' W	2633	11.08.01	09:45	83° 36.5'	027° 02.1' W	2633	TV-Gab, MAFR	redfish / redfish + sandeels	
217	12.08.01	12:07	83° 04.6'	026° 02.2' W	3543	83° 04.6'	026° 02.2' W	3543	12.08.01	12:07	83° 04.6'	026° 02.2' W	3543	TV-Gab, MAFR	redfish / redfish + sandeels	
218	12.08.01	16:25	83° 04.6'	026° 02.2' W	3543	83° 04.6'	026° 02.2' W	3543	12.08.01	16:25	83° 04.6'	026° 02.2' W	3543	TV-Gab, MAFR	redfish / redfish + sandeels	
219	12.08.01	20:24	83° 08.7'	026° 02.2' W	3543	83° 08.7'	026° 02.2' W	3543	12.08.01	20:24	83° 08.7'	026° 02.2' W	3543	TV-Gab, MAFR	redfish / redfish + sandeels	
220	13.08.01	00:24	83° 05.0'	026° 45.1' W	3628	83° 05.0'	026° 45.1' W	3628	13.08.01	00:24	83° 05.0'	026° 45.1' W	3628	TV-Gab, MAFR	redfish / redfish + sandeels	
221	13.08.01	13:10	82° 53.7'	026° 16.7' W	4063	82° 53.7'	026° 16.7' W	4063	13.08.01	13:10	82° 53.7'	026° 16.7' W	4063	TV-Gab, MAFR	redfish / redfish + sandeels	
222	13.08.01	19:40	82° 54.2'	026° 19.3' W	4155	82° 54.2'	026° 19.3' W	4155	13.08.01	19:40	82° 54.2'	026° 19.3' W	4155	TV-Gab, MAFR	redfish / redfish + sandeels	
223	13.08.01	21:41	82° 54.2'	026° 19.3' W	4155	82° 54.2'	026° 19.3' W	4155	13.08.01	21:41	82° 54.2'	026° 19.3' W	4155	TV-Gab, MAFR	redfish / redfish + sandeels	
224	14.08.01	01:10	83° 16.7'	026° 32.2' W	4474	83° 16.7'	026° 32.2' W	4474	14.08.01	01:10	83° 16.7'	026° 32.2' W	4474	TV-Gab, MAFR	redfish / redfish + sandeels	
225	14.08.01	15:55	83° 16.7'	026° 32.2' W	4474	83° 16.7'	026° 32.2' W	4474	14.08.01	15:55	83° 16.7'	026° 32.2' W	4474	TV-Gab, MAFR	redfish / redfish + sandeels	
226	15.08.01	01:10	83° 22.7'	026° 42.0' W	4599	83° 22.7'	026° 42.0' W	4599	15.08.01	01:10	83° 22.7'	026° 42.0' W	4599	TV-Gab, MAFR	redfish / redfish + sandeels	
227	15.08.01	08:11	83° 22.7'	026° 42.0' W	4599	83° 22.7'	026° 42.0' W	4599	15.08.01	08:11	83° 22.7'	026° 42.0' W	4599	TV-Gab, MAFR	redfish / redfish + sandeels	
228	15.08.01	19:27	83° 33.8'	026° 35.1' W	2987	83° 33.8'	026° 35.1' W	2987	15.08.01	19:27	83° 33.8'	026° 35.1' W	2987	TV-Gab, MAFR	redfish / redfish + sandeels	
229	16.08.01	01:36	83° 41.8'	026° 11.9' W	4039	83° 41.8'	026° 11.9' W	4039	16.08.01	01:36	83° 41.8'	026° 11.9' W	4039	TV-Gab, MAFR	redfish / redfish + sandeels	
230	16.08.01	09:46	82° 46.5'	026° 04.4' W	2934	82° 46.5'	026° 04.4' W	2934	16.08.01	09:46	82° 46.5'	026° 04.4' W	2934	TV-Gab, MAFR	redfish / redfish + sandeels	
231	16.08.01	15:47	82° 46.5'	026° 04.4' W	2934	82° 46.5'	026° 04.4' W	2934	16.08.01	15:47	82° 46.5'	026° 04.4' W	2934	TV-Gab, MAFR	redfish / redfish + sandeels	
232	16.08.01	22:28	82° 53.2'	026° 08.8' W	2928	82° 53.2'	026° 08.8' W	2928	16.08.01	22:28	82° 53.2'	026° 08.8' W	2928	TV-Gab, MAFR	redfish / redfish + sandeels	
233	16.08.01	23:28	82° 53.2'	026° 08.8' W	2928	82° 53.2'	026° 08.8' W	2928	16.08.01	23:28	82° 53.2'	026° 08.8' W	2928	TV-Gab, MAFR	redfish / redfish + sandeels	
234	17.08.01	04:52	83° 06.2'	026° 08.8' W	2928	83° 06.2'	026° 08.8' W	2928	17.08.01	04:52	83° 06.2'	026° 08.8' W	2928	TV-Gab, MAFR	redfish / redfish + sandeels	
235	17.08.01	07:38	83° 06.2'	026° 08.8' W	2928	83° 06.2'	026° 08.8' W	2928	17.08.01	07:38	83° 06.2'	026° 08.8' W	2928	TV-Gab, MAFR	redfish / redfish + sandeels	
236	17.08.01	11:41	83° 56.0'	026° 24.8' W	4020	83° 56.0'	026° 24.8' W	4020	17.08.01	11:41	83° 56.0'	026° 24.8' W	4020	TV-Gab, MAFR	redfish / redfish + sandeels	
237	17.08.01	18:25	84° 37.9'	026° 25.8' W	3930	84° 37.9'	026° 25.8' W	3930	17.08.01	18:25	84° 37.9'	026° 25.8' W	3930	TV-Gab, MAFR	redfish / redfish + sandeels	
238	18.08.01	00:45	84° 10.8'	026° 51.9' E	3995	84° 10.8'	026° 51.9' E	3995	18.08.01	00:45	84° 10.8'	026° 51.9' E	3995	TV-Gab, MAFR	redfish / redfish + sandeels	
239	18.08.01	07:43	84° 16.0'	026° 25.9' E	3771	84° 16.0'	026° 25.9' E	3771	18.08.01	07:43	84° 16.0'	026° 25.9' E	3771	TV-Gab, MAFR	redfish / redfish + sandeels	
240	18.08.01	17:43	84° 16.0'	026° 25.9' E	3771	84° 16.0'	026° 25.9' E	3771	18.08.01	17:43	84° 16.0'	026° 25.9' E	3771	TV-Gab, MAFR	redfish / redfish + sandeels	
241	19.08.01	00:08	84° 34.3'	026° 56.4' E	4020	84° 34.3'	026° 56.4' E	4020	19.08.01	00:08	84° 34.3'	026° 56.4' E	4020	TV-Gab, MAFR	redfish / redfish + sandeels	
242	19.08.01	00:08	84° 34.3'	026° 56.4' E	4020	84° 34.3'	026° 56.4' E	4020	19.08.01	00:08	84° 34.3'	026° 56.4' E	4020	TV-Gab, MAFR	redfish / redfish + sandeels	
243	19.08.01	06:45	84° 30.3'	026° 12.2' E	5263	84° 30.3'	026° 12.2' E	5263	19.08.01	06:45	84° 30.3'	026° 12.2' E	5263	TV-Gab, MAFR	redfish / redfish + sandeels	
244	19.08.01	13:46	84° 43.9'	026° 32.7' E	5263	84° 43.9'	026° 32.7' E	5263	19.08.01	13:46	84° 43.9'	026° 32.7' E	5263	TV-Gab, MAFR	redfish / redfish + sandeels	
245	19.08.01	15:20	84° 43.9'	026° 32.7' E	5263	84° 43.9'	026° 32.7' E	5263	19.08.01	15:20	84° 43.9'	026° 32.7' E	5263	TV-Gab, MAFR	redfish / redfish + sandeels	
246	19.08.01	15:20	84° 43.9'	026° 32.7' E	5263	84° 43.9'	026° 32.7' E	5263	19.08.01	15:20	84° 43.9'	026° 32.7' E	5263	TV-Gab, MAFR	redfish / redfish + sandeels	
247	19.08.01	15:20	84° 43.9'	026° 32.7' E	5263	84° 43.9'	026° 32.7' E	5263	19.08.01	15:20	84° 43.9'	026° 32.7' E	5263	TV-Gab, MAFR	redfish / redfish + sandeels	
248	19.08.01	15:20	84° 43.9'	026° 32.7' E	5263	84° 43.9'	026° 32.7' E	5263	19.08.01	15:20	84° 43.9'	026° 32.7' E	5263	TV-Gab, MAFR	redfish / redfish + sandeels	
249	19.08.01	15:20	84° 43.9'	026° 32.7' E	5263	84° 43.9'	026° 32.7' E	5263	19.08.01	15:20	84° 43.9'	026° 32.7' E	5263	TV-Gab, MAFR	redfish / redfish + sandeels	
250	19.08.01	15:20	84° 43.9'	026° 32.7' E	5263	84° 43.9'	026° 32.7' E	5263	19.08.01	15:20	84° 43.9'	026° 32.7' E	5263	TV-Gab, MAFR	redfish / redfish + sandeels	
251	19.08.01	15:20	84° 43.9'	026° 32.7' E	5263	84° 43.9'	026° 32.7' E	5263	19.08.01	15:20	84° 43.9'	026° 32.7' E	5263	TV-Gab, MAFR	redfish / redfish + sandeels	
252	19.08.01	15:20	84° 43.9'	026° 32.7' E	5263	84° 43.9'	026° 32.7' E	5263	19.08.01	15:20	8					

5. Station Log POLARSTERN (PS 52)

Profile/Station No	Start			On bottom			Off bottom			End			Equipment Used	Comments/ Results
	Date	Time (UTC)	Position Latitude (N) Longitude (E/W)	Date	Time (UTC)	Position Latitude (N) Longitude (E/W)	Date	Time (UTC)	Position Latitude (N) Longitude (E/W)	Date	Time (UTC)	Position Latitude (N) Longitude (E/W)		
282-1	09.09.01	03.20	87° 30.0' N 081° 56.3' E	09.09.01	04.26	87° 37.0' N 081° 56.3' E	09.09.01	04.36	09.09.01	05.09	87° 37.8' N 081° 53.0' E	4445	HF successful	
282-2	09.09.01	03.32	87° 30.0' N 081° 56.3' E	09.09.01	04.46	87° 37.0' N 081° 56.3' E	09.09.01	04.56	09.09.01	05.39	87° 36.0' N 081° 56.3' E	4441	Seach depth 21m	
283-1	10.09.01	08.06	87° 03.3' N 076° 37.5' E	10.09.01	08.52	87° 03.3' N 076° 37.5' E	10.09.01	09.03	10.09.01	09.17	87° 03.3' N 076° 38.4' E	4138	4.8 m sediments, HF successful	
284-1	10.09.01	08.18	87° 03.3' N 076° 38.4' E	10.09.01	09.22	87° 03.3' N 076° 38.4' E	10.09.01	09.34	10.09.01	09.41	87° 03.3' N 076° 38.4' E	4138	Seach depth 21m	
285-1	10.09.01	22.15	85° 43.3' N 074° 31.4' E	10.09.01	22.22	85° 43.3' N 074° 31.4' E	10.09.01	22.44	10.09.01	22.44	85° 43.3' N 074° 31.4' E	3303	0.69 m sediments, no HF data	
286-1	10.09.01	01.32	85° 41.8' N 074° 18.2' E	10.09.01	01.38	85° 41.8' N 074° 18.2' E	10.09.01	01.50	10.09.01	01.50	85° 41.8' N 074° 18.2' E	3480	0.95 m sediments, no HF data	
286-2	10.09.01	11.01	85° 33.3' N 074° 11.0' E	10.09.01	11.40	85° 33.3' N 074° 11.0' E	10.09.01	11.50	10.09.01	11.50	85° 33.3' N 074° 17.8' E	3468	HF successful	
287-1	11.09.01	18.01	85° 29.0' N 073° 51.0' E	11.09.01	18.44	85° 29.0' N 073° 51.0' E	11.09.01	18.45	11.09.01	18.45	85° 29.0' N 073° 52.0' E	3609	0.41 m sediments	
287-2	11.09.01	19.48	85° 29.0' N 073° 55.5' E	11.09.01	20.53	85° 28.8' N 074° 24.7' E	11.09.01	21.03	11.09.01	21.03	85° 29.0' N 073° 55.5' E	3810	Seach depth 11m	
287-3	11.09.01	22.12	85° 28.8' N 074° 20.9' E	11.09.01	23.00	85° 28.8' N 074° 24.7' E	11.09.01	23.08	11.09.01	23.08	85° 28.1' N 074° 17.8' E	3022	2.83 m sediments, HF successful	
288-1	12.09.01	07.16	85° 20.9' N 073° 35.0' E	12.09.01	08.01	85° 20.9' N 073° 35.0' E	12.09.01	08.11	12.09.01	08.11	85° 20.9' N 073° 38.8' E	4130	HF successful	
288-2	12.09.01	08.06	85° 20.9' N 073° 35.0' E	12.09.01	08.57	85° 21.0' N 073° 42.8' E	12.09.01	10.46	12.09.01	10.46	85° 20.9' N 073° 38.8' E	4137	no parameters, HF successful	
288-3	12.09.01	09.15	85° 20.9' N 073° 41.6' E	12.09.01	09.57	85° 21.0' N 073° 42.8' E	12.09.01	10.56	12.09.01	10.56	85° 20.9' N 073° 35.0' E	4137	Seach depth 21m	
289-1	13.09.01	05.17	85° 33.0' N 069° 43.7' E	13.09.01	05.33	85° 33.0' N 069° 43.7' E	13.09.01	05.56	13.09.01	05.56	85° 33.0' N 069° 43.7' E	3622	HF successful	
290-1	13.09.01	06.18	85° 33.0' N 069° 25.2' E	13.09.01	06.33	85° 33.0' N 069° 25.2' E	13.09.01	06.31	13.09.01	06.31	85° 33.0' N 069° 16.7' E	2824	69 kg basalt + glass	
290-2	13.09.01	06.18	85° 33.0' N 069° 25.2' E	13.09.01	06.33	85° 33.0' N 069° 25.2' E	13.09.01	06.31	13.09.01	06.31	85° 33.0' N 069° 16.7' E	2824	133.77 kg basalt	
291-1	14.09.01	03.32	85° 44.2' N 065° 22.9' E	14.09.01	03.40	85° 44.0' N 065° 21.6' E	14.09.01	03.40	14.09.01	03.40	85° 42.3' N 065° 33.0' E	4557	0.429 kg others + basalt	
292-1	14.09.01	03.32	85° 44.2' N 065° 22.9' E	14.09.01	03.40	85° 44.0' N 065° 21.6' E	14.09.01	03.40	14.09.01	03.40	85° 42.3' N 065° 33.0' E	4557	med only	
292-2	14.09.01	03.32	85° 44.2' N 065° 22.9' E	14.09.01	03.40	85° 44.0' N 065° 21.6' E	14.09.01	03.40	14.09.01	03.40	85° 42.3' N 065° 33.0' E	4557	Seach depth 21m	
292-3	14.09.01	08.10	85° 46.3' N 065° 29.3' E	14.09.01	08.20	85° 46.1' N 065° 30.7' E	14.09.01	08.17	14.09.01	08.17	85° 47.1' N 065° 27.7' E	5016	HF successful	
293-1	15.09.01	02.50	85° 54.4' N 059° 40.8' E	15.09.01	03.04	85° 54.4' N 059° 40.8' E	15.09.01	03.04	15.09.01	03.04	85° 53.9' N 059° 25.8' E	3300	165 kg basalt + others	
293-2	15.09.01	03.20	85° 54.4' N 059° 40.8' E	15.09.01	03.30	85° 54.3' N 059° 24.3' E	15.09.01	03.30	15.09.01	03.30	85° 53.2' N 059° 01.4' E	3713	263 kg basalt + others + glass	
293-3	15.09.01	08.52	85° 49.3' N 052° 07.4' E	15.09.01	09.47	85° 49.4' N 052° 05.8' E	15.09.01	11.32	15.09.01	11.32	85° 47.9' N 052° 19.7' E	4282	85.295 kg basalt + glass	
294-1	17.09.01	02.28	85° 40.5' N 047° 51.0' E	17.09.01	02.27	85° 40.4' N 047° 51.5' E	17.09.01	02.21	17.09.01	02.21	85° 40.6' N 047° 07.8' E	4901	med only	
294-2	17.09.01	11.02	85° 43.1' N 047° 38.2' E	17.09.01	11.54	85° 43.1' N 047° 38.2' E	17.09.01	12.08	17.09.01	12.08	85° 42.8' N 047° 34.6' E	4874	197.4 kg basalt + glass	
298-1	17.09.01	12.07	85° 44.5' N 046° 16.2' E	17.09.01	12.10	85° 44.4' N 046° 16.2' E	17.09.01	12.22	17.09.01	12.22	85° 45.3' N 046° 18.0' E	4653	HF successful	
300-1	18.09.01	03.10	85° 40.0' N 045° 40.0' E	18.09.01	03.20	85° 40.2' N 045° 38.5' E	18.09.01	03.28	18.09.01	03.28	85° 40.0' N 045° 38.5' E	4653	116 kg basalt + others	
301-1	18.09.01	18.41	85° 33.4' N 040° 35.2' E	18.09.01	19.28	85° 33.0' N 040° 33.8' E	18.09.01	19.35	18.09.01	19.35	85° 32.5' N 040° 31.6' E	2286	69.3 kg basalt + others	
302-1	19.09.01	00.50	85° 32.0' N 040° 23.5' E	19.09.01	02.07	85° 32.0' N 040° 23.5' E	19.09.01	02.10	19.09.01	02.10	85° 30.0' N 040° 31.6' E	2286	18.43 kg basalt + others	
303-1	19.09.01	06.43	85° 23.8' N 041° 06.4' E	19.09.01	08.03	85° 23.9' N 040° 59.8' E	19.09.01	08.05	19.09.01	08.05	85° 23.0' N 040° 58.0' E	4515	33 kg basalt	
305-1	19.09.01	13.30	85° 25.7' N 040° 58.0' E	19.09.01	14.30	85° 25.3' N 040° 57.7' E	19.09.01	15.56	19.09.01	15.56	85° 24.7' N 040° 58.0' E	4515	220.83 kg basalt, others + glass	
307-1	20.09.01	03.45	85° 28.6' N 039° 10.1' E	20.09.01	03.52	85° 28.6' N 039° 10.1' E	20.09.01	04.23	20.09.01	04.23	85° 24.1' N 038° 08.0' E	4309	177.6 kg basalt, others + glass	
308-1	20.09.01	08.37	85° 20.2' N 038° 40.0' E	20.09.01	09.32	85° 20.2' N 038° 37.8' E	20.09.01	09.32	20.09.01	09.32	85° 19.0' N 038° 28.6' E	5209	94.9 kg basalt + glass	
308-2	20.09.01	08.46	85° 20.2' N 038° 40.0' E	20.09.01	10.12	85° 20.1' N 038° 38.8' E	20.09.01	10.22	20.09.01	10.22	85° 20.1' N 038° 38.8' E	5219	HF successful	
309-1	20.09.01	15.55	85° 15.0' N 032° 54.0' E	20.09.01	16.54	85° 14.8' N 032° 46.8' E	20.09.01	16.46	20.09.01	16.46	85° 13.6' N 032° 57.0' E	5200	Seach depth 21m	
310-1	21.09.01	06.34	85° 01.3' N 032° 08.8' E	21.09.01	07.19	85° 01.1' N 032° 31.2' E	21.09.01	09.06	21.09.01	09.06	85° 00.7' N 032° 23.0' E	4622	127.5 kg basalt + others	
310-2	21.09.01	09.40	85° 58.0' N 027° 18.2' E	21.09.01	10.15	85° 58.0' N 027° 18.2' E	21.09.01	10.06	21.09.01	10.06	85° 59.0' N 032° 21.4' E	3787	21.16 kg basalt + others	
312-1	21.09.01	20.32	85° 55.4' N 027° 22.7' E	21.09.01	21.33	85° 55.4' N 027° 22.7' E	21.09.01	21.33	21.09.01	21.33	85° 56.7' N 031° 06.2' E	3365	Seach depth 21m	
313-1	22.09.01	02.50	85° 50.2' N 025° 46.8' E	22.09.01	03.30	85° 50.2' N 025° 47.4' E	22.09.01	03.30	22.09.01	03.30	85° 53.3' N 027° 18.2' E	3823	3.373 kg basalt + others	
313-2	22.09.01	02.50	85° 50.2' N 025° 46.8' E	22.09.01	03.30	85° 50.2' N 025° 47.4' E	22.09.01	03.30	22.09.01	03.30	85° 54.4' N 025° 40.0' E	4302	56.41 kg basalt, pebbles + others med only	

5. Station Log POLARSTERN (PS 59)

Profile/Station No	Start				On Bottom				Off Bottom				End				Equipment used	Comments/ Results			
	Date	Time (UTC)	Position		Date	Time (UTC)	Position		Date	Time (UTC)	Position		Date	Time (UTC)	Position						
			Latitude (N)	Longitude (E/W)			Latitude (N)	Longitude (E/W)			Latitude (N)	Longitude (E/W)			Latitude (N)	Longitude (E/W)			Latitude (N)	Longitude (E/W)	
313-2	22.09.01	00.00	85° 55.4'	025° 43.9' E	4739	22.09.01	10.31	85° 55.1'	025° 41.4' E	4610	22.09.01	12.14	85° 53.3'	025° 42.5' E	4150	22.09.01	13.00	85° 53.2'	025° 42.1' E	4143	Frame Dredge (1st-1st one) Pipe Dredge TV-Grab MAPIR Frame Dredge Suez-Diak Frame Dredge Pipe Dredge Pipe Dredge TV-Grab Argun-Army, Sonnbobys Argun-Army, Multichannel-Streamer, Sonnbobys Argun-Army, Multichannel-Streamer, Sonnbobys reflection seismic profile 20010400 reflection seismic profile 20010400 reflection/refraction seismic profile 20010400
314	22.09.01	19.20	85° 56.0'	025° 03.8' E	4833	22.09.01	17.15	85° 56.0'	025° 03.1' E	4831	22.09.01	19.16	85° 54.4'	024° 47.3' E	4635	22.09.01	20.05	85° 53.3'	024° 47.2' E	4626	
315-1	23.09.01	02.15	85° 46.0'	020° 27.2' E	4739	23.09.01	03.53	85° 46.5'	020° 27.0' E	4782	23.09.01	04.00	85° 50.2'	021° 22.0' E	5019	23.09.01	05.50	85° 48.5'	020° 26.2' E	4792	
315-2	23.09.01	03.24	85° 50.3'	021° 22.2' E	5037	23.09.01	09.38	85° 50.2'	021° 22.0' E	5019	23.09.01	11.21	85° 49.4'	021° 10.1' E	4876	23.09.01	12.13	85° 49.4'	021° 09.5' E	4871	
317	23.09.01	14.45	85° 50.3'	021° 22.0' E	5119	23.09.01	15.05	85° 49.7'	021° 30.8' E	4935	23.09.01	16.52	85° 47.7'	021° 30.6' E	4245	23.09.01	17.42	85° 50.3'	021° 22.9' E	5019	
318	23.09.01	14.45	85° 52.4'	022° 19.9' E	5042	23.09.01	22.30	85° 52.3'	022° 19.9' E	4909	23.09.01	19.37	85° 53.5'	022° 35.2' E	4659	23.09.01	20.32	85° 50.5'	022° 34.9' E	4578	
319	24.09.01	07.35	85° 57.0'	022° 40.9' E	4829	24.09.01	08.35	85° 57.0'	022° 40.7' E	4803	24.09.01	10.00	85° 56.5'	022° 35.2' E	4659	24.09.01	10.30	85° 50.5'	022° 34.9' E	4415	
320	24.09.01	16.45	85° 54.7'	022° 35.6' E	5051	24.09.01	17.47	85° 54.7'	022° 31.5' E	5123	24.09.01	19.37	85° 53.5'	022° 35.2' E	4659	24.09.01	20.32	85° 50.5'	022° 34.9' E	4415	
321	24.09.01	23.42	85° 56.2'	023° 51.1' E	4465	25.09.01	02.00	85° 56.1'	023° 38.8' E	4540	25.09.01	03.35	84° 55.4'	020° 06.7' E	4293	26.09.01	15.30	84° 55.4'	020° 06.7' E	4293	
322	26.09.01	02.05	85° 40.5'	020° 01.2' E	3960	26.09.01	03.10	84° 35.1'	020° 01.2' E	3790	26.09.01	10.13	83° 52.8'	019° 03.8' E	4097	26.09.01	10.13	83° 52.8'	019° 03.8' E	4097	
323	26.09.01	03.10	84° 35.1'	020° 01.2' E	3790	26.09.01	10.13	83° 52.8'	019° 03.8' E	4097	26.09.01	10.13	83° 52.8'	019° 03.8' E	4097	26.09.01	10.13	83° 52.8'	019° 03.8' E	4097	
324	26.09.01	19.25	83° 52.3'	027° 30.6' E	4070	26.09.01	19.25	83° 52.3'	027° 30.6' E	4070	26.09.01	21.28	81° 27.8'	032° 03.8' E	374	26.09.01	21.28	81° 27.8'	032° 03.8' E	374	

Chapters 6 to 16: only on CD-ROM.

17. List of Abbreviations and Acronyms

AGL	Above Ground Level
AMORE	Arctic Mid-Ocean Ridge Expedition
ARGOS	Automatic Remote Geomagnetic Observatory
AVHRR	Advanced Very High Resolution Radiometer
CS	Clear Sky
CTD	Conductivity, Temperature, Density
DAPI	4,6-diamidino-2-phenylindol
DAU	Digital Acquisition Unit
DCS	Data Collection and Positioning System
DWD	Deutscher Wetterdienst (= German Weather Service)
EEZ	Exclusive Economic Zone
EM	Electromagnetic
FLB	Fluorescently Labelled Bacteria
FOV	Field Of View
GKG	GroßKastenGreifer (= box corer)
GMT	Generic Mapping Tool
GPS	Global Positioning System
HDCS	Hydrographic Data Cleaning System
HELI-MAG	Helicopter Magnetic
HEM	Helicopter Electro-Magnetic
HRPT	High Resolution Picture Transmission
IABP	International Arctic Buoy Programme
IBCAO	International Bathymetric Chart of the Arctic Ocean
ISC	International Seismological Centre
IUGS	International Union of Geological Sciences
LSS	Light Scattering Sensor
MAPR	Miniature Autonomous Plume Recorder
MAR	Mid-Atlantic Ridge
MELT	Mantle Electromagnetic and Tomographic
MOU	Memorandum Of Understanding
MSRC	Marine Sciences Research Center, Stony Brook University, USA
MT	Magnetotelluric
NEIC	National Earthquake Information Center
NOAA	National Oceanic and Atmospheric Administration, USA
NPEO	North Pole Environmental Observatory
OC	OverCast

OFOS	Ocean Floor Observation System
PDF	Probability Density Function
PFB	Preformed Beams
PODAS	POLARSTERN Data Acquisition System
PPM	Proton-Precision-Magnetometer
RAMESSES	Reykjanes Axial Melt Experiment Structural Synthesis From Electromagnetics and Seismics
RAYINVR	RAY INVeRsion (raytracing programm)
SAR	Synthetic Aperture Radar
SCAMP	Seafloor Characterization And Mapping Pods
SCICEX	Scientific Ice Expeditions
SEM	Surface Electromagnetic Probe
SIMS	Sea Ice Monitoring System
SMT	Seismological Magnetotelluric
UTC	Universal Time Coordinator
VLF	Very Low Frequency

18. Karasik Seamount: only on CD-ROM.

„Berichte zur Polarforschung“

Eine Titelübersicht der Hefte 1 bis 376 (1981 - 2000) erschien zuletzt im Heft 413 der nachfolgenden Reihe „Berichte zur Polar- und Meeresforschung“. Ein Verzeichnis aller Hefte beider Reihen sowie eine Zusammenstellung der Abstracts in englischer Sprache finden Sie im Internet unter der Adresse: <http://www.awi-bremerhaven.de/Resources/publications.html>

Ab dem Heft-Nr. 377 erscheint die Reihe unter dem Namen: „Berichte zur Polar- und Meeresforschung“

- Heft-Nr. 377/2000 – „Rekrutierungsmuster ausgewählter Wattfauna nach unterschiedlich strengen Wintern“ von Matthias Strasser
- Heft-Nr. 378/2001 – „Der Transport von Wärme, Wasser und Salz in den Arktischen Ozean“, von Boris Cisewski
- Heft-Nr. 379/2001 – „Analyse hydrographischer Schnitte mit Satellitenaltimetrie“, von Martin Losch
- Heft-Nr. 380/2001 – „Die Expeditionen ANTARKTIS XI/1-2 des Forschungsschiffes POLARSTERN 1998/1999“, herausgegeben von Eberhard Fahrback und Saad El Naggar.
- Heft-Nr. 381/2001 – „UV-Schutz- und Reparaturmechanismen bei antarktischen Diatomeen und *Phaeocystis antarctica*“, von Lieselotte Riegger.
- Heft-Nr. 382/2001 – „Age determination in polar Crustacea using the autofluorescent pigment lipofuscin“, by Bodil Bluhm.
- Heft-Nr. 383/2001 – „Zeitliche und räumliche Verteilung, Habitatspräferenzen und Populationsdynamik benthischer Copepoda Harpacticoida in der Potter Cove (King George Island, Antarktis)“, von Gritta Veit-Köhler.
- Heft-Nr. 384/2001 – „Beiträge aus geophysikalischen Messungen in Dronning Maud Land, Antarktis, zur Auffindung eines optimalen Bohrpunktes für eine Eiskerntiefbohrung“, von Daniel Steinhage.
- Heft-Nr. 385/2001 – „Actinium-227 als Tracer für Advektion und Mischung in der Tiefsee“, von Walter Gelbert.
- Heft-Nr. 386/2001 – „Messung von optischen Eigenschaften troposphärischer Aerosole in der Arktis“ von Rolf Schumacher.
- Heft-Nr. 387/2001 – „Bestimmung des Ozonabbaus in der arktischen und subarktischen Stratosphäre“, von Astrid Schulz.
- Heft-Nr. 388/2001 – „Russian-German Cooperation SYSTEM LAPTEV SEA 2000: The Expedition LENA 2000“, edited by Volker Rachold and Mikhail N. Grigoriev.
- Heft-Nr. 389/2001 – „The Expeditions ARKTIS XVII/1 and ARKTIS XVII/2 of the Research Vessel 'Polarstern' in 2000“, edited by Gunther Krause and Ursula Schauer.
- Heft-Nr. 390/2001 – „Late Quaternary climate variations recorded in North Atlantic deep-sea ostracodes“, by Claudia Didié.
- Heft-Nr. 391/2001 – „The polar and subpolar North Atlantic during the last five glacial-interglacial cycles“, by Jan. P. Helmke.
- Heft-Nr. 392/2000 – „Geochemische Untersuchungen an hydrothermal beeinflussten Sedimenten der Bransfield Straße (Antarktis)“, von Anke Dähmann.
- Heft-Nr. 393/2001 – „The German-Russian Project on Siberian River Run-off (SIRRO): Scientific Cruise Report of the Kara-Sea Expedition 'SIRRO 2000' of RV 'Boris Petrov' and first results“, edited by Ruediger Stein and Oleg Stepanets.
- Heft-Nr. 394/2001 – „Untersuchung der Photooxidation von Wasserstoffperoxid, Methylhydroperoxid und Formaldehyd in der Troposphäre der Antarktis“, von Katja Riedel.
- Heft-Nr. 395/2001 – „Role of benthic cnidarians in the energy transfer processes in the Southern Ocean marine ecosystem (Antarctica)“, by Covadonga Orejas Saco del Valle.
- Heft-Nr. 396/2001 – „Biogeochemistry of Dissolved Carbohydrates in the Arctic“, by Ralph Engbrodt.
- Heft-Nr. 397/2001 – „Seasonality of marine algae and grazers of an Antarctic rocky intertidal, with emphasis on the role of the limpet *Nacilla concinna* Strebel (Gastropoda: Patellidae)“, by Dohong Kim.
- Heft-Nr. 398/2001 – „Polare Stratosphärenwolken und mesoskalige Dynamik am Polarwirbelrand“, von Marion Müller.
- Heft-Nr. 399/2001 – „North Atlantic Deep Water and Antarctic Bottom Water: Their Interaction and Influence on Modes of the Global Ocean Circulation“, by Holger Brix.
- Heft-Nr. 400/2001 – „The Expeditions ANTARKTIS XVIII/1-2 of the Research Vessel 'Polarstern' in 2000“ edited by Victor Smetacek, Ulrich Bathmann, Saad El Naggar.
- Heft-Nr. 401/2001 – „Variabilität von CH₂O (Formaldehyd) - untersucht mit Hilfe der solaren Absorptionsspektroskopie und Modellen“ von Torsten Albrecht.
- Heft-Nr. 402/2001 – „The Expedition ANTARKTIS XVII/3 (EASIZ III) of RV 'Polarstern' in 2000“, edited by Wolf E. Arntz and Thomas Brey.
- Heft-Nr. 403/2001 – „Mikrohabitatsprüche benthischer Foraminiferen in Sedimenten des Südatlantiks“, von Stefanie Schumacher.
- Heft-Nr. 404/2002 – „Die Expedition ANTARKTIS XVII/2 des Forschungsschiffes 'Polarstern' 2000“, herausgegeben von Jörn Thiede und Hans Oerter.
- Heft-Nr. 405/2002 – „Feeding Ecology of the Arctic Ice-Amphipod *Gammarus wilkitzkii*. Physiological, Morphological and Ecological Studies“, by Carolin E. Arndt.
- Heft-Nr. 406/2002 – „Radiolarienfauna im Ochootskischen Meer - eine aktuopaläontologische Charakterisierung der Biozönose und Taphozönose“, von Anja Nimmergut.
- Heft-Nr. 407/2002 – „The Expedition ANTARKTIS XVIII/5b of the Research Vessel 'Polarstern' in 2001“, edited by Ulrich Bathmann.
- Heft-Nr. 408/2002 – „Siedlungsmuster und Wechselbeziehungen von Seepocken (Cirripedia) auf Muschelbänken

(*Mytilus edulis* L.) im Wattenmeer", von Christian Buschbaum.

Heft-Nr. 409/2002 – „Zur Ökologie von Schmelzwassertümpeln auf arktischem Meereis - Charakteristika, saisonale Dynamik und Vergleich mit anderen aquatischen Lebensräumen polarer Regionen“, von Marina Carstens.

Heft-Nr. 410/2002 – „Impuls- und Wärmeaustausch zwischen der Atmosphäre und dem eisbedeckten Ozean“, von Thomas Garbrecht.

Heft-Nr. 411/2002 – „Messung und Charakterisierung laminarer Ozonstrukturen in der polaren Stratosphäre“, von Petra Wahl.

Heft-Nr. 412/2002 – „Open Ocean Aquaculture und Offshore Windparks. Eine Machbarkeitsstudie über die multifunktionale Nutzung von Offshore-Windparks und Offshore-Marikultur im Raum Nordsee“, von Bela Hieronymus Buck.

Heft-Nr. 413/2002 – „Arctic Coastal Dynamics. Report of an International Workshop, Potsdam (Germany) 26-30 November 2001“, edited by Volker Rachold, Jerry Brown and Steve Solomon.

Heft-Nr. 414/2002 – „Entwicklung und Anwendung eines Laserablations-ICP-MS-Verfahrens zur Multielementanalyse von atmosphärischen Einträgen in Eisbohrkernen“, von Heiko Reinhardt.

Heft-Nr. 415/2002 – „Gefrier- und Tauprozesse im sibirischen Permafrost – Untersuchungsmethoden und ökologische Bedeutung“, von Wiebke Müller-Lupp.

Heft-Nr. 416/2002 – „Natürliche Klimavariationen der Arktis in einem regionalen hochauflösenden Atmosphärenmodell“, von Wolfgang Dorn.

Heft-Nr. 417/2002 – „Ecological comparison of two sandy shores with different wave energy and morphodynamics in the North Sea“, by Iris Menn.

Heft-Nr. 418/2002 – „Numerische Modellierung turbulenter Umströmungen von Gebäuden“, von Simón Domingo López.

Heft-Nr. 419/2002 – „Scientific Cruise Report of the Kara-Sea Expedition 2001 of RV „Academic Petrov“: The German-Russian Project on Siberian River Run-off (SIRRO) and the Project „ESTABLISH“, edited by Ruediger Stein and Oleg Stepanets.

Heft-Nr. 420/2002 – „Vulkanologie und Geochemie pliozäner bis rezenter Vulkanite beiderseits der Bransfield-Straße / West-Antarktis“, von Andreas Veit.

Heft-Nr. 421/2002 – „POLARSTERN ARKTIS XVII“ Cruise Report: AMORE 2001 (Arctic Mid-Ocean Ridge Expedition)“, by J. Thiede et al.

* vergiffen/out of print.

** nur noch beim Autor/only from the author.